TECHNISCHE UNIVERSITÄT MÜNCHEN

TUM School of Engineering and Design

Design and Optimisation of Solar-Assisted Urban District Heating Systems

Daniel Beckenbauer

Vollständiger Abdruck der von der *TUM School of Engineering and Design* der *Technischen Universität München* zur Erlangung des akademischen Grades eines

Doktors der Ingenieurwissenschaften

genehmigten Dissertation.

Vorsitzender:

Prof. Dr.-Ing. Klaus Peter Sedlbauer

Prüfer der Dissertation:

1. Dr. Vicky Albert-Seifried
2. Prof. Dr.-Ing. Wilfried Zörner
3. Prof. Dr. rer. nat. Thomas Hamacher

Die Dissertation wurde am 12.04.2021 bei der *Technischen Universität München* eingereicht und durch die *TUM School of Engineering and Design* am 29.06.2022 angenommen.

Abstract

The reduction of greenhouse gas emissions and fossil energy consumption has been one of the mostly discussed topics in society and science for the past years. The dissemination of solar district heating systems provides the opportunity of a more climate-friendly heat supply in urban areas. Many research projects focus on the utilisation of central solar plants and large-scale seasonal thermal storages to achieve high solar fractions in the heat supply of the districts. However, in case of energetic renovation of a densely built-up area, the feasible dimensions of collector arrays and thermal storages as well as their distribution are often limited. Moreover, high storage capacities come along with high investment and, thus, high heat generation costs.

Another approach is the installation of small detached solar thermal plants for domestic hot water production and space heating. These systems are easy to install and, therefore, suitable for retrofitting but usually allow only a limited solar fraction for single buildings. These problems impede a decent contribution of solar energy in the heat supply of many urban housing estates.

The question arises, whether there is potential to further increase the solar fraction of decentralised solar thermal plants with diurnal storages. Therefore, the objective of this research was the analysis of an improved hydraulic design of distributed solar heat generators and storage tanks in combination with suitable control strategies for an optimised utilisation of the solar heat in urban district heating networks.

After a literature review on the current state of science and technology of solar district heating, a simulation model was set up based on a field test system in Ingolstadt. This system was equipped with four medium-scale solar thermal plants and analysed in a comprehensive metrological study for the validation of the simulation model. Based on this validation, an extension of the model for bidirectional flow in the district heating pipes was performed. The extended model served as the basis for a simulation study of various integration concepts of solar thermal plants regarding size, hydraulics, distribution and control strategy. A parametric study allowed the assessment of the concepts under different boundary conditions.

It is shown in this thesis, that the field test installation works reliable and the planned cost level is reached. From the simulation study it was derived that even with decentralised plants, solar fractions of up to 40 % are possible, depending on the climate and heat demand. Many configurations of distributed plants allow fossil energy savings of approximately 25 % at costs between 10 Ct/kWh and 15 Ct/kWh. The results can serve as design recommendations for further retrofitting projects of existing small-scale district heating systems.

Acknowledgements

Firstly, I would like to express my gratitude to Prof. Wilfried Zörner and Dr. Christoph Trinkl, who gave me the opportunity to work at the *Institute of New Energy Systems* and for initiating the cooperation with *TUM*.

Furthermore, I would like to thank Dr. Vicky Albert-Seifried for supervising the project at the *Munich School of Enginering* for many years, Prof. Hamacher, who liberally volunteered to be the third examiner of the thesis as well as Prof. Sedlbauer, who took the chair of the examining committee.

I would also like to thank all my former colleagues at the *Institute of New Energy Systems* for their support in daily work and the good times we had, regardless of all challenges, that occurred.

The patience, motivation and support from my whole family helped me to carry on with my work and made things much easier.

Last but not least, I would like to thank Corinna for pushing me patiently through the final phase of the work after my time at the institute, when it was sometimes difficult to stay on task.

Table of Contents

List of Figures

List of Tables

Abbreviations and Subscripts

BMU	Bundesministerium für Umwelt, Naturschutz und Reaktorsicherheit / Federal Ministry for the Environment, Nature Conservation and Nuclear Safety
BMWi	Bundesministerium für Wirtschaft und Energie / German Federal Ministry for Economic Affairs and Energy
C	Central
CARNOT	Conventional And Renewable eNergy systems OpTimization Blockset
CHP	Combined heat and power plant
Ct	Euro-Cent
DH	District heating
DHW	Domestic hot water
EPDM	Ethylene propylene diene monomer rubber
HGC	Heat generation costs
KfW	Kreditanstalt für Wiederaufbau
kW	Kilowatt
kWh	Kilowatthour
MAP	Marktanreizprogramm / market incentive programme
MWh	Megawatthour
RR	Return-return
RS	Return-supply
SDH	Solar district heating
SF	Solar fraction
spec	Specific
SR	Supply-return
SS	Supply-supply
th	Thermal
THI	Technische Hochschule Ingolstadt
THV	Thermo-Hydraulic Vector
TRNSYS	Transient Systems Simulation Software
TWh	Terawatthour
US-FM	Ultrasonic flow meter
VDI	Verein Deutscher Ingenieure / Association of German Engineers

1 Introduction

1.1 Motivation

Multi-storey residential buildings provide high potential for solar-assisted local district heating. Current research projects, as described in section 2, focus on the utilisation of large seasonal storages and large centralised collector arrays to achieve a solar fraction[1] of above 50 %. However, for retrofitting densely built-up urban areas, the feasibility of solar district heating is often restricted by the limited available space for collector arrays and heat storages. Moreover, high storage capacities come with high investment and heat generation costs. These drawbacks impede the application of large centralised system concepts in existing urban areas and hinder the dissemination of solar thermal district heating.

1.1.1 Energy Consumption and Future Transition

To understand the relevance of solar thermal plants in urban districts, a look at the current situation of the energy supply in Germany and an outlook on its future development has to be taken with an emphasis on the role, solar district heating can play in the transition to a more climate-friendly structure.

According to the *BMWi (German Federal Ministry for Economic Affairs and Energy)*, the total final energy consumption in Germany in 2016 was 2,542 TWh, which is even 1.7 % more than four years before (Figure 1) [1]. The fraction of energy for space heating and domestic hot water production is around 33 % of this total energy consumption. As space heating and domestic hot water are supplied at temperature levels below 100 °C, a considerable fraction of this energy can be covered by renewable low temperature heat sources like solar thermal, to reach a higher independence from fossil fuels and to reduce carbon dioxide emissions.

Taking the data from the scenarios, which Nitsch et al. [2] developed for the *BMU (Federal Ministry for the Environment, Nature Conservation and Nuclear Safety)*, a renewable heat production of more than 350 TWh is necessary in 2050 to reach the government's aims for carbon dioxide reduction of at least 80 % compared to 1990. The current renewable heat production is dominated by biomass applications and the solar thermal contribution is less than 4 %. As the biomass resources are limited and there is only small potential for further growth in this sector, geothermal and solar

[1] The portion of energy provided by the solar thermal systems divided by the total energy production in %.

thermal energy have to be expanded. Amongst these, the greatest effort has to be devoted to additional solar thermal installations as more than 25 % of the renewable heat in 2050 is expected to be provided by solar thermal plants (Figure 2).

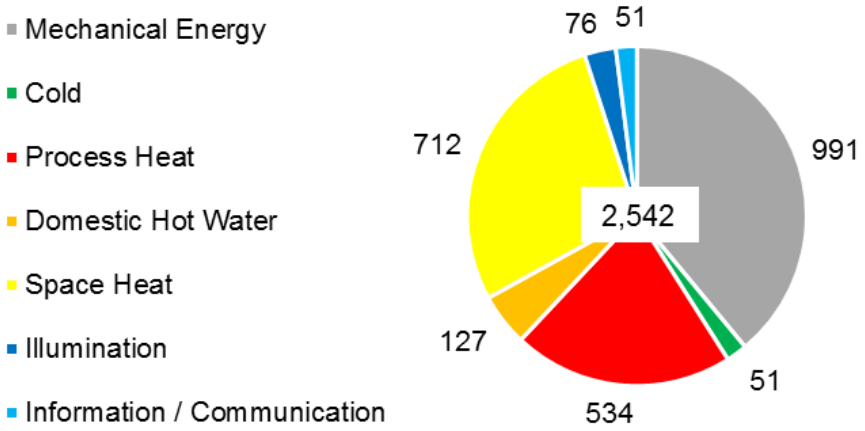

Figure 1: Final energy consumption in Germany 2016 in TWh (based on [1])

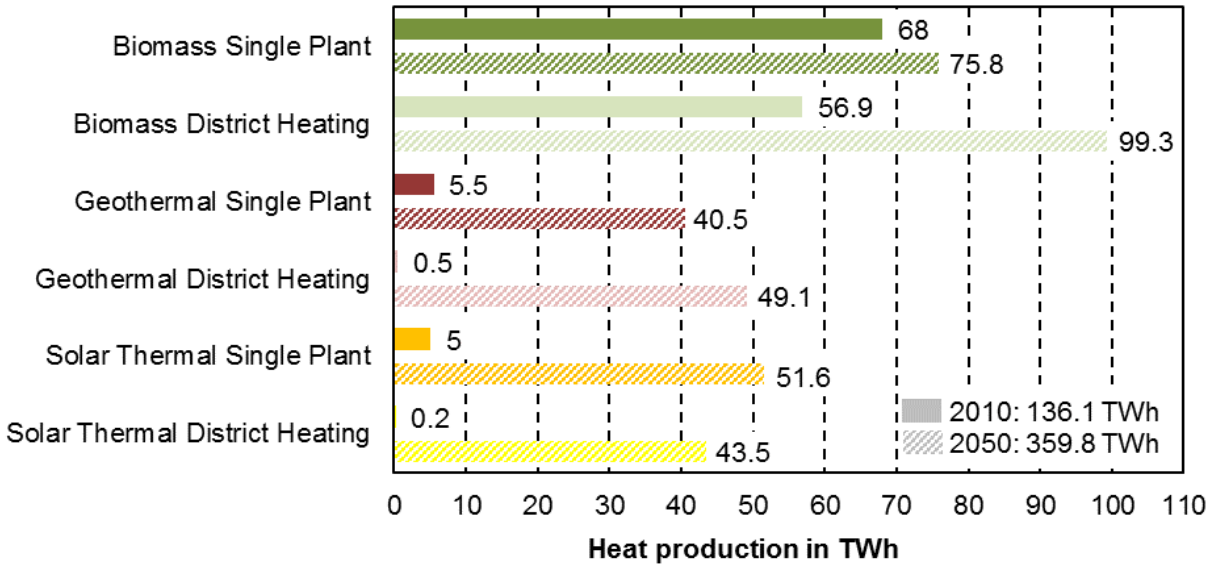

Figure 2: Renewable heat production in Germany (based on [2])

Within this expansion, in particular the combination with district heating has to be significantly enhanced. The heat production from solar district heating in 2050 will be more than 200 times higher than today according to the *BMU* scenario. The need for district heating systems is additionally intensified by the necessity of thermal load compensation abilities for a more flexible electricity production ([2], [3]).

1.1.2 Solar Applications in Urban Areas

Loga et al. [4] showed, that 18 % of the residential buildings in Germany are multi-family houses with three or more flats. These houses contain 54 % of all residential units. In larger cities, the number is even higher. One half of the residential buildings

was built before 1970. Figure 3 shows the distribution of the heated living area in multi-family buildings with 3 – 12 residential units and large multi-family buildings with 13 or more residential units for different years of construction (class A to J).

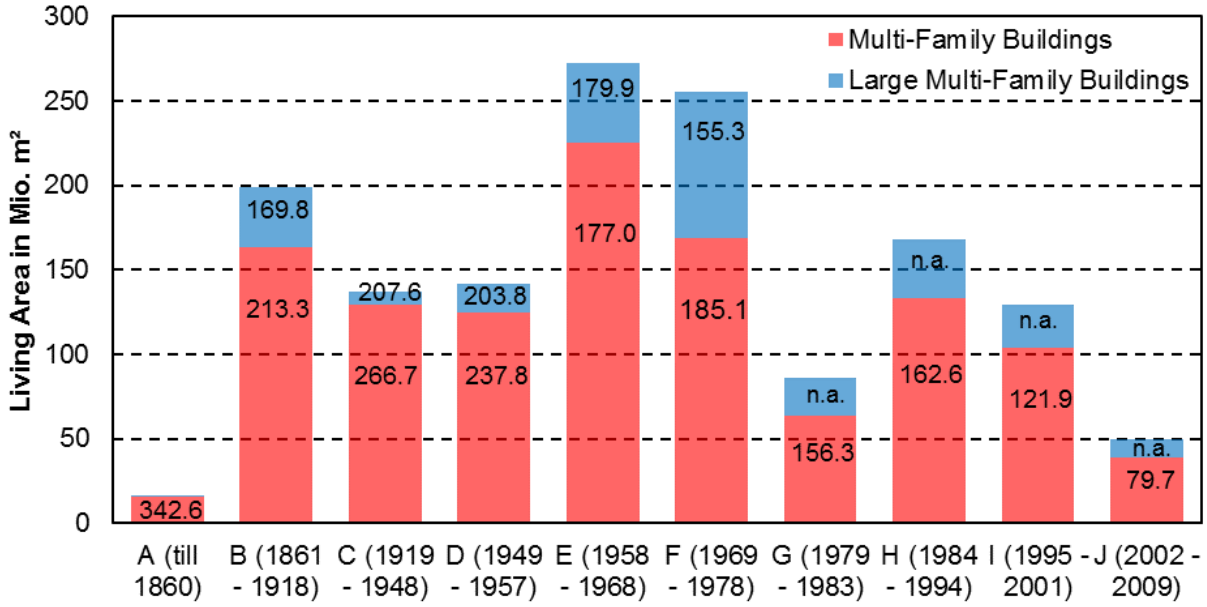

Figure 3: Heated living area in multi-family buildings of different ages; values at the columns show the average specific annual heat demand of the building type in kWh/m² (based on [4])

It can be seen that a considerable fraction of the living area is located in buildings with a high specific heat demand. Therefore, multi-family buildings, particularly existing buildings, have a significant relevance in the progress of retrofitting the German energy supply. On the other hand, only 5.4 % of all buildings are supplied by district heating systems up to now [5] and the fraction of multi-family buildings supplied by district heating is around 13 % [4]. As new buildings have to fulfil stricter regulations for the heat protection [6], the demand for space heating will be lower in the future. The same holds true for retrofitting of existing buildings, where improved insulation reduces the heat losses through building envelopes. Nevertheless, due to a currently low retrofitting rate of only 1 %, it will take several decades, until the standard of the majority of the buildings will reach the level of newer ones [7]. Besides that, there is no high potential to decrease the demand for the domestic hot water consumption as it mostly depends on the behaviour of the inhabitants and less on the technology of supply. It can be expected that the fraction of domestic hot water of the total heat consumption in residential buildings will increase in the future, while the total consumption will be reduced by around 47 % [2].

There are hardly any data available on the utilisation of solar thermal heat in multi-family buildings. However, in 2007 Stryi-Hipp et al. [8] showed that only 1 % of the newly installed solar thermal systems, funded by the German *MAP (market incentive*

programme) at this time were mounted on multi-storey buildings. This results from technical problems, e.g. not enough space for the installation of heat storages, on one hand and from economic aspects on the other hand. Many of the flats in these buildings are rented out. The owners of the buildings have limited interest in new heating systems even if they had lower heat generation costs, as the heat is paid by the tenants but investments in new heating systems are primarily covered by the owners. When it comes to the installation of a new heating system, conventional gas or oil-fired furnaces are preferred, as they come with less planning and installation effort, low investment costs and are judged as a reliable technology by many building owners.

Based on these determining factors, it can be concluded that the investigation of solar thermal plants in urban residential areas as well as of district heating systems is an important field of research. While the installation and operation of simple solar thermal systems in single-family houses is well known and mostly impeded by personal or economic considerations (depending on current funding by the government and fossil fuel prices), the integration of solar energy into district heating is in its infancy and still faces technological challenges besides these financial aspects.

1.2 Objectives and Procedure of the Research

This work aims to tackle the challenges mentioned above by investigating a novel solar district heating design, based on distributed solar collector arrays and thermal heat storages in multi-storey residential buildings, with bidirectional heat distribution capability. The network design and yield optimisation of such a system is examined in various urban contexts. Figure 4 summarises the thesis structure.

After describing the technology of solar thermal energy and district heating as well as their current role in the energy sector and the expected future transition, a review on past and ongoing research in solar district heating is presented in section 2. Besides the design of the plants and the current research activities on the improvement of the solar yield, the economic and energetic performance of existing plants is an aspect of this review.

The novelty of the proposed solar thermal systems lies in the concept of smart bidirectional heat distribution, which allows flexible responses to the concurrent heat demands of buildings in the heating network. The bidirectional approach enables solar thermal plants in buildings with a lower heat demand to supply buildings with higher demand in the heating network. In addition, solar thermal energy can be transferred from the collector arrays to storages and consumers anywhere in the heating network

and the network itself can act as short-term buffer. This concept is described in detail in section 3.

As basis for the optimisation of the plant layout and operation, a suitable simulation model is set up based on a field test installation in South Germany, which is described in section 4. The modelling approach is validated with decentralised solar thermal plants, integrated into this district heating system and additional laboratory tests in section 5.

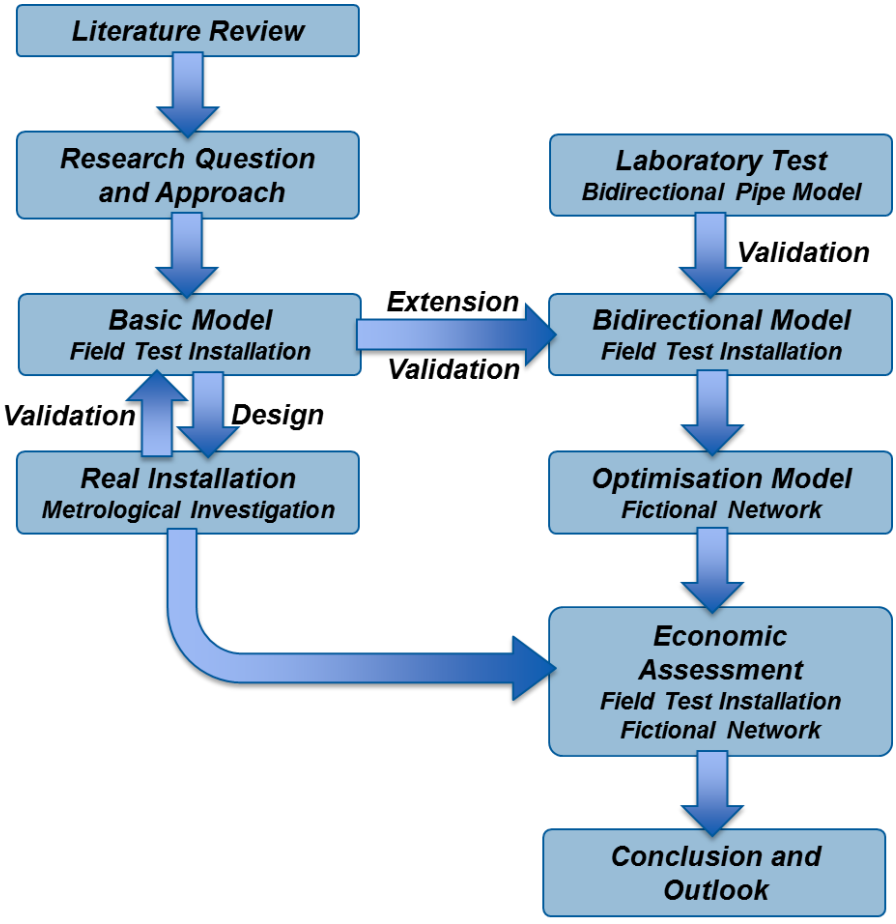

Figure 4: Scheme of the thesis structure

The most promising designs of the system in terms of hydraulic schemes, dimensioning and positioning of the storages and the solar collector arrays are determined by a simulation study. This study is conducted with an additional model of a fictional network, capable of bidirectional flow. For an appropriate operation of this system, superior control algorithms for managing the heat generators and storages in the system are implemented. A model-based parametric study is carried out to examine the impacts of various boundary conditions (e.g. available space, heat demand, climate conditions etc.) and the performance of the new concept is compared to existing approaches for solar district heating (section 0).

Based on the results of the study, the economic and ecological advantages and disadvantages of various solar district heating systems are assessed in section 7 and a conclusion with an outlook on future research is presented in section 8.

2 Literature Review

2.1 Solar Thermal Technology

As the thesis deals with the integration of solar thermal plants into district heating, some basic principles of solar thermal technology, including the layout and operation of a solar thermal plant and their influences on the plant´s efficiency are shown in this chapter.

2.1.1 Solar Thermal Collectors

A solar thermal collector, the main component of a solar thermal system, is a device to transform the energy of the sunlight into heat for multiple purposes and. In domestic applications, the purposes can either be domestic hot water preparation or space heating. There are different kinds of collectors – flat plate collectors, evacuated tube collectors and pool absorbers. Figure 5 shows efficiency curves of several of these collectors [9]. It can be seen, that with increasing temperature differential to the ambient, the efficiency gets lower. This is due to the increasing thermal losses. The value on the x-axis is denoted “reduced temperature”, which means the temperature differential in K divided by the solar irradiation in W/m². The solar irradiation is the second important factor on the thermal power of the collector. Higher irradiation leads to higher power input to the collector and increases the thermal output.

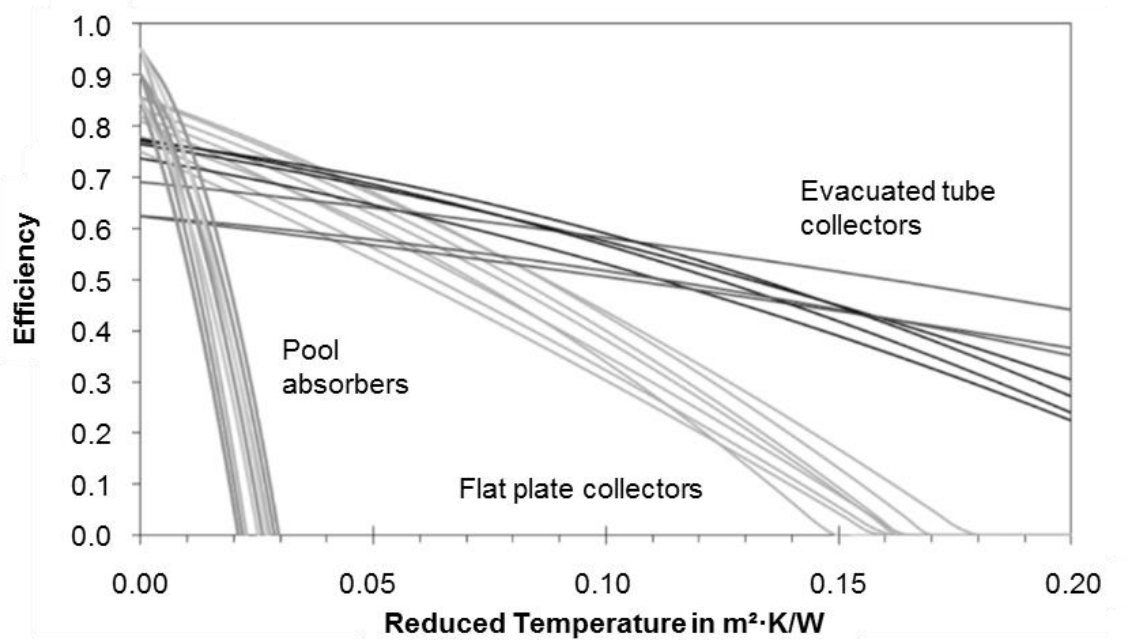

Figure 5: Efficiency curves of collectors (based on [9])

It is obvious that the uncovered pool absorbers have the highest efficiency when operating at a mean temperature equal to ambient temperature. This point is called zero-loss efficiency or optical efficiency (η_0) as it mostly depends on the optical properties of the collector. On the other hand, the decrease of efficiency is very steep at higher temperatures and lower irradiation. The evacuated tube collectors have the lowest η_0 value but suffer less from higher operating temperatures or low irradiation. Flat plate collectors are in between. This behaviour indicates that it is most suitable to work on a low temperature level for reaching a high efficiency of a solar thermal system.

2.1.2 Solar Thermal Systems

The solar yield, gained by the collector array is transferred and distributed in the heating system of the building. Figure 6 shows a scheme of an exemplary solar thermal system used for domestic hot water production and space heating [10]. The described functionality is similar for all solar thermal systems in residential applications.

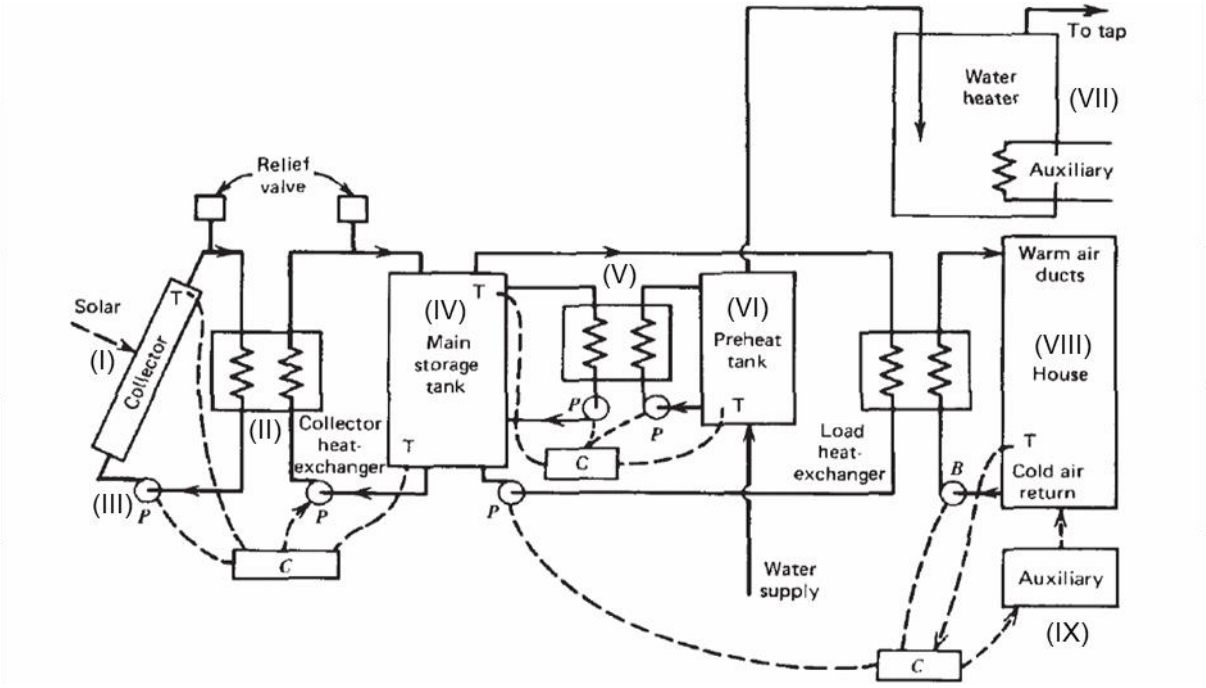

Figure 6: System for domestic hot water production and space heating (based on [10])

In this system, the heat from the collectors (I) is transferred to the fluid in the primary circuit. This fluid is conducted through the collector heat exchanger (II) by the pump (III). In domestic solar thermal systems, it is common to transport the energy absorbed by the collector via a heat transfer fluid. Depending on the system this can be water or a mixture of water and an anti-freeze like glycol. There are also air collectors, which

transfer the energy to an air stream flowing through the collector. This type is not considered in this study because it is only relevant for process heat or energy efficient new buildings with air heating systems and less for retrofitting projects, which are the focus of this investigation.

The secondary circuit transfers the energy to the main storage tank (IV). This hot water tank serves as a buffer to store solar heat if it is not consumed immediately. A second heat exchanger (V) connects the storage tank with the preheat tank (VI). The preheat tank is filled with drinking water, which is heated up if the temperature in the buffer storage exceeds the temperature in the preheat tank. In case of hot water tap, cold water from the water supply flows into the preheat tank and the already heated water is transferred to the water heater. If the temperature of this water is below the desired temperature, it is additionally heated by an auxiliary source (VII). A second circuit connects the main storage tank with the building's space heating system (VIII). Like for the domestic hot water production, auxiliary heat (IX) is used to fill gaps between heat demand and available solar heat. Of course, there are variations of the layout. E.g., an integrated domestic hot water heating via a pipe or plate heat exchanger can be included in the solar buffer. The auxiliary heat source is often connected to the same storage tank and heats up the upper part of the volume, while the lower storage volume is reserved for the solar thermal system.

The tasks of the controller in a large solar thermal system for domestic hot water preparation are according to Bollin et al. [11] the management of:

- Transporting away the heat from the solar collector array
- Loading the storage
- Unloading the storage
- Heating the domestic hot water and space heating
- Thermal disinfection (legionella) and temperature control

For the control of the collector array, temperature and irradiation sensors are used, where irradiation is more likely to be a control parameter in larger systems or systems with evacuated tube collectors. When using temperature sensors at the collector, the pump is activated, when the collector temperature is higher than the storage temperature plus a certain offset for the compensation of losses in the pipes and the temperature difference in the heat exchanger. When an irradiation sensor is available, a check is performed to determine whether the irradiation is higher than a predefined threshold, e.g. 200 W/m². In that case, the pump in the collector circuit is switched on and a temperature sensor close to the plate heat exchanger is used to start the pump for loading the storage. All other pumps in the system have a similar behaviour and

are activated, if there is a sufficient temperature differential between heat source and heat sink. For thermal disinfection, which is performed to prevent legionella contamination, usually a time-controlled heating of the complete drinking water in the system above 60 °C is set once a day. To increase the efficiency, additional checks can be done to determine if the temperature was already reached during the last 24 h due to high solar yields. In that case, the disinfection can be skipped.

2.2 District Heating Technology

The basic principles of district heating technology are presented in this chapter in addition to the already mentioned solar heat generation. The reasons for setting up district heating networks are shown as well as the components and the operation.

2.2.1 System Layouts

District heating is a technology to supply several buildings or even complete districts or towns with heat from one or more large heating plants. These plants are either included in one of the supplied buildings or in a dedicated building for the heating devices. The three elements of a district heating system are according to Krimmling [12]:

- Heat generators
- Distribution network
- Customer substations

The reasons for setting up district heating systems include:

- Utilisation of excess heat (from power plants or industrial processes)
- Utilisation of heat sources, which are difficult to exploit with small plants (e.g. deep geothermal energy, wood chips, biogas)
- Higher flexibility for combined heat and power generation
- Higher efficiency of one large heat generator over many small plants
- Lower space demand in the supplied buildings
- Easier treatment of exhaust gases
- Easier optimisation and maintenance of one large compared to many small plants

These reasons are in particular relevant in urban contexts, where a high density of buildings leads to a high density of heat consumption. In this case, the installation of a central heat generator for several buildings not only has a positive effect on the available space in the buildings and the amount of exhaust gas but also comes with a high efficiency due to the low fractional distribution losses of the piping network.

Fossil- and biomass-fired boilers are an established technology in such district heating networks. For standard systems, there are two main principles for the piping architecture, the 2-pipe network and the rarely used 4-pipe network (Figure 7). The 2-pipe network has one supply pipe and one return pipe. These pipes are filled with heating water (or sometimes steam) and the production of domestic hot water is done in the substations in a separate circuit. A 4-pipe network has a supply and a return pipe for the space heating as well as a pipe for supplying the substations directly with domestic hot water and a circulation pipe, leading back to the central heating station. A 2-pipe network is less expensive to build but for a 4-pipe network, the temperatures and the mass flows of space heating and domestic hot water supply can be controlled separately [13].

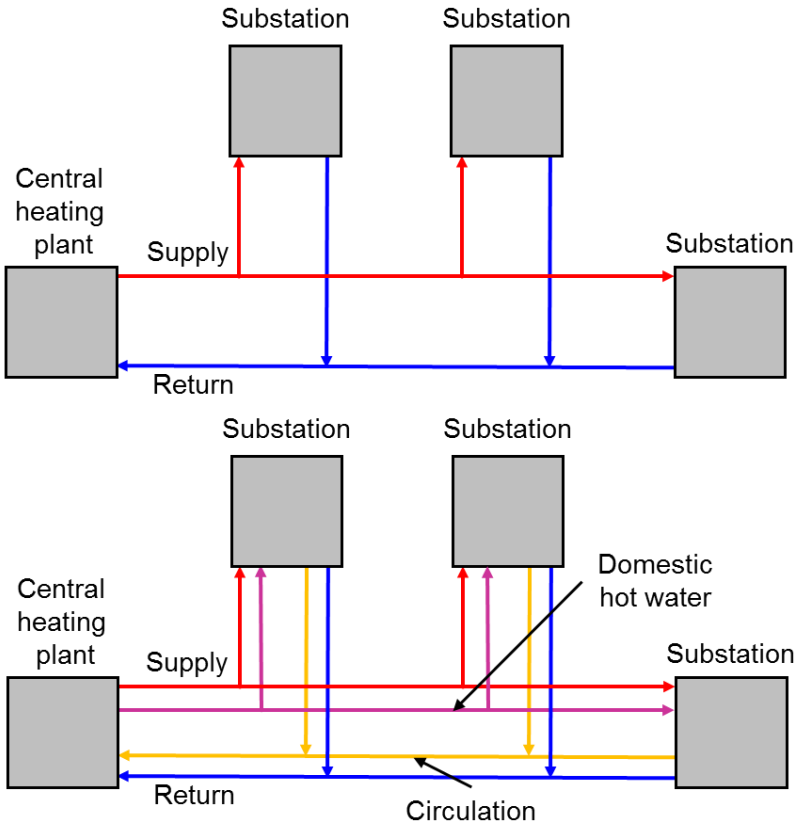

Figure 7: 2-pipe (top) and 4-pipe (bottom) architecture of district heating networks

2.2.2 Central Heating Stations

A typical layout of a central heating station is shown in Figure 8. A furnace is connected to the piping network via a hydraulic compensator. Pumps on the primary and the secondary side control the mass flow in the network. If the heating power of the furnace is difficult to control, e.g. for wood fired plants, or in case of other special requirements like an electricity driven generation in combined heat and power plants (CHP), the hydraulic compensator can be substituted with a larger buffer storage to compensate a higher power mismatch between generation and consumption. An alternative to the

hydraulic compensator is a controlled three-way valve for bypassing the network. This allows a better temperature control for the heat generator. Instead of only one furnace, it is common to use several devices to increase the power of the central heating station or to allow the combination of e.g. a CHP plant for base load and an additional gas furnace to cover peak demands. These generators can be connected in parallel or in series. A group of gas furnaces can have a higher efficiency when all devices work in part load, while a CHP plant or a condensing boiler can profit from a serial connection directly to the return pipe, where the temperature level is the lowest in the system.

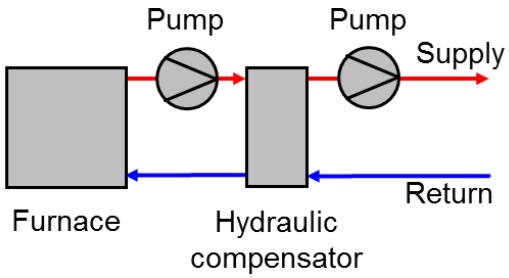

Figure 8: Exemplary design of a central heating station

To control the thermal power of the district heating system, the temperature as well as the mass flow can be modified. A common approach is to change the supply temperature depending on the ambient temperature (Figure 9).

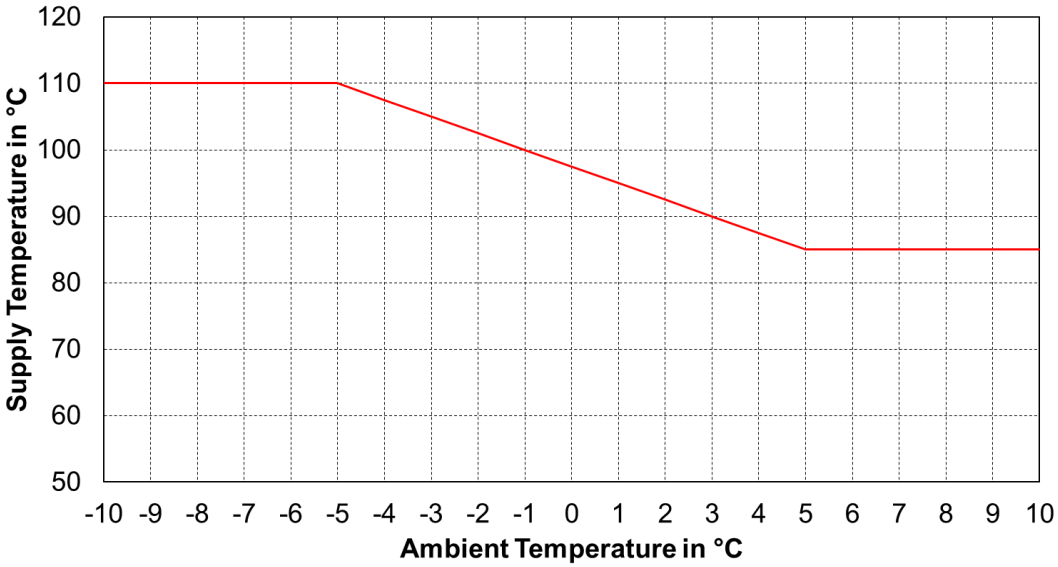

Figure 9: Supply temperature as function of ambient temperature (based on [14])

During winter season, the set temperature is higher to increase the amount of energy transferred per fluid volume. The modification of the temperature is a slow process as all capacities, like heat transfer fluid, pipes and other devices in the system have to be heated up. To compensate short-term fluctuations, it is therefore common to change the flow rates by closing and opening valves in the substations. This has an immediate effect in the network.

2.2.3 Piping Network

The transfer of the heated water from the central heating station to the consumer is realised through insulated pipes. These pipes are nowadays usually built of an inner steel shell, insulated by polyurethane foam and covered with an outer polymeric surface to prevent humidity from influencing the insulation. For lower temperatures and fluid pressures there are also pipes available, which are completely built of polymers. The pipes are either small in diameter, flexible and can be installed directly from coils or come as single straight pipes, which are connected by welding or, in case of polymers, crimping. Usually, the pipes are laid underground but there are systems as well, where the pipes lie on the surface or are mounted in concrete channels.

The pressure difference between the supply and return pipes is the driving force to conduct the water in the system. In addition to the system pressure, the central pump creates a pressure difference between pump inlet and pump outlet. The consumer with the longest piping distance to the central heating station has the highest pressure loss in the pipe connection and therefore defines the minimum static head, the pump has to maintain.

2.2.4 Substations

The substation is the connection between the network and the consumers. It can be connected directly to the district heating network with the same fluid circulating in the network and in the buildings. Nevertheless, a more common design is the indirect connection with a plate heat exchanger or a pipe heat exchanger in decentralised buffer storages (Figure 10). This enables different pressure levels in the buildings and the network and problems in single substations, like leakages or contaminations, have no effect on the operation of the whole district heating system. Direct connections prevent a temperature difference between district heating and building system and are less costly as the plate heat exchangers are not necessary. Therefore, it is more common in small systems, supplying several buildings or small districts. For the space heating circuit, there is usually a mixing valve to set the supply temperature to the desired level of each individual building.

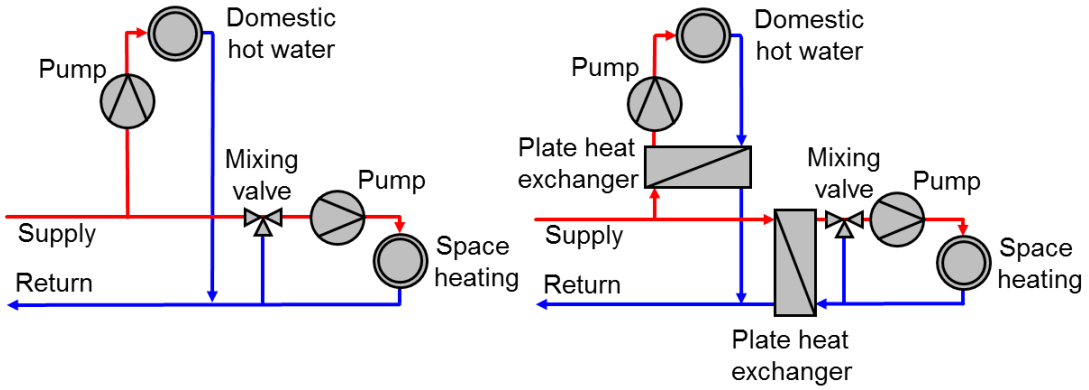

Figure 10: Exemplary substation design: direct connection (left) and connection via plate heat exchanger (right)

Independent of the connection type, relevant components of the substation (besides safety devices) are:

- Gate valve to disconnect the building from the district heating network
- Filter to separate contaminations from the heating water
- Energy meter to log the heat consumption of the building
- Differential pressure valve to control the mass flow through the substation
- Pumps for space heating or domestic hot water circuit
- Controller

The domestic hot water in a substation is usually produced by a plate heat exchanger, a storage tank or a combination of both (Figure 11). The use of a heat exchanger has hygienic benefits, as there is only a small amount of drinking water stored and legionella contamination is minimised. The space demand and the heat losses are very low. On the other side, a large heat exchanger and larger pipe diameters are necessary, as the peak hot water tap power of the building has to be completely covered by this heat exchanger. If the water is very chalky, there can be deposits, when the temperature in the plate heat exchanger reaches higher levels. Systems with additional storages provide the possibility to buffer a part of the necessary energy. Therefore, the maximum heat transfer power can be reduced at the substation.

In Germany, for systems in multi-family buildings with a higher volume than 400 l in total or 3 l in the longest pipe between heating and tapping on the drinking water side, the temperature must reach 60 °C at least once a day for disinfection [15]. A system with heat exchanger for every single flat in the building is therefore more beneficial from the energetic view, as the hot water supply temperature can be reduced to below 60 °C, which allows a lower temperature level in the complete system.

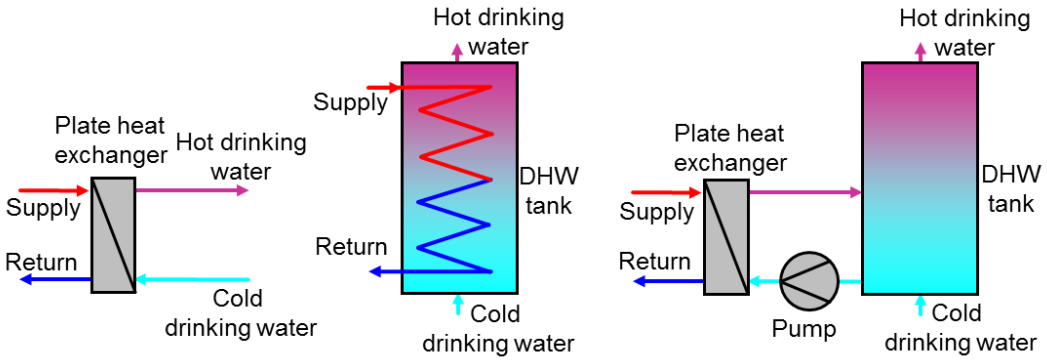

Figure 11: Domestic hot water production with heat exchanger (left), storage (centre) and combined system (right)

2.3 Research Activities and Existing Concepts for Solar District Heating

After discussing the principles of solar thermal plants and district heating, a summary of several relevant research projects, dealing with the integration of solar thermal technology into single buildings as well as districts is given. Several approaches have been developed in the past and can be seen as basis or supplement of the presented research.

In the project *SDHtake-off - Solar District Heating in Europe* from 2009 until 2012 and the follow-up project *SDHplus* (2012 – 2015), the research aimed at promoting the implementation of large solar thermal plants across Europe. Around 200 large solar thermal plants in Europe are currently listed on the website [16]. Here, in addition, guidelines for planning and operation were created from a technological and economic point of view [17].

Most of the plants were built in Denmark, Sweden, Austria and Germany. While in most of these countries, the implementation of large solar thermal systems began in the early 1980s, the German efforts on this technology only started in the 1990s, mainly in the context of (federal) research programmes (e.g. *Solarthermie 2000*, and *Solarthermie 2000plus*). In these projects, several pilot plants were realised and scientifically analysed.

The following sections give an overview of the concepts and the research on efficient solutions for the integration of large solar thermal plants into heat supply systems. Collected data for the operation of realised plants are presented and the performance of these plants is compared.

2.3.1 Decentralised Plants for Domestic Hot Water and Space Heating

Most of the systems in the *Solarthermie 2000* programme were plants for domestic hot water production (DHW) in individual multi-family buildings and had a similar hydraulic layout as shown in Figure 12. Here, the solar heat is used for preheating the domestic hot water. With some modifications, it can be used to additionally cover the circulation losses to achieve a higher solar fraction. Furthermore, connecting the solar collectors to a buffer storage can enable the system to partly cover space heating demand. A variant of such a system was already shown in Figure 6. Generally, these plants use the same principles as smaller plants, which are well known from single-family houses but with larger storage volume and collector area.

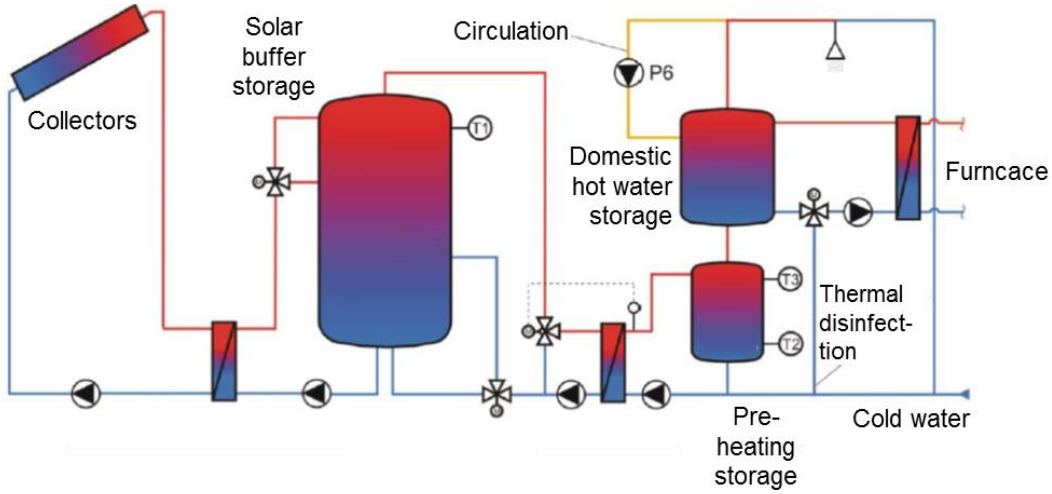

Figure 12: Typical layout of large DHW plants (based on [18])

2.3.2 Central Solar District Heating

To further enlarge the collector area, the connection to a district heating system is beneficial. Central solar district heating plants were part of the investigation in *Solarthermie 2000plus*. Central means that the collector arrays are located at the main heat production unit, either on the roof of the central heating station, a nearby building or ground mounted next to the station. While in Germany and Austria, the roof-mounted variant is more common, ground-mounted systems are well established in Denmark and Sweden.

A buffer storage is common for solar-supported district heating systems. Besides the auxiliary heat source (fossil or biomass), a solar circuit is connected to the buffer (Figure 13). Another possibility is to use the storage only for the solar heat generator and connect the auxiliary heat source e.g. via an additional hydraulic compensator at the supply pipe exiting the buffer. The storage may be a short-term buffer for storing

energy for several hours or days or a larger tank with a suitable capacity to buffer up to several months of heat demand in case of seasonal concepts (see section 2.3.4).

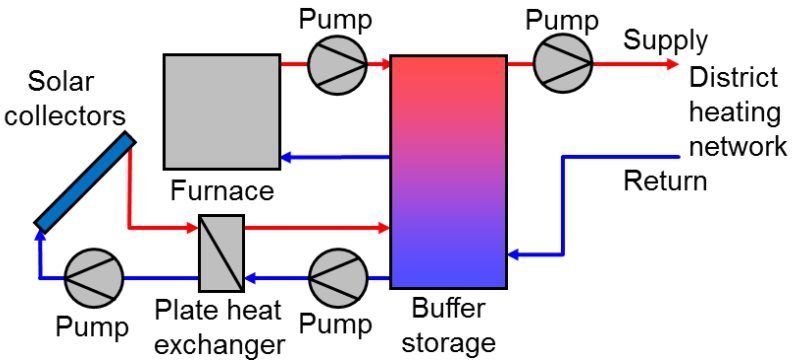

Figure 13: Central heating station with additional solar heat generation

2.3.3 Decentralised Solar District Heating

Although there are different solutions for the decentralised integration of solar thermal plants into district heating systems the term “decentralised” generally means that the collector arrays are not next to or on the roof of the central heating station. Additional pipes can be used to transfer the solar heat from decentralised plants to the central heating station. In this case, the solar circuit may have its own supply and return pipe (2+2 system) or only one supply pipe while drawing fluid from the network return (2+1 system). The two layouts are shown in Figure 14.

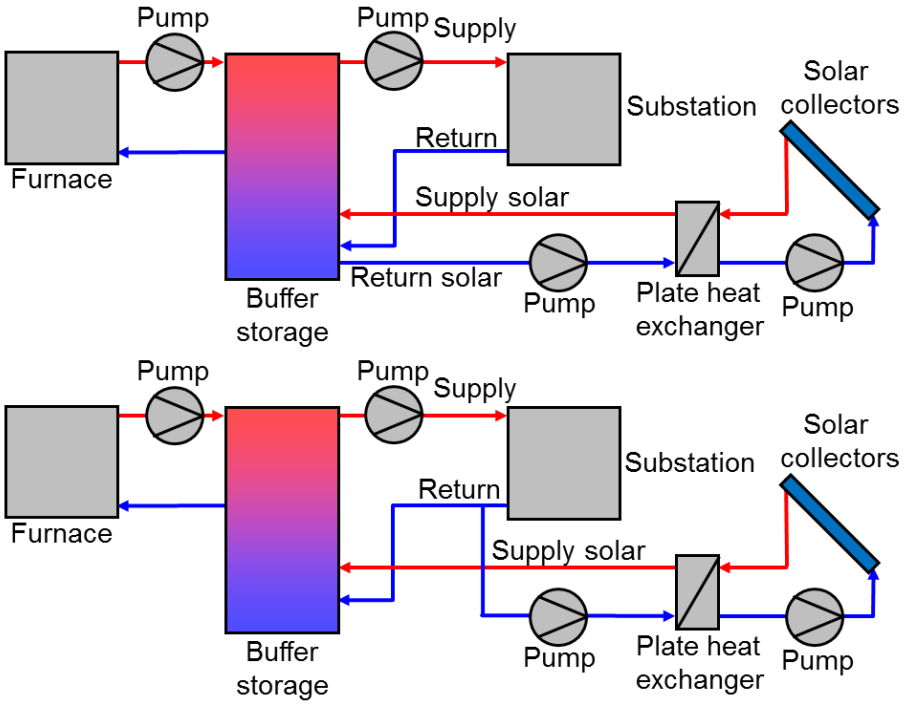

Figure 14: 2+2 (top) and 2+1 (bottom) network design with decentralised solar heat generation

Another possibility of realising decentralised feed-in is the abdication of additional solar pipes and the utilisation of the existing network supply and return pipes. The basic principles are Return-Return (RR), Return-Supply (RS), Supply-Supply (SS) and Supply-Return (SR). The hydraulic layouts are shown in Figure 15.

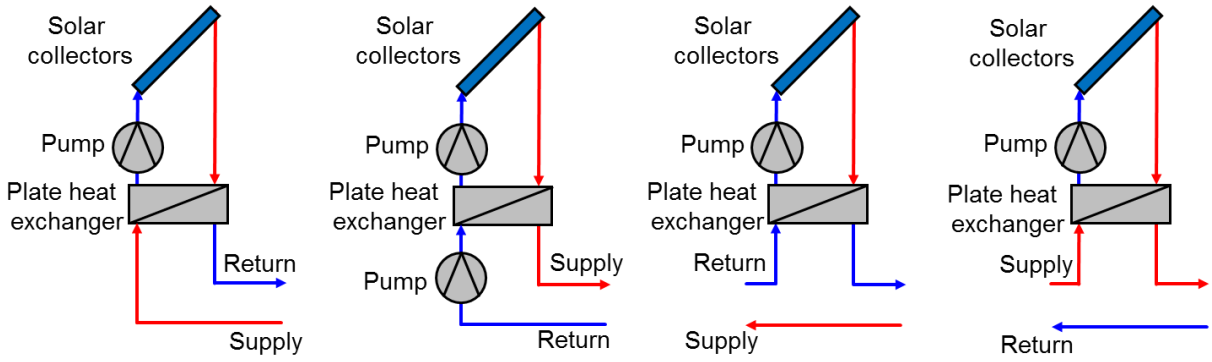

Figure 15: Solar feed-in principles (SR, RS, RR, SS from left to right)

Schäfer et al. [19] created an overview of decentralised solar district heating plants in Europe using these types of feed-in. The authors found, that only 2 out of 31 analysed plants were capable of an RR feed-in, which can lead to the highest efficiency as the temperature level is the lowest. The most common solution is the RS feed-in, where most district heating operators claim it enables constant temperatures in the network. As the flow direction in the network pipes changes when solar energy is produced, this concept will be referred to “bidirectional” feed-in. However, while the control of pressure, temperature and flow rate of these systems is very complex, the energy management is quite simple and just feeds in a surplus of solar heat, when the solar yield is higher than the current local consumption and storage capacity. Some plants feed in the total solar energy. The SS and SR solutions are energetically disadvantageous and preferred neither by the owners of the solar thermal system, nor by the district heating operators.

While other concepts are well scientifically analysed (e.g. in the *Solarthermie 2000* programme), there is hardly any information available on the detailed layout and operation of existing plants with bidirectional feed-in to the district heating network. This is remarkable as most of the decentralised plants without additional solar network use this method. Dalenbäck [20] created an overview of the annual yield of several of these plants (Figure 16).

The annual yields range between 100 and 350 kWh/m², which is quite low compared to other plants shown in section 2.5. While part of the lower yield can be explained by lower solar irradiation in Sweden compared with Austria or Germany, it still indicates that there is potential to improve the efficiency of these bidirectional feed-in concepts.

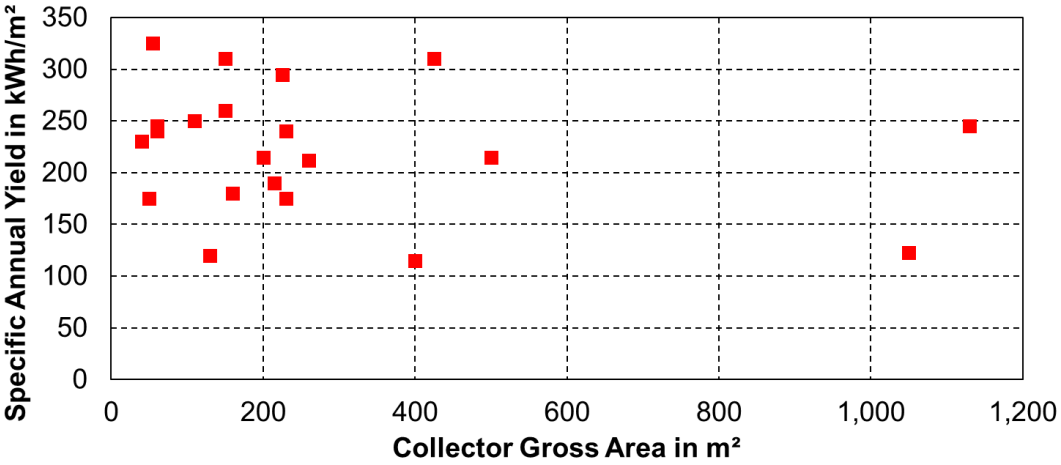

Figure 16: Annual yield of existing decentralised SDH systems in Sweden (based on [20])

Another example for the research on decentralised feed-in is the work of Papillon and Paulus [21], who conducted an investigation of different substation layouts and network designs for a decentralised solar-supported district heating system in France. They built up a model of a network consisting of 12 substations in the TRNSYS simulation environment and compared different design principles:

- No local use of solar energy
- Domestic hot water preheating via heat exchanger
- Domestic hot water preheating via storage tank
- Solar preheating of DH return
- Solar preheating of DH return before preheating of building return
- Solar preheating of DH return after preheating of building return

On top of that, the authors compared a 2-pipe network architecture with a 3-pipe architecture. The 3-pipe system has an extra pipe from a central solar buffer storage to the decentralised collector arrays. This is beneficial as the inlet temperature and flow rate of the collectors are independent from the current conditions in the district heating network in this case. In addition, in the 2-pipe network the returning fluid reaching the solar plants closer to the central heating plant is already preheated by other plants installed upstream and limits their efficiency. This is of importance especially when low energy buildings are supplied and a high solar fraction is reached during summer. In that case, the 3-pipe architecture performs better than the 2-pipe variant. Taking a high-performance (double glazed) and a low-performance flat plate solar thermal collector into account, it was confirmed that the solar yield primarily depends on the return temperature of the network. Nevertheless, the high-performance collector enables higher yields at higher network temperatures.

Dealing with decentralised feed-in into the district heating network comes along with complex pressure and volume flow control tasks. Lennermo and Lauenberg [22] showed in the course of a metrological investigation of substations that both, rapid and large differential pressure changes can occur. This leads to the necessity of a controller for the solar feed-in that can adapt to these changes in order to maintain the currently necessary volume flow. This can be done by either an improved pump control or a constant pump power in combination with regulating valves.

The research project *DEZENTRAL* [23] dealt with the investigation of decentralised feed-in of solar thermal plants regarding the network as well as the single plant layout. Three existing district heating systems were taken to define different types of networks in terms of the temperature level. Further studies were reduced to a Low-Ex[2] System with supply temperatures of 60 °C and return temperatures of 30 °C. Two different RS feed-in stations were defined of which one has no storage and the other one uses a storage between collector array and network. A local consumption was neglected in the work. Analytical calculations and numerical simulations showed that with an optimised control strategy, the supply temperature can be kept during feed-in phases. A limitation is seen in the utilisation of the available roof area, in particular without heat storages, due to a lack of heat transfer capacity of the exiting pipes. On the other hand, the installation of a storage reduces the specific annual solar yield from 370 kWh/m² to 258 kWh/m², respectively 278 kWh/m² for the two different feed-in stations.

In addition to the contemplation of the solar thermal plants, the effects on the district heating network were simulated and an experimental feed-in and consumption test rig set up [24, 25]. The authors found that an installed solar thermal power of 10 % of the design consumption can be handled without storages and only short stagnation periods by utilising the return pipes as additional buffer volume. In case of feed-in by substations close to the end of the supply lines, a reverse flow is established in the pipes and a part of the network is supplied independently of the central heating station. A more detailed discussion of the effect of decentralised or central storage capacities was recommended by the authors. Measurements at the test rig showed that the combined feed-in and consumption works by utilising adapted control algorithms of the feed-in pump.

[2] Low exergy demand due low temperature difference of the heating system over the ambient temperature (cf. section 2.3.5)

2.3.4 Seasonal Storage Concepts

As in Europe, solar energy is mostly available during summer, the only opportunity to increase the solar fraction above a certain level is to implement large storage tanks, which are capable of storing heat for several months. If such a high capacity is desired, there are options to use aquifer storages, borehole storages or pit storages, which can be easier and less expensive to build compared to hot water storage tanks, depending on the geological conditions [17].

A possible layout of a solar assisted district heating system with a seasonal storage is shown in Figure 17. Centralised and decentralised collector arrays feed a storage tank which is connected to the central heating station. Due to the high capacity of this storage, solar heat is available even during the winter season.

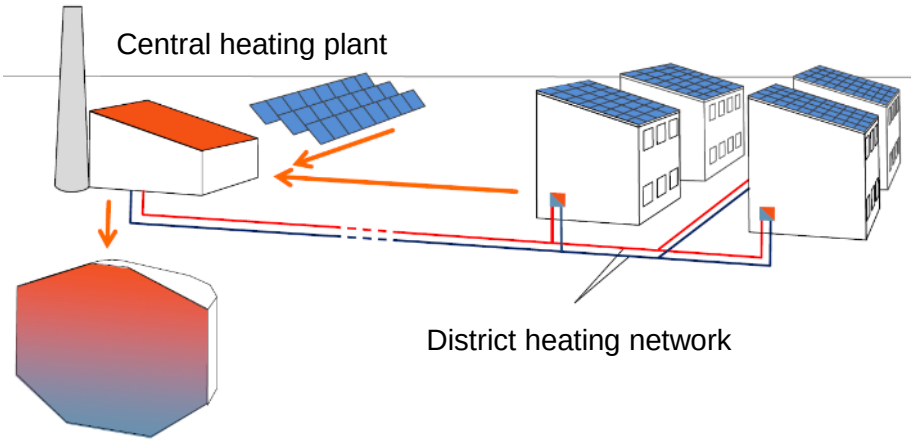

Figure 17: Centralised feed-in of solar heat in a district heating system [17]

Studies of seasonal storages like aquifers, borehole, gravel-water and hot water storages still have a high priority in the current research environment. Several prototypes were built in the past and the development of the storage technology still continues. An example is the work of Lundh and Dalenbäck [26], who performed a metrological investigation of a 60,000 m³ borehole storage for supporting a solar district heating system with 50 residential units in Sweden. This storage provides a high capacity and beneficial conditions for the connected 2,400 m² solar thermal collector array. In this case, a solar fraction of about 70 % was intended.

An example of a large hot water storage tank is the *Ackermannbogen* project in Munich, Germany. Here, an additional heat pump is used to cool down the storage to temperatures below 10 °C for further increasing the solar yield. Decentralised collector arrays are connected to the storage via a 2+2 network. Optimised substations reduce the return temperature by a serial connection of radiators and floor heating and decentralised hot water production in the individual flats. Despite some unexpected

problems with the solar yield, the stratification in the storage and the control system, the solar fraction is around 45 % in this system. [27]

2.3.5 Low-Ex Systems

Apart from the approach of a seasonal storage to increase the solar yield, there are further research activities dealing with the improvement of the efficiency of district heating systems and their components.

A low temperature level in the heating system is an important factor to increase the solar yield. Besides the irradiation, the power output of solar thermal collectors depends on the difference between collector temperature and ambient temperature. The mean collector temperature depends on the flow rate of the fluid and mainly on the inlet temperature. The reduction of the temperature of the incoming fluid can increase the energy output of a collector significantly. Figure 18 shows the exemplary annual yield of different collector types (evacuated tube collector, medium- and high-performance flat plate collector) depending on the temperature in the heat exchanger.

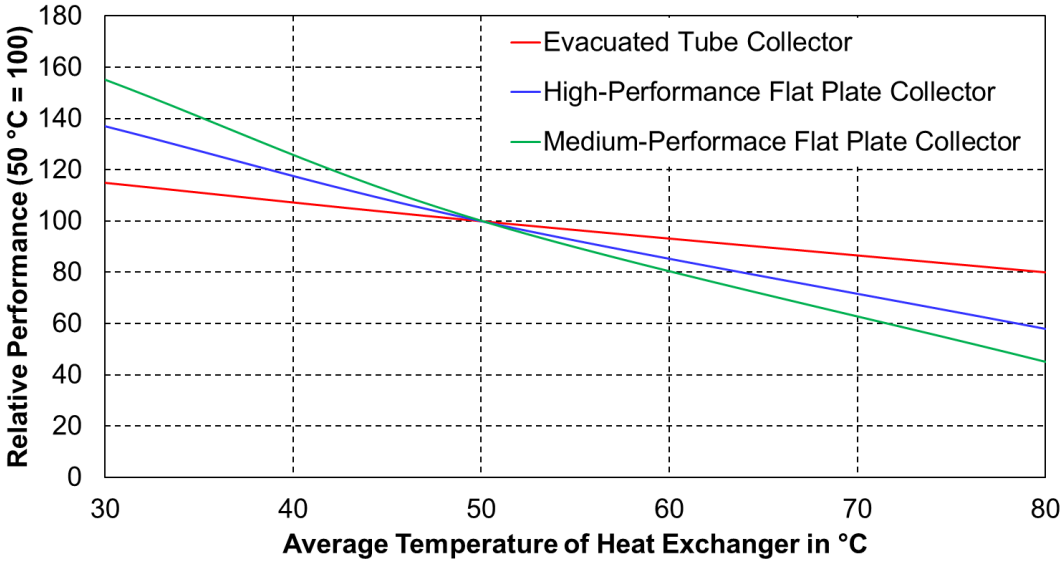

Figure 18: Annual solar yield depending on the average temperature of the district heating heat exchanger (based on [17])

As the temperature differential constitutes a crucial point in optimising a solar district heating system, there are efforts to reduce the network temperature level of district heating systems in various ways.

Gustafsson et al. [28] discussed the effects of an improved space heating control of buildings connected to a district heating network. Due to a mass flow control strategy of the radiators, lower pump energy consumption and a reduced return temperature

were achieved in the heating network. This led to a higher efficiency of the heat generator and lower heat losses of the piping system.

Felsmann et al. [29] examined the possibilities and effects of reduced supply and return temperatures in Low-Ex district heating systems. Small and medium standard district heating systems work at supply temperature levels of 70 °C up to 100 °C. By utilisation of low temperature space heating systems, decentralised domestic hot water production via plate heat exchangers or integration of decentralised auxiliary heat pumps and electric heaters, the necessary temperatures can be lowered to approximately 50 °C. This enables the operation of CHP plants and solar thermal systems at higher efficiencies. Within the research project, software tools for the optimisation of the network architecture (*STEFaN*) and the control strategy (*FreeOpt*) were developed.

Also aiming at low system temperatures to provide favourable conditions for solar thermal plants, Szablinski [13] investigated the effects on the solar yield and possible energy savings of different hydraulic connections. The focus was on the central heating station as well as on the substations and included e.g. serial and parallel boiler integration, instantaneous heating systems and storage charging systems or return flow mixing into the supply pipe. The study is based on the simulation of a district heating system with central feed-in of the solar energy and different numbers of buildings as well as different solar thermal plant dimensions. In the considered systems, the solar yield could be increased by individual measures by up to 15 %.

2.4 Performance of Existing Large Solar Thermal Systems

To better classify the technical and economic possibilities and limits of the approaches, described above, an overview of several existing larger solar thermal plants in Europe was conducted. It is based on the reports of accompanying research projects and online monitoring platforms and includes solar-supported district heating as well as large plants for domestic hot water production and space heating in multi-family buildings. The following graphs show a comparison of performance data collected from 28 German plants as well as from 53 plants from Denmark, Sweden, France, Austria and the Netherlands. The data were taken from [8, 16, 27, 30–70].

Figure 19 shows the solar fraction plotted against the specific storage volume. The specific storage volume V_{spec} is calculated according to equation (2). It relates the installed storage volume to the energy consumption for domestic hot water production and space heating. This enables an easier comparison of plants of different absolute size as the storage volumes of the investigated objects reach from 0 to 110,000 m³.

For DHW plants, only the hot water consumption is taken into account for the energy consumption. For plants providing domestic hot water and space heating as well as for district heating systems, the total heat consumption is taken.

$SF = \frac{E_{solar}}{E_{prod}}$	*(1)*
$V_{spec} = \frac{V_{storage}}{E_{total}}$	*(2)*

with:

E_{prod}	*total heat production*	*MWh/year*
E_{solar}	*heat provided by solar thermal plant*	*MWh/year*
E_{total}	*energy consumption for domestic hot water (and space heating)*	*MWh/year*
SF	*solar fraction*	*%*
V_{spec}	*specific storage volume*	*m³·year/MWh*
$V_{storage}$	*installed storage volume*	*m³*

It can be seen that even with relatively low storage volume, a solar fraction of up to 20 % is possible. The highest solar fraction of the total energy consumption is 56 % for a solar district heating system with seasonal storage in Denmark. The solar fraction of the domestic hot water production goes up to 70 % for a single plant in France.

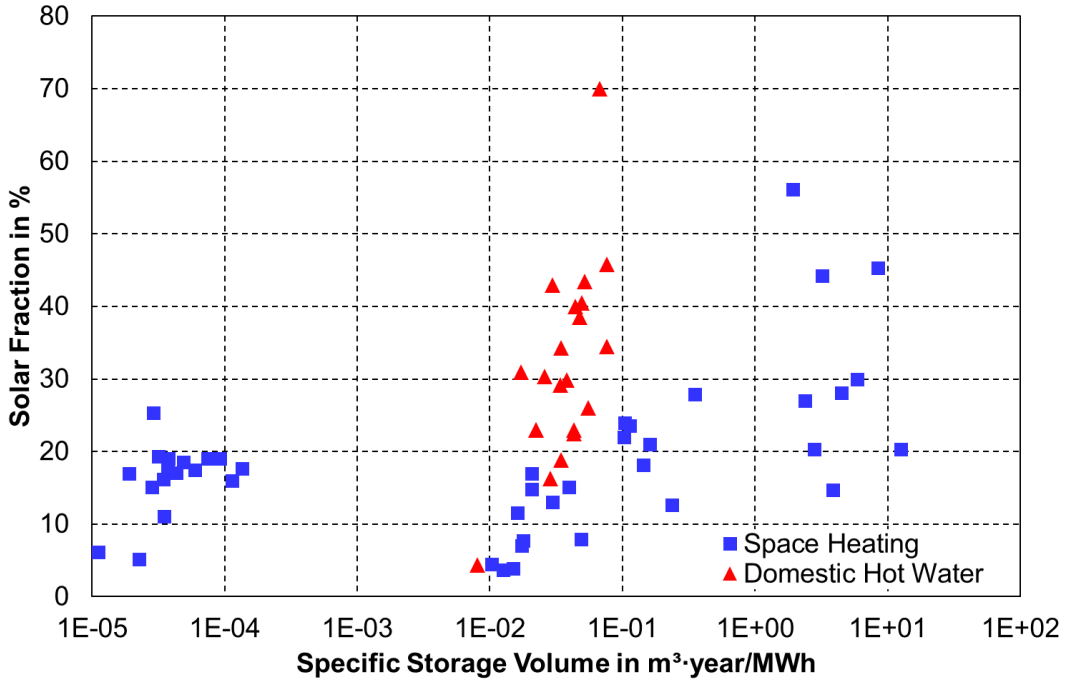

Figure 19: Solar fraction of existing large solar thermal plants depending on the specific storage volume

Having a look at the system efficiency η_{sys} (Figure 20), it is obvious that plants with a low storage volume tend to have a higher efficiency. Up to a specific volume of 0.1 m³·year/MWh, the efficiency is almost constant. This storage size equals about 80 l per person for domestic hot water production.

Plants with a higher storage volume (seasonal concept) show a slight decrease of the collector efficiency η_{col} and a more noticeable decrease in the system efficiency. This indicates that a large fraction of up to half of the solar yield is lost, for instance through heat losses of the large storages. On the other hand, large storages benefit from the lower specific investment costs per volume as compared to smaller plants.

$$\eta_{sys} = \frac{E_{solar}}{E_{irr}} \quad (3)$$

$$\eta_{col} = \frac{E_{col}}{E_{irr}} \quad (4)$$

with:

η_{col}	*efficiency of the solar thermal collector array*	*%*
η_{sys}	*efficiency of the solar thermal system (incl. thermal losses of pipes and storages)*	*%*
E_{col}	*heat provided by solar thermal collectors*	*MWh/year*
E_{irr}	*irradiated energy on the solar collector surface*	*MWh/year*
E_{solar}	*heat provided by solar thermal plant*	*MWh/year*

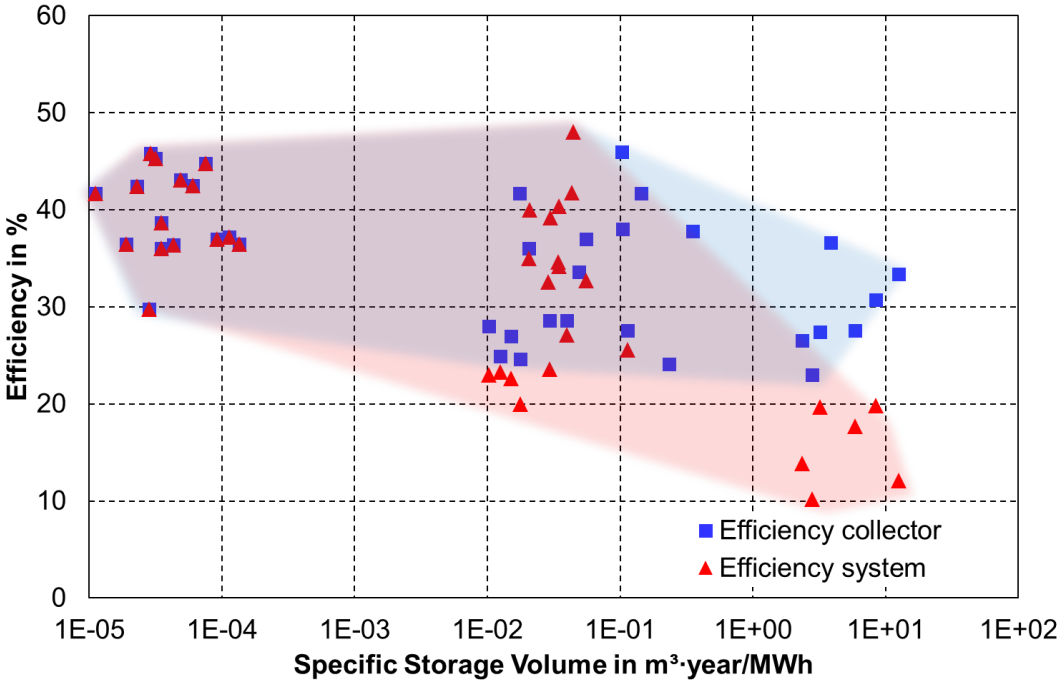

Figure 20: Efficiency of existing large solar thermal plants depending on the specific storage volume

Coming back to the results for bidirectional feed-in plants (Figure 16), the comparison to the plants of this review shows that specific annual yields of up to 500 kWh/m² can be achieved regardless of the absolute size of the collector array (Figure 21). The bidirectional plants are in the lower range of this overview and pure DHW systems are limited to collector areas below 1,200 m².

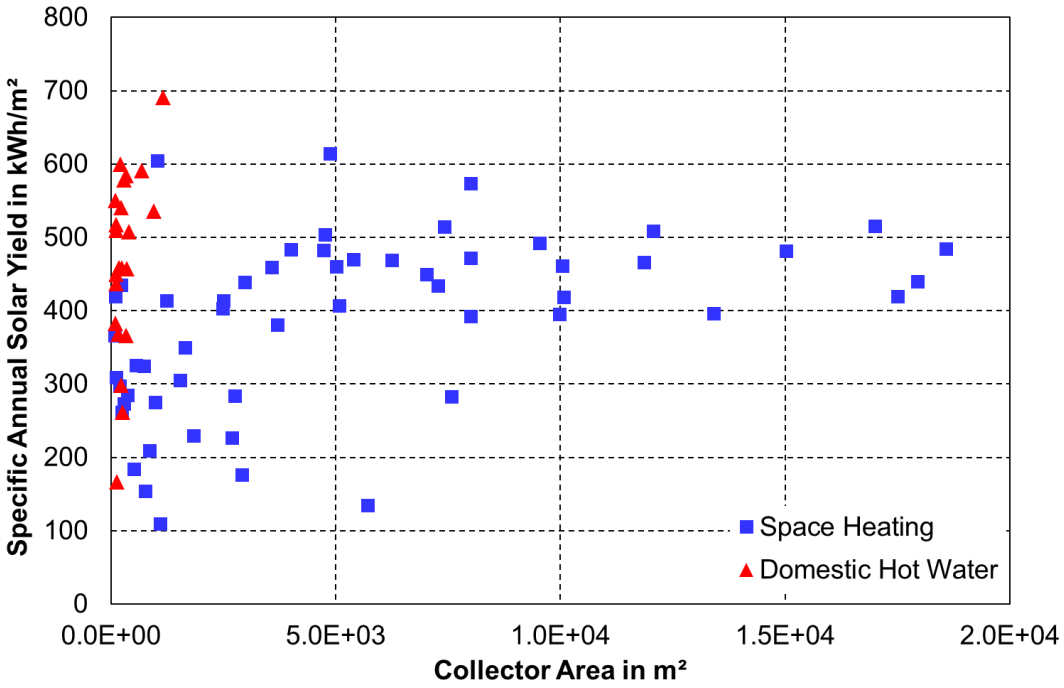

Figure 21: Specific solar yield depending on the absolute collector area

To reach the necessary fraction of the total heat production without needing government funding, solar thermal systems have to be economically competitive to other heat production devices. Zech et al. [71] conducted a literature review on the heat generation costs of different technologies (Figure 22).

It is evident that small solar thermal systems in single-family houses, followed by solar-supported district heating (yellow), have the highest average costs. Biomass (green) and fuel oil (blue) fired district heating systems perform more cost effective. The high spread of the costs of solar heating systems compared to fossil or biomass systems indicates an uncertainty in the planning and operation of these plants as well as a higher dependency on the boundary conditions like supply temperature, consumption and climate. Many of the existing district heating systems are prototypes and therefore less cost effective than conventional systems that use more mature technologies. This holds true in particular for the systems including a seasonal storage.

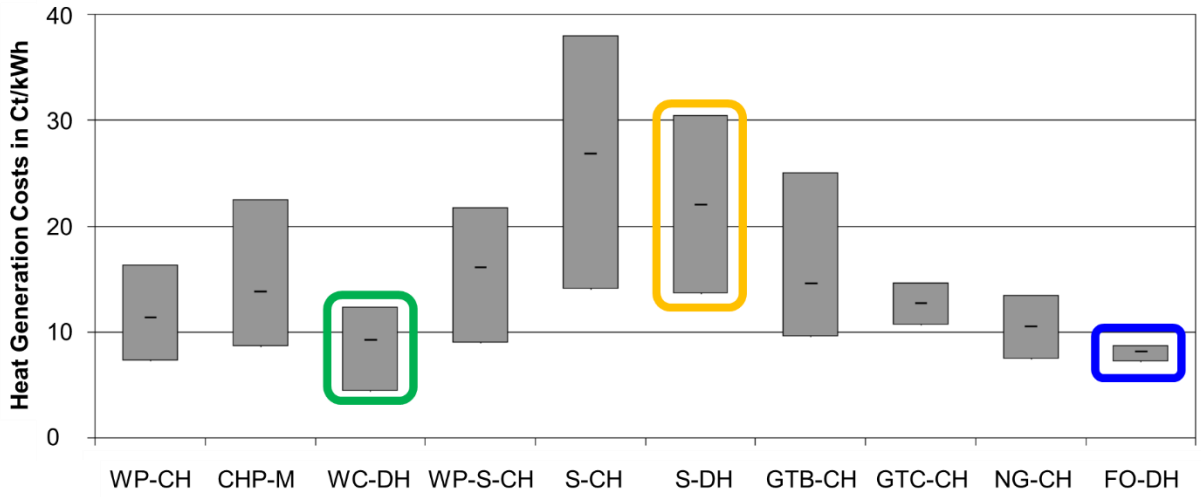

WP-CH	Wood pellet, central heating
CHP-M	Combined heat and power plant, micro district heating, plant oil
WC-DH	Wood chip heating plant, district heating
WP-S-CH	Wood pellet, solar heat, central heating
S-CH	Solar heat, central heating
S-DH	Solar heat, district heating
GTB-CH	Geothermal heat, borehole, central heating
GTC-CH	Geothermal heat, collector, central heating
NC-CH	Natural gas condensing boiler, central heating
FO-DH	Fuel oil heating plant, district heating

Figure 22: Heat generation costs of different technologies (based on [71])

The heat generation costs of the investigated plants are calculated according to equation (4) and (5). The calculation of the annuity[3] depends on the lifetime of the plant and the level of interest rate. According to the *Solarthermie 2000* programme, a lifetime of 20 years and an interest rate of 6 % was assumed. The real values may vary depending on the location and the time when the plant is built. To enable a comparison, the different tax levels and funding were neglected.

$$HGC = \frac{Annuity}{E_{solar}} \qquad (5)$$

with:

$Annuity$	*annuity of the investment costs*	*€/year*
HGC	*heat generation costs*	*Ct/kWh*

Figure 23, shows an advantage of the Danish plants without, respectively with short-term storages. Additionally to the low installation costs of the collector arrays due to ground mounting and the use of large scale collectors of up to 15 m² aperture area, the simple plant layout and the abdication of large storages lead to low investment costs. The high system efficiency of these plants, as already shown in Figure 20, is the second reason for the low heat generation costs.

[3] An equal annual payment to pay off the capital and running costs of an investment.

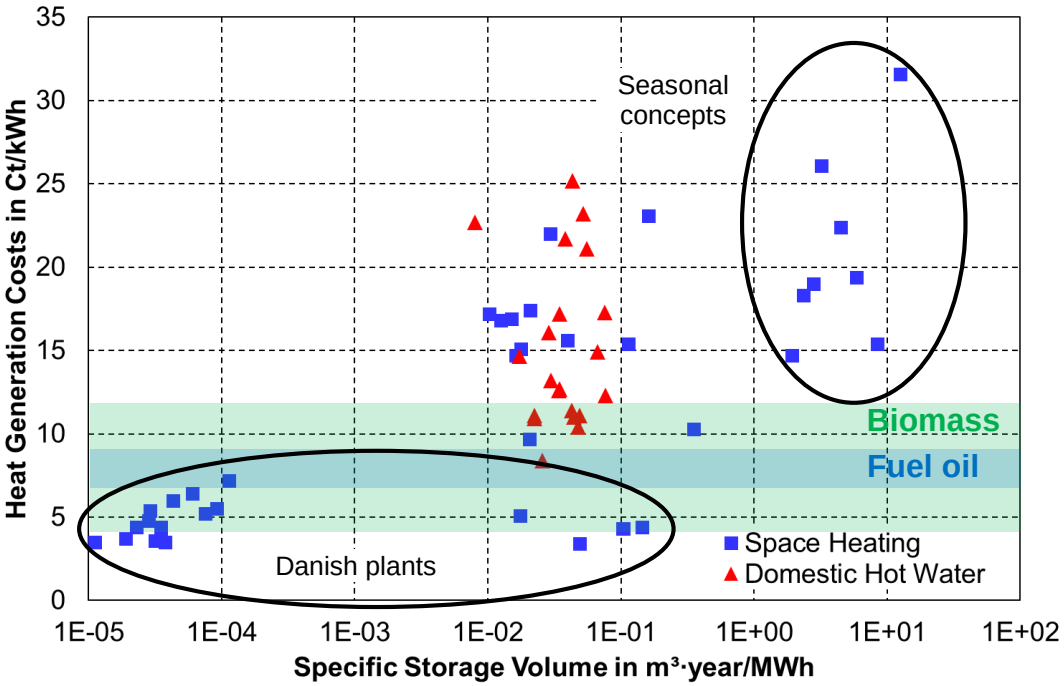

Figure 23: Heat generation costs of existing large solar thermal plants depending on the specific storage volume

3 Research Question and Approach

3.1 Research Question

In section 2.3, several existing approaches for the integration of solar thermal systems into urban structures were introduced. From the comparison of the plants' performance in section 2.4 it can be seen that there are concepts, where solar energy can be integrated into the heat supply of a town on a competitive cost level. This applies to many plants in Denmark with lower solar fraction. Most of these plants have a high system efficiency and low investment costs due to mounting on the ground and simple system layout. The disadvantage is that the concept only works in areas which are not densely built-up and where the land is not expensive and not needed for other purposes, like agriculture. Therefore, it is difficult to apply to districts in larger cities.

For the decentralised plants, which are integrated to urban districts to supply domestic hot water or space heating for single houses, the heat generation costs are higher and the solar fraction may even be lower as compared to the Danish plants. This is due to the higher investment costs for roof mounting and the smaller absolute plant size, meaning less economies of scale, as some costs show no linear correlation with the collector array size, e.g. installing pipes from roof to basement or scaffolding.

Larger plants would increase the solar fraction of the single house but rapidly decrease the efficiency, respectively the specific yield as shown in Figure 24, where the two parameters are plotted depending on the utilisation of the collectors i.e. the annual heat load per square meter collector area. It can be seen, that for higher utilisation (low collector area per consumed energy) the solar fraction goes down to low levels, while the specific yield reaches higher values. In case of a low utilisation (large collector area), the solar fraction increases, while the specific yield is reduced rapidly. On top of that, these large collector areas come with higher investment costs.

Integrating collectors into a district heating system provides the possibility of enlarging single collector arrays without automatically generating a high local solar fraction, as the produced energy can be distributed to more consumers. The utilisation of the collectors is therefore increased. The heat is produced and fed in at the central heating station or transferred from decentralised arrays to the central heating station for distribution to the consumers. However, the conventional solar-assisted district heating concept comes along with increased collector temperatures and higher piping heat losses as the minimum working temperature is the district heating return temperature and the energy is produced far away from the consumers. Some of these

drawbacks can be reduced by using bidirectional feed-in, which allows the transport of the energy directly to nearby buildings without the detour to the central heating station. Nevertheless, the few existing plants with bidirectional feed-in are not well documented or scientifically analysed. Based on available literature, it can be concluded that the performance of existing bidirectional feed-in plants is not sufficient to reach low solar heat generation costs.

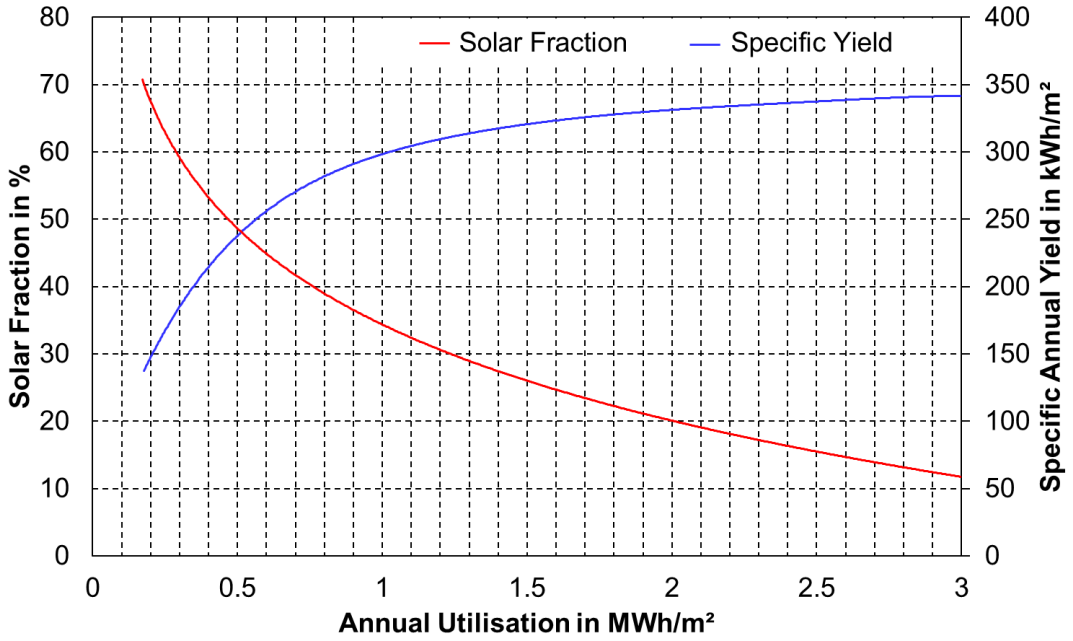

Figure 24: Specific solar yield and solar fraction depending on the specific collector utilisation in multi-storey residentail buildings (based on [72])

To develop an efficient solar-assisted district heating system for urban applications, this thesis proposes a novel concept with intelligent interaction between decentralised solar thermal collector arrays and decentralised short-term storages connected via a bidirectional heat distribution network. The heat generated by the decentralised collectors is directly used at the production site. Excess heat during times of high solar irradiation or low local consumption is fed into the district heating network and distributed to other consumers. To reduce piping heat losses, this system can be used to temporary shut down certain branches in the network or even the complete network, while supplying the consumers with decentrally stored energy. Hence, similar to smart grids in the electricity sector, interacting producers, storages and consumers in a district heating network can help to improve the system efficiency and to find a new way of integrating solar thermal energy into densely built-up urban areas.

The resulting scientific contribution of this work lies in answering the following questions:

- How should a smart solar district heating system be designed and operated?

- How should the components of a smart solar district heating system be dimensioned and arranged?
- What are the optimal plant configurations and control parameters depending on various boundary conditions (heat consumption, climate, etc.)?
- How does a smart solar district heating system perform against existing concepts of solar energy in urban areas regarding solar yield, fossil energy savings and cost effectiveness?
- Can smart solar district heating contribute to the necessary expansion of solar heat generation in the residential sector?

3.2 Approach

The primary objective of this thesis is the investigation of smart solar district heating systems. This section describes the approach, regarding the design and operation of such a system on a more detailed level, in order to define the concept and the requirements it needs to fulfil.

For the smart solar district heating approach, decentralised solar thermal plants are integrated into a district heating network. The main purpose of these plants is to supply domestic hot water and, if desired, space heating to the buildings they are mounted on, following the concept of simple detached solar thermal systems. Taking into account that not all buildings in a network may have beneficial conditions for the installation of solar thermal collectors and other necessary system components, the viable plants can be oversized to produce excess heat during summer. This excess heat is fed into the network via bidirectional substations to supply the other buildings. Depending on the structure and storage capacities, the temporary shutdown of branches in the network is discussed to reduce pipe heat losses. The aim is to reach a high solar fraction during summer without having a considerable decrease of the system efficiency due to stagnation[4]. An interconnected controller is considered to operate the system and the substations for an optimised managing of the heat flow in the network. Figure 25 shows a scheme of the approach to illustrate the function.

Figure 26 classifies the intended performance of the proposed smart solar district heating approach amongst other concepts. By eliminating the disadvantages of short-term solar district heating and decentralised DHW plants while keeping their advantages, the proposed system can lead to competitive solar fractions and heat generation costs.

[4] Overheating and shutdown of the solar thermal system. This is usually the case, when the solar heat production is higher than consumption and available storage capacity.

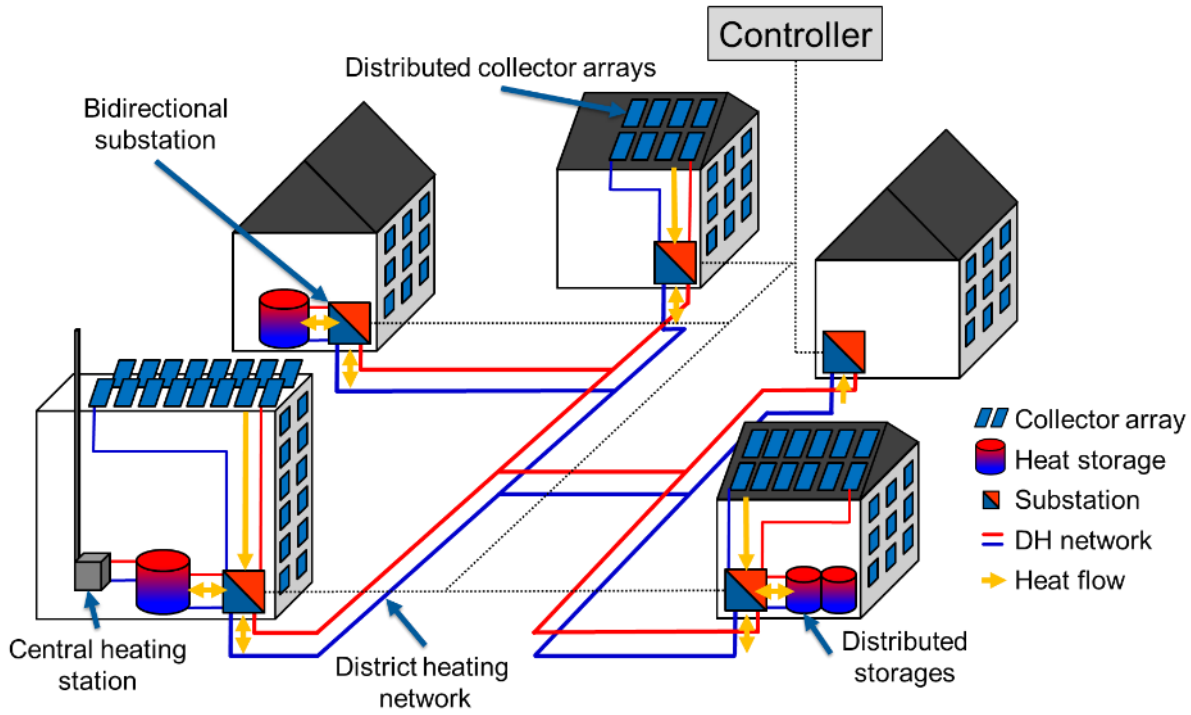

Figure 25: Illustration of the investigated approach

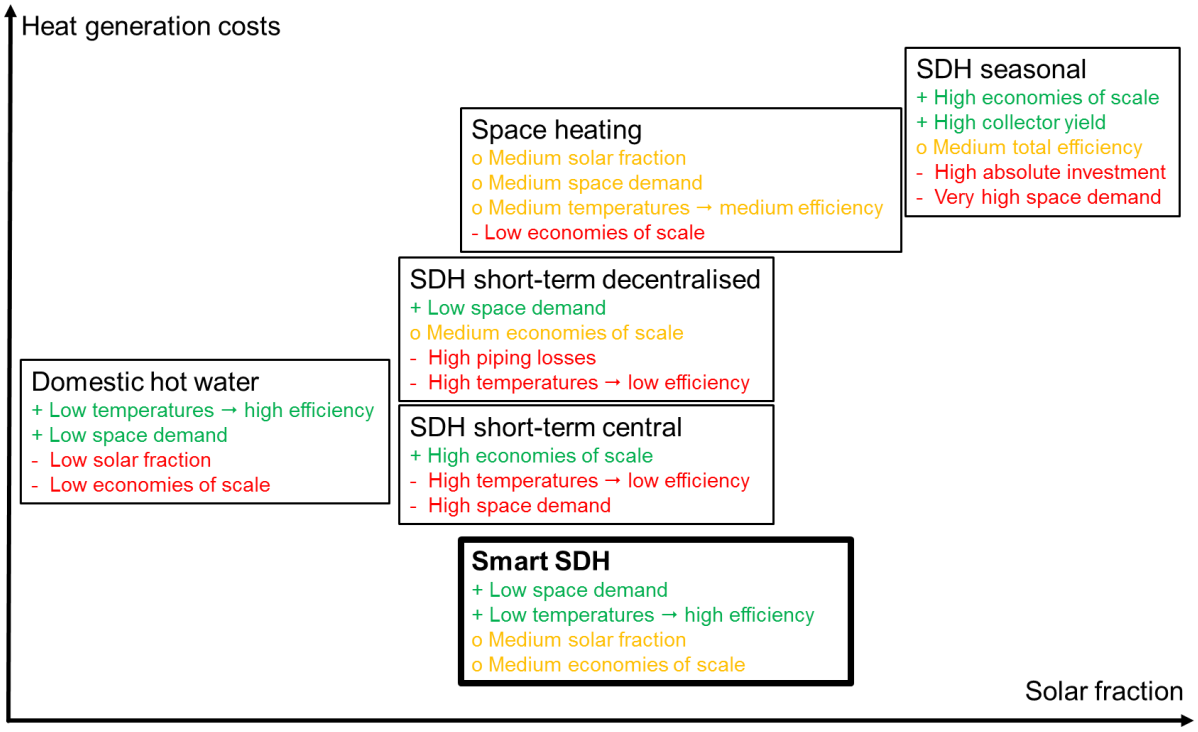

Figure 26: Approach of smart solar district heating combining solar fraction and plant size of decentralised short-term district heating with the higher efficiency of DHW systems

It is expected to achieve an advantageous performance due to:

- Better economies of scale of several medium-sized plants compared to many small decentralised domestic hot water and space heating plants

- Better system efficiency than central solar district heating due to reduced average system temperatures by partial domestic hot water production and avoidance of stagnation
- Lower space demand than centralised solar district heating due to the avoidance of large (seasonal) storages and utilisation of available roof areas
- Solar fraction of up to 100 % during summer with distributed collector arrays and short-term storages
- Reduced losses of the district heating network due to temporary shutdown of branches
- Utilisation of the network itself for heat buffering

3.2.1 Network Level

The idea of smart solar district heating in a 2-pipe network is based on an RS feed-in of the decentralised solar thermal plants for a dedicated loading or unloading of buffers in the network via the supply pipes. A feed-in to the return pipes has advantages for low solar fractions due to the lower temperature level. Nevertheless, it would never enable an independent operation of sub-networks. I.e. a building with solar heat generator supplies one or more nearby buildings without any heat flow from or to the central heating station. A pure supply by decentralised plants is possible for return feed-in as well but always utilises a volume flow via the return pipe to the central heating station.

Scheme 1 in Figure 27 shows the behaviour of an exemplary small network during standard operation (supply only by central heating station).

The scheme below (2) shows the same network during decentralised SR feed-in. In this case, a decentralised pump or valve reduces the pressure drop across the substation. This leads to a higher volume flow through this substation to enable the feed-in of solar excess heat. If the pressure drop is too low, it can lead to an undersupply of the other substations, as a large amount of the water takes the path through the substation with the lowest pressure drop. This is a situation, that can occur in RR systems as well.

If it is intended to use an RS feed-in, there are two conditions to consider. Scheme 3 shows the operation of the decentralised pump on a pressure level that compensates the pressure imprinted by the central pump. In this case, there is a section in the network (grey lines) where there is no volume flow due to the pressure equilibrium of the two pumps.

If one of the pumps has a significantly lower static head than the other pump, only a lower fraction of the volume flow is provided by this substation. The building located next to the pump is then partly supplied by each of the heat generators (scheme 4). Details on this behaviour can be found in [73].

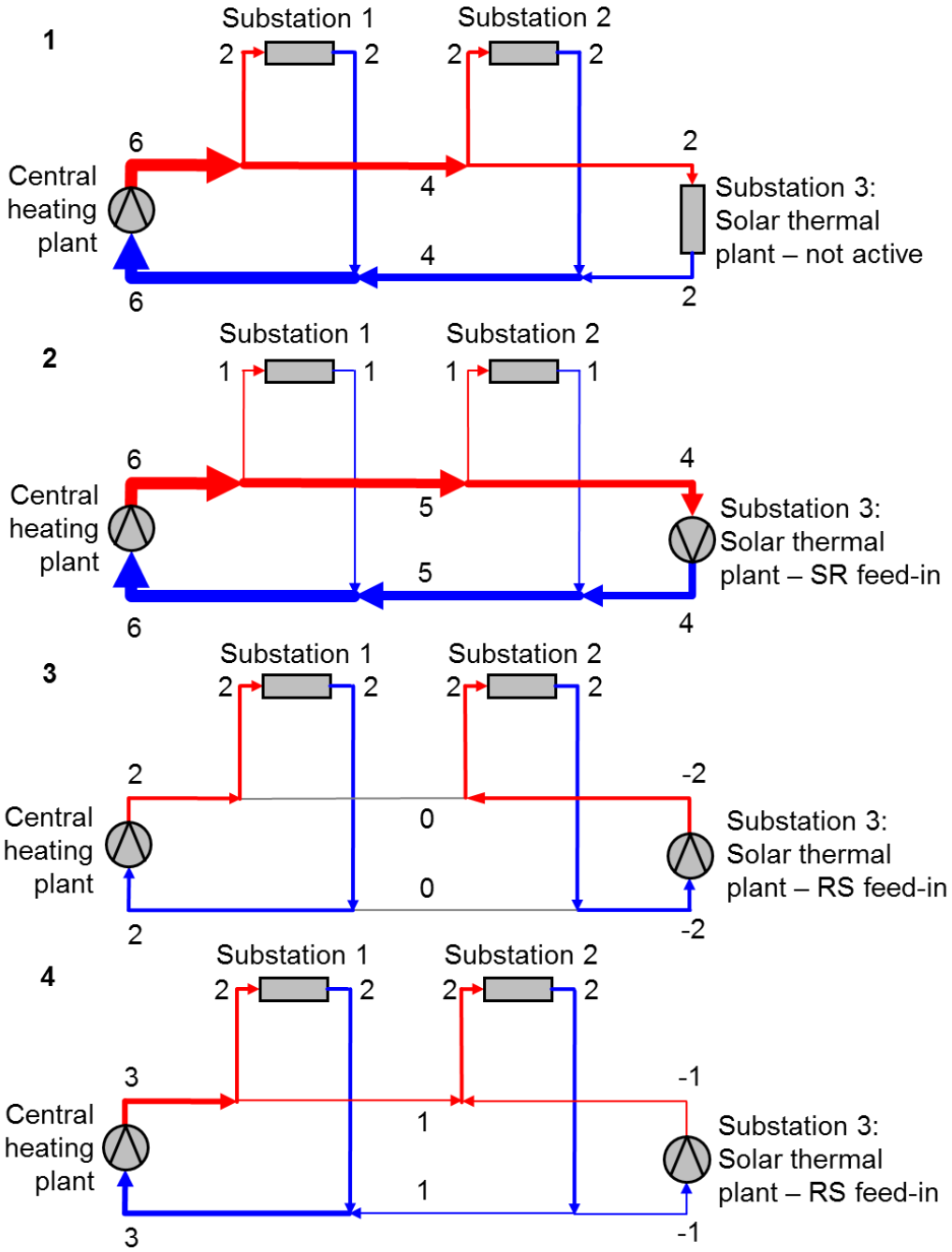

Figure 27: 1: Standard operation of network with volume flow defined solely by central pump (numbers show nominal flow rates)
2: Additional pump for decentralised feed-in to the return, parallel branches can be undersupplied
3: Additional feed-in to the supply pipe at a balanced differential pressure, standstill of connection branch between left and right side occurs
4: Additional feed-in to the supply pipe at low differential pressure, decentralised producer partly supplies neighbour-building

If the solar yield of the decentralised plant is high enough to supply the building itself and the nearby building (substation 2) at a sufficient temperature, a decentralised pump is switched on to reverse the flow in the pipes of substation 3. Therefor it is necessary to overcome the pressure differential of the central pump. An equilibrium of the pressure differential in the connection pipes between central heating station and substation 1 on the one side and substations 2 and 3 on the other side leads to a standstill of the flow in these pipes. The pipes will cool down and the heat losses will decrease until they are in operation again. As the central pump only circulates the water through the branch of substation 1 and not through the complete network, the pump power can be decreased.

The energy saving effect of shutting down pipes is higher, when the shutdown period is longer. It is beneficial, if the independent supply of substation 2 and 3 can be continued after the period of high solar yields, i.e. during evening and night. A short-term storage can provide this opportunity. VDI 6002 [74] assumes a domestic hot water consumption of 40 l at 60 °C for a standard person per day. Taking a cold water temperature of 10 °C, this means an energy of around 2.3 kWh. For multi-family buildings, the circulation losses can easily reach the same level. 100 l of storage volume per inhabitant is therefore a sufficient storage size to ensure an almost 100 % solar supply during sunny periods in summer. The district heating pipes can support the energy storage by a temporary overheating. A sub-grid would have to store enough energy to supply all the inhabitants of two or more connected buildings during night.

3.2.2 Substation Level

As already discussed in Section 2.2.4, the substation designs are manifold. To describe the behaviour of the substations, an example with a connection to the district heating network via a buffer storage is given. Figure 28 shows substations 2 and 3 of the example during decentralised feed-in. The solar collectors produce heat to support the supply of substation 3. The feed-in pump is off and bypassed until the collectors produce more energy than can be consumed and stored in substation 3. From that point on, hot water at the design supply temperature or above is conducted from the buffer storage to the consumers in substation 2. There is no volume flow in the connection pipes to the rest of the network (grey) anymore. This mode of operation can be maintained, until the temperature at the top level of the buffer storage is below the necessary supply temperature of the consumers (plus an offset due to the temperature loss in the pipe connections). From that point onwards, the feed-in pump is switched off again and the central heating station is in charge of the supply of substation 2. The collectors may still produce energy to supply substation 3 during that

period. If there is space available to install a storage in substation 2, it is possible to load this storage with energy from the decentralised plant to provide an independent operation of the building over a longer period.

If the solar collectors are not directly connected to the district heating network but to the domestic hot water storage, it is possible to further increase the efficiency and yield, as the heat can be supplied at a lower temperature (e.g. 10 °C cold water instead of 40 – 70 °C district heating return temperature). For dimensioning variants, where the installed solar thermal power is higher, further buildings in the network would be loaded during the feed-in of substation 3.

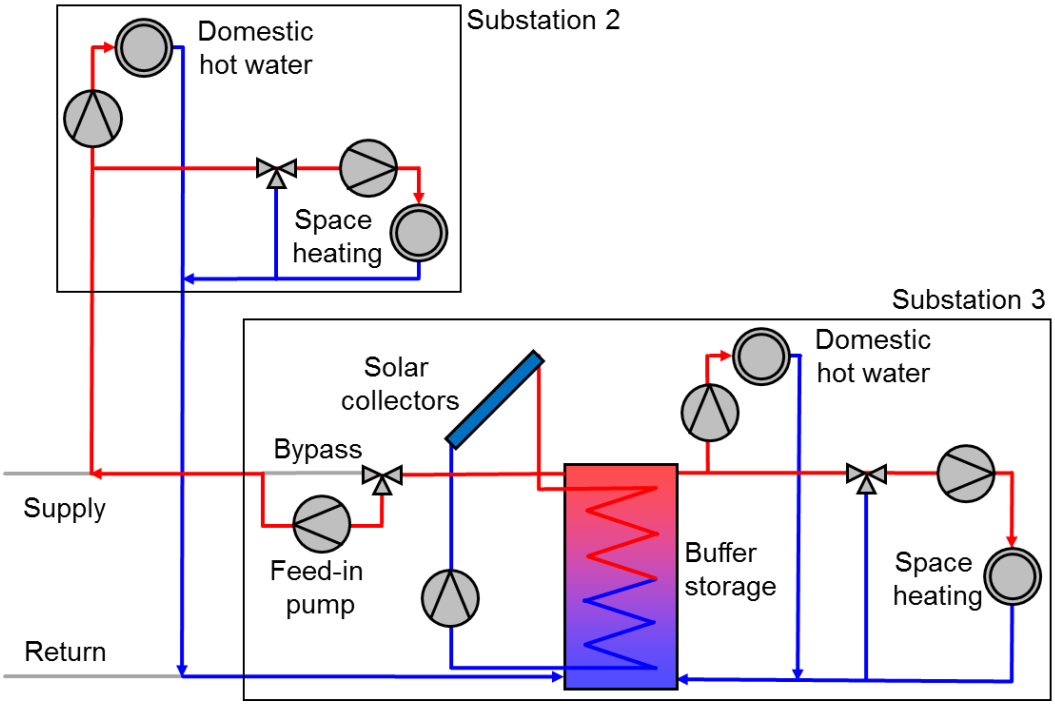

Figure 28: Substations during decentralised feed-in

After the discussion of the approach, the next section will introduce a field test installation, where several concepts of integrating solar thermal plants were tested. Due to the necessity of keeping a reliable operation of the inhabited district, not all options of hydraulic integration and control could be tested. Nevertheless, it serves as a proof of concept for some of the ideas and allows the setup of a validated simulation model.

4 Field Test Installation

In the course of the research project *smartSOLgrid – Solar Smart Grid for the Heating Sector*, a retrofit of a district heating system in the South of Germany was available to serve as a field test object for the approach of this thesis. The setup of the solar thermal plants was done between mid of 2015 and end of 2016. The study area is typical for many urban residential areas and composed of a group of multi-storey buildings, connected by a district heating network from the 1970s. Only a few of the roofs have favourable orientations and inclinations for the installation of large, contiguous solar collector arrays. The available space inside and outside the buildings is limited. Therefore, the utilisation of a large-scale seasonal storage and large ground-mounted collector arrays is impossible. Due to the age of the buildings and the high number of residents, these limitations face a high consumption of space heating and domestic hot water. The goal of the retrofit was a concept, which provides low solar heat generation costs at a system design that prevents overheating during summer.

This district heating system is described in detail in section 4.1 with the design and simulation of the additional solar thermal plants in sections 4.2 and 4.3 and is the basis for the simulation model validation in section 4.6. Section 4.4 gives an overview of the metrological equipment of the system and 4.5 shows the measurement results of the operation, which serve as data source for the validation. An outlook on the effect of a modified operation of the network and an increase of the collector area is given in sections 4.8 and 4.9. The validated model, modified with bidirectional feed-in properties, was used to investigate further concepts of decentralised feed-in as described in Section 6.

4.1 Description of the Field Test District Heating System

The research site is shown in Figure 29 and consists of a total of 13 buildings, which are supplied by 8 substations via a 2-pipe network (red lines) from the central heating station. Some buildings are supplied by a 4-pipe sub-network from the neighbouring building (red/orange lines for space heating supply respectively for domestic hot water and circulation). The central heating station, which consists of three gas boilers with a total thermal power of 1,945 kW, is located in building 1 in the southeast of the quarter. The network length is 500 m.

Figure 30 shows a photograph of the district from the roof of building 1. The steep saddle roofs (40° inclination) with the brick roofing that most of the connected buildings have are clearly visible. These have, with one exception, an east-west orientation. In

between, there are three buildings with flat saddle roofs (10° inclination in east-west as well as north-south orientation). Building 1 is the only building with a flat tin roof (Figure 31). The roof of the building in the furthest northwest of the quarter was already covered by a solar thermal system for domestic hot water preheating and a photovoltaic system. In building 3 and building 4, smaller solar thermal systems for local domestic hot water preheating were already installed.

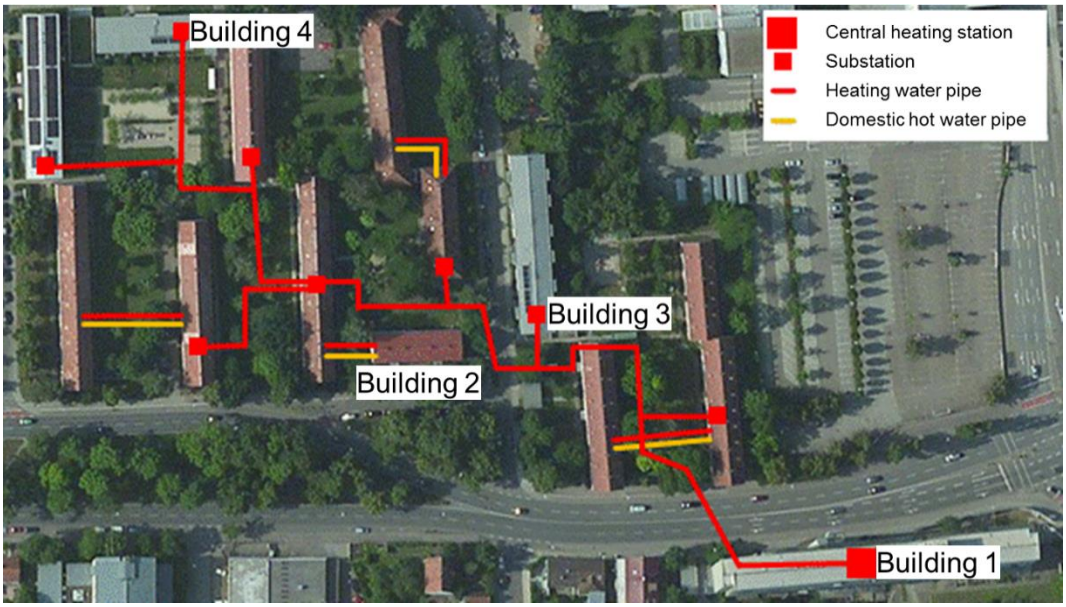

Figure 29: Existing district heating network in Ingolstadt

Figure 30: Photograph of the district with older buildings (brick roofs, foreground) and newer buildings (tin roofs, background)

Figure 31: Flat tin roof of building 1 (west side)

According to the architecture of the 1950s, very limited space is available in the basements of the buildings, impeding the installation of additional heating components. Figure 32 shows the central heating station with the three gas boilers on the left and an exemplary boiler room in a substation on the right.

Figure 32: Central heating station with three gas boilers (building 1, left) and example of a substation with limited space (right)

Table 1 shows the three-year average heat consumption of the single substations. Only buildings with direct connection to the network are listed. The consumption of buildings supplied indirectly by the 4-pipe networks are included in the neighbouring substations. The limited available space and the unfavourable roof orientation in most buildings led to a focus on a few potential solar thermal systems. These are building 1, building 2, building 3 and building 4. Amongst these, a high heat consumption is found in building 1 due to the high number of residential units. Building 3 and building 4 are newer buildings with fewer residential units, built around the turn of the millennium. Due to the lower number of residents and the better energy standard of the building envelope, the hot water consumption and, in particular, the space heating consumption is reduced significantly compared to the older buildings. Building 2 dates back to the 1950s and, like some other buildings, does not have its own substation but is supplied by the neighbouring building via a 4-pipe network.

Table 1: Annual heat consumption of the substations

Building	Residential units	Space heating in MWh	Domestic hot water in MWh	Circulation in MWh
1	85	906	145	135
3	24	69	39	25
4	12	34	22	14
5	30	759	57	34
6	48	444	37	42
7	60	472	46	52
8	24	78	38	23
9	36	240	42	39
10	24	281	19	23
Sum	343	3,282	447	387
Total consumption				4,116
Network heat losses				284
Heat production				4,400

The structure of the substations is basically identical in all buildings and is shown in Figure 33. There is a direct connection to the district heating network without plate heat exchangers. This means, the heating water of the network is conducted directly through the radiator-based space heating. There is no variation of the supply temperature in the district heating network itself. However, the supply temperature of the space heating in the individual buildings is regulated by means of a return admixture in the substation. The loading of the domestic hot water storage is done either via integrated tube heat exchangers or tank-in-tank systems. A regulation of the supply temperature of the hot water storage is only performed in some of the buildings.

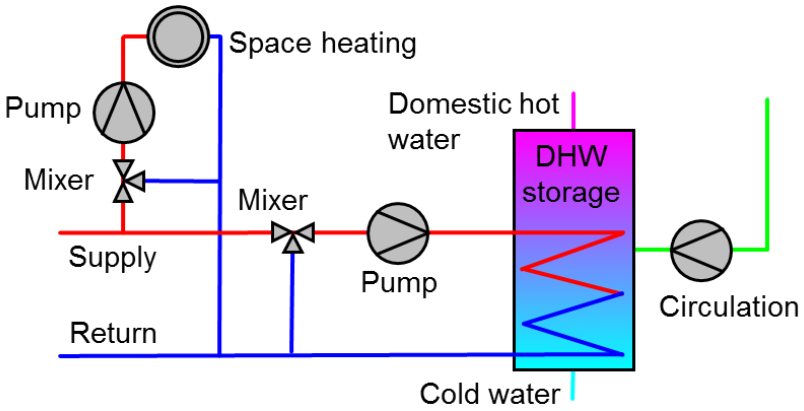

Figure 33: Hydraulic scheme of the existing substations with space heating circuit, domestic hot water circuit and domestic hot water circulation

4.2 Selection of Plant Concepts

The load profile of the domestic hot water consumption was derived from an on-site measurement of the tap volume flow on a weekly basis as shown in Figure 34. It was determined with a clamp-on flow meter and a superposition with seasonal effects according to VDI 6002 [74]. The calculation of the space heating is based on an annual simulation of the buildings, as described in section 5.2.5. The building geometries were adapted to the real objects and the insulation of the building envelopes selected according to the building ages. In order to fit the actually measured annual consumption, minor modifications of the heat losses through the envelopes were performed by adjusting the heat transfer coefficients of the walls, roofs and windows.

Figure 34: Acquisition of hot water consumption profiles by means of an ultrasonic clamp-on flow meter at the cold water inlet of a hot water storage

Based on the boundary conditions and the determined heat consumption, it was decided to focus on the connection of the solar thermal systems to domestic hot water production. In addition, the dimensioning had to be adapted to the roof areas and available space in the basements. The aim of the selection was primarily to realise a cost-effective and easy-to-implement retrofit solution, feasible for many existing urban district heating networks. Another demand of the system operator was, due to previous experiences with solar thermal plants, a low complexity and high reliability. Therefore, the investigation of a medium-sized ground-mounted system north of building 3 for pure feed-in via a plate heat exchanger was part of the initial considerations.

For this ground-mounted plant as well as building 2 (where there is no substation but a supply from the neighbour building), a simple return feed-in to the district heating network was examined, which is shown in Figure 35. Since the involved housing association operates both the buildings with the solar thermal plants and the district heating network, there is no conflict with regard to the allocation of revenues and losses to plant- and network operator. This would be the case for a feed-in to a district

heating network operated by a third party. The district heating network was designed to operate at a supply temperature of 80 °C with a return temperature between 60 °C and 70 °C depending on the load. Due to the connection to the return pipe, the high temperature can be reduced compared to an injection into the network supply pipe and collector temperatures above 65 °C can already lead to a solar feed-in.

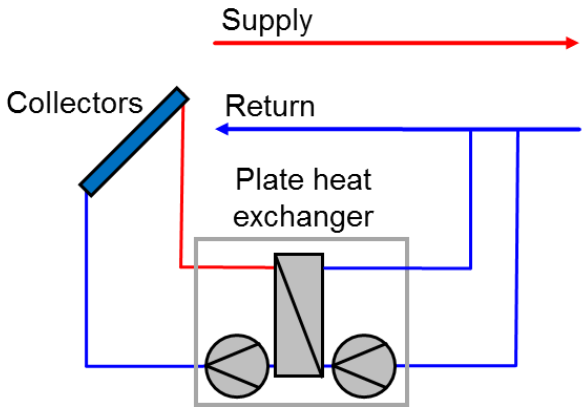

Figure 35: Scheme of the plants for pure feed-in to the return pipe

As the ratio of roof area to heat consumption is low in the 9-storey building 1, limiting the possible solar fraction, the focus was on a pure domestic hot water system. Like for the existing solar thermal systems of the housing association, the approach of domestic hot water preheating was considered as an appropriate solution (Figure 36).

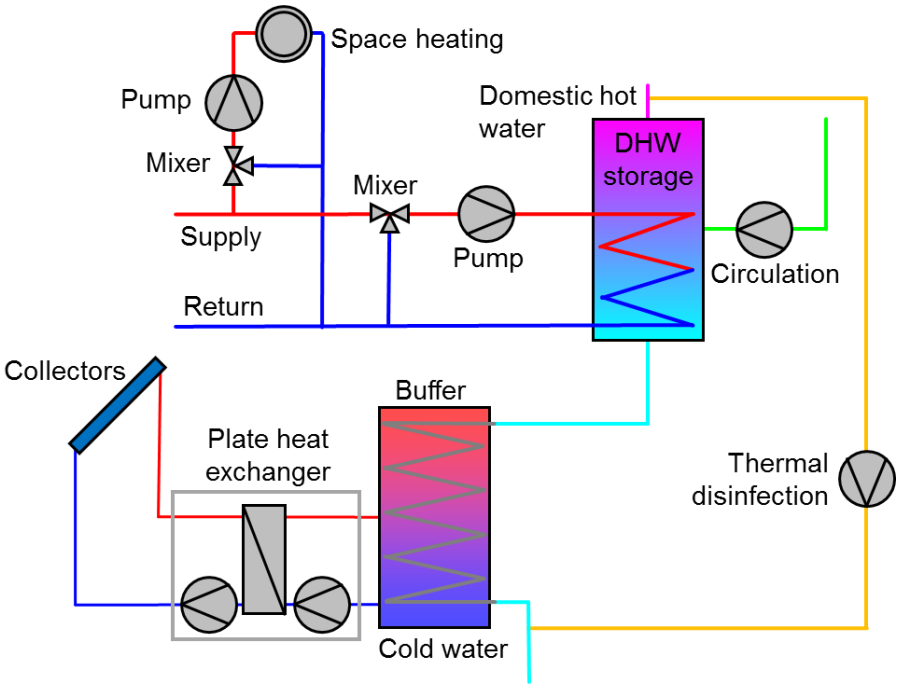

Figure 36: Scheme of the plant for pure local domestic hot water preheating

In contrast to these existing systems, it was decided not to use a drinking water tank for this purpose but a buffer storage with an internal stainless steel corrugated tube heat exchanger. This minimises the reduction of the solar yield due to daily thermal

disinfection. The volume of drinking water within the corrugated pipes is 60 l and thus a very short dwell time in the preheating tank for the development of bacteria is given. Nevertheless, a thermal disinfection pump was planned for safety reasons. Compared to a buffer storage with fresh water station, this approach provides lower complexity and a lower pump power consumption through the forced flow in the pipe heat exchanger during hot water tapping.

Building 3 and Building 4 are very similar, apart from roof orientation and number of residential units. In both buildings there was an existing solar thermal plant consisting of a 750 l preheating storage and 21 m² of evacuated tube collectors in case of building 3 respectively 17 m² of flat plate collectors on building 4. In these buildings, the ratio of roof area to heat consumption is significantly higher than in building 1. Therefore, solar excess heat is generated during summer, if the available roof area is completely utilised for solar thermal collectors. The obvious solution was therefore to optimise and extend the existing systems for local domestic hot water production and to feed the resulting excess heat into the district heating network analogously to the plant in building 2. A space heating support was discarded, since the excess heat occurs mostly in summer and therefore cannot be used for space heating purposes. The hydraulic scheme of this concept is shown in Figure 37.

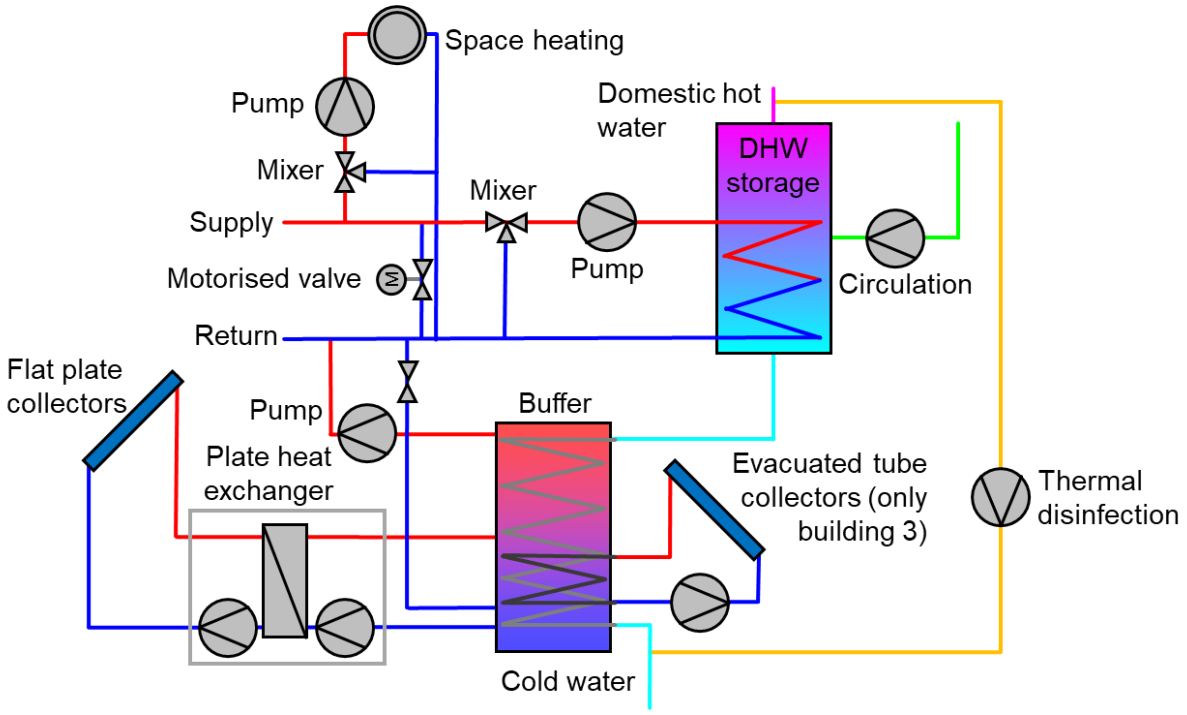

Figure 37: Scheme of the plants for combined local utilisation of solar heat and feed-in of excess heat (building 3 and building 4)

In case of solar excess heat, the buffer storage is discharged via an additional feed-in pump into the return pipe. This avoids stagnation of the collectors and ensures continuous operation during the summer despite the oversized collector area. In

winter, the solar fraction of the domestic hot water supply is increased compared to a standard-size plant.

All plants were planned using flat plate collectors. The collector efficiency data (related to the aperture area) are shown in Table 2.

Table 2: Data of the installed collector

Gross area in m²	2.57
Aperture area in m²	2.38
Optical efficiency	0.825
Linear heat loss coefficient a_1 in W/(m²·K)	3.49
Quadratic heat loss coefficient a_2 in W/(m²·K²)	0.0184

4.3 Simulation-Based Plant Design

The simulation-based design was performed using the simulation models of the individual plants and the district heating network as described in section 5. The initially considered maximum size of the collector arrays, taking into account shading, roof structures and installation effort, was 150 m² on building 1, 100 m² on the south side of building 2, 450 m² on building 3 (east and west side) and 100 m² on building 4. For the ground-mounted system, a maximum size of 160 m² was determined. The maximum storage sizes were set between 2 and 4 m³, depending on the space available in the basements of the buildings. Table 3 shows an overview of selected variants for all objects and the calculated specific solar yields. The finally implemented plants are highlighted in grey.

Due to the long piping distances to the nearest possible connection point of the district heating network and the associated heat losses, no adequate efficiency could be achieved for the ground-mounted system and the annual yields were below 200 kWh/m² for all variants. Taking into account the challenge of reaching and ensuring the necessary supply temperatures, the system was therefore discarded.

The system at building 2 follows the same concept. Here, however, the main return pipe of the district heating network is only 5 m away from the building. Additional transmission losses are thus almost completely avoided. The specific annual yields are at a higher level of up to 256 kWh/m². A change of the collector area has no considerable influence on the specific yield, due to the low dependence of the network return temperature on the relatively low total solar fraction of this plant. In order to keep the system design simple and the investment costs low, the variant with 71 m² collector area was selected, which can be connected to a standard solar station.

Table 3: Selection of variants for the dimensioning with solar yield for ground-mounted plant, building 1, building 2, building 3 und building 4 (realised plants are highlighted in grey)

Variant	Collector area in m²	Inclination in °	Storage volume in m³	Specific annual yield in kWh/m²
Ground v1	142	30	0	174
Ground v2	71	30	0	159
Ground v3	71	40	0	167
Building 1 v1	114	30	4	544
Building 1 v2	114	30	2	469
Building 1 v3	71	30	4	643
Building 1 v4	71	30	2	601
Building 1 v5	71	40	2	609
Building 2 v1	95	40	0	254
Building 2 v2	71	40	0	256
Building 3 v1	114	10	2	313
Building 3 v2	71	10	2	359
Building 3 v3	71	10	1	345
Building 3 v4	92	10	2	346
Building 4 v1	95	40	2	344
Building 4 v2	95	10	2	283
Building 4 v3	71	40	2	364
Building 4 v4	71	40	1	382

The flat roof of building 1 allows greater scope for the design of the system. Here, the simulation results show that a stagnation-free operation in summer is possible with 71 m² collector area and 2 m³ buffer storage. Thus, a high specific annual yield of 609 kWh/m² can be achieved. The inclination of 40° instead of the standard 30° leads to a slightly higher yield without additional costs. As this allows a direct comparison of the concept with the identically oriented and dimensioned building 2, this variant was chosen. In order to reduce shading of the second row of collectors, a horizontal installation was done with a variant of the same collector, dedicated for this type of mounting. Increasing the storage volume would increase yields even further. However, in order to keep the investment costs and installation costs low, the variant with 2 m² was chosen. Thus, it was possible to install both storage tanks and all other system components in one room in the basement.

Due to the west orientation with 10° roof inclination and the already installed evacuated tube collectors, a special situation is given in building 3. Using the eastern half of the roof is less efficient due to the frequent fogs in the morning caused by the nearby Danube. The existing evacuated tube collector array was integrated into the new

system. Due to the smaller area of approximately 21 m², the connection to the buffer tank could be realised via an internal tube heat exchanger with a lower power compared to the plate heat exchangers in the solar station. Since an area of the newly installed flat plate collectors of 71 m² allows a good compromise between system size and the use of standard components, this size was selected here as well. An increase would lead to an increased proportion of feed-in to the network, meaning a lower efficiency compared to the domestic hot water pre-heating. The target of a maximised solar yield, could be promoted but this would be contrary to the request of the operator of having low costs and simple systems. An increase of the buffer volume results only in a small increase of the solar yield, since the capacity of the buffer storage and the existing domestic hot water storage correspond approximately to the daily demand of domestic hot water. Nevertheless, in order to integrate the tube heat exchangers for the evacuated tube systems, two 1 m³ tanks were planned. These tanks contain a corrugated stainless steel heat exchanger for the domestic hot water and a heat exchanger for the evacuated tube collectors. In the other plants, two heat exchangers for domestic hot water were integrated in parallel in one buffer tank.

The same concept as in building 3 is used in building 4. However, there is no integration of the existing collectors. Although initially planned, it was finally discarded due to the bad condition of these old collectors. Hence, the existing collector array was uninstalled. This resulted in a simpler installation of the new collector arrays. The hot water demand of the building is approx. 60 % of the value of building 3. A buffer of 1 m³ is therefore sufficient here as well. An increase would even lead to a slight reduction of the yield due to the higher heat losses.

4.4 Metrological Concept

4.4.1 Overview

Goal of the metrological concept was to get results for the scientific investigation of the system on a detailed level as well as providing easy-to-use long-term monitoring for the operator. While the operator is primarily interested in the solar yield and in ensuring a long lifetime of the plant, additional data was necessary for the validation of the simulation model. This includes temperatures and volume flow rates in all relevant branches of the systems.

Due to a lack of information on the design and current condition of the district heating piping, the simulated energy balance of the complete network suffers from some uncertainties. To get a more precise model for further optimisations, a continuous logging of the transferred thermal power at all substations is conducted. This is done

by installing clamp-on ultrasonic flow sensors and temperature sensors at the building´s substations. By choosing clamp-on sensors, an interference with the running system is prevented. Besides that, the pipes of the network are too large in diameter for most of the common stationary flow rate sensors. The heat flow information is transferred by an impulse output of the sensor and the joining with the temperature sensor signals for supply and return pipe to a data logger. The data loggers store the information on SD-cards. As these values are only relevant for validating the model, a continuous monitoring is not necessary and reading the data from the cards at certain intervals is sufficient.

Figure 38 shows the district heating network with the realised metrological equipment. The solar thermal systems with extensive monitoring of all heat flows in the building are highlighted in white, the measurements at the substations of the network with clamp-on technology in yellow.

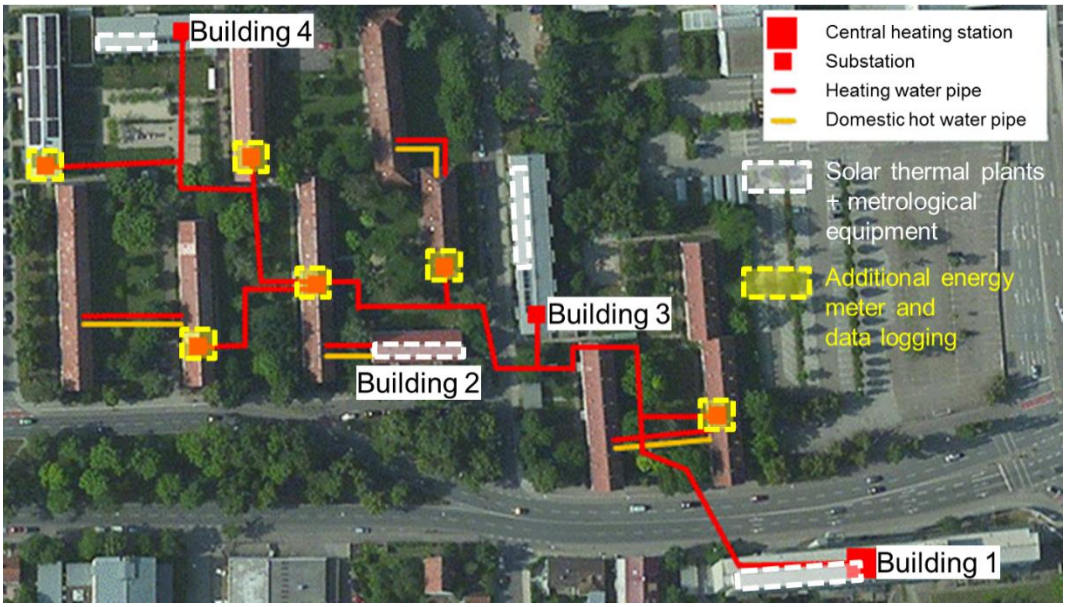

Figure 38: Solar thermal plants and metrological equipment in the district heating system

A balancing of all heat flows in the buildings with a high sample rate is possible. To gather the data of the electricity that is necessary to run the solar thermal systems, additional electricity meters are installed for the pumps, valves and controllers. The calculation of the solar thermal system efficiency is enabled via the pyranometers installed parallel to the collector arrays on building 1 and building 3 (40° inclination, south and 10° inclination, west). Additionally, data from the weather station, installed at *THI* is available, which is approximately one kilometre away from the plants.

The objects with solar thermal systems have real-time monitoring with online access to the system data. Therefore, an internet connection of the data loggers was set up

with routers to enable a monitoring via an online platform. The data recorded in the facilities includes:

- All heat flows in the plants
  - Consumption/feed-in district heating network
  - Consumption space heating
  - Consumption domestic hot water
  - Circulation losses
  - Yield of the collector circuit
  - Yield of the solar thermal system (from storage to consumers)
- Electricity consumption of pumps and controllers
- Irradiation at building 1 and building 3 (40° south and 10° west)
- Temperature, global irradiation and wind speed at the weather station of *THI*

Figure 39 shows a scheme of the data logging from the single sensors up to the computer-based data evaluation.

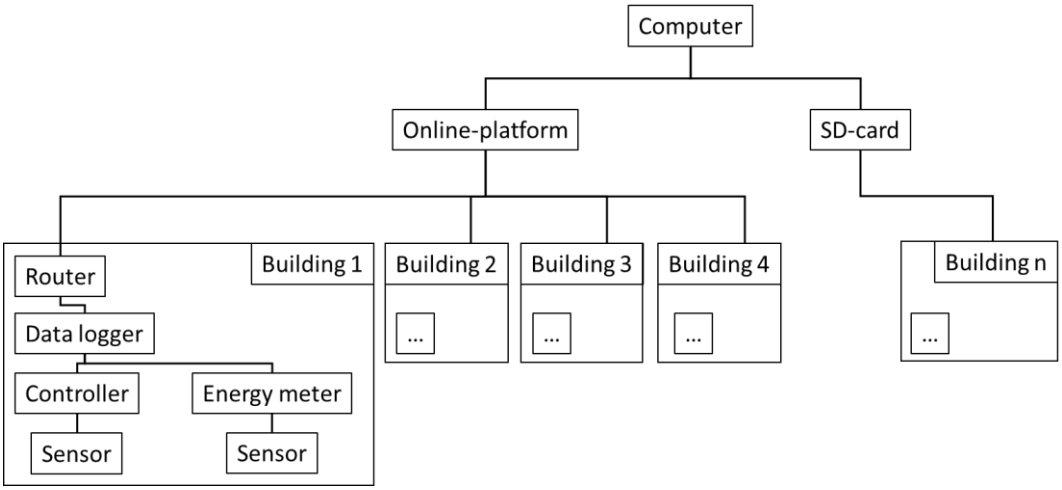

Figure 39: Scheme of the data logging and data transmission

4.4.2 Measurement Accuracy

In order to assess the uncertainty of the measured values for the model validation and the evaluation of the test systems, an estimation of the measurement accuracy is given below. Table 4 shows the accuracies of the individual sensors, which are used for the calculation of the thermal power and energy.

Considering the effect of these deviations on the calculated thermal power at the mostly used heat flow measurement with the combination of two PT1000 sensors plus one impeller flowmeter (V40) leads to the maximum measurement uncertainty as shown in Figure 40 as a function of the solar thermal power measured in the secondary circuit of the plant. The other circuits are evaluated analogously.

Table 4: Overview of sensor accuracies

Sensor	Measured value	Accuracy
PT1000	Temperature	0.1+0.0017·T °C
VFS/VFD	Temperature	± 2 °C, ± 1 °C @ 25…80 °C
VFS	Volume flow	1.5…5 %
VFD	Volume flow	± 2 %
V40	Volume flow	2.1 % (own laboratory measurement)
US-FM	Volume flow	1 % resp. 0.003 m/s
RPS/RPD	Temperature	± 3 °C, ± 1 °C @ (25…80 °C)
RPS/RPD	Pressure	± 0.25 bar, ± 0.2 bar @ 25…80 °C

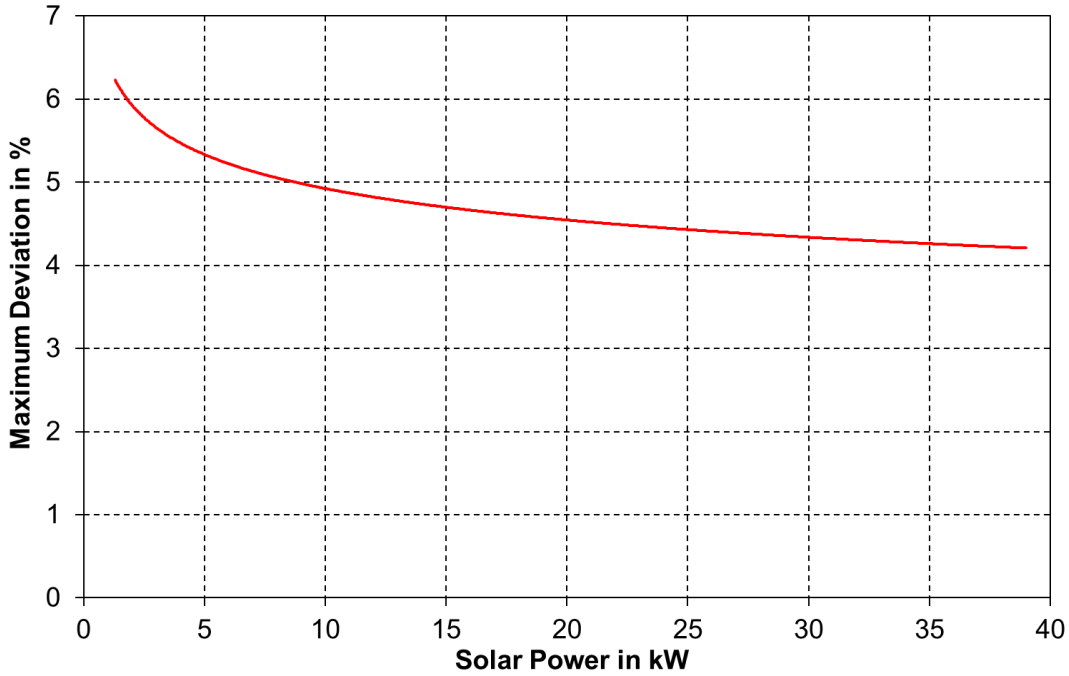

Figure 40: Maximum deviation of the combination of two PT1000 plus one impeller-flowmeter for thermal power measurement of the secondary circuit

It can be seen that over the relevant power range, the maximum deviation is between 4 % and 6 %. This represents the maximum expected deviation in case of unfavourable, opposite deviations of the temperature sensors. However, all PT1000 sensors were previously calibrated with reference sensors in the laboratory of *THI* and pairs with similar resistance characteristics were formed for the heat flow measurement. Any deviations were corrected in the controllers, energy meters and data loggers with an offset. The real deviations can therefore be assumed to be less than the maximum value shown in the graph. The relative error is calculated as stated below:

$$f_{Power} = f(T) + f(\dot{V}) \quad (6)$$

$$f_{Power} = \frac{2 \cdot (0.1\ K + 0.0017 \cdot T)}{\Delta T} + 2.1\ \% \quad (7)$$

with:

f_{Power}	*relative error of thermal power*	*%*
$f(T)$	*relative error of temperature sensors*	*%*
$f(\dot{V})$	*relative error of flow meter*	*%*

4.5 Metrological Investigation

The following explications show measurement results recorded during one year of operation of the plants and allow to assess the yield achieved in reality as well as the system behaviour.

4.5.1 Building 1

The grey dots in Figure 41 represent the daily solar yields as a function of the irradiation per square meter of collector area for the simulated yields from the design phase. The red dots show the measured values in the period from 1st January 2017 until 31st January 2017. It can be seen that these initially measured values are clearly below the point cloud of the expected values. This can be explained by the control of thermal disinfection. At the beginning of the plant operation, a daily heating of the entire buffer storage was carried out, which increased its temperature until the morning and thus, particularly in winter, resulted in correspondingly lower yields. After the switch of the thermal disinfection to a brief flushing of the pipes with hot water, the solar yield improved significantly. This can be seen from the green dots in the graph, which represent the measured values from 1st February 2017 until 31st December 2017. These points are in the lower expected range of the system design. An offset can be explained by cold-water temperatures that are in average 3 °C higher than assumed during the design phase.

In order to prevent overheating of the buffer storage, both a forced circulation by the thermal disinfection pump from the buffer storage to the domestic hot water storage and the possibility of feed-in to the return pipe of the central heating station right before the gas boilers were planned. The latter should never have been used according to the simulation results, but was integrated as an additional backup. The evaluation of the measurement results shows that the real operation corresponds to this prediction and no buffer storage temperatures beyond 80 °C were reached. The few temporary temperature peaks were compensated by the thermal disinfection pump. This is

exemplified in Figure 42, where the operation during a week with very high yields (up to 265 kWh per day) is shown. The red curve shows the temperature of the preheated drinking water at the outlet of the buffer storage, the orange curve the temperature at the outlet of the domestic hot water storage, which is subsequently conducted to the consumers in the building. It can be seen that on several days the thermal disinfection is activated in order to lower the buffer storage temperatures during periods of insufficient tapping. Although preheated water of up to 78 °C was conducted to the domestic hot water storage during this time, there was no critical increase in the temperature on the consumer side.

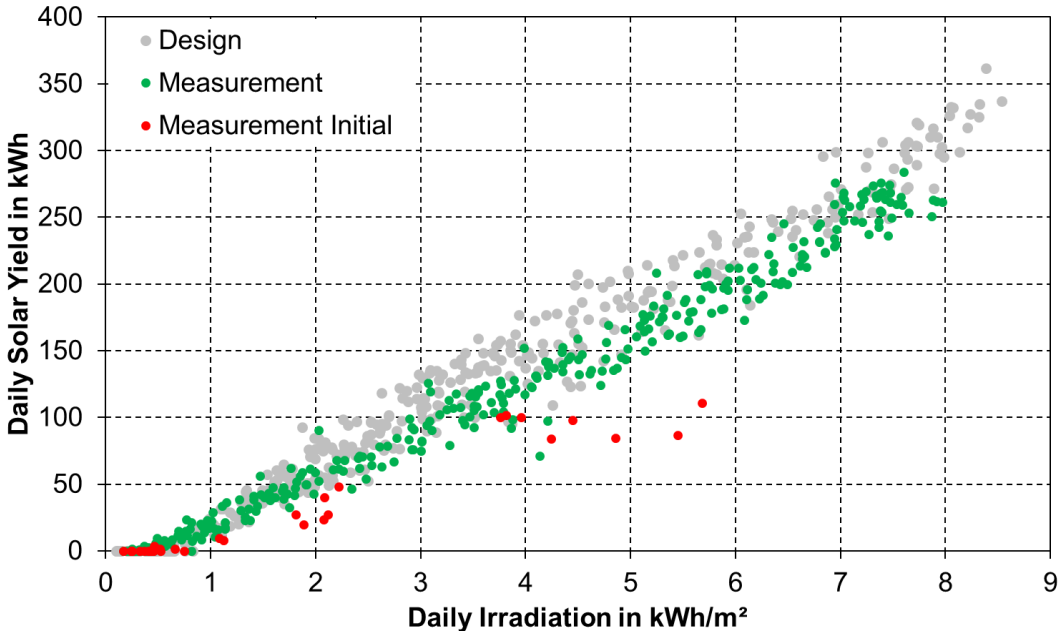

Figure 41: Building 1 – daily yields of design (complete year, grey) and measurements from 1st January 2017 until 31st January 2017 (red) as well as after the change of the thermal disinfection from 1st February 2017 until 31st December 2017 (green)

Another effect can be observed during night and early morning hours. At these times, a temperature increase in the upper part of the buffer storage occurs. This presumably results from a return flow caused by the circulation pump in combination with a malfunctioning check valve. However, an increase in the temperature can only be observed in the upper part of the storage and therefore has no relevant influence on the solar yield of the following day, as already in the early morning the storage is cooled down by the beginning tapping of the residents. This can be seen from the temperature drop at the buffer storage outlet to about 20 °C, which takes place before the temperature increase due to the solar yield of that day.

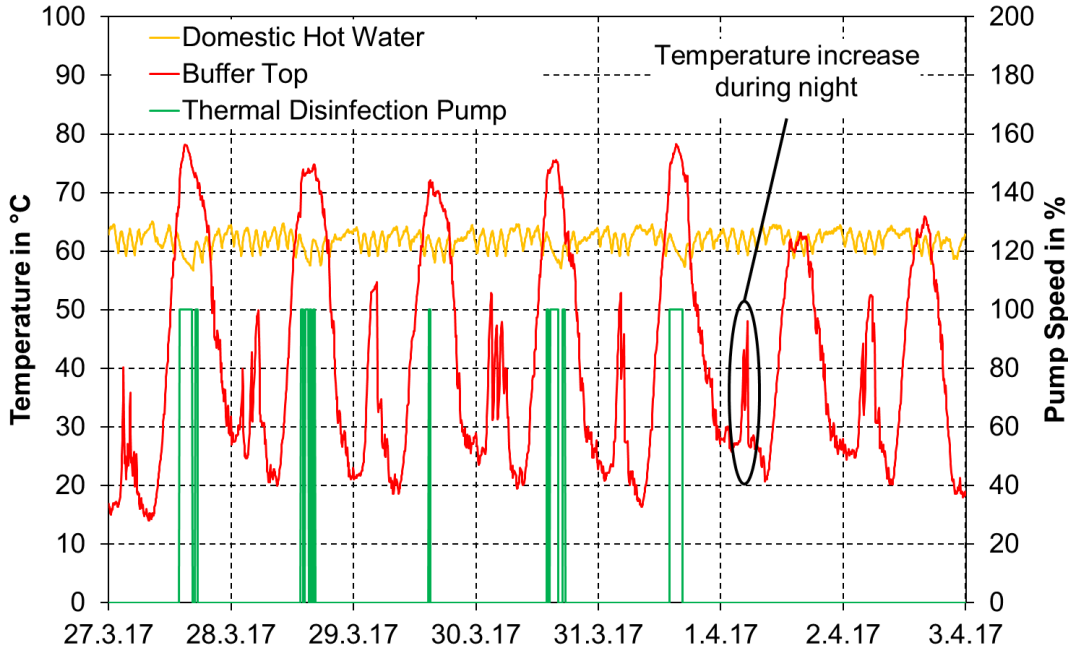

Figure 42: Building 1 – temperature between buffer and domestic hot water storage as well as at the outlet of the domestic hot water storage; thermal disinfection pump speed

4.5.2 Building 2

The plant at building 2 started operation in November 2016. Since the concept is a pure feed-in to the district heating network, significantly higher collector temperatures are required to achieve solar yields. Figure 43 shows the daily solar yields as a function of the irradiation per square meter of collector area for the design simulation as well as the measured values recorded between January and December 2017. In the considered measurement period, yields in the lower half of the expected corridor of the design simulation (grey dots) are usually achieved during the winter (marked in red). With increasing outside temperatures and irradiation values in summer, significantly higher yields can be observed (values from April until September, highlighted in green). It can also be seen that no relevant yield is achieved at daily irradiation values below 1.5 kWh/m². The operation of the plant is, however, not least due to the simple hydraulic design and the associated simple control, without complications and thus fulfils the claim of the operator for a simple and less failure-prone concept.

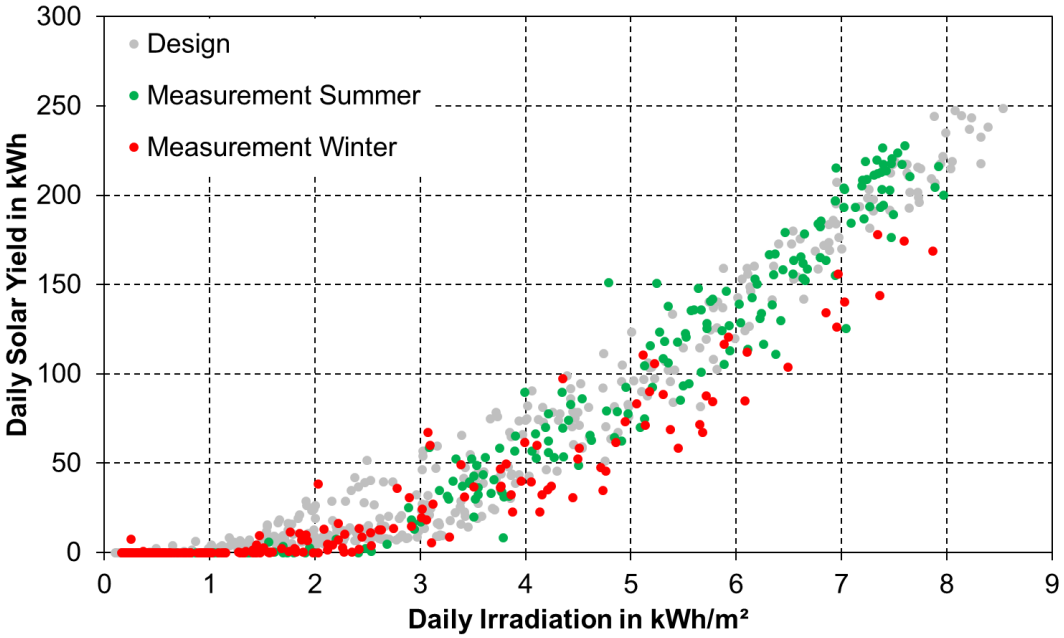

Figure 43: Building 2 – daily yield of design simulation (whole year, grey), measurement in summer (April until September, green) and winter (red) 2017

Figure 44 and Figure 45 show the operation during a week in March 2017. On days with low irradiation (18th and 19th March) there is no solar yield due to the necessary high supply temperatures of approximately 80 °C. On sunny days (13th to 17th March), the expected performance and yields are reached. The controller activates the primary circuit at a collector temperature of more than 60 °C, and tries in a second step to maintain a defined temperature difference between the primary circuit and district heating return via the speed of the secondary circuit pump. In addition, it can be seen that the return temperatures of the network are on a very high level of up to 73 °C.

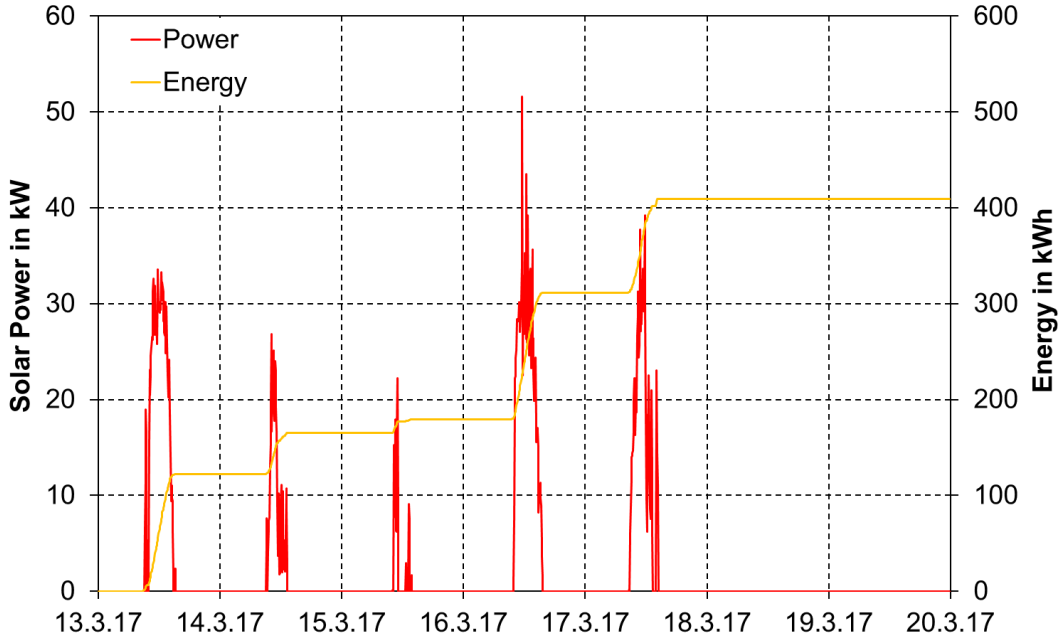

Figure 44: Building 2 – thermal power and energy during a week in March 2017

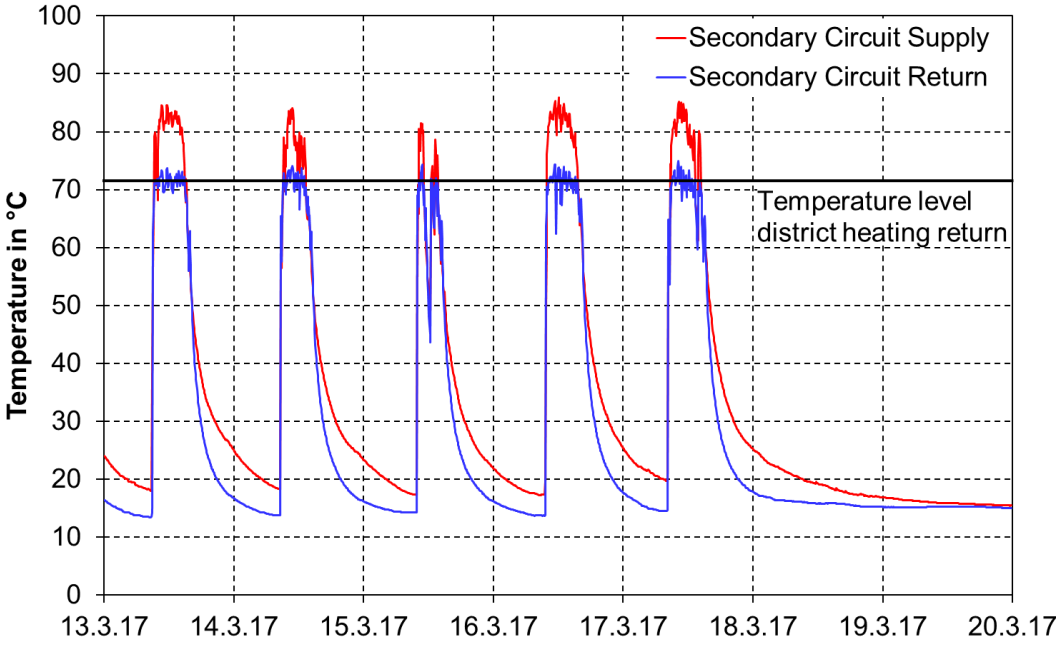

Figure 45: Building 2 – temperatures in the secondary circuit (district heating return) during a week in March 2017

4.5.3 Building 3

The system at building 3 is the most complex regarding the hydraulics and control strategy and was the last one to start operation. The hydraulic construction was completed in December 2016. However, it took several weeks to reach a state of regular operation with appropriate data recording. Other malfunctions during summer led to a lack of reliable metrological data in 2017. As for the comparison of the plant concepts and for validation purposes, it is sufficient to compare the three plants with similar orientation and collector array size, building 3 is neglected in this consideration.

4.5.4 Building 4

Building 4 differs from building 3 only by the orientation to the south, the lack of additional evacuated tube collectors and the fact that only one 1 m³ buffer instead of two is installed. The plant, which was also commissioned in November 2016, worked without any difficulties at the beginning. In the period until early February 2017, some adjustments were made to the control. This also includes the conversion of thermal disinfection analogous to building 1. The measured yields shown in Figure 46 are in the range predicted in the design phase.

In order to analyse the feed-in of the plant, a few days at the end of February and beginning of March 2017 are particularly of interest. In this period the existing domestic hot water storage was unmounted in the course of maintenance work and the solar thermal system was disconnected from the building's domestic hot water supply. The items "Domestic Hot Water Shutdown" in Figure 46 show the operation of the system

during this phase of pure feed-in. A stagnation and thus an increased load on the system and energy losses could be avoided over the period of the maintenance work. The plant achieved solar yields that correspond to about half of the design value in normal operation. The temperature thresholds for the beginning of the feed-in were chosen higher in this object than in building 2, since preferably a local use of solar heat should take place. Therefore, the yields in this operating state are relatively low. Individual outliers amongst the measuring points can be explained by modifications of the system or the control and measurement devices during the start-up phase and the accompanying inaccuracies on these days.

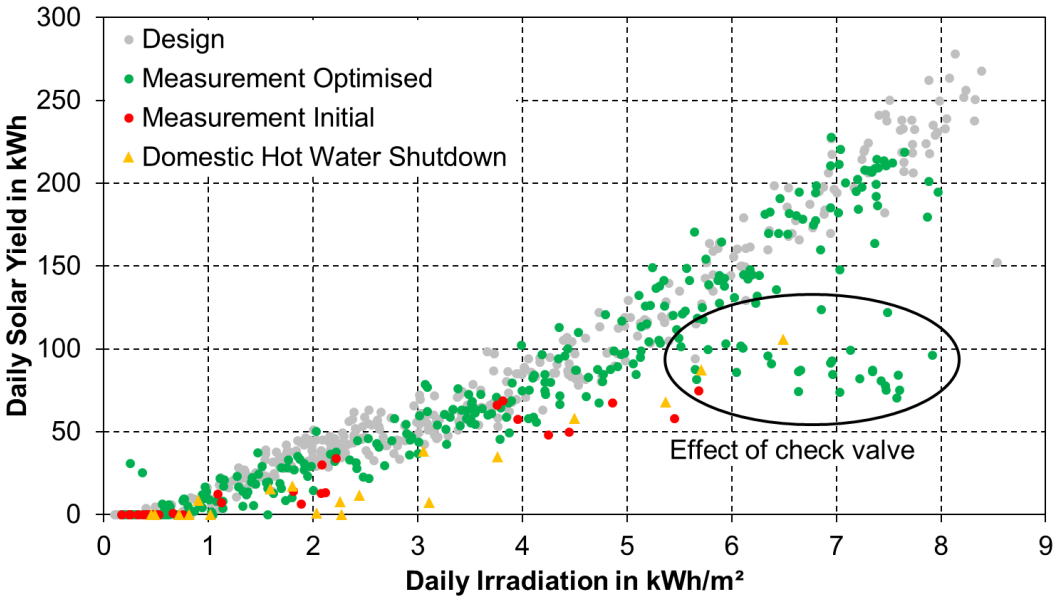

Figure 46: Building 4 – daily solar yield of design (complete year, grey), initial measurement data (1st January 2017 till 31st January 2017, red) as well as after the change of the thermal disinfection from 1st February 2017 till 31st December 2017 (green resp. yellow)

While the feed-in worked without any problems until March, increasing ambient temperatures resulted in increasing deviations from the expected values (circled points, bottom right in Figure 46). A more detailed analysis showed that in periods, where there was no flow through the space heating circuit of the building, a sufficiently high flow through the substation was not reached. This should have been compensated by opening an additional motorised valve between supply and return pipe in the building. During a lack of flow through the substation and a subsequent increase of the temperature in the feed-in circuit, it should have opened step by step and thus allow a flow from the district heating supply to keep the temperature in the feed-in circuit on a predetermined level.

An on-site assessment of the system showed that a check valve was installed between the two connections of the buffer to the return line, which was not planned (Figure 47). This valve prevented a reversed flow through this pipe section by the feed-in pump.

To circumvent the problem, the control of the motorised valve was changed in a way, that no longer a target temperature is maintained in the feed-in pipe but in the buffer storage. If the sensor at the top of the storage exceeds 90 °C, the valve opens at intervals and attempts to maintain this temperature. It is closed below 90 °C. This changed mode of operation proved to be just as functional as the one originally planned and brought the later measurements close to the expected range. The selected temperature of 90 °C represents a variant for the preferred local use of the yield. With lower set temperatures, the yield can be increased through an earlier cooling by the district heating network.

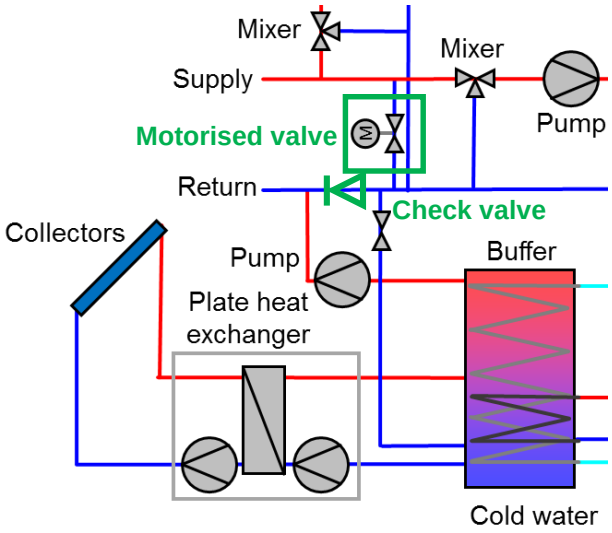

Figure 47: Part of the hydraulic scheme of building 4 with motorised valve and check valve (highlighted in green)

The cascaded behaviour of the system with the hot water preheating, the energy shift to the domestic hot water storage and the network feed-in for stagnation prevention can be very well monitored by having a closer look at the recorded temperature curves. As shown in Figure 48, on 13th, 16th and 17th March, the maximum tolerated temperatures of the buffer were reached. At the beginning, the thermal disinfection pump tried to dissipate the heat by shifting it to the domestic hot water storage (green curve). This also took place on 15th March but the temperatures only reached 80 °C on that day. After a further temperature increase, the feed-in pump switched on and transferred energy into the return pipe of the building and thus, into the district heating network. The maximum collector temperature could be limited to approximately 100 °C, which prevented stagnation and maintained plant operation throughout the entire day. This operating condition is increasingly found during summer, when the yields continue to increase and can no longer be completely consumed in the building.

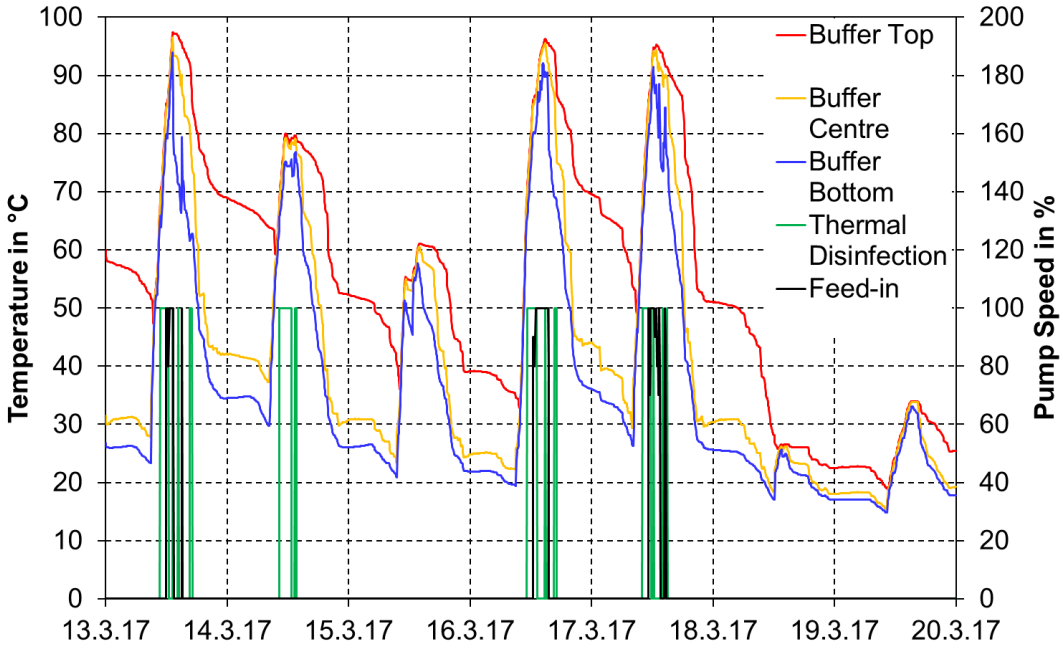

Figure 48: Building 4 – buffer temperatures at top, centre and bottom as well as dissipation of excess heat via shift to the domestic hot water storage and feed-in to the district heating network during a week in March 2017

4.6 Validation of the Solar Thermal Plant Model

In order to be able to gather further knowledge on controller optimisation and plant design for different types of districts in the following simulation study, the models were validated with the available metrological data and modified for a better fitting with reality. In addition, more accurate forecasts of the average annual yield can be derived for the subsequent economic evaluation of the installation.

The validation of the complete network model is described at hand of two exemplary weeks (week 16 and week 20) in 2017. These two weeks represent both, higher and lower ambient temperatures as well as high and average irradiation in the collector plane (Table 5), which ensures, that all of these conditions are covered by the validation. Ambient temperatures and weekly in-plane irradiations of 4.6 °C and 23.9 kWh/m² respectively 16.1 °C and 46.1 kWh/m² are typical for the heating period and summer.

Table 5: Average ambient temperature and irradiation in week 16 and 20 2017

Week	Average ambient temperature in °C	Irradiation on collector plane in kWh/m²
16	4.6	23.9
20	16.1	46.1

The individual components, the complete system and the control devices were validated in the model. The same collectors and solar stations are installed in all buildings. A distinction is only made in the length of the collector array piping, the array connection and the orientation of the collectors. In addition, the downstream components, e.g. buffer storage, and the connections to the existing district heating network respectively local domestic hot water system in the basements have variable designs.

In order to make a reliable statement about all different concepts of solar thermal systems, the three types of installations "local domestic hot water", "network feed-in" and "combined solution" are presented using building 1, building 2 and building 4. Of particular importance are the deviations of solar yields between measurement and simulation over a week, which are defined as follows:

$$Dev = \frac{E_{solar,simulated} - E_{solar,measured}}{E_{solar,measured}} \quad (8)$$

with:

Dev	*deviation of simulation and measurement*	*%*
$E_{solar,measured}$	*solar yield from the metrological analysis*	*kWh*
$E_{solar,simulated}$	*solar yield from the system simulation*	*kWh*

The measured network temperatures, cold water temperatures and domestic hot water consumptions as well as the irradiation in the collector plane and the ambient temperature were set as boundary conditions for the simulations.

4.6.1 Building 1

Table 6 shows the measured solar yields of building 1 and the associated simulated values. In week 16, a larger deviation than in week 20 is observed. However, it is only 3.3 % and therefore still within an acceptable range. Figure 49 shows the simulated and measured curves of solar power and yield as an example for week 20. Figure 50 shows the temperatures in the secondary circuit supply pipe and the associated volume flows. In Figure 51, the temperatures of the buffer storage top, centre and bottom are plotted. These values also show a good correspondence of reality and simulation. The unwanted temperature increase in the upper storage, caused by the circulation pump, was neglected in the model.

The simulated values are based on adjusted components. For this purpose, slight corrections of the heat exchanger capacity as well as the heat losses of the heat exchanger and the piping had to be carried out compared to the design models. In addition, the pump flow rates were adapted to the actually measured values as a function of the current pump speed. A shading model was introduced for the second

row of collectors, which reduces the irradiation during the winter months. In the design phase, this shading was not planned, as a different distribution of the collectors on the roof was assumed. The influence of shading is about 2 % yield reduction per year. In addition, it was found by the continuous temperature measurement that the cold water temperature is subject to a significant seasonal change. At the inlet to the buffer storage, the temperature fluctuates between minimum values of 9 °C in February and maximum values of 21 °C in July, while for the plant design, a constant temperature of 12 °C was assumed.

Table 6: Data of the model validation of building 1

Measured value	**Measurement in kWh**	**Simulation in kWh**	**Deviation in %**
Solar yield week 16 (secondary circuit)	671	693	3.3
Solar yield week 20 (secondary circuit)	1,492	1,499	0.5

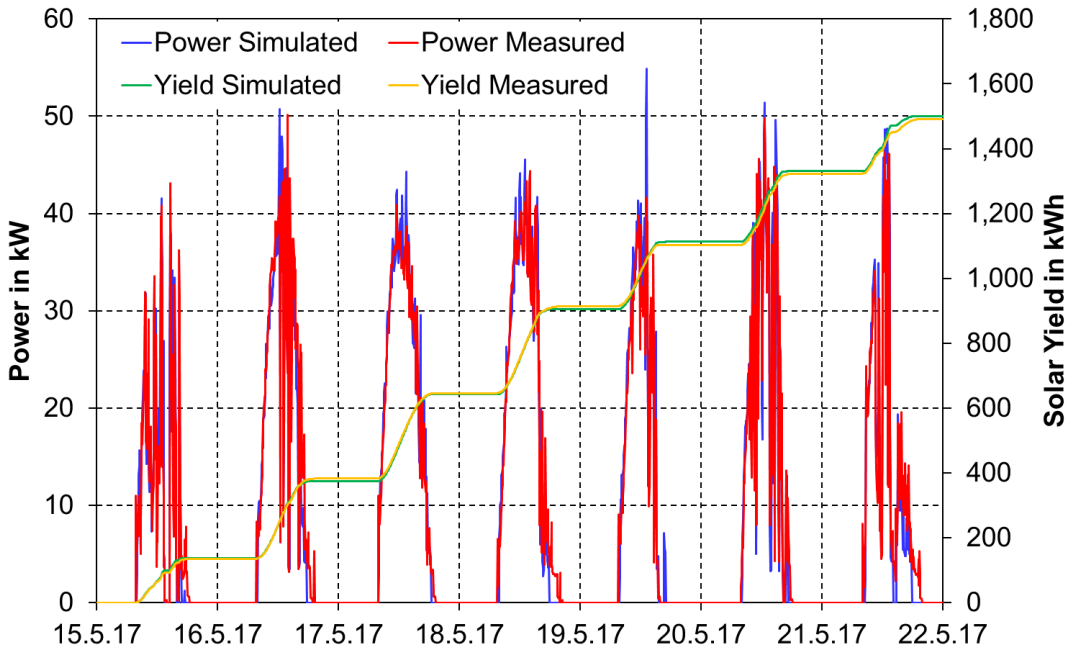

Figure 49: Building 1 – simulated and measured thermal power and solar yield in secondary circuit in week 20

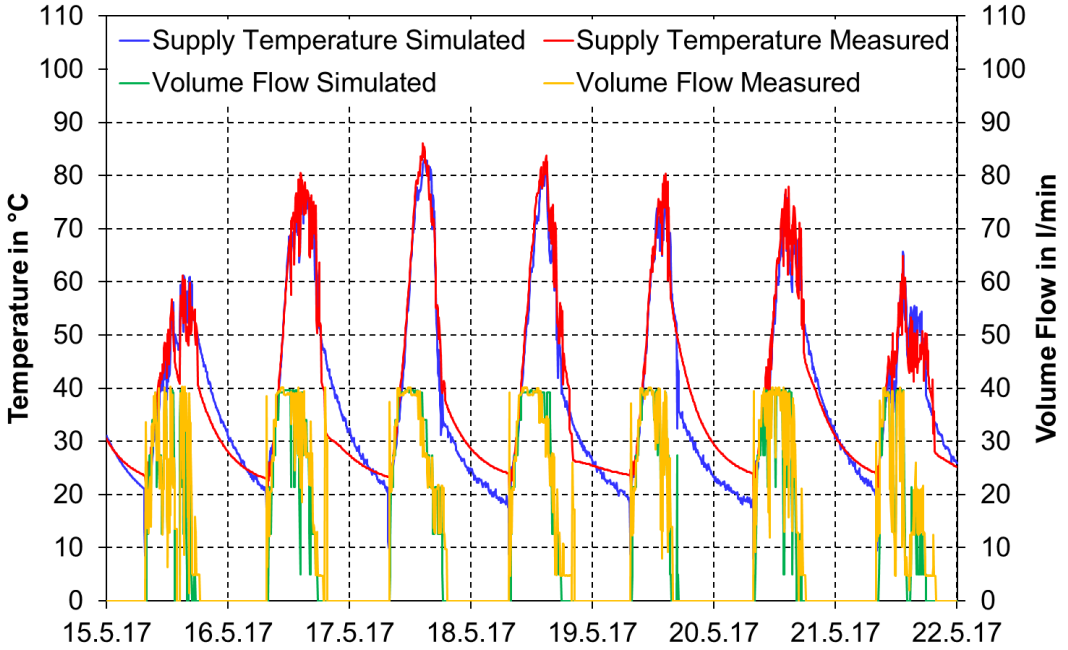

Figure 50: Building 1 – simulated and measured supply temperatures and volume flows in secondary circuit in week 20

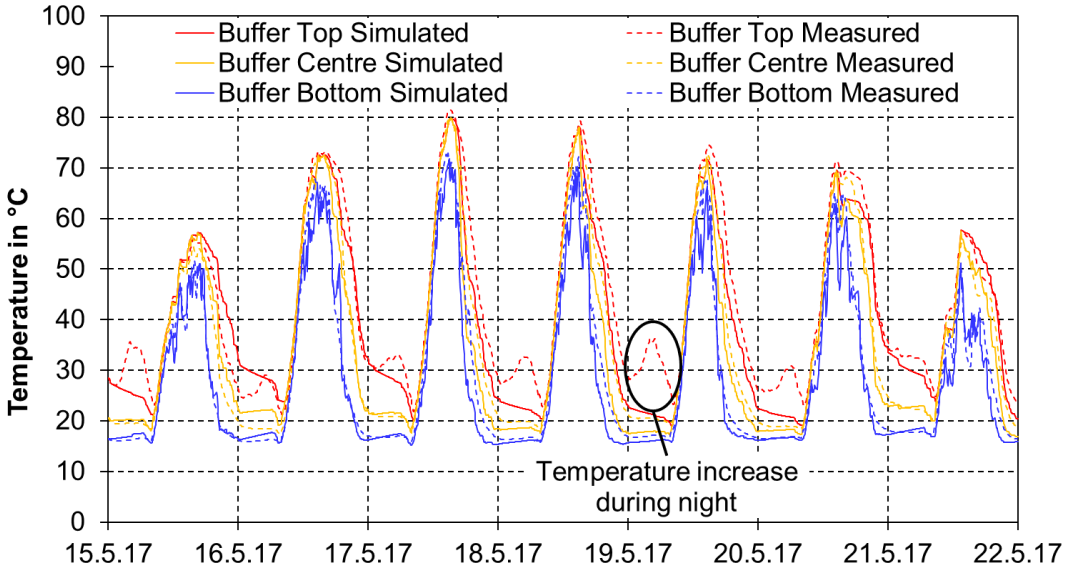

Figure 51: Building 1 – simulated and measured buffer temperatures in week 20

4.6.2 Building 2

Table 7 shows the measured solar yield of the real plant in building 2 and the simulated values of the model. Deviations of up to 0.8 % are given, with the simulation predicting slightly lower yields in the week with lower irradiation values. This replication by the model can be regarded as sufficiently accurate within the scope of the measuring accuracy of the test system.

Table 7: Data of the model validation of building 2

Measured value	Measurement in kWh	Simulation in kWh	Deviation in %
Solar yield week 16 (secondary circuit)	253	250.9	-0.8
Solar yield week 20 (secondary circuit)	1,033	1,041	0.8

Figure 52 shows the measured and simulated thermal power and solar yield, Figure 53 the supply temperature and volume flow in the secondary circuit of the system in week 20 from 15th May 2017 to 21st May 2017. Both, the power and the yield of the validated model match the measured curves very well. On some days, there are positive or negative deviations of the solar yield, which compensate each other over time. For the annual simulations, these deviations can therefore be accepted. It can be seen from the temperature curves that the model accurately reproduces the behaviour of the system. Only the cooling curves of the components (pipes and heat exchangers) show a different behaviour. However, since these effects are not within the operating hours of the collectors, this has no significant impact on the yield. The function of the control can be demonstrated with the curves of the volume flows in the secondary circuit. The activation and deactivation of the pumps as well as the speed control correspond well between the model and the test system.

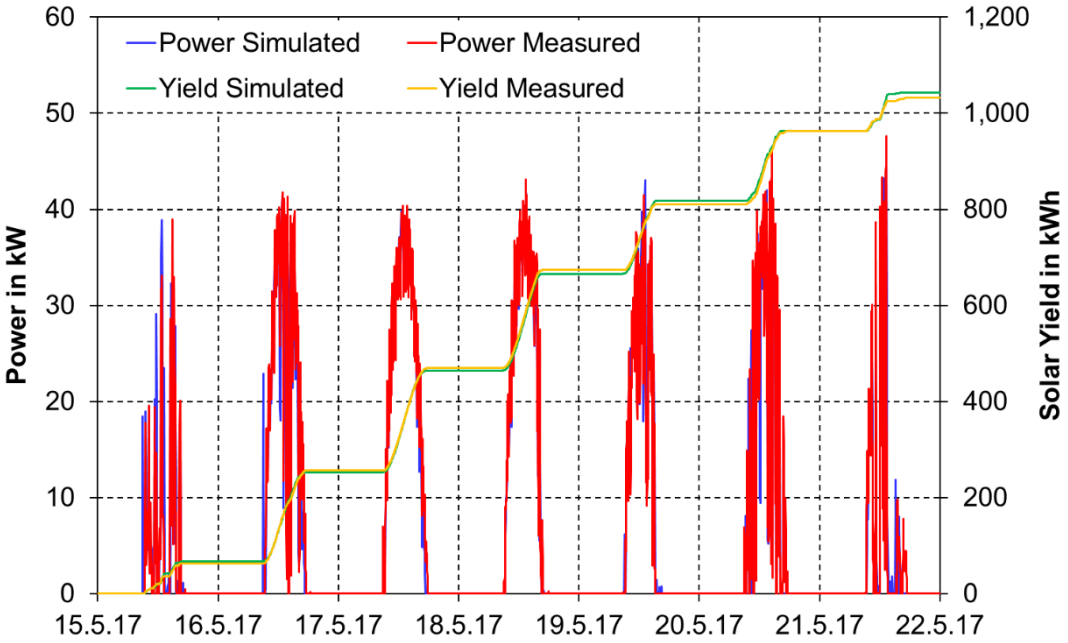

Figure 52: Building 2 – simulated and measured thermal power and solar yield in secondary circuit in week 20

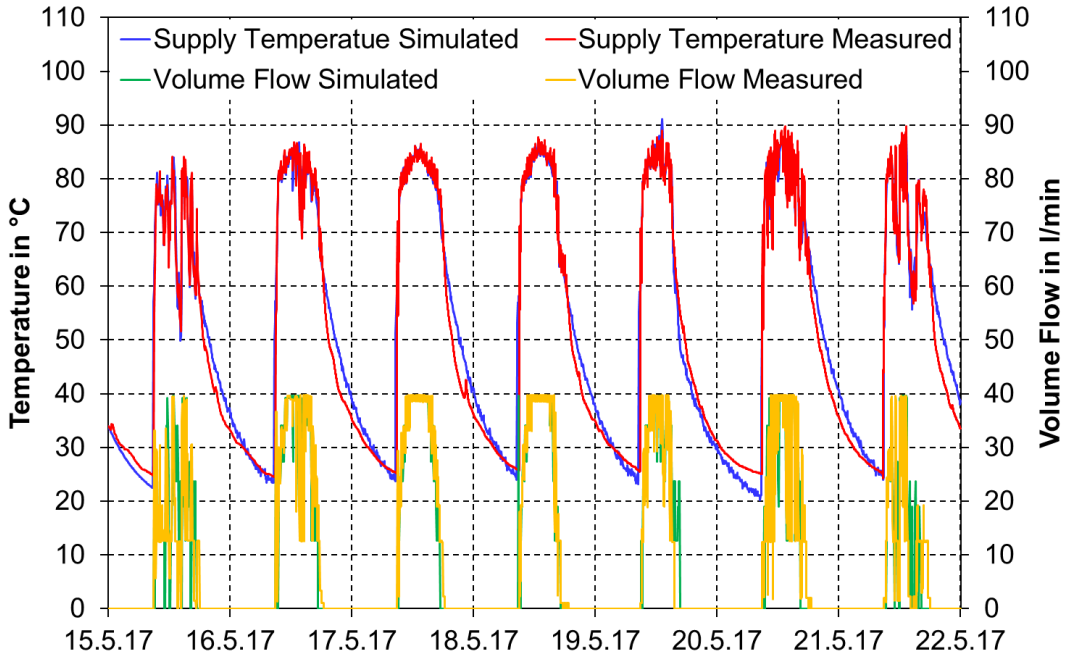

Figure 53: Building 2 – simulated and measured supply temperatures and volume flows in secondary circuit in week 20

4.6.3 Building 4

Compared to building 1, building 4 is more complex and associated with correspondingly more uncertainties and potential sources of error in modelling. As described earlier, in the metrological investigation section, due to the check valve at the feed-in in week 16 and week 20, the plant did not operate completely without stagnation. Nevertheless, these two weeks are used for validation as well and the lack of possibility of feed-in during the shutdown of the space heating considered in the model. Table 8 shows the measured and simulated yields. In this plant, the deviations can be classified as acceptable, too.

Table 8: Data of the model validation of building 4

Measured value	Measurement in kWh	Simulation in kWh	Deviation in %
Solar yield week 16 (Secondary circuit)	386	381	-1.3
Solar yield week 20 (Secondary circuit)	591	611	3.4

A look at the solar power and yield in week 16 shows that differences in yield occur on individual days, but these are compensated in the long term (Figure 54). The supply temperatures correspond well in general, but have slight deviations at certain times (Figure 55). If this is observed in conjunction with the buffer storage temperatures from Figure 56, it becomes clear that the reason of the partially deviating yields and temperatures in the secondary circuit is due to different storage temperatures.

Obviously, the measurement accuracy of the cold water inlet with only one volume flow sensor is lower than the accuracy of the sum of the 4 parallel sensors used at building 1. Since this value is given as a boundary condition on the buffer storage, there may be deviations. However, this does not represent an inadequacy of the model.

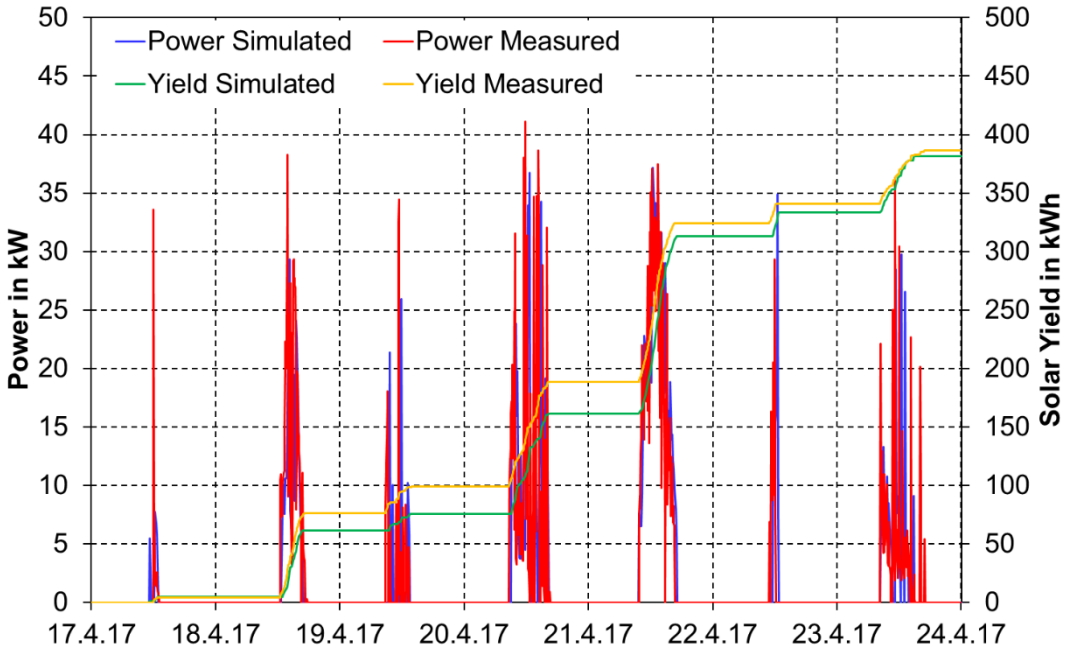

Figure 54: Building 4 – simulated and measured thermal power and solar yield in secondary circuit in week 16

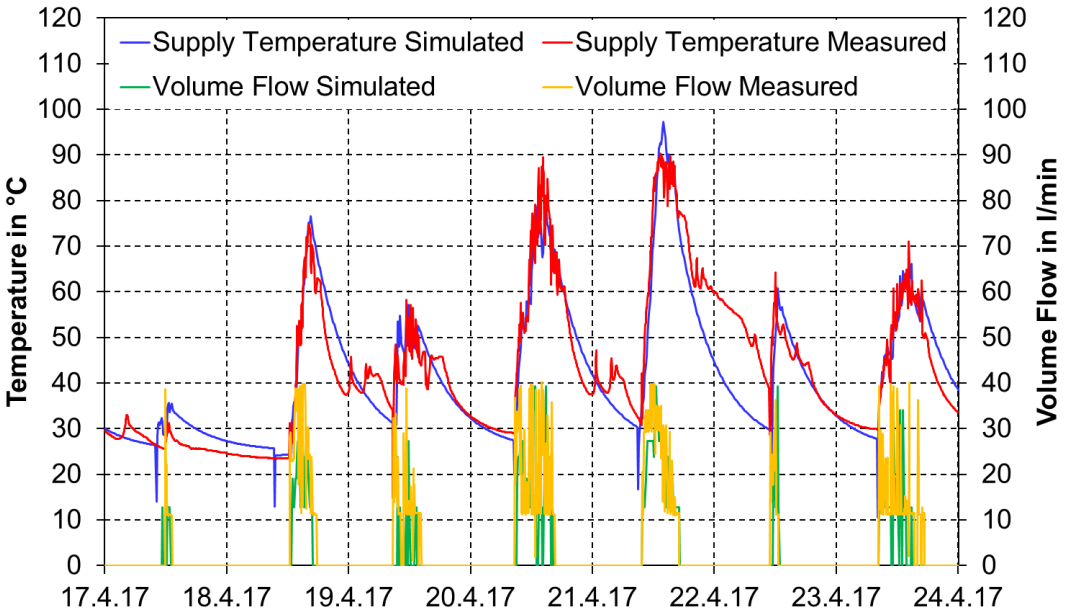

Figure 55: Building 4 – simulated and measured supply temperatures and volume flows in secondary circuit in week 16

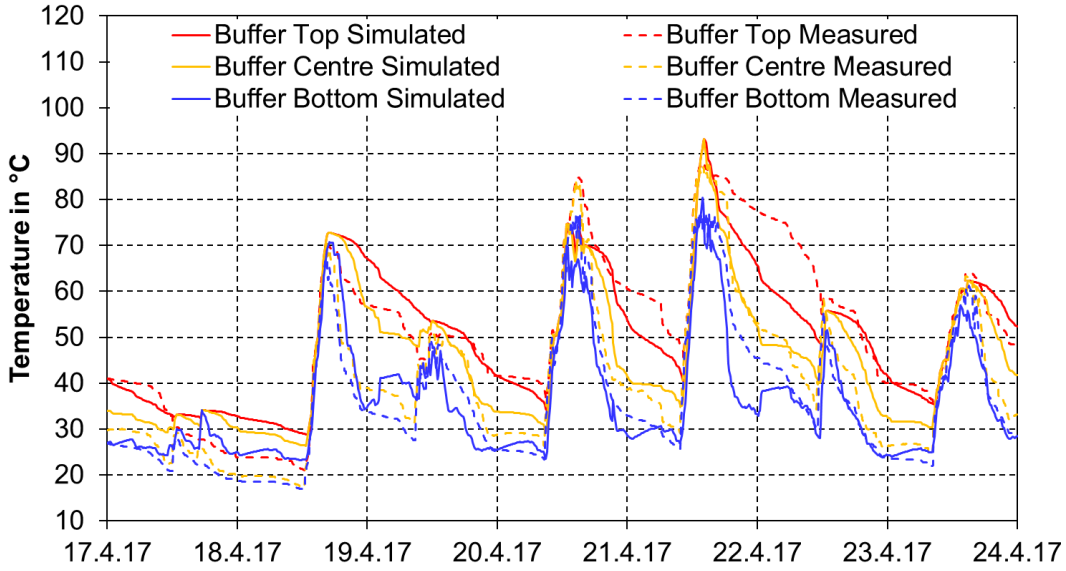

Figure 56: Building 4 – simulated and measured buffer temperatures in week 16

4.7 One-Year-Simulation of Validated Models

Based on the models, validated on a weekly basis, the yield resulting from annual simulations was evaluated in order to give an outlook on an average year of operation of the field test plant. Analogous to the design simulation, the average weather data was used, as well as the average annual heat consumption of the objects. The layout of the models is described in section 5. These models were considered both individually and in combination with the district heating network in order to be able to record reciprocal interactions.

Table 9 shows the total solar yield of the four plants during one year of operation separated into the local consumption and the network feed-in. In total, all four plants generate 117.5 MWh or 356 kWh/m² of solar heat.

Table 9: Annual yields of all solar thermal plants in the network

	Local use in MWh	**Feed-in in MWh**
Building 1	42.5	-
Building 2	-	17.0
Building 3	26.0	6.0
Building 4	19.2	6.8
Total	**87.7**	**29.8**

4.7.1 Building 1

The pure preheating at building 1 results in a forecasted annual yield of 42.5 MWh or 551 kWh/m². This is 10 % lower than the original design of 609 kWh/m², which is

mainly caused by the increased cold water temperatures in summer and due to the partial shading of the second row of collectors. Nevertheless, the yield is satisfactorily high and the plant operation reliable. Figure 57 shows the monthly yield and the solar fraction of the domestic hot water including circulation losses. The average annual solar fraction is 15 %.

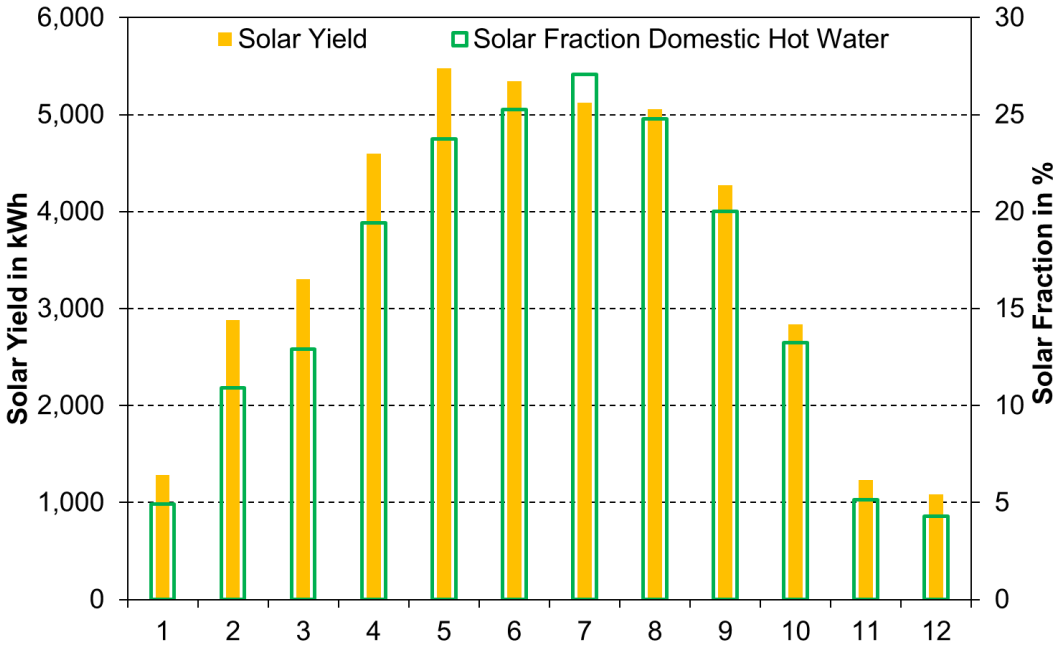

Figure 57: Building 1 – forecast of the average monthly solar yield and solar domestic hot water fraction

4.7.2 Building 2

In the considered measurement period, return temperatures of 73 °C in average at supply temperatures of 78 °C can be observed due to not optimally adjusted control of the district heating network. During the design of the plants it was calculated with an average value of 70 °C, based on the available data at that time. The temperatures in the current operation are higher outside the heating season, but during the heating season they are lower. The increase in the return temperature due to the feed-in of building 4 also affects the yield during summer. Figure 58 shows the monthly forecasted solar yield of the plant. The solar fraction supplied by the plant of building 2 of the total heat demand of the complete district is between almost zero and 3 % in the individual months. For an average operating year, a yield of 17.0 MWh compared to the planned 19.8 MWh is expected. This corresponds to a specific yield of 220 kWh/m² compared to 256 kWh/m² and an annual solar fraction of 0.4 %.

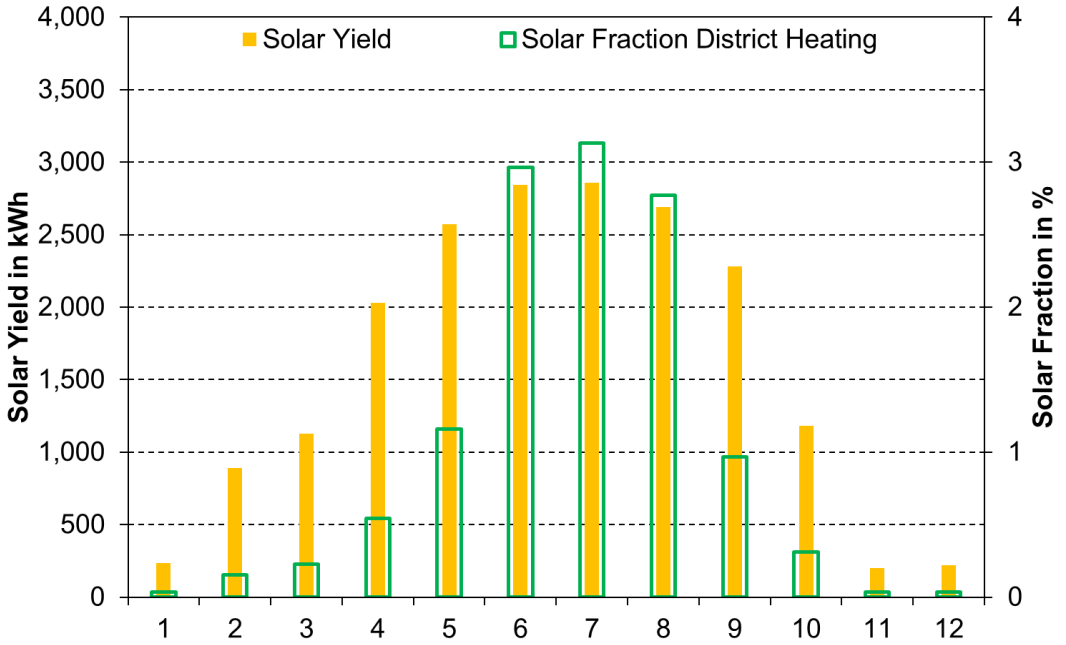

Figure 58: Building 2 – forecast of the average monthly solar yield and solar fraction of the complete district heating network

4.7.3 Building 3

At building 3, which is based on the validated model of building 4, the distribution of the utilisation of solar yields for feed-in and local consumption is of interest. Figure 59 shows the solar yield as well as the local domestic hot water fraction and the energy fed into the district heating network over the course of the year.

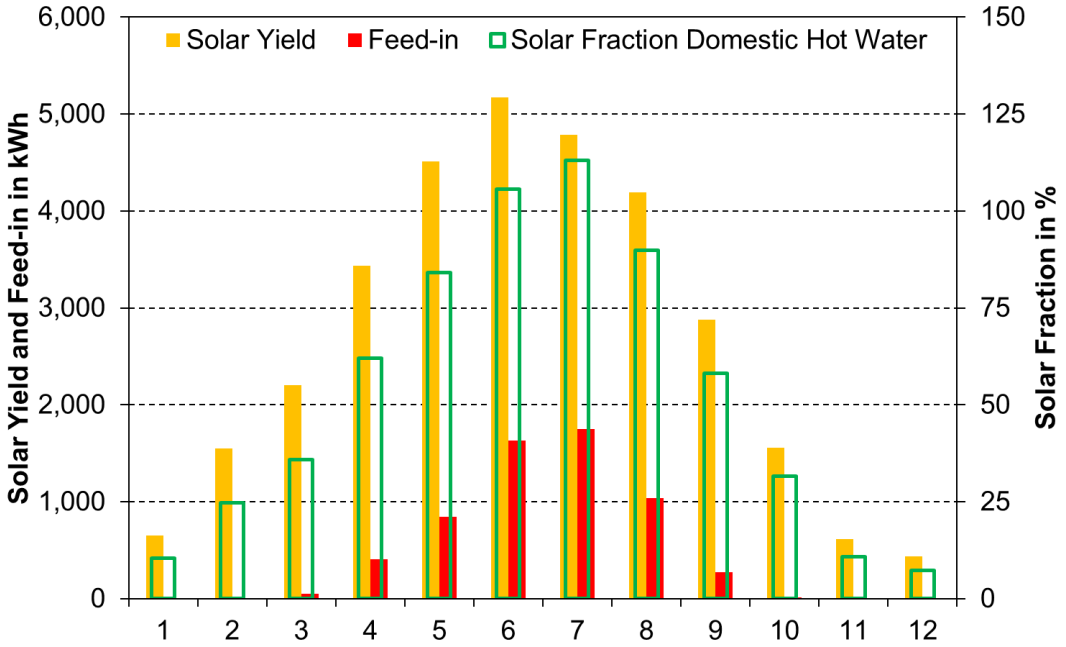

Figure 59: Building 3 – forecast of the average monthly solar yield, the feed-in and the solar domestic hot water fraction

In total, the flat-plate collectors and the existing evacuated tube collectors generate 32.0 MWh or 325 kWh/m² respectively. 6.0 MWh are fed into the district heating network. For this simulation, an optimised feed-in control was used, operating at buffer storage temperatures above 75 °C, which is close to the design values and represents the current control of the field test plant. The first weeks of operation, including the model validations, were still carried out at temperatures thresholds of 90 °C. The solar fraction in July amounts to more than 110 % of the consumption of hot water including circulation. The average solar fraction is 49 %. Compared to the design values of 34.2 MWh, the yield is 6 % lower.

4.7.4 Building 4

Figure 60 shows the solar yield, the local solar domestic hot water fraction and the energy fed into the district heating network during one year for the plant in building 4. From the 26.0 MWh, respectively 337 kWh/m², generated by the solar thermal system, 6.8 MWh are fed into the network. The solar fraction in July is in the range of more than 140 % of domestic hot water consumption including circulation, with an annual solar fraction of 73 %. In comparison to the design with 29.4 MWh, the yield is reduced by 12 %. Again, the increased cold water temperature is mainly responsible for the lower yield compared to the design simulation.

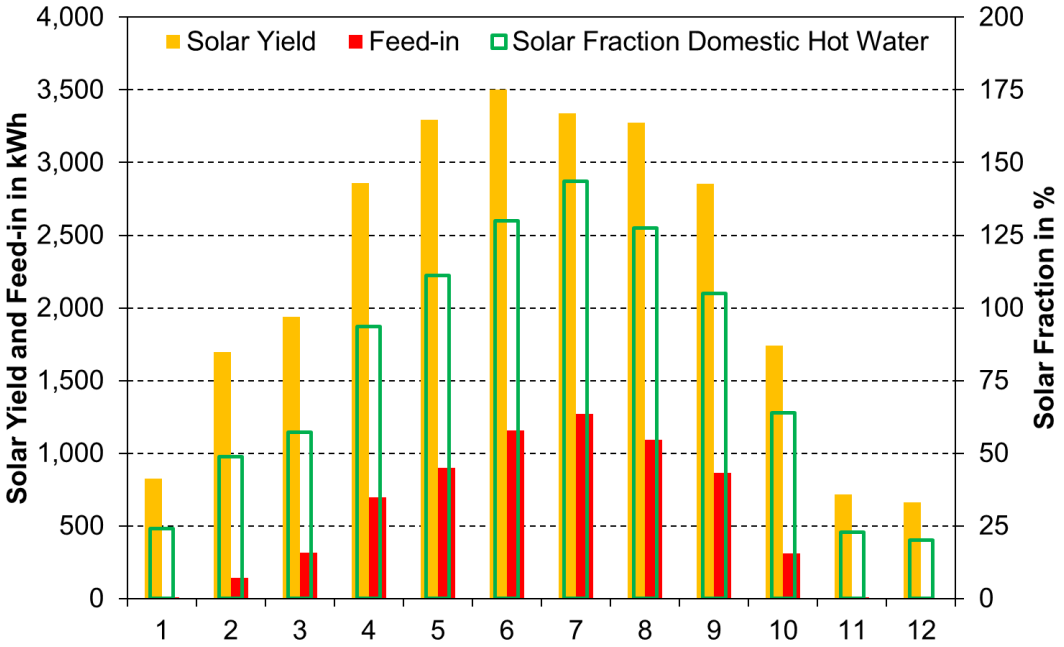

Figure 60: Building 4 – forecast of the average monthly solar yield, the feed-in and the solar domestic hot water fraction

4.8 Modified Operation

In order to further increase the yield of the realised plants, adjustments can be made on the operation of the district heating network or on the control of the solar thermal systems. As already mentioned, the lower yield compared to the design simulation partly results from the fact that the return temperatures in the network are higher than expected. This can have two reasons:

1. The supply temperature is too high or
2. The mass flow in the network is too high

The supply is set to a temperature of approximately 80 °C throughout the year. This is a typical value for this kind of system, but can be further reduced, if necessary. The measured values show an average supply temperature of 78 °C. The return temperature fluctuates between 72 and 75 °C inside and outside the heating period. The volume flow is typically between 60 m³/h and 50 m³/h inside and outside the heating period. On the basis of the network model, it was investigated how a reduced supply temperature affects the solar yield.

An even more decisive approach of reducing the temperature in the return is to increase the temperature drop in the substations by an adapted volume flow of the central pump and a better control of the substations. Therefore, an optimised control was tested in the model, to reduce the return temperatures to an average of 60 °C by adjusting the volume flow through the substations. Since the system of building 1 does not feed energy into the district heating network, a closer look at this object is not reasonable. Yields remain at the same level, regardless of network temperatures and volume flows. Table 10 shows the changes in solar yield for the individual variants.

Table 10: Improvements of solar yields of building 2, building 3 and building 4 by an optimised operation of the network

		Improvement of annual solar yield at current volume flow control in MWh	**Improvement of annual solar yield at optimised volume flow control in MWh**
Supply temperature 80 °C	**Building 2**	-	+4.8
	Building 3	-	-0.2
	Building 4	-	0
Supply temperature 75 °C	**Building 2**	+1.5	+6.2
	Building 3	+0.8	+0.5
	Building 4	+0.7	+0.6

For building 2, simulations show a possible increase of the feed-in from 220 kWh/m² in the current operation mode to 282 kWh/m² at optimised return temperatures. The adaptation of the supply temperature to 75 °C in summer has less influence and results in 240 kWh/m².

The systems in building 3 and building 4 for combined use of the yield show, as expected, a lower dependency on the network operation. A change in the volume flow has hardly any impact on the yield. The best variant for further optimisation in this case is the supply temperature reduction. This can be explained by the following considerations:

- The systems only feed in a part of the produced solar heat into the network. The local use is independent of network operation, like in building 1.
- In spring and autumn, the supply of the systems depends on the return temperature of the building itself and not on the total network temperature. Building 3 and building 4 are already better adjusted regarding the flow conditions than the older buildings in the network.
- If there is feed-in for which the return volume flow rate of the building is not sufficient, an admixture from the supply is done. Therefore, a temperature reduction of the supply has the most significant influence on the operation in this case.

4.9 Parametric Study

After considering the existing system with regard to an optimisation of the operation, it is of interest to clarify, how an extension of the implemented systems would affect the solar yield of this improved system. The available roof areas have not been fully utilised to enable the installation of existing standard components and to ensure a better comparability of the systems by equal dimensioning. Therefore, another simulation study was carried out applying different sizes of the systems. For this purpose, more of the available roof area of the buildings was occupied regardless of the installation effort and finally the impact on the yield and the network operation was examined under these changed conditions. Building 2 was kept as in reality as there is only minor potential for further collectors. An important point of this consideration lies in the determination of interaction between the plants. This is particularly important during summer, when the solar power is in the order of magnitude of the heat consumption of the district, which is not yet the case with the currently implemented systems.

The following configurations were examined:

- Building 1 with 3 times 71 m² flat plate collectors and utilisation of surplus feed-in to the district heating network
- Building 3 with 3 times 71 m² flat plate collectors on the west roof (unmounting of evacuated tube collectors)
- Building 4 with 3 times 71 m² flat plate collectors

The storage sizes remained unchanged, since there is, in contrast to the roof areas, no space for further installations. Table 11 shows the annual yields of this study divided into local use and network feed-in.

Table 11: Annual solar yields of the existing and the extended solar thermal plants

	Local use in MWh		**Feed-in in MWh**	
	Existing	**Extended**	**Existing**	**Extended**
Building 1	42.5	83.9	-	4.8
Building 2	-	-	17.0	20.0
Building 3	26.0	35.6	6.0	17.5
Building 4	19.2	25.9	6.8	37.3
Total	87.7	145.4	29.8	79.6

The fraction of feed-in increases significantly for the larger-sized plants. In the case of building 3, the solar fraction increases to 205 % during summer, at building 4 to 365 %. Even in the winter months there is now a minor network feed-in. While there are no surpluses to be injected at the realised plant in building 1, the solar fraction now rises to 55 % in summer and the share of feed-in in the total yield of the plant is 5 %. If larger storage tanks are used or occasional stagnation is tolerated, the same collector area can be used without feed-in. In summer, there are several periods, in which the production of the solar thermal systems exceeds the consumption in the district. In these cases, a positive heat transfer into the central heating station with short-term peak values of 60 kW can be monitored.

5 Modelling of the Bidirectional Network

5.1 Requirements of the Model

The model for the simulation-based investigation of the smart district heating system has to be capable of calculating the energy production, distribution and storing processes of solar thermal plants and district heating systems. Therefore, it has to fulfil several requirements:

- Replication of realistic solar yield
- Replication of realistic storage stratification and heat loss
- Replication of realistic network heat loss
- Replication of the dynamics of the network regarding transport delay of the fluid and thermal capacity of the components and the contained water

All simulations were carried out using the CARNOT toolbox in MATLAB/Simulink, which provides a block library with all relevant components to model heating systems – including district heating – for the conceptual design of such systems [75]. Due to the unidirectional information flow between blocks in the Simulink modelling concept, it is, nevertheless, not straightforward to model reversed flow in pipe connections between components like boilers, storages and heat exchangers. A modification and extension of the available CARNOT library was therefore done to enable the design of a district heating system with decentralised solar thermal plants utilising an RS feed-in. As it was intended to investigate only the energetic behaviour of a smart solar district heating system and not the detailed hydraulics, it was on the other hand not necessary to implement a sophisticated pressure calculation. The used modelling approach is presented in following section and validated by additional laboratory measurements.

Figure 61 describes how a calculation is processed using the CARNOT Thermo-Hydraulic Vector (THV) on the example of a small district heating system. The supply pipe model connects the outlet of the central heating station model with the inlet of a building model. The numbers at the connecting lines indicate the dimension of the vector. The ambient temperature of the pipes, in this case the ground temperature, is a time-dependent scalar value. The THV connections are 20-component vectors of which the most relevant components are the temperature of the fluid in °C, the mass flow in kg/s, the pressure in Pa, the fluid type (e.g. water or water/glycol mixture) and pressure drop coefficients. The THV leaves the central heating station with a defined mass flow and pressure at a defined temperature. These values are determined by the pump and heat source. The vector containing this information is processed in the

pipe model in a way that the temperature is decreased by a thermal loss calculation depending on the pipe dimensions and insulation. The pressure drop coefficients are increased depending on the pipe dimensions and roughness. The modified THV with lower temperature and higher pressure drop is conducted to the building model and further modified by the consumption in this building. The return flow is conducted through the return pipe, where the same calculations are performed like in the supply pipe. Finally, the heat generator and the pump in the central heating station set the THV temperature and pressure to the desired values and the circuit is closed.

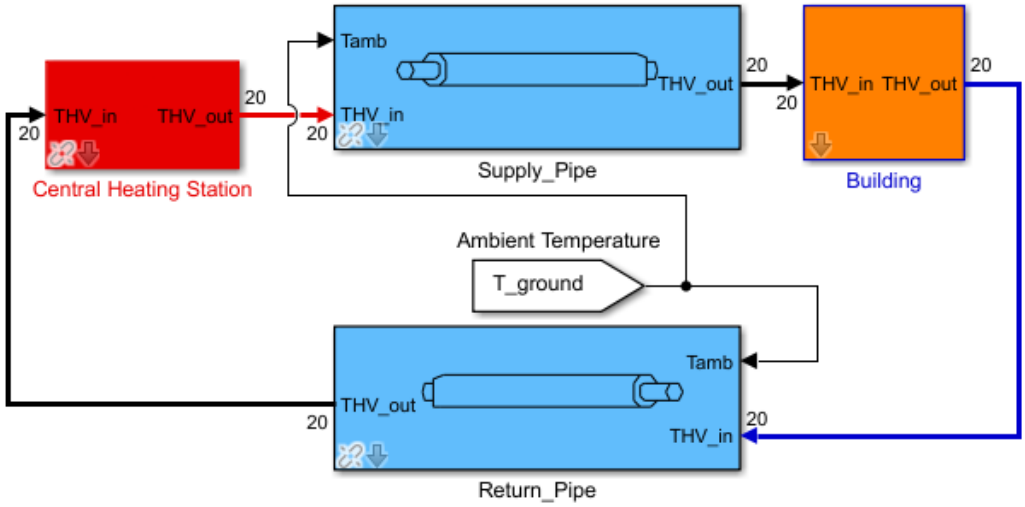

Figure 61: Example of a simple CARNOT-based district heating model

If the building model is not only a consumer but also a prosumer, the mass flow cannot simply be redirected to leave the building inlet port and enter the central heating station outlet port. A negative mass flow definition for the THV results in unrealistic high temperature values, as the temperature calculation is not defined for this condition. While the CARNOT pipe model was sufficient for the design of the field test installation, this circumstance leads to the necessity of modifying the district heating pipe model to include RS-schemes in the simulation study.

5.2 Definition of the Model Components

5.2.1 Network Structure

Figure 62 shows the layout of the complete district heating network model for the optimisation in section 6. The single components, used in this model, are introduced subsequently. The network model consists of the connected buildings, a central heating station, pipes and connections (junctions) between these pipes.

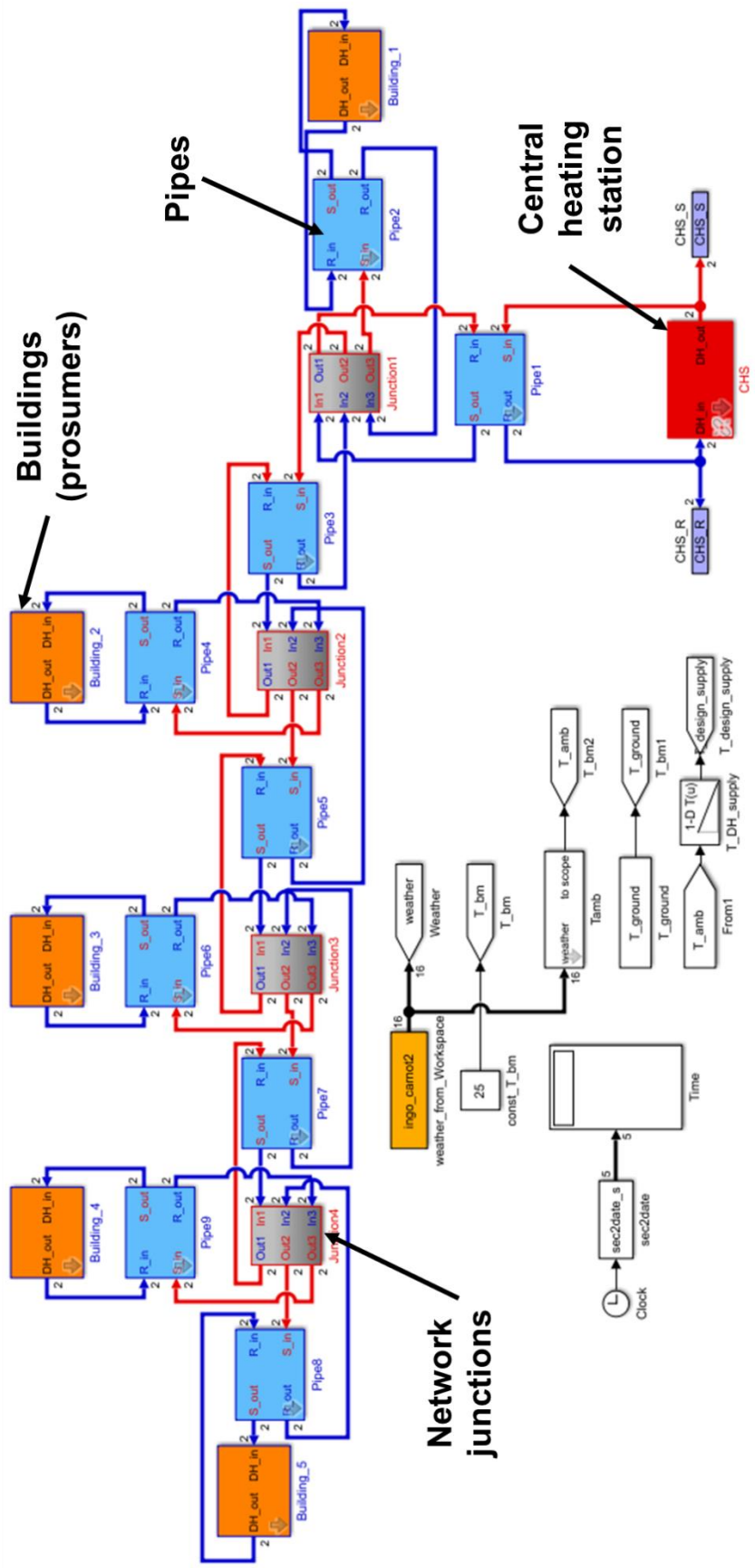

Figure 62: Depiction of the district heating network simulation model with central heating station and five connected buildings

5.2.2 Central Heating Station

Basis of the heat production in the network is the central heating station. Such a station can be included in one of the supplied buildings or installed in a separate building. Another possibility can be the supply via a larger district heating system, connected to the investigated district. As it is not intended to discuss the heat production at the central heating station in detail but only to assess the energy savings due to the different integration concepts of solar thermal plants, the heat generator is modelled as a simplified thermal power source at the top level of the central buffer. This leads to a neglect of efficiency changes of e.g. the temperature level on a gas boiler.

The thermal power source is integrated in a buffer storage model and represents an ideal heat source, feeding in the energy on the upper level of the storage. The connecting ports are positioned on 95 % respectively 75 % of the storage height to keep this part of the storage on the desired supply temperature. A modulation of the heating power is integrated, which allows three levels at 50 %, 75 % and 100 % of the installed power. Depending on the difference between design supply temperature and actual supply temperature, the power is increased or decreased.

Heat losses are included by assuming a constant ambient temperature of 25 °C in the heating station building and a storage insulation thickness of 100 mm at a thermal conductivity of 0.04 W/(m·K). The same applies to all other storages in the model. All thermal energy entering and leaving the storage as well as the storage temperatures are logged in a 5 minutes interval.

5.2.3 Pipes

For the simulation of a district heating network with decentralised feed-in, four aspects of the pipe model are particularly relevant:

- Calculation of the heat losses
- Calculation of the stored energy due to the thermal capacity of pipe and fluid
- Calculation of time delays of the fluid flow in the network
- Ability to simulate a reversed flow in the pipe

To cope with these demands, a new setup of pipe model was developed based on Simulink. As the buildings and other system components are modelled in CARNOT, the THV was the basis for the new calculation procedure. Besides the temperature and the mass flow, the THV contains information, which is not relevant to the energy balance of the district heating network and can be simplified without losing accuracy in this application. As the fluid is always pure water and pressure loss calculations are only of interest for the detailed system design but not for the conceptual layout and

energy management, only the temperature and the mass flow were selected and structured in a 2-component vector for all calculations in the network.

Some definitions regarding the physics are introduced in this pipe model. Firstly, the heat capacity of the water is assumed to be constant at 4,188 J/(kg·K). This is justified as the maximum deviation of the real value within the temperature range between 0 °C and 100 °C is less than 0.5 %. Secondly, the temperature of the pipe wall is assumed to be the same as the fluid temperature, which is acceptable if the thermal resistance of the pipe insulation is much higher than the thermal resistance of the pipe wall and the convective heat transfer between fluid and pipe wall. For thermal conductivities of the insulation material around 0.04 W/(m·K) and thicknesses in the range of the pipe diameter, this assumption is sufficient. For the calculation of the insulation capacity, an average insulation temperature was defined. This results from the fact that for the assumption of a linear temperature gradient along the insulation thickness, more than half of the insulation material mass is closer to ambient than to fluid temperature due to the increasing lateral surface at larger distances from the pipe wall. For a pipe with an insulation thickness equal to the inner diameter, this results in a weighted temperature of 37 % of the inner temperature compared to ambient, meaning that e.g. at 80 °C fluid and 20 °C ambient temperature, the average insulation temperature is only at 42 °C. To cope with this fact, 37 % of the total capacity of the insulation are added to the fluid capacity and set to fluid temperature whereas the other 63 % are neglected. Figure 63 illustrates this correlation.

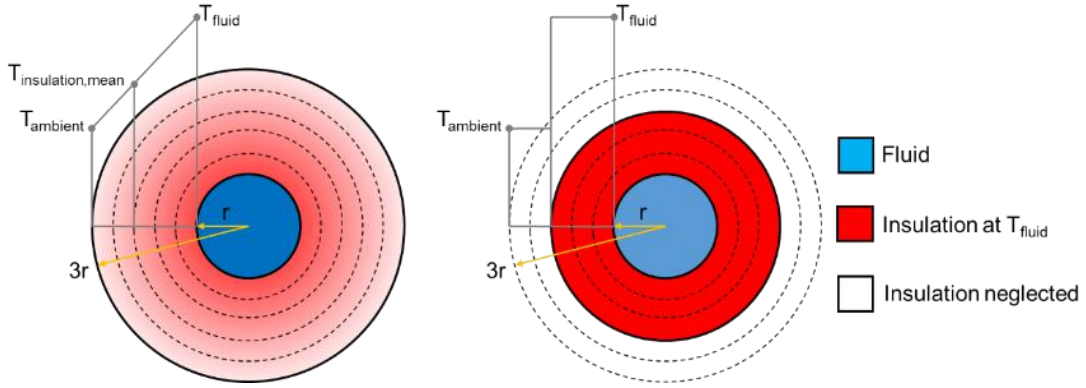

Figure 63: Real (left) and discretised (right) temperature distribution across the pipe cross-section with equal stored energy

As the thermal conductivity of insulation materials can be highly dependent on the temperature, a temperature-conductivity function was introduced using a set of temperature-conductivity pairs and a linear interpolation between the known values. Equation (9) gives the heat loss of the pipe [76]:

$$\dot{Q}_{loss} = \frac{2 \cdot \pi \cdot l \cdot (T_{fluid} - T_{ambient})}{\frac{1}{\lambda} ln\left(\frac{D + \frac{2 \cdot P_i}{100} \cdot D}{D}\right)} \quad (9)$$

The thermal capacity of the fluid, the pipe wall and the insulation can be calculated by:

$$mc_f = l \cdot (\frac{D}{2})^2 \cdot \pi \cdot \rho_f \cdot c_f \quad (10)$$

$$mc_w = l \cdot D \cdot \pi \cdot t_w \cdot \rho_w \cdot c_w \quad (11)$$

$$mc_i = l \cdot \left[(0.5 \cdot D + \frac{D \cdot P_i}{100})^2 - (0.5 \cdot D)^2\right] \cdot \pi \cdot \rho_i \cdot c_i \quad (12)$$

The delay time of the fluid particle and temperature information between inlet and outlet of the pipe is given by:

$$Del = \frac{l}{\frac{\dot{m}}{\left(\frac{D}{2}\right)^2 \cdot \pi \cdot \rho_f}} \quad (13)$$

The change of the internal energy of the fluid in the pipe is:

$$\dot{E}_{fluid} = (T_{in} - T_{out}) \cdot c_w \cdot \dot{m} \quad (14)$$

With the change in internal energy and the loss, the new outlet temperature of the pipe can be calculated by:

$$T_{fluid} = \int \frac{1}{mc_f + mc_w + 0.37 \cdot mc_i} \cdot (\dot{E}_{fluid} - \dot{Q}_{loss}) \delta t \quad (15)$$

with:

$c_{w,f,i}$	*specific thermal capacity of the pipe wall material, fluid or insulation*	*J/(kg·K)*
D	*inner diameter of the pipe*	*m*
Del	*time delay*	*s*
$\dot{E}_{fluid}$	*internal energy change of the fluid*	*W*
l	*length of the pipe*	*m*
λ	*heat loss coefficient of insulation*	*W/(m·K)*
$\dot{m}$	*mass flow in the pipe*	*kg/s*
$mc_{w,f,i}$	*mass times thermal capacity of the pipe wall, fluid or insulation*	*J/K*
P_i	*relative insulation thickness based on pipe diameter*	*%*

$\dot{Q}_{loss}$	*heat loss of the pipe*	*W*
$\rho_{w,f,i}$	*density of the pipe wall material, fluid or insulation*	*kg/m³*
$T_{ambient}$	*ambient temperature*	*°C*
T_{fluid}	*temperature of the fluid*	*°C*
t_w	*wall thickness of the pipe*	*m*

Another definition is to calculate the pipe as a one-node capacity along the pipe length. This results in the fact that a temperature gradient along the pipe length is not simulated in detail. In addition, the heating and cooling process of the pipe wall and insulation are neglected, as the temperature of these parts is assumed to be immediately at fluid temperature.

To realise the reversed flow in Simulink, the pipe model consists of a supply- and a return-pipe, merged in one block. Figure 64 shows the structure of this block. It is connected via the “Supply_in”, “Supply_out”, “Return_in” and “Return_out” ports to the superior model. Depending on the sign of the mass flow (positive = heat generation, negative = heat consumption), the “Switch” blocks conduct the information from the “Supply_in” port to the supply pipe and the “Supply_out” port for standard operation. During a decentralised feed-in, the return pipe is connected to the “Supply_in” and “Supply_out” ports to establish the reversed flow. The memory blocks are used to break algebraic loops by adding a one integration step time delay. As the time step is always below 10 s (approximately 3 s in average), this does not lead to a significant error in the simulation.

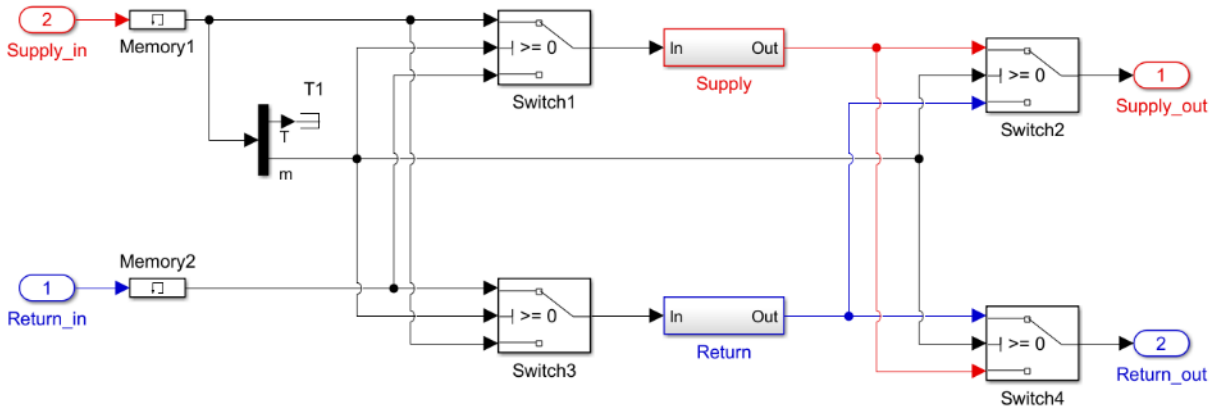

Figure 64: Pipe block with supply and return pipe and switches for change of the flow direction

Inside the “Supply” and “Return” blocks, the defined calculations are performed to emulate the pipe behaviour (Figure 65). The “Delay” sub-model takes the current mass flow of the fluid in the pipe, calculates the fluid velocity and, based on the pipe length, the transport delay from the inlet to the outlet. The temperature information at the inlet

is then kept for the calculated delay duration until the fluid is conducted to the “Q_loss” and the “E_pipe” block. These blocks represent the energy balance at the pipe (losses through insulation, stored internal energy due to fluid, pipe wall and insulation capacity). Integrating the sum of these two terms after multiplication with the total pipe capacity leads to the time-dependent outlet temperature. The same calculation is performed in the return pipe of the block.

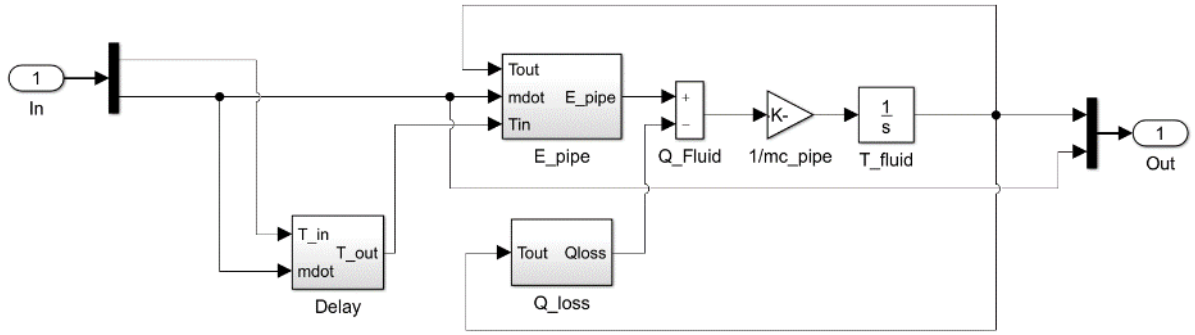

Figure 65: Layout of a single pipe component with time delay, energy loss, energy balance of inlet and outlet and thermal node of the pipe

5.2.4 Network Junctions

Besides the pipe model, the existing flow diverter and flow mixer models in CARNOT cannot handle changes of the flow direction. Therefore, a dedicated “junction” component is used for the pipe couplings of the network. As at every point in the network, there is a supply and a return temperature, this component has an “upper” and a “lower” node, representing these temperatures. The upper temperature is calculated as the mass-flow-weighted mean value of all incoming supply flows, whereas the lower temperature represents the mass-flow-weighted mean value of all incoming return flows. The decision of whether an incoming flow is directed to the upper or lower node depends on the sign of the mass flow. Similar to the pipe supply and return component, this is performed by switch blocks in the junction. As on the network level, the mass flows are calculated in a bottom-up approach from the single buildings back to the flow at the central heating station, the flow in branch one, connected to the junction is the sum of branch two and branch three:

$$\dot{m}_1 = \dot{m}_2 + \dot{m}_3 \tag{16}$$

$$T_U = \frac{T_1\dot{m}_{1U} + T_2\dot{m}_{2U} + T_3\dot{m}_{3U}}{\dot{m}_{1U} + \dot{m}_{2U} + \dot{m}_{3U}} \tag{17}$$

$$T_L = \frac{T_1\dot{m}_{1L} + T_2\dot{m}_{2L} + T_3\dot{m}_{3L}}{\dot{m}_{1L} + \dot{m}_{2L} + \dot{m}_{3L}} \tag{18}$$

with:

$\dot{m}_n$	*mass flow of the pipe connection n*	*kg/s*
$\dot{m}_{nL}$	*mass flow of the pipe connection n lower node*	*kg/s*
$\dot{m}_{nU}$	*mass flow of the pipe connection n upper node*	*kg/s*
$T_{1,2,3}$	*temperature at connection 1, 2, 3*	*°C*
T_L	*resulting temperature at lower node*	*°C*
T_U	*resulting temperature at upper node*	*°C*

Figure 66 shows the junction sub-model.

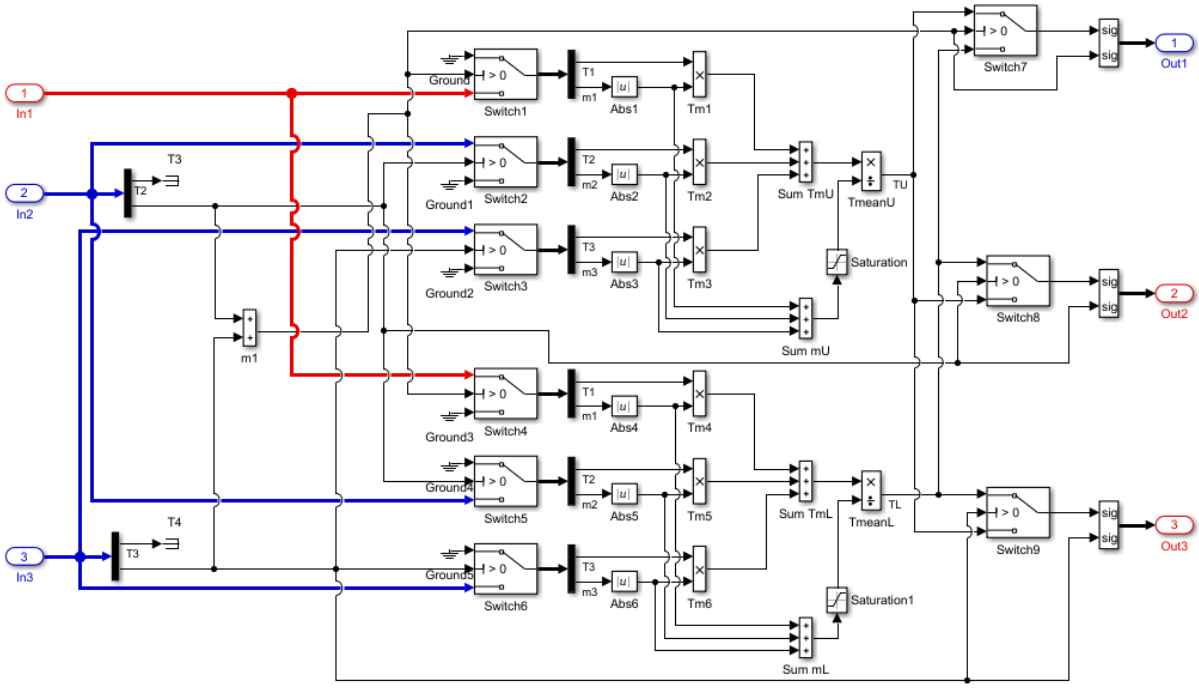

Figure 66: Sub-model of a network junction with flows at connection one resulting from the flows at connection two and three

5.2.5 Prosumers

The prosumers are composed of several main components:

- Building space heating model
- Hydraulic compensator as connection to the network
- Buffer (domestic hot water preheating) storage
- Domestic hot water storage
- Solar collectors
- Controller

The building model itself is based on the CARNOT one-node building. It has a single capacity and a heat transfer system from the space heating circuit to the building node.

The temperature from the weather data is taken to calculate the heat losses by conduction through the building's envelope and by ventilation losses. On top of that, the passive solar yields are calculated depending on the size and orientation of the windows. Further information on the parameters of the different buildings is given in section 6.1.1.

The connection of the modified network model to the CARNOT-based building models is realised by a hydraulic compensator that is based on the CARNOT storage model. Figure 67 shows the sub-model with the relevant connections for space heating, domestic hot water storage, solar thermal plant and the bidirectional connection to the district heating network. Inside this block, the same switch-based decision is performed as described for the pipe and the junction components, to allow a consumption from or a feed-in to the network. By selecting the storage connection heights (either a flow from top to bottom or vice-versa), the bidirectional flow is implemented.

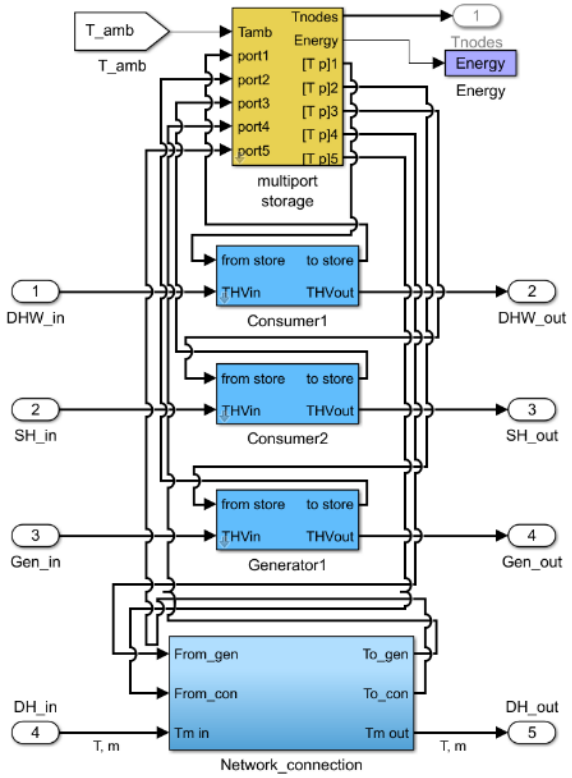

Figure 67: Substation between modified district heating network model and CARNOT-based building model with domestic hot water and space heating connections as well as solar heat geneartor and district heating connections

The buffer storages in the buildings are similar to the buffer in the central heating station besides the fact, that there are further connections for domestic hot water preheating and thermal disinfection, respectively energy transfer from buffer to domestic hot water storage (10 % to 90 % storage height). The third connection is for

the energy transfer between hydraulic compensator and buffer. Depending on the controller signal, the connection for feed-in to the network (bottom to top flow) or for loading the storage from the network (top to bottom flow) is selected.

The domestic hot water storage is fed by the preheated water from the buffer and additionally loaded by the network, if the temperature is below 58 °C. The loading is stopped at 62 °C. The thermal disinfection circuit is, like the drinking water, conducted from bottom to top, the network supply from top to bottom. To include the circulation losses in a multi-family building, a flow with a constant temperature loss is taken from the storage top and fed back at 77 % of the height.

Figure 68 shows the model of building 4 from the field test as basis for all substations in the optimisation model. Here, an additional small storage model below the hydraulic compensator is used to handle the feed-in to the return (cf. Table 17). For the other hydraulic approaches, this component is not necessary.

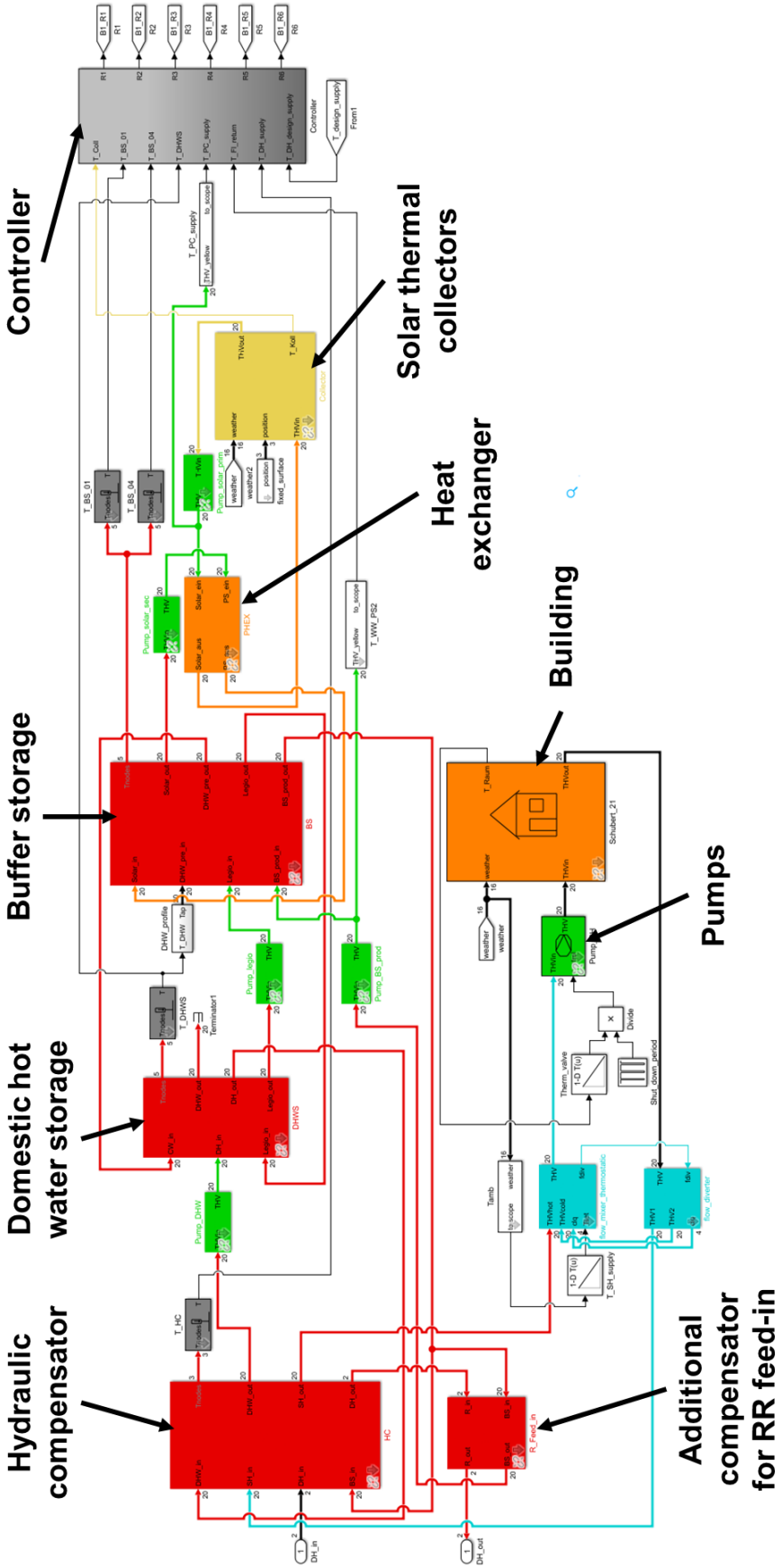

Figure 68: Model of building 4 with RR feed-in

5.2.6 Solar Thermal Plant and Controller

As shown in section 2.1.1, the power of a solar thermal collector depends on the irradiation on the collector surface and on the collector efficiency. The efficiency depends on the reduced temperature, which represents the difference between collector temperature and ambient temperature divided by the current irradiation. To describe the efficiency, a parabolic approximation according to EN 12975 [77] is used. The parameters for this approximation are determined in standardised test procedures, taking into account the incidence angle modifier (IAM). The IAM describes the reduction of incoming irradiation on the absorber surface by additional reflection at the collector glazing. The CARNOT toolbox provides a collector model including these parameters and the collector capacity to account for the system dynamics. A detailed description of this model can be found in [75].

The controller for each system is modelled in MATLAB/Stateflow. Like in the field test installation, the controller has several sensor inlets and relay outlets. The solar primary, secondary and the feed-in pump are speed-controlled and increase the volume flow in 10 % steps, starting at a minimum of 30 %, if the temperature difference between heat source and heat sink increases. This is as well analogous to the field test system.

5.3 Validation of the Pipe Model

5.3.1 Description of the Laboratory Test

While the network junctions and the connections between district heating network and buildings can be solved by a purely logical approach, the pipe model includes physical properties, which need to be examined in detail. Due to the choice of a one-node model for the pipe, the question arises of how the pipe performs under a sudden temperature change e.g. caused by a reversion of the flow direction. To answer this question, a laboratory test was set up to validate the pipe model. The layout of the test rig is shown in Figure 69. Main component of this test was a 2.12 m long copper pipe with an inner diameter of 20 mm and a wall thickness of 1 mm. The pipe was equipped with five thermocouples along the length and insulated with a 19 mm EPDM foam insulation. The parameters of the components are listed in Table 12. A computer-controlled thermostat maintained a constant temperature at the pipe inlet. A pump and a motorised valve were used to set the volume flow in the circuit. To get an immediate temperature load on the pipe, the heated water was conducted through a bypass tube in the first step (green arrow), while cold water was flowing through the pipe (blue

arrow). After starting the data logging, valve 2 and valve 1 were closed while valve 3 was opened and the 3-way-valve 4 set to connect the inlet with the pipe sample for starting the temperature load (red arrow). The temperatures of the inlet and outlet sensors as well as the five temperatures along the pipe and the ambient temperature were logged in a one-second interval. In addition, the volume flow was monitored with a magnetic flow meter.

Table 12: Parameters of the laboratory test for validating the pipe model

Length of pipe in m	2.12
Inner diameter of pipe in mm	20
Wall thickness of pipe in mm	1
Thickness of insulation in mm	19
Thermal conductivity of insulation in W/(m·K)	0.04
Temperature sensor inlet / outlet	PT100 4-wire 1/10 DIN EN 60751
Pipe temperature sensors	Thermocouple type T

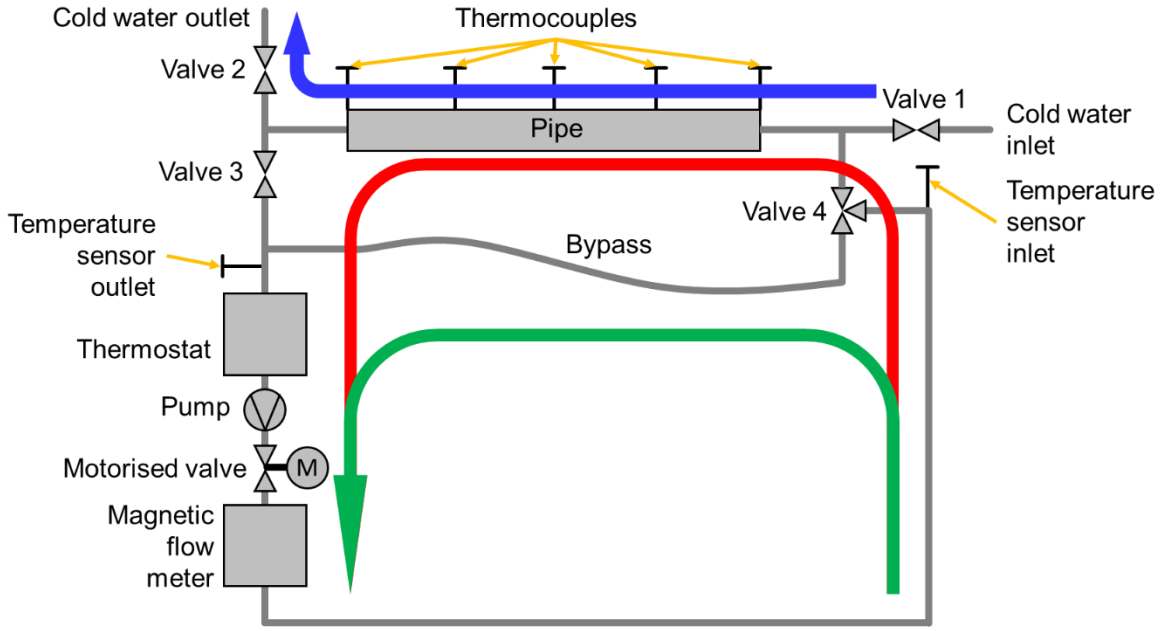

Figure 69: Layout of the test rig for validating the pipe model

Two test cases were defined to validate the model at different conditions. The conditions of these tests are listed in Table 13. In the test “Step Response”, the step response of the pipe was tested at a volume flow of 150 l/h and a sudden inlet temperature change from 22 °C to 47 °C. In the test “Heat Loss”, the pipe was heated up to 70 °C and then the volume flow set to zero to observe the cooling behaviour.

Table 13: Conditions of the laboratory test for validating the pipe model

Test name	Initial temperature in °C	Inlet temperature in °C	Volume flow in l/h
Step Response	22	47	150
Heat Loss	71	-	-

5.3.2 Assessment of the Model

The most interesting results of the first test are the time delay of the temperature change along the pipe length and the shape of the temperature curve after the heating process starts. Figure 70 shows the comparison of the temperature sensors of the measurement and the outlet temperature of the simulation model for the scenario of a sudden inlet temperature increase from 22 to 47 °C. The curve “Inlet” describes the measured temperature step at the inlet, which was set as inlet temperature for the simulation. “Outlet Measured” is the measured value of the temperature at the outlet of the pipe.

For the CARNOT pipe, two models were simulated. The first one has only one node (“Outlet CARNOT 1 Node”). This leads to an instant but slow temperature increase at the outlet. The second model with 100 nodes along the pipe length (“Outlet CARNOT 100 Nodes”) describes the time delay very well but shows a too steep temperature increase when the hot fluid reaches the outlet-node. No node number could be found, for which the time delay and the slope of the curve fitted the measured data. While the heating of the newly set up model (“Outlet New Model”) is not as steep as for the real pipe, it still fits the measured curve better than the CARNOT model. The fractional capacity of the insulation, as described in 5.2.3, was also added to the capacity of the pipe wall in the CARNOT models for better comparison.

Another important information when discussing the control strategy of the district heating network is the stored energy in the pipes. Figure 71 shows this energy for the measured pipe, the CARNOT pipes (1 node and 100 nodes) and the new model. As expected from the faster temperature increase at the outlet, the CARNOT pipe model stores less energy than the measured pipe. The new model calculates slightly higher energies within the period of observation but differs by only 6.3 % in this case according to equation (19):

$$f_{Energy} = \frac{E_{pipe,simulated} - E_{pipe,measured}}{E_{pipe,measured}} \qquad (19)$$

with:

$E_{pipe,measured}$	*measured final energy of the pipe*	*kJ*
$E_{pipe,simulated}$	*simulated final energy of the pipe*	*kJ*
f_{Energy}	*relative error of the final thermal energy*	*%*

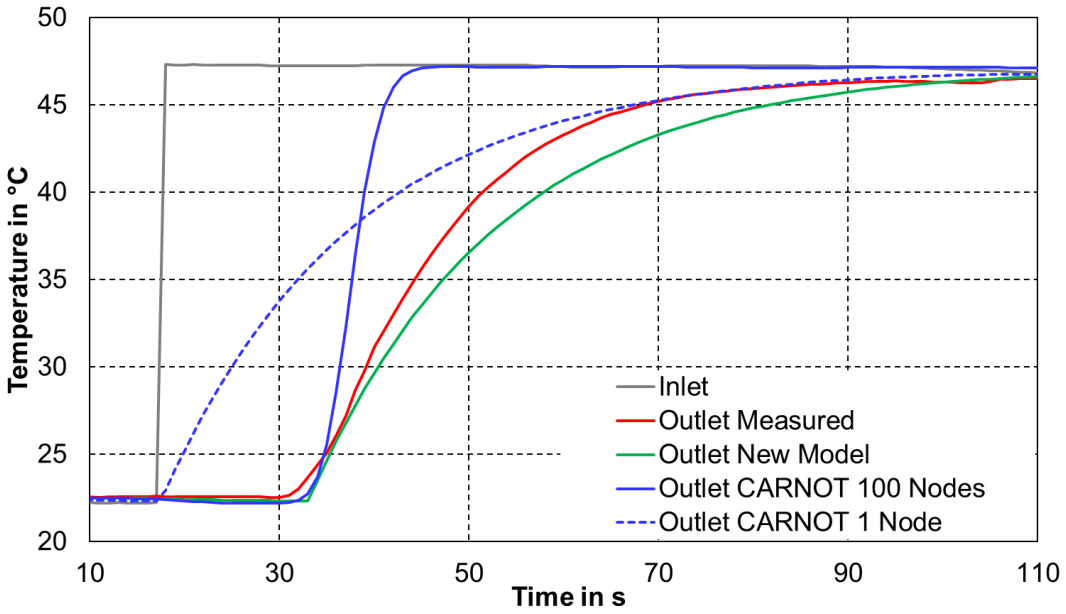

Figure 70: Temperature curves over time for the step response from 22 to 47 °C

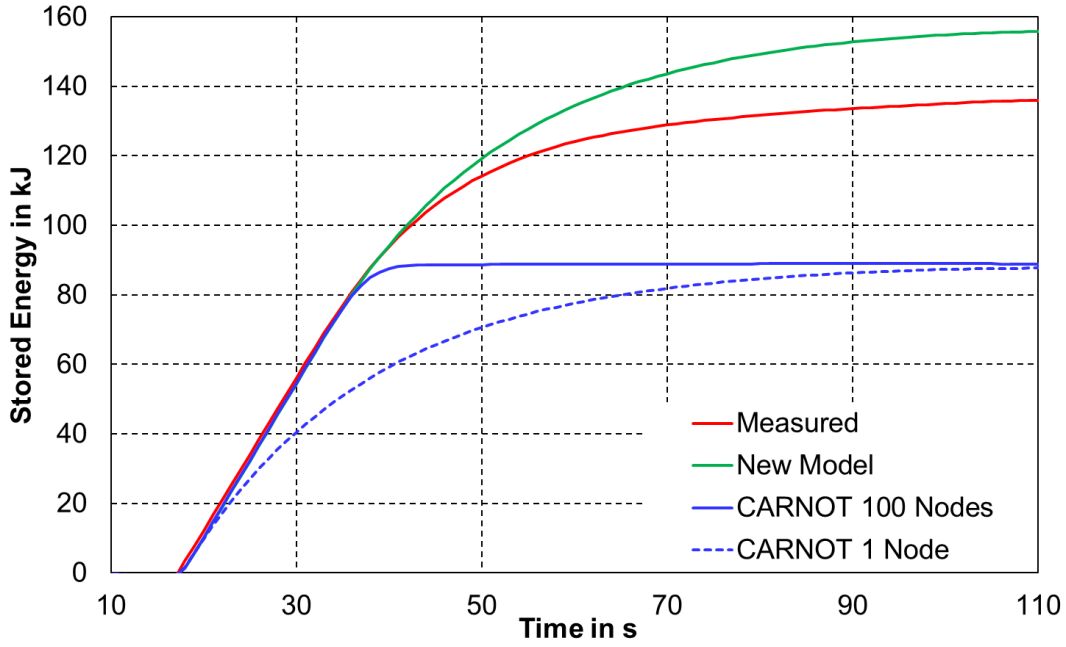

Figure 71: Stored energy over time for the step response from 22 to 47 °C

The third important point is the calculation of the heat losses in the district heating network. The pipe in the laboratory test was heated up to a constant temperature of 71 °C and then cooled down by the losses through the insulation for approximately 50 minutes. The temperature decrease of the sensor in the centre of the pipe was

evaluated. It revealed that both models are within acceptable tolerance and the temperature loss is 0.8 % too low respectively 1.7 % too high for the new model and the CARNOT model according to following equation:

$$f_{Temp} = \frac{T_{pipe,simulated} - T_{pipe,measured}}{T_{pipe,measured}} \qquad (20)$$

with:

f_{Temp}	*relative error of the final pipe temperature*	*%*
$T_{pipe,measured}$	*measured final pipe temperature*	*°C*
$T_{pipe,simulated}$	*simulated final pipe temperature*	*°C*

5.4 Setup of the System Model

As the goal of this work package was to define a Simulink-based model for the investigation of intelligent feed-in concepts under various boundary conditions, a final simulation-based validation with the operational network, introduced in section 4, is discussed. While in this network, only an RR feed-in could be implemented, the simulation model allows additional investigations of the influence of an RS feed-in and larger solar thermal plants. The following designs are compared based on a one-year simulation of the complete network:

- Type 1: Model of the field test system and RR feed-in based on CARNOT toolbox
- Type 2: Model of the field test system and RR feed-in based on new components
- Type 3: Model of the field test system and RS feed-in based on new components

Type 1 represents the existing, operational network, using only CARNOT components. The operation strategy and the solar thermal plants are designed like in reality. The model is valid, as introduced in section 4. Type 2 is the same but using the modified model components for the network. Type 3 is based on type 2 but includes the change from RR feed-in to RS feed-in for the plants with combined utilisation, while the pure feed-in plant (building 2) keeps the RR concept. Nevertheless, the network operation and plant dimensions are still the same.

For this comparison, average climate data for Ingolstadt were used. The thermal load in the district heating network is equal to the model validation. Table 14 shows the solar yields for the plants of all types and their contribution to the heat production of the complete network. Several conclusions can be drawn from the simulation results:

- Firstly, due to the modified pipe components and resulting variations in the temperatures of the network, there is a difference of the solar yield between the

pure CARNOT model and the modified model of 1.6 %. This is considered as acceptable within the scope of this work and taking into account the measurement accuracy.

- Secondly, RS feed-in has no significant benefit over the less complex RR feed-in in case of the investigated network. It increases the solar fraction from 2.63 % to 2.65 %.

Table 14: Annual solar yield and solar fraction of decentralised plants of the simulated system types

	Annual solar yield Building 1 in MWh	**Annual solar yield Building 2 in MWh**	**Annual solar yield Building 3 in MWh**	**Annual solar yield Building 4 in MWh**	**Fossil heat production in MWh**	**Solar fraction in %**
Type 1	42.5	16.9	31.8	26.6	4,289	2.67
Type 2	42.5	16.6	31.1	25.9	4,299	2.63
Type 3	42.5	16.6	31.6	26.2	4,294	2.65

From these results it can be seen, that besides the initial pure CARNOT model, also the modified model shows a good correlation to the metrological data of the field test network. The optimisations in section 6 were conducted based on this model.

While all plant types of the operational network were validated, it is sufficient to focus on building 4 for the further investigation, as this building represents the integration concept with local use and feed-in of solar heat. From the validated model to the model for the optimisation study, some additional definitions were applied:

- No pipe heat losses of solar circuit but higher pump and plate heat exchanger losses
- Linear increase of pump volume flow as well as heat transfer coefficients of plate heat exchangers with increasing number of collectors
- No shading simulation and no separation of single collector arrays, as roofs are assumed to be steep saddled roofs
- Enhancement of controller functions for further investigations and RS feed-in
- Height-diameter ratio of buffer storages 3:1 for all storage volumes
- Heat losses of storages set to design data (insulation thickness times heat conductivity of insulation material)

6 Optimisation

After describing a modified simulation model for the set-up of systems with RS feed-in and the analysis of the RS feed-in in the field test object, an additional study on a fictional network is introduced. Basic scenarios are shown with different sizing of collector arrays and buffer storages as well as different collector orientations. For the most suitable plant dimensions, a further parametric study reveals the effect of an uneven distribution of the solar thermal systems across the district and variations of climate, consumption and district size. In a final step, optimised control strategies are tested on this district.

6.1 Methodology

6.1.1 Definition of Boundary Conditions

To get an idea of the range of possible benefits of the decentralised solar heat production, two types of buildings, interconnected by a district heating network were defined. As shown in Figure 3, a large number of multi-family buildings was built in the 1960´s and 1970´s with an average annual heat demand of 155 – 185 kWh/m². On the other hand, buildings from the early 2000s on (class J in the figure) have to fulfil harder legislative restrictions and therefore have a lower annual demand of 80 kWh/m² or even less. Although the renovation rate is on a low level, it can be expected, that older buildings will be optimised in future regarding their heat demand, as this is an obligatory addition to non-energetic measures like the installation of new windows, new roof envelopes or new plastering. This is particularly the case in combination with the retrofitting of the heating system, making it relevant to account for these building types, too.

Therefore, two energetic standards were defined for the simulation study. The first is denoted “1970” or “non-renovated” with typical heat transfer values of the envelope of that time. The second is a “renovated” version of the same building with additional insulation of roof, walls, bottom (respectively basement ceiling) and substitution of the windows according to the current legislative regulations for a substitution of these parts (“2010”). The building is based on the data of building 4 from the investigated field test network, which represents the heat demand of the renovation variant. As most of the buildings according to Figure 3 are in the range of up to 12 residential units, this is considered to represent a large amount of the existing multi-family homes. Table 15 gives the relevant data for the building types.

Table 15: Overview of investigated buildings

	1970 (non-renovated)	2010 (renovated)
Number of residential units	12	12
Length in m	30	30
Width in m	11	11
Height in m	12	12
Heat transfer walls in W/(m²·K)	0.8	0.24
Heat transfer roof in W/(m²·K)	0.8	0.24
Heat transfer bottom in W/(m²·K)	0.8	0.3
Heat transfer windows in W/(m²·K)	1.6	1.3
Area of windows (south, east, north, west) in m²	40, 5, 40, 5	40, 5, 40, 5
Space heating max. supply temperature in °C	75	50
Space heating max. mass flow in kg/s	0.8	0.4
Heat transfer radiators in kW/K	1.4	1.4
Ventilation rate in 1/h	0.38	0.38
Thermal capacity in MJ/K	700	700
Internal gains in kW	6.3	6.3
Space heating demand in MWh	109	34
Domestic hot water tapping in MWh	22.5	22.5
Circulation losses in MWh	13.5	13.5
Specific total heat demand in kWh/m²	115	56
Max/min supply temperature DH in °C	80/65	65/65

According to [78], smaller district heating networks in Germany with less than 1 km piping length account only for 1.6 % of the supplied heat, while larger systems of more than 100 km length account for 86 %. On the other hand, the number of these small systems is very high with 823 compared to 38 systems of more than 100 km. Besides these numbers, many small networks, connecting only several buildings are in operation.

Against this background, a system was set up for the simulation-based investigation with five buildings of 12 residential units. The number of buildings was chosen, as it is the necessary minimum number to set up all variants of different plant distributions. On the other hand, more connected buildings do not necessarily improve the validity of the results. The heat source can be considered as either the central heating station of this small network or a connection to a larger district heating system. Figure 72 shows a scheme of the network with all investigated variations.

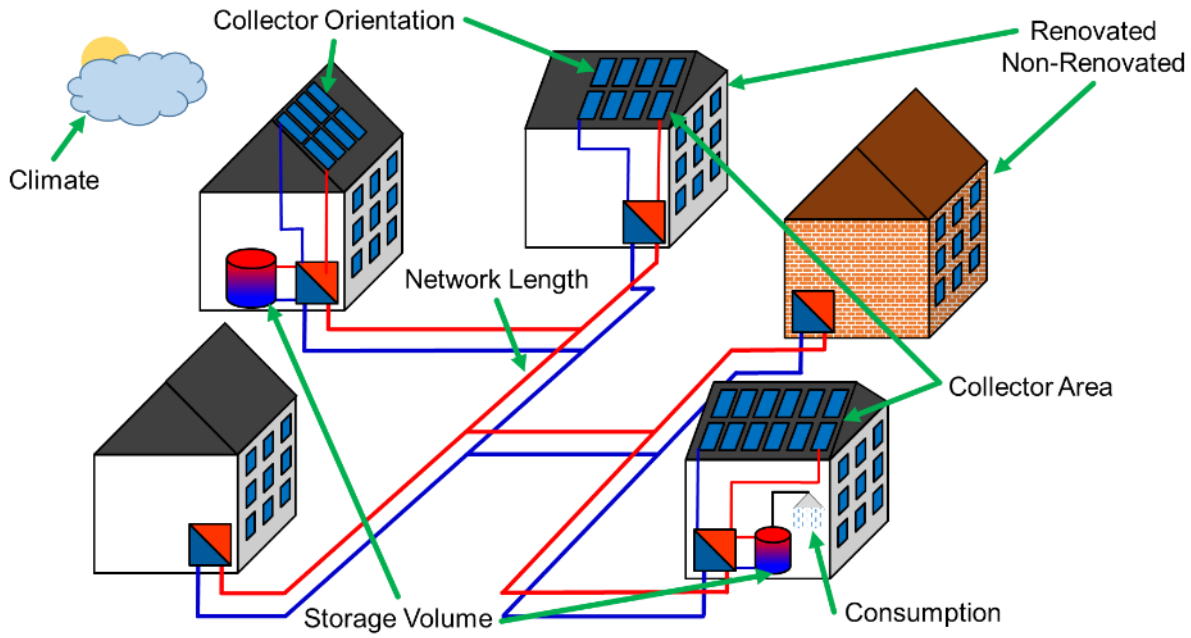

Figure 72: Structure and variations of the investigated district heating network

The space heating is transmitted by a radiator system (high temperature level) for the buildings with high heat demand. The supply temperature of these radiators can be reduced for the renovated buildings due to the lower heat load from 75 °C to 50 °C. The type of domestic hot water production is the same for both variants, meaning that a domestic hot water storage is installed in the buildings, which is kept at 60 °C throughout the year. Although an alternative legionella prevention by a reduced supply temperature in the network and a decentralised domestic hot water production in the flats can improve the integration of low temperature heat sources, it is not considered in this investigation as there is already a lot of literature available on this topic, as well as on other optimisations of the substations (e.g. [13, 79]). Instead, the coupled control of heat producers and storages is used to enable a temporary shutdown of the network during the times, when domestic hot water storages are not loaded. This makes the approach suitable for retrofitting purposes, as the interior piping of the buildings can be kept in the original layout.

6.1.2 Sensitivity Analysis

To prevent incorrect statements drawn from the comparison of the variants, each variant has to be optimised in the possible range of the plant design and dimensioning. This includes sufficient heat transfer of the heat exchangers, pump volume flows and temperature threshold of the controllers for activating and deactivating the pumps in the solar thermal system. A sensitivity analysis was therefore performed for each hydraulic scheme and one sizing variant of collector area and buffer volume. All the parameters were tested in a range of ± 10 % around the design value. The design

value itself was taken from the experience gained during the setup and operation of the field test installation in Ingolstadt. Each of the parameter variations was tested in a characteristic summer and winter week to examine the influence of the different weather conditions during a year.

Table 16 gives an overview of the influence of the variation of these parameters on all hydraulic systems. It can be seen, that no relevant change in the solar yield occurs. This indicates that the results are very stable around the selected parameters and no faulty design was chosen.

Table 16: Results of the sensitivity analysis for the basic variants

		Winter week		Summer week	
		Solar yield in kWh	**Change in %**	**Solar yield in kWh**	**Change in %**
Central plant with 205 m² collector area and 10 m³ buffer					
	Basis	682.9	-	2,369.4	-
Temperature threshold	**-10 %**	682.5	-0.05	2,372.0	+0.11
	+10 %	681.7	-0.17	2,363.4	-0.25
Volume flow	**-10 %**	682.5	-0.05	2,365.2	-0.18
	+10 %	681.7	-0.17	2,365.2	-0.18
Heat transfer heat exchanger	**-10 %**	679.7	-0.46	2,360.8	-0.36
	+10 %	685.0	+0.32	2,369.9	+0.02
Decentralised domestic hot water preheating with 41 m² collector area and 1 m³ buffer per building					
	Basis	888.2	-	2,199.5	-
Temperature threshold	**-10 %**	890.5	+0.26	2,200.5	+0.05
	+10 %	883.2	-0.56	2,198.9	-0.02
Volume flow	**-10 %**	890.9	+0.31	2,203.1	+0.17
	+10 %	884.5	-0.41	2,194.9	-0.21
Heat transfer heat exchanger	**-10 %**	885.7	-0.28	2,196.7	-0.13
	+10 %	890.4	+0.25	2,201.3	+0.08
Decentralised RR-feed-in with 82 m² collector area and 2 m³ buffer per building					
	Basis	1,471.8	-	3,436.8	-
Temperature threshold	**-10 %**	1,475.0	+0.21	3,452.4	+0.45
	+10 %	1,463.6	-0.56	3,440.5	+0.11
Volume flow	**-10 %**	1,476.2	+0.29	3,443.3	+0.19
	+10 %	1,466.7	-0.35	3,433.2	-0.11
Heat transfer heat exchanger	**-10 %**	1,468.4	-0.24	3,437.8	+0.03
	+10 %	1,475.2	+0.23	3,445.1	+0.24

Decentralised RS-feed-in with 82 m² collector area and 2 m³ buffer per building					
	Basis	1472.2	-	3476.0	-
Temperature threshold	**-10 %**	1475.2	+0.21	3487.7	+0.34
	+10 %	1463.4	-0.59	3471.6	-0.13
Volume flow	**-10 %**	1476.1	+0.27	3500.6	+0.71
	+10 %	1466.9	-0.36	3476.9	+0.03
Heat transfer heat exchanger	**-10 %**	1468.4	-0.26	3477.3	+0.04
	+10 %	1475.3	+0.21	3482.0	+0.17

6.1.3 Hydraulic Schemes and Method of Assessment

For all considered variants, an energy balance is derived for one year of operation. All relevant heat flows are considered. The assessment of the variants is done by the fractional fossil energy savings, which are defined as:

$$f_{Sav} = \frac{E_{generation} - E_{generation\_with\_solar}}{E_{generation}} \qquad (21)$$

with:

$E_{generation}$	*heat generation at central heating station without solar thermal plants*	*kWh*
$E_{generation\_with\_solar}$	*heat generation at central heating station with solar thermal plants*	*kWh*
f_{Sav}	*fractional fossil energy savings of the solar assisted system*	*%*

Having a closer look on the different hydraulic variants with decentralised solar thermal plants, the energy flows can be comprehended. For all five buildings in the basic network (cf. section 6.2), this flow is very similar, as all have the same consumption and the same installed collector area and buffer volume. There is only a slight increase in the feed-in of the energy from the building closest to the central heating station to the building at the end of the network, as the average temperature in the network is lower there due to the network losses.

The top left scheme in Table 17 shows a Sankey diagram of the heat flow in building 1 of the variant with 82 m² collector area, 2 m³ buffer volume and RS feed-in for the non-renovated district. The collectors produce 27.7 MWh of heat. 122.6 MWh have to be provided by the network. The highest fraction (18.8 MWh) of the solar heat is transferred to the domestic hot water via pre-heating. 3.6 MWh are shifted to the domestic hot water storage by the thermal disinfection pump. This pump transfers heat from the buffer to the domestic hot water tank in case of an overheating of the buffer.

From the remaining energy, a part is transferred to the substation and a part compensates for the thermal losses of the storage. The domestic hot water storage as well as the buffer lose 0.8 MWh. 14.5 MWh of the energy needed for the domestic hot water and circulation system cannot be provided by the solar thermal plant and are taken from the district heating network. The space heating accounts for 109.1 MWh. From the 4.7 MWh transferred to the substation, 0.9 MWh are consumed by the building itself, 3.8 MWh are fed into the network. The feed-in is very low in this variant, as all buildings in the network produce their own solar heat and the feed-in can only be considered as a storing of energy in the network by increasing the supply temperature and a compensation of network heat losses. For variants where the collector areas are not equal in each building, the feed-in increases (section 6.2.7).

The top right scheme shows the same variant without buffer storage. The different options of transferring heat in the system can in reality be kept the same by installing a plate heat exchanger instead of the buffer for the hot water preheating. In the simulation model, this is simplified by reducing the storage volume to an amount of 50 l to account for the capacities of heat exchanger and piping.

For the other hydraulic schemes, including the central heating station, exemplary energy flows are depicted in the following cells of Table 17. For the RR variant, it can be seen, that the connection between buffer and district heating is at the return connection of the building and not directly at the hydraulic compensator, which impedes a local use of the excess heat for e.g. space heating. The dotted connections represent a switching of the connections during the loading process of the buffer with excess heat from the network, which enables a top to bottom loading. This is automatically done for the RS scheme.

Table 17: Overview of variants with energy flows for one sizing of collectors and buffers in the non-renovated district, numbers show the annual heat transfer in MWh

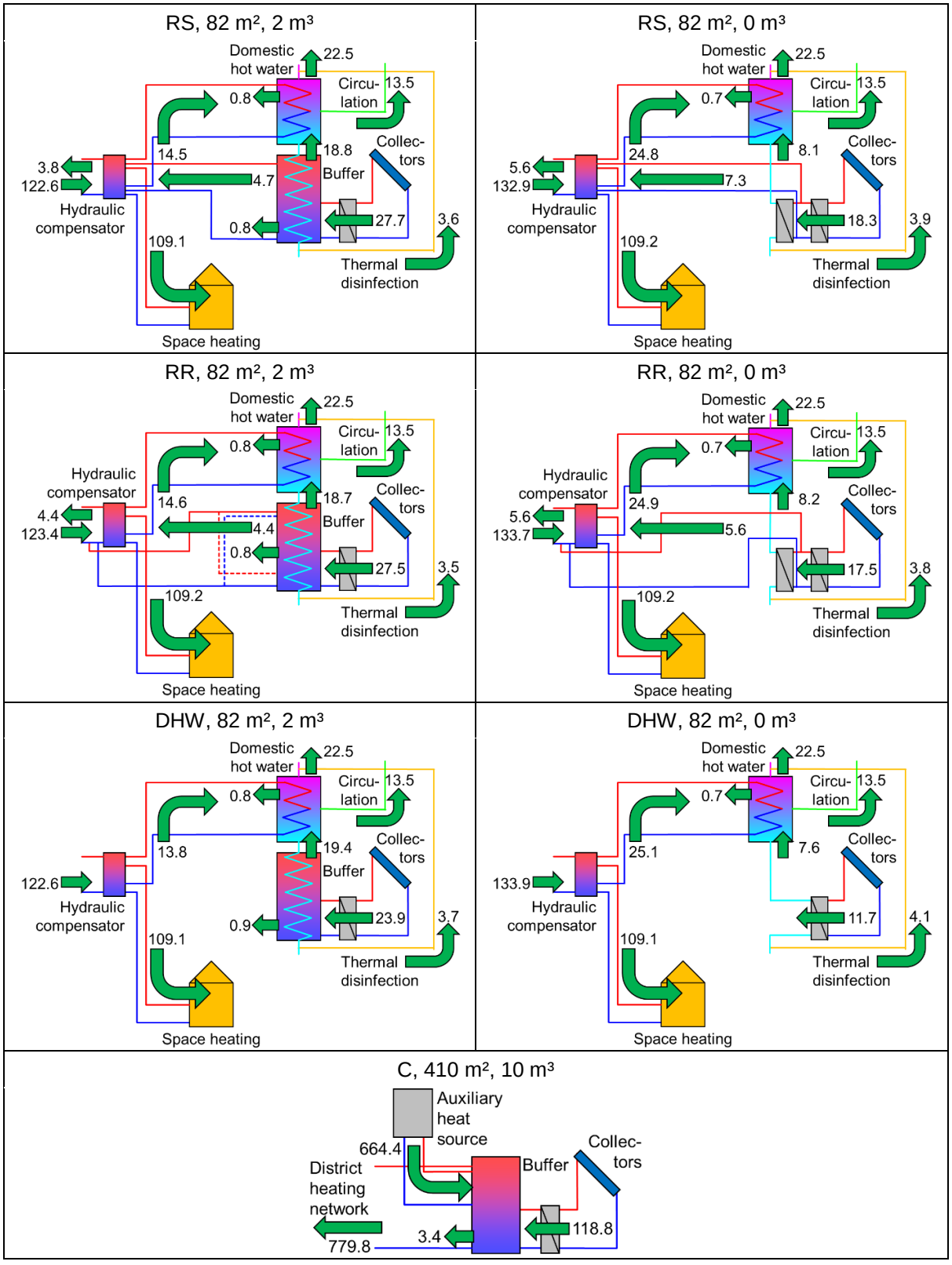

6.2 Basic Variants

6.2.1 Overview of Variants

To examine the differences of the hydraulic integration concepts, a basic district is defined to test several variations of the plant design and dimensioning. Standard configurations of solar thermal plants in a district are decentralised plants for local use or central plants for pure feed-in to the district heating network. These, in addition to the complete abdication of solar thermal energy, are the concurrent solutions, the smart solar district heating approach has to compete with. Table 18 gives an overview of the variants for the initial design, which serve as basis for the following analysis.

Table 18: Parameters for the basic study

	Collector area in m²	**Buffer volume in m³**
Central solar thermal plant (C)	0, 205, 410, 820	0, 10, 20
Decentralised domestic hot water systems (DHW)	5 x (0, 41, 82, 164)	5 x (0, 2, 4)
Decentralised system with local domestic hot water preheating and RR feed-in (RR)	5 x (0, 41, 82, 164)	5 x (0, 2, 4)
Decentralised system with local domestic hot water preheating, partial space heating and RS feed-in (RS)	5 x (0, 41, 82, 164)	5 x (0, 2, 4)

For the investigation, the same flat plate collector as in the field test study site was used (Table 2). This type has a gross area of 2.57 m², leading to total areas of 41 m², 82 m² and 164 m² for the decentralised systems respectively 206 m², 411 m² and 822 m² for the central plant (denoted 205, 410 and 820).

6.2.2 Central Plant

A central solar thermal plant is one of the most common approaches for the solarisation of district heating networks. While the installation of such a system is not possible in every district, it is still one of the benchmarks, the smart district heating approach has to compete with. To compare the decentralised solution with this system design, a simulation study was done with 0 m³, 10 m³ and 20 m³ of central buffer volume in combination with 0 m², 205 m², 410 m² and 820 m² collector area installed at the central heating station. The design and operation of the central heating station is described in section 5.

Non-Renovated District

Figure 73 shows the savings in fossil energy for the district with non-renovated buildings. The maximum saving is 21.9 % for the variant with 820 m² collector area and 20 m³ buffer volume. By reducing the buffer volume to 10 m³, a saving of 17.6 % is possible, which is on the same level of the variant with 410 m² collector area and 20 m³ buffer. Without any buffer, only a small fraction of the possible solar yield can be used during summer as the network cannot consume the energy and stagnation occurs. The savings go down to 10.3 % for 820 m².

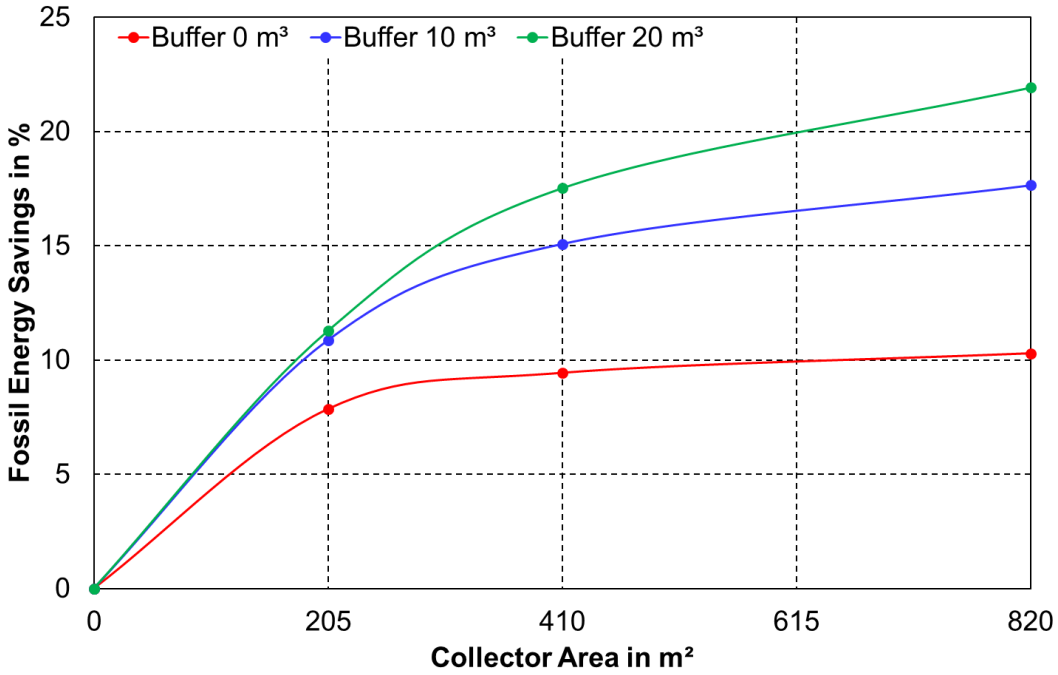

Figure 73: Fossil energy savings for central solar thermal plants in the non-renovated district

Table 19 shows the annual specific yield of the plants, based on the gross area of the collectors. These range between 96 kWh/m² and 437 kWh/m². The results show, that even the installation of a small buffer storage leads to a significant increase of the system efficiency and the solar yield.

Table 19: Specific annual yield of the central solar thermal plants in the non-renovated district in kWh/m²

		Buffer volume in m³		
		0	**10**	**20**
Collector area in m²	**205**	288	415	437
	410	175	289	340
	820	96	170	213

Renovated District

For the renovated buildings, some modifications have been done to the heat supply system. As already mentioned, the supply temperature of the space heating was decreased from a maximum of 75 °C to 50 °C. Therefore, the supply temperature of the district heating network can be reduced from a range between 65 °C and 80 °C to a constant level of 65 °C, which is sufficient to supply the domestic hot water as well as the space heating. Like for the non-renovated buildings, a variety of collector numbers and buffer volumes was tested.

The central plant concepts show savings in fossil energy between 11.8 % and 37.1 % (Figure 74). There is a significantly flat correlation between collectors and energy savings, if there is no storage installed. Due to the lower demand of the quarter, the collectors often reach the maximum temperature, where the controller shuts down the system. Nevertheless, for the variants with storage higher relative savings can be reached than for the non-renovated system

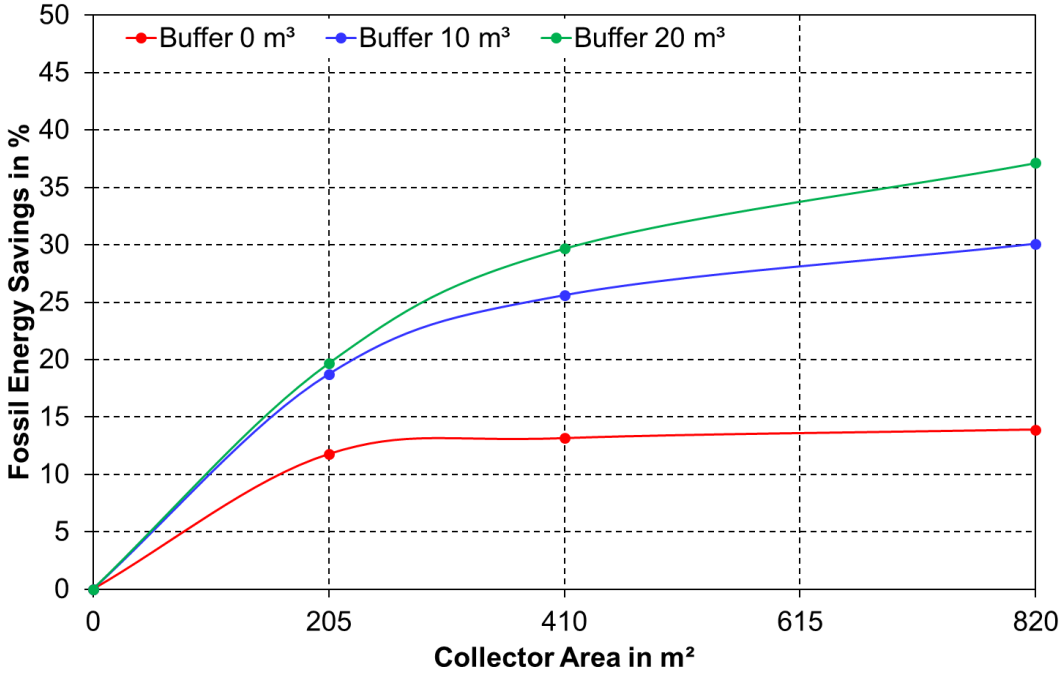

Figure 74: Fossil energy savings for central solar thermal plants in the renovated district

Table 20 shows the annual specific yield of the variants. These range between 67 kWh/m² and 397 kWh/m². It is visible, that the specific yield goes down compared to the non-renovated district due the reduced utilisation by the more efficient buildings.

Table 20: Specific annual yield of the central solar thermal plants in the renovated district in kWh/m²

		Buffer volume in m³		
		0	**10**	**20**
Collector area in m²	**205**	223	372	397
	410	126	255	300
	820	67	151	188

6.2.3 Decentralised Domestic Hot Water Production

The second widely spread integration variant for solar thermal plants is a pure domestic hot water production. Like described for the existing plants in section 4, a domestic hot water preheating was investigated in the parametric study. As the collector area for pure domestic hot water plants is smaller than for additional space heating supply, the smallest variant with 41 m² can be considered as a standard design, resulting in 1.4 m² per habitant, while larger collector arrays are oversized.

Non-Renovated District

Figure 75 shows the fossil energy savings for all non-renovated variants. The collector area and the installed buffer volume is given per building. This means, that in total five times the stated number respectively volume is installed in the complete district, which results in the same overall sizing as in the central integration variants. The maximum fossil energy saving is 19.9 % for 164 m² and 4 m³ per building. However, even for the standard layout with 41 m² and 2 m³ already 12.0 % are reached, meaning 51 % solar fraction of the domestic hot water and circulation consumption.

Table 21 shows the annual specific yield of the plants. These lie in the range of 76 kWh/m² to 466 kWh/m². As the solar heat cannot be transferred to other consumers in the network for this hydraulic layout, the disadvantage of the abdication of a storage has a higher influence on the yield than for the central integration. On the other hand, an extension of the volume from 2 to 4 m³ only leads to a small improvement.

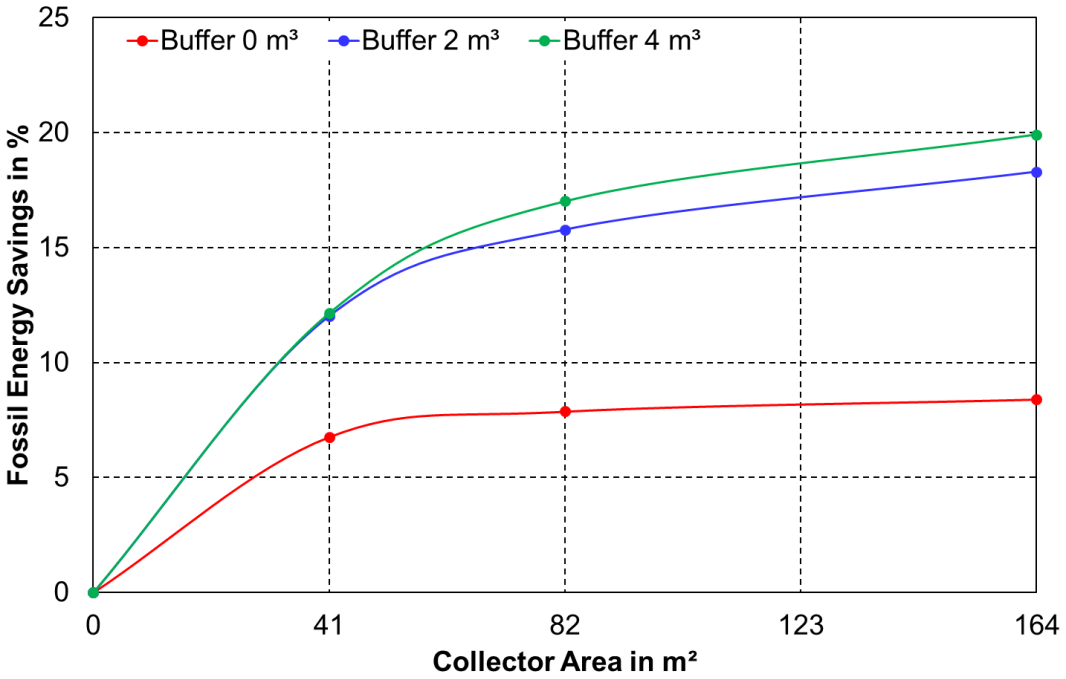

Figure 75: Fossil energy savings for decentralised domestic hot water plants in the non-renovated district

Table 21: Specific annual yield of the decentralised domestic hot water plants in the non-renovated district in kWh/m²

		Buffer volume in m³		
		0	**2**	**4**
Collector area in m²	**41**	245	450	466
	82	142	290	318
	164	76	167	185

Renovated District

The pure domestic hot water preheating in the renovated district shows savings in fossil energy between 12.8 % and 39.8 % (Figure 76), meaning up to 84 % solar fraction of the domestic hot water consumption. Like for the central system, a flat shape of the curve without buffer storage is obvious.

Table 22 shows the annual specific yield of the variants. These range between 74 kWh/m² and 466 kWh/m². As there is no relevant influence of the network temperature and the space heating demand on the hot water preheating, these values are almost the same like for the non-renovated system.

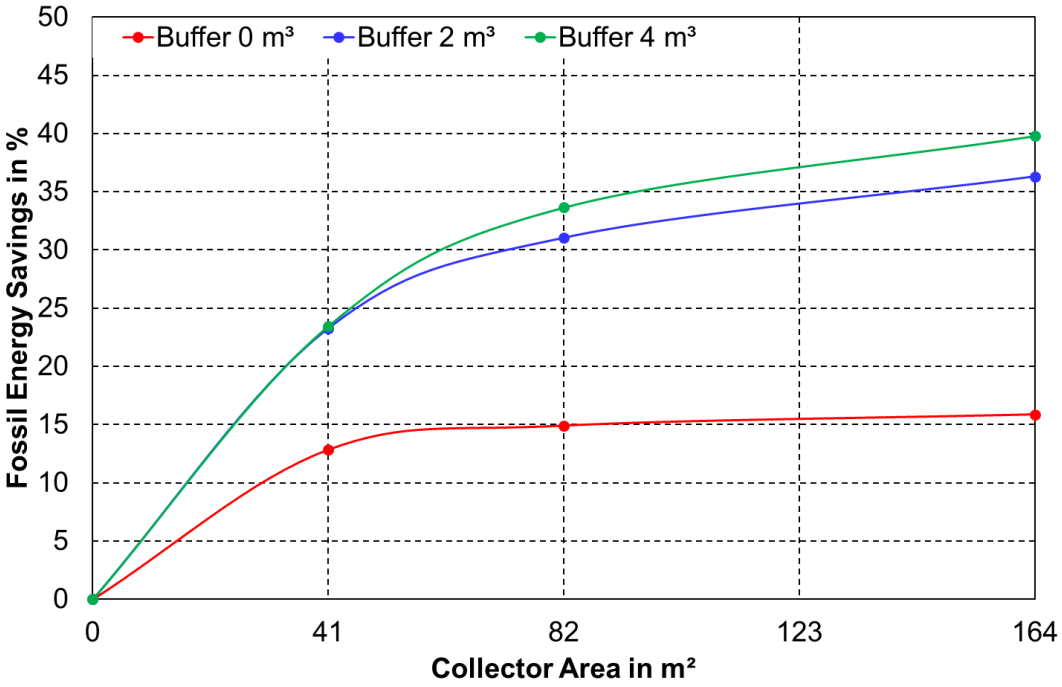

Figure 76: Fossil energy savings for decentralised domestic hot water plants in the renovated district

Table 22: Specific annual yield of the decentralised domestic hot water plants in the renovated district in kWh/m²

		Buffer volume in m³		
		0	**2**	**4**
Collector area in m²	**41**	243	449	466
	82	140	290	318
	164	74	166	185

6.2.4 RR Feed-in

The simpler variant of decentralised feed-in, which was also selected for the study site in Ingolstadt, is the RR feed-in. The same type of system was set up for the parametric study and simulated with the same collector areas and storage volumes like the pure domestic hot water variant.

Non-Renovated District

Figure 77 shows the fossil energy savings for all simulations of the non-renovated district. Again, the collector area and the buffer volume are given per building. The maximum fossil energy saving is 22.9 % for 164 m² collector area and 4 m³ buffer volume per building. The variants with 2 m³ show almost the same performance, while the variants without any storage are much more inefficient, regardless of the additional

possibility of a feed-in to the network and therefore extended consumption and storage capacities.

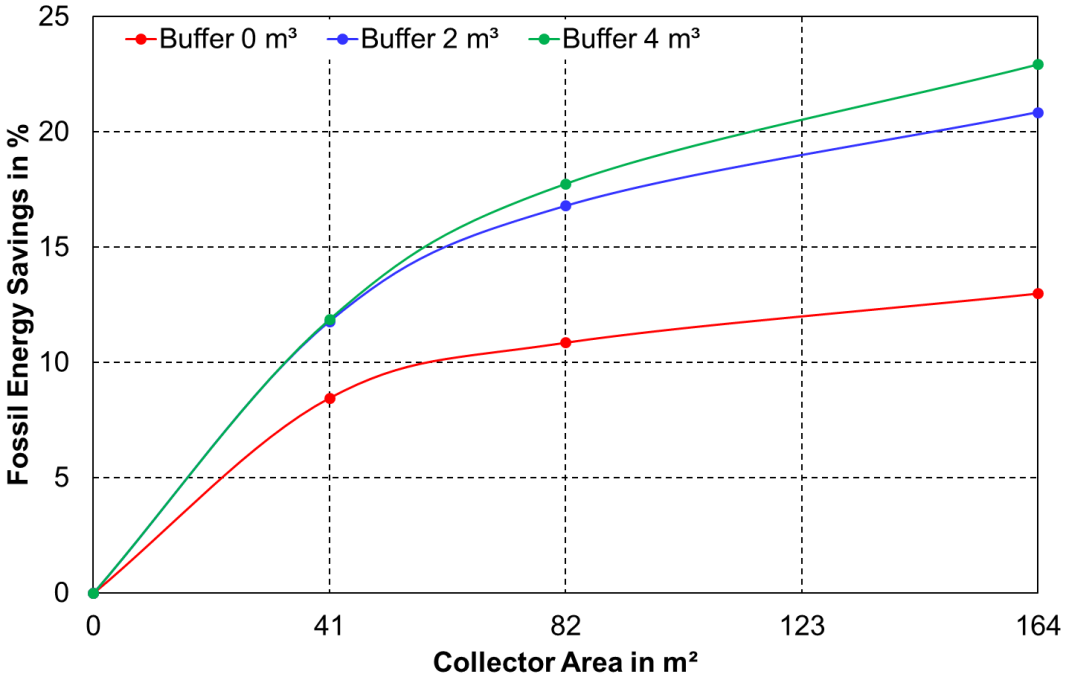

Figure 77: Fossil energy savings for decentralised plants with RR feed-in in the non-renovated district

Table 23 shows the annual specific yield of the plants. These range between 131 kWh/m² and 471 kWh/m². It is obvious, that for all variants, the RR feed-in improves the performance of the plants compared to the pure domestic hot water system as it allows to transfer excess heat to the district heating network that would otherwise be lost due to stagnation of the collector array. This is in particular true for the variants without storage. Nevertheless, the fossil energy savings are not significantly higher than for the domestic hot water system, as all buildings in the network produce excess heat at the same time, meaning that the additional solar yields result primarily in higher network losses and not in a consumption of the energy by the inhabitants.

Table 23: Specific annual yield of the decentralised plants with RR feed-in in the non-renovated district in kWh/m²

		Buffer volume in m³		
		0	**2**	**4**
Collector area in m²	**41**	334	462	471
	82	217	338	360
	164	131	212	234

Renovated District

The RR feed-in system for the renovated district shows savings in fossil energy between 15.5 % and 41.5 % (Figure 78). Again, the effect of missing storage volume is not as significant as for the central plant and the hot water preheating, as the buffering of the district heating network itself can be utilised. Nevertheless, the influence is higher than for the non-renovated RR variant, as the consumption is lower.

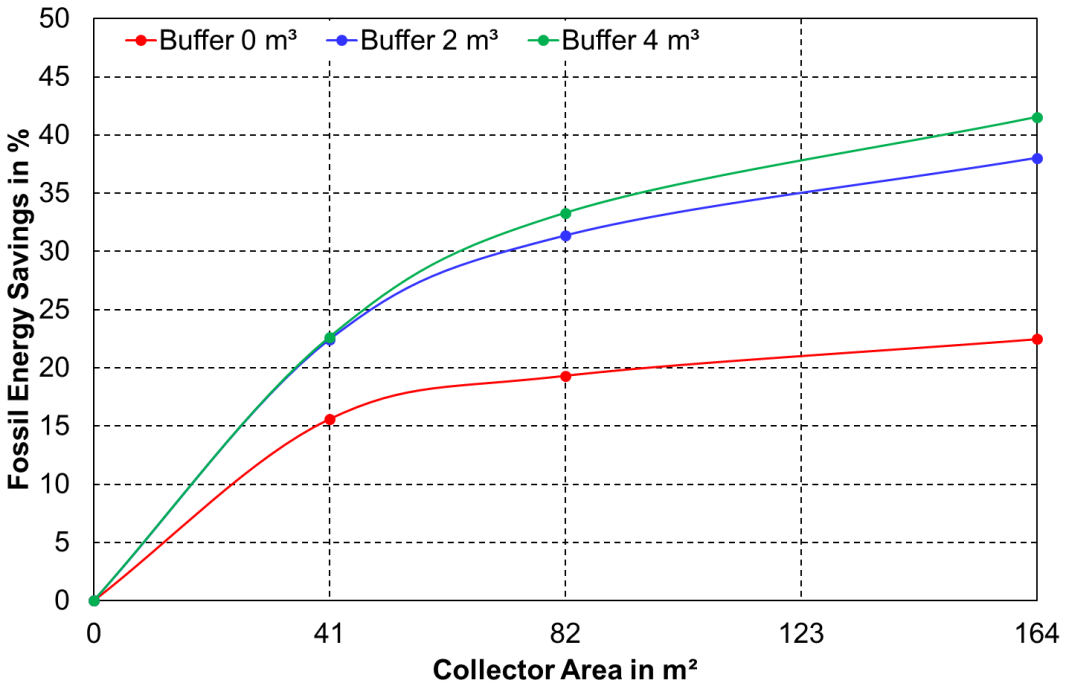

Figure 78: Fossil energy savings for decentralised plants with RR feed-in in the renovated district

Table 24 shows annual specific yields between 120 kWh/m² and 471 kWh/m².

Table 24: Specific annual yield of the decentralised plants with RR-feed-in in the renovated district in kWh/m²

		Buffer volume in m³		
		0	**2**	**4**
Collector area in m²	**41**	327	460	471
	82	205	332	353
	164	120	204	221

6.2.5 RS Feed-in

The more complex variant of decentralised feed-in, promising higher solar fractions and more possibilities in managing the energy in the network, is the RS feed-in. It was simulated with the same collector and storage sizes like the previous systems.

Non-Renovated District

Figure 79 shows the fossil energy savings for this integration concept. The collector area and the installed buffer volume is, like for all decentralised variants, given per building. The maximum fossil energy saving is 22.7 % for 164 m² collector area and 4 m³ buffer volume per building. Like for the RR feed-in, the variants with 2 m³ show almost the same performance.

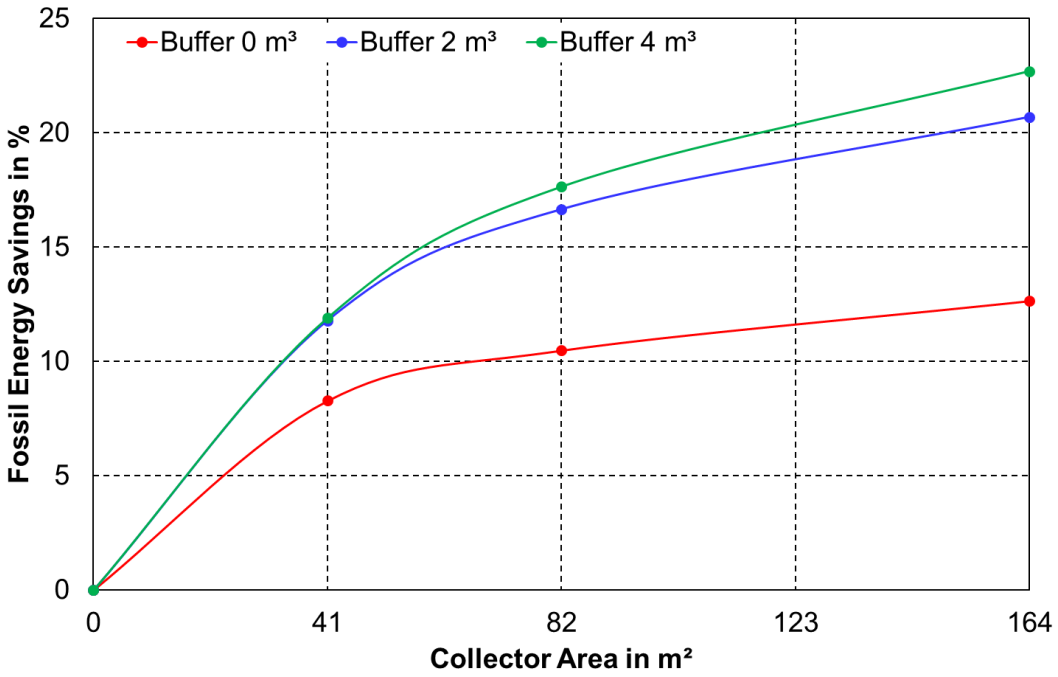

Figure 79: Fossil energy savings for decentralised plants with RS feed-in in the non-renovated district

Table 25 shows the annual specific yields of the plants. These range between 135 kWh/m² and 473 kWh/m². For all variants, the RS feed-in has slightly higher specific yields than the pure domestic hot water system as well as the RR feed-in. Nevertheless, the fossil energy savings are not higher and the additional solar yields result in higher network losses.

Table 25: Specific annual yield of the decentralised plants with RS feed-in in the non-renovated district in kWh/m²

		Buffer volume in m³		
		0	**2**	**4**
Collector area in m²	**41**	342	465	473
	82	226	341	361
	164	135	214	235

Renovated District

The renovated RS variants show savings in fossil energy between 15.5 % and 41.4 % (Figure 80). There is no significant difference in performance to the RR variants.

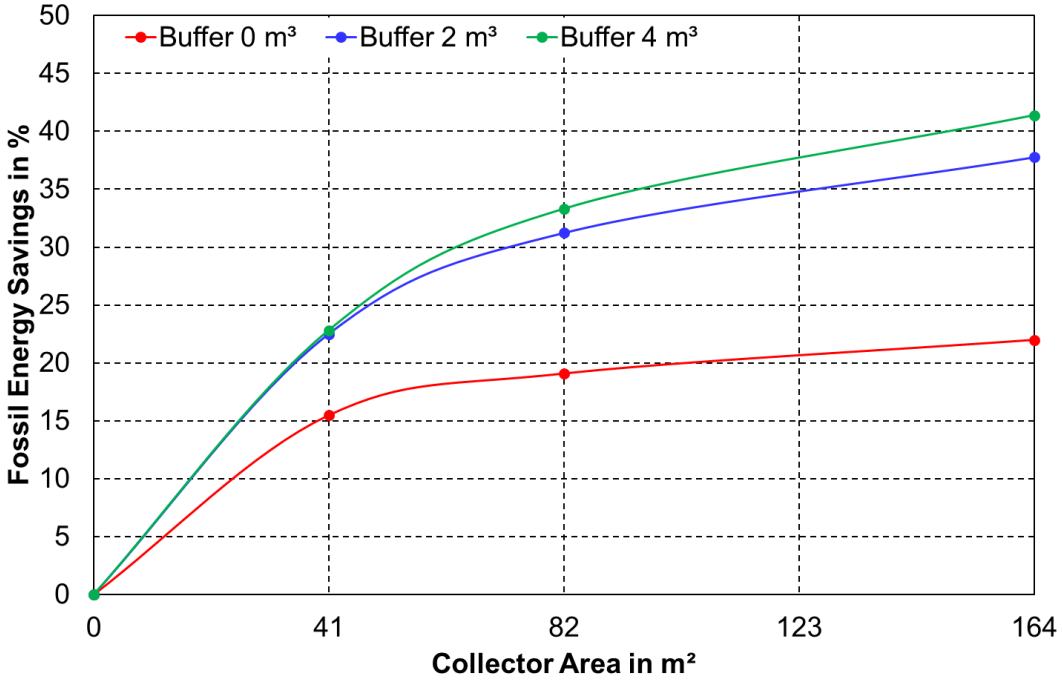

Figure 80: Fossil energy savings for decentralised plants with RS feed-in in the renovated district

Table 26 shows the annual specific yields of the variants. These range between 122 kWh/m² and 472 kWh/m² and are only slightly higher than for the RR system.

Table 26: Specific annual yield of the central solar thermal plants in the renovated district in kWh/m²

		Buffer volume in m³		
		0	**2**	**4**
Collector area in m²	**41**	334	463	472
	82	212	335	353
	164	122	204	222

6.2.6 Comparison of Integration Variants

Having a look at the central plant with 410 m² collector area and 10 m³ buffer volume respectively at the decentralised plants with 82 m² and 2 m³, resulting in the same total size, conclusions can be drawn on the energy savings and stagnation of the different integration concepts. This sizing seems to result in a good compromise of energy saving and investment into solar thermal system components. In Table 27, the energy

savings, specific yields and stagnation times of these variants are compared for the non-renovated district.

Table 27: Results of all integration concepts for a total of 410 m² collector area and 10 m³ buffer volume (82 m² and 2 m³ per building) for the non-renovated district

	Energy savings in %	Specific annual yield in kWh/m²	Annual stagnation time in h
Central	15.1	289	132
Decentralised DHW	15.8	290	145
Decentralised RR feed-in	16.8	338	47
Decentralised RS feed-in	16.7	342	63

While the central plant for the non-renovated district enables fossil energy savings of 15.1 %, the decentralised variants result in 15.8 % for the pure domestic hot water and even higher values of 16.7 and 16.8 % for the plants with additional feed-in. Like already mentioned, the higher specific yield of the feed-in concepts partly results only in higher network losses. These losses are 50.9 MWh for the central, 43.4 MWh for the domestic hot water, 56.2 MWh for the RR feed-in and 57.9 MWh for the RS feed-in.

Table 28 shows the same results for the renovated district. The results are similar, but on a higher level of fractional energy savings on the one hand as well as higher stagnation times and lower specific yield on the other hand.

Table 28: Results of all integration concepts for a total of 410 m² collector area and 10 m³ buffer volume (82 m² and 2 m³ per building) for the renovated district

	Energy savings in %	Specific annual yield in kWh/m²	Annual stagnation time in h
Central	25.6	256	143
Decentralised DHW	31.0	290	145
Decentralised RR feed-in	31.3	332	54
Decentralised RS feed-in	31.2	335	74

The large deviation of the network losses results from the different influences of the concepts on the network temperature. Figure 81 shows the average daily supply and return temperatures of all variants during one year of operation for the non-renovated district. It can be seen, that for the domestic hot water system, the return pipe cools

down significantly on many summer days when there is no consumption from the network. A temperature increase of the supply pipe cannot be observed. The central concept results in higher supply temperatures during summer, while the two variants for decentralised feed-in increase the temperature of both, supply and return pipe. It is also obvious, that for the RR-feed-in the temperature increase of the return pipe is higher, as the excess heat is directly fed in. For the RS-feed-in, there is only an indirect heating of the return via the reversed flow across the central heating station.

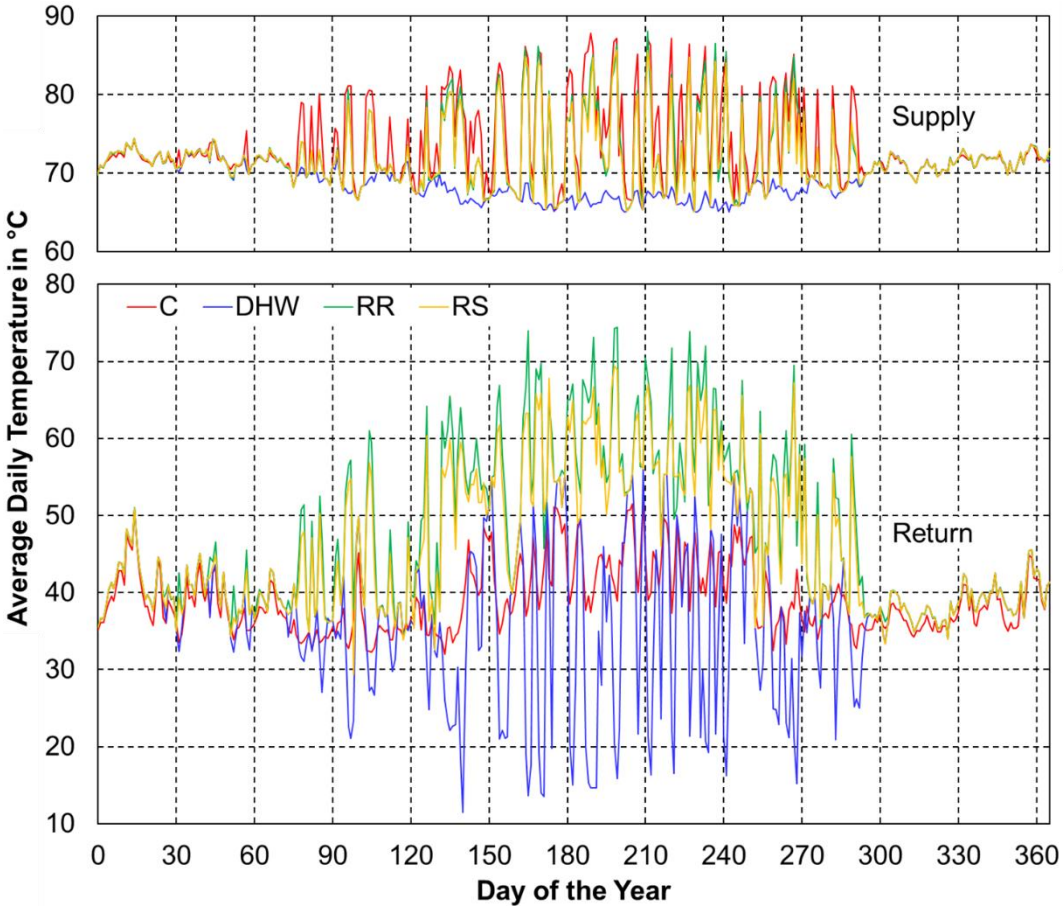

Figure 81: Daily average supply and return temperatures of all integration variants with a total of 410 m² collector area and 10 m³ buffer volume during one year for the non-renovated district

In Figure 82, it can be seen, that the concept with decentralised feed-in already shows benefits for an equal distribution of collectors due to the buffering of excess heat in the network, while the domestic hot water system is the most efficient for lower collector area and sufficient storage volume. The reduced energy savings for the abdication of additional storages are obvious for all variants. Nevertheless, the effect is lower for the feed-in systems than for the central and the domestic hot water systems.

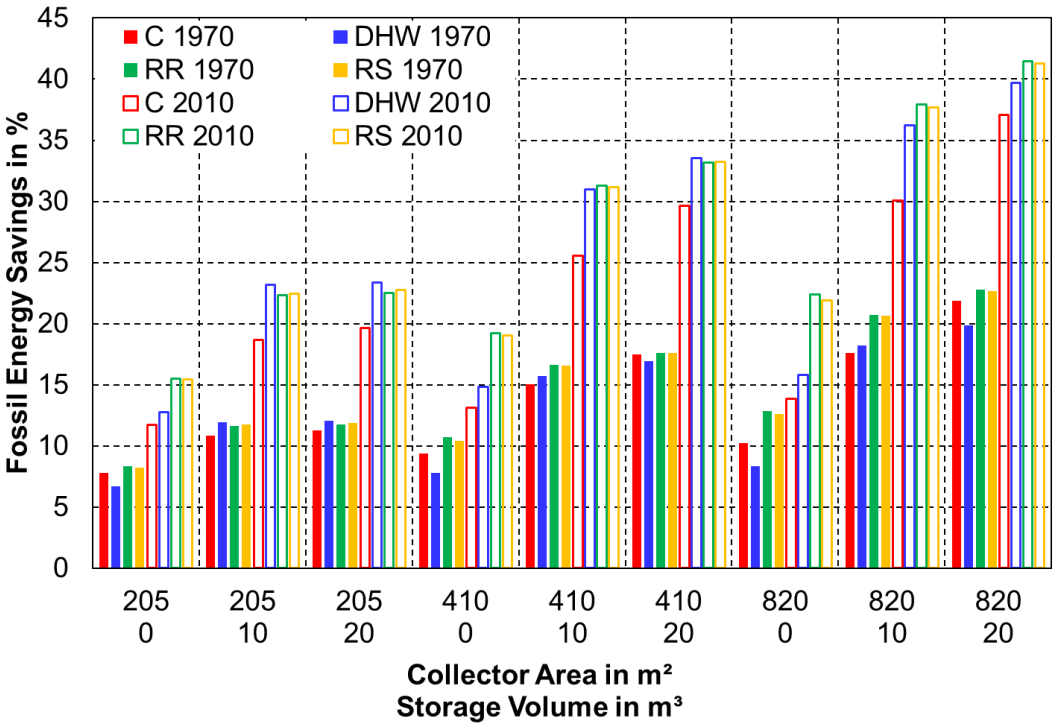

Figure 82: Fossil energy savings for all basic variants

6.2.7 Unequally Distributed Plants

From the presented results, it can be concluded, that for equally distributed plants, there is no significant benefit of the more complex RS feed-in over the RR feed-in as for both variants, the consumption in the network goes down to zero, when the feed-in starts. On the other hand, for some dimensioning variants, both have a benefit over the pure domestic hot water preheating by utilising additional storage capacities in the district heating pipes.

Nevertheless, it was the starting point of this thesis, that there are situations, where the roof orientation or other roof installations, like antennas or photovoltaic modules prevent the integration of solar thermal collectors on some of the buildings. The same holds true for the possibilities of installing buffer storages. Therefore, the basic variants are compared with additional configurations, investigating non-homogenously distributed collector arrays and storages. As the roof area of the building with 12 residential units is approximately 215 m² on one side, a maximum number of 80 collectors with 205 m² gross area per building is investigated. Having two buildings with this maximum number of collectors and a 2 m³ buffer in each of the five buildings of the district or 5 m³ in the buildings with collectors, gives the same overall system size as the 82 m², 2 m² respectively the 410 m², 10 m³ variants and enables a comparison with these. The same holds true for a single central buffer of 10 m³ in combination either with five equally sized decentralised collector arrays or with two

larger arrays. Another option is the installation of buffer storages in the three buildings without collectors, if the collectors are disturbed on two of the buildings. This gives a variety of systems, which are characterised in Table 29. All of these systems can be combined either with an RR or with an RS feed-in strategy.

Table 29: Dimensioning variants of unequally distributed collector arrays and storages (A_{Col} = area of collectors in m², V_{Buf} = buffer volume in m³)

Central heating station		**Building 1**		**Building 2**		**Building 3**		**Building 4**		**Building 5**	
A_{Col}	**V_{Buf}**	**A_{Col}**	**V_{Buf}**	**A_{Col}**	**V_{Buf}**	**A_{Col}**	**V_{Buf}**	**A_{Col}**	**V_{Buf}**	**A_{Col}**	**V_{Buf}**
		205	5							205	5
		205	2		2		2		2	205	2
		82	5	82		82		82		82	5
410			2		2		2		2		2
410			5								5
	10	82		82		82		82		82	
	10	205								205	
		205			3.3		3.3		3.3	205	

To operate these systems efficiently, some adaptions on the control strategy have to be made. When a loading of the buffers in buildings without collectors is necessary, a simple measurement of the network temperature at the substation of this building is not sufficient. This is due to a time delay of the increasing temperature from e.g. the central heating station to the last building as well as a temperature decrease from the heat source to the consumer resulting from the pipe heat losses. The same holds true for a feed-in from a decentralised buffer. A lower temperature at the substation due to the heat losses of the pipes can start a feed-in when the buffer is loaded, regardless of possibly higher temperatures at the central heating station. A superior control of the temperatures at the central heating station is used to start and stop the feed-in and consumption at the substations. This means that all decentralised plants are used to keep the network temperature at the desired level.

Table 30 shows the selected thresholds for the two hydraulic schemes. The temperature thresholds for the RR feed-in are on a lower level, as it does not necessarily have to keep the network supply temperature due to the possible additional temperature increase at the central heating station before the fluid reaches other consumers in the network.

Table 30: Selected temperature thresholds for the feed-in and consumption control of the decentralised plants

	RR	RS
Feed-in start	Buffer > DH supply + 2 °C AND Buffer > DH design supply + 2 °C	Buffer > DH supply + 5 °C AND Buffer > DH design supply + 5 °C
Feed-in stop	Buffer < Substation OR Buffer < DH design supply – 2 °C	Buffer < Substation OR Buffer < DH design supply
Consumption start	DH supply > 80 °C AND DH supply > Buffer + 5 °C	DH supply > 80 °C AND DH supply > Buffer
Consumption stop	DH supply < 78 °C OR DH supply > Buffer + 2 °C	DH supply < 78 °C OR DH supply > Buffer + 2 °C

This behaviour is exemplary shown in Figure 83 for the system with a central collector array and five decentralised storages in the renovated district for a period of 24 hours during summer.

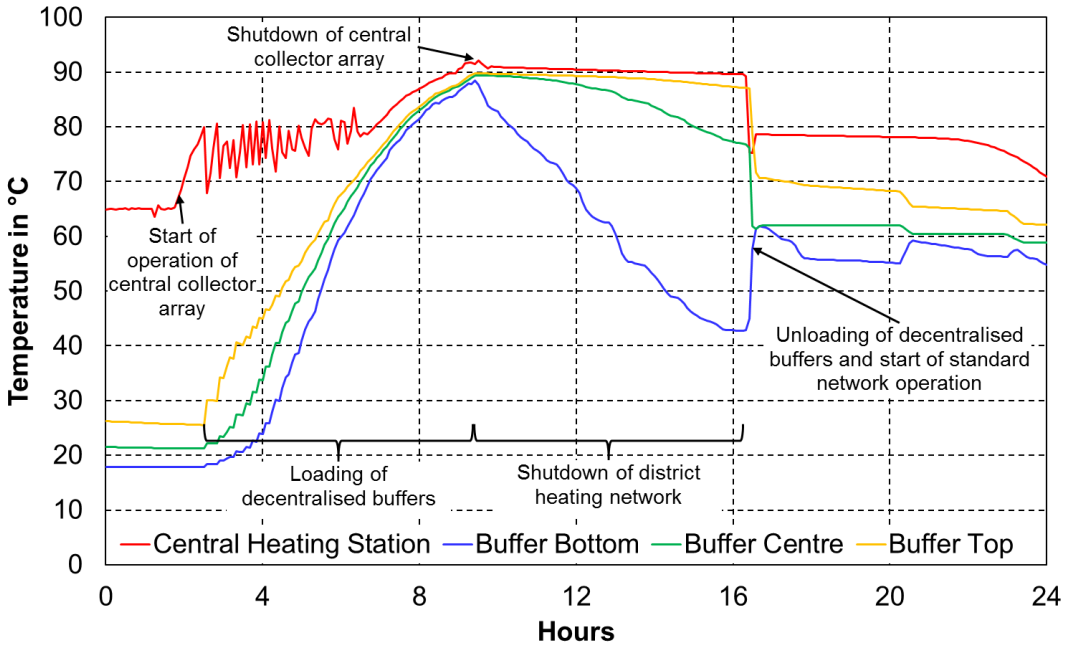

Figure 83: Temperatures of the central heating station and the decentralised buffer in building 5 for 24 hours of operation of the system with 410 m² central collector area and 5 decentralised storages of 2 m³ with RR feed-in

The central heating station temperature is at 65 °C in the morning. After the solar collectors start producing energy, the temperature rises, as it cannot be completely consumed by the connected buildings. After exceeding the 70 °C threshold, the buffer temperature in building 5 increases, as the loading from the network starts. The same holds true for the other buildings. Following the period of fluctuating temperatures at the central heating station and continuously increasing temperatures of the decentralised buffers, a saturation is reached and the solar thermal plant is shut down. The buffers continue loading until the central temperature is less than 5 K above the

buffer temperature. This is followed by 7 hours of complete shutdown of the network with unloading of the decentralised buffers and a slight temperature decrease at the central heating station due to thermal losses. As soon as one of the buffers is unloaded by the consumers to a temperature below the central heating station temperature, it starts drawing energy from the network and the other buffers, including the plotted buffer 5, respond with a short unloading into the network. This results in a de-stratification of the temperature levels in the buffer and finally in a stop of the feed-in due to the low storage top-temperature.

The results of the unequally distributed systems for the non-renovated basic district are shown in Table 31. The results of the equally distributed basic variants are depicted in the last four lines of the table.

Table 31: Fossil energy savings of unequally distributed variants compared to basic variants with a total of 410 m² collector area and 10 m³ buffer volume

Hydr. scheme	Central heating station		Building 1		Building 2		Building 3		Building 4		Building 5		Fossil energy savings in %	
	A_{Col}	V_{Buf}	A_{Col}	V_{Buf}	A_{Col}	V_{Buf}	A_{Col}	V_{Buf}	A_{Col}	V_{Buf}	A_{Col}	V_{Buf}	1970´s district	2010´s district
RR	410			2		2		2		2		2	16.2	27.5
RS	410			2		2		2		2		2	16.5	28.3
RR	410			5								5	15.1	25.5
RS	410			5								5	15.1	25.6
RR		10	205								205		12.2	23.9
RS		10	205								205		13.0	24.4
RR			205	2		2		2		2	205	2	14.6	27.3
RS			205	2		2		2		2	205	2	15.1	28.2
RR			205			3.3		3.3		3.3	205		12.9	24.3
RS			205			3.3		3.3		3.3	205		13.1	25.0
RR			205	5							205	5	13.2	25.1
RS			205	5							205	5	13.5	25.4
DHW			205	5							205	5	8.3	16.4
RR		10	82		82		82		82		82		13.9	26.1
RS		10	82		82		82		82		82		14.3	26.7
RR			82	5	82		82		82		82	5	14.7	27.8
RS			82	5	82		82		82		82	5	14.6	27.8
C	410	10											15.1	25.6
DHW			82	2	82	2	82	2	82	2	82	2	15.8	31.0
RR			82	2	82	2	82	2	82	2	82	2	16.7	31.3
RS			82	2	82	2	82	2	82	2	82	2	16.6	31.2

Compared to the basic central variant, some of the systems have higher energy savings while the decentralised equally distributed systems show a more efficient behaviour in most cases. Nevertheless, the central collector array with distributed storages, in particular if the storages are equally distributed, is even competitive to the distributed domestic hot water preheating. These variants enable fossil energy savings of up to 16.5 %. Distributed collectors have a lower efficiency. The only exception is

the system with two collector arrays and equally distributed storages using the RS feed-in, which is competitive to the basic central variant. Regarding the differences between RR and RS feed-in, there is a benefit of the RS approach for most of the systems. Only for the central collector array and the equally distributed arrays with 5 m³ storages, the two hydraulic variants are almost equal. The domestic hot water system with only two plants in the district is the least efficient with only 8.3 % energy savings.

The results of the unequally distributed systems for the renovated district are shown in the second column. Compared to the basic central variant, many of the systems have higher or equal energy savings while the decentralised equally distributed systems show a more efficient behaviour in all cases. Decentralised collectors are competitive to a central collector array with equally distributed storages and only the variants with two arrays and three, respectively one central storage are outperformed by the basic central system. The lowest energy savings can be observed for the pure domestic hot water systems with two oversized plants of 205 m² collector area and 5 m³ buffer each. Opposite to the non-renovated district, the variant with distributed storages and two collector arrays is even competitive to the central collector array with distributed storages. The RR scheme shows less energy savings, except the variants 410 m² and 5 m³ respectively 82 m² and 5 m³, which are competitive to the RS-scheme.

6.3 Variation of Boundary Conditions

After investigating different integration variants for smart solar district heating systems, a further relevant point to discuss is the influence of changing boundary conditions on the fossil energy savings to assess the solutions for the application on other sites. Possible changes in these boundary conditions can be:

- Roof orientation
- Climate
- District size / piping length
- Heat demand

Therefore, a further simulation study was done on variations of these conditions for the most relevant system configurations of the basic district. A distribution of the collector arrays on east, west or east and west roofs was simulated as well as the location of the network in Stockholm (Sweden) and Davos (Switzerland). Regarding the district size, a variant with 340 m piping length is discussed, while the basic variants have approximately 170 m. The consumption profiles were modified in a way,

that a shift of the consumption from daytime to night-time and vice versa took place, simulating different behaviour and daily routine of the inhabitants.

6.3.1 Variation of Collector Orientation

Not all roofs may have a south-orientation but can also face east and west, as seen in the field test case. The influence of different orientations on the district was investigated. Only certain variants are described for this investigation, which either have a total collector area of 410 m² with 10 m³ buffer, 820 m² without buffers or 820 m² with 20 m³ buffer volume. Figure 84 shows the relative fossil energy savings compared to the variant without solar thermal plants for the non-renovated and the renovated district with a central collector array as well as a central buffer storage.

There is a clear ranking from lower to higher energy savings going from east to east-west to west and finally south. This is due to the already mentioned mists in the morning hours. Nevertheless, for the variants without storage, the east-west configuration is even better than the pure west configuration and very close to south configuration, which can be explained by a better fitting of the load curve during the day and the temporary wider distributed solar yield, which is higher in the morning and in the afternoon. A similar behaviour can be observed for the other hydraulic schemes. The results are shown in Figure 85, Figure 86 and Figure 87.

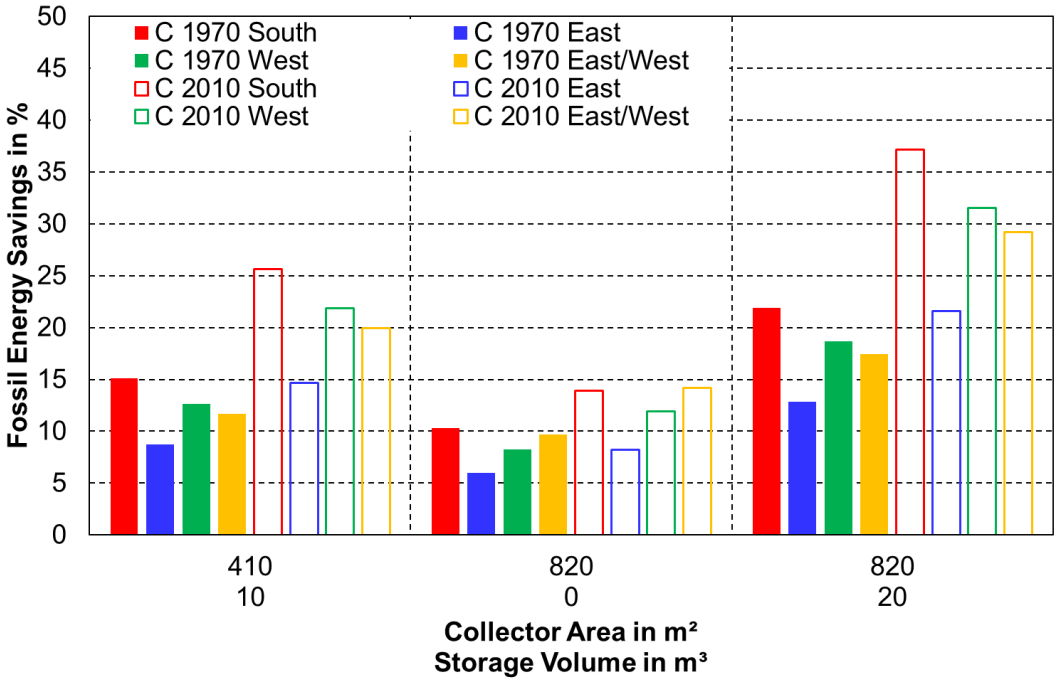

Figure 84: Influence of the collector orientation on the performance of the central solar thermal plant

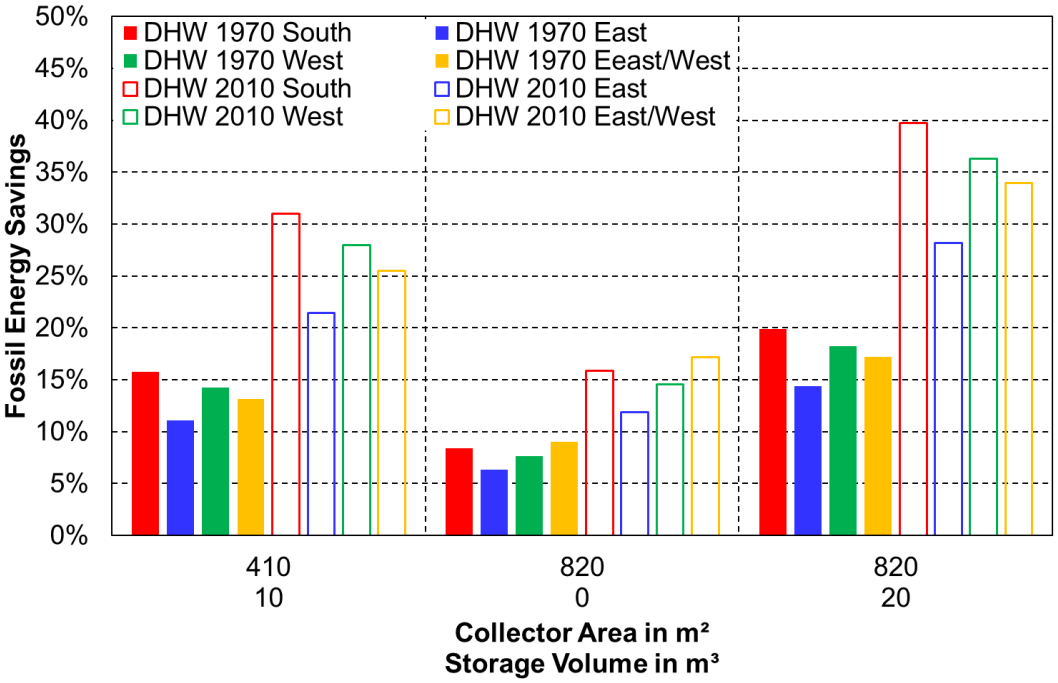

Figure 85: Influence of the collector orientation on the performance of the domestic hot water preheating system

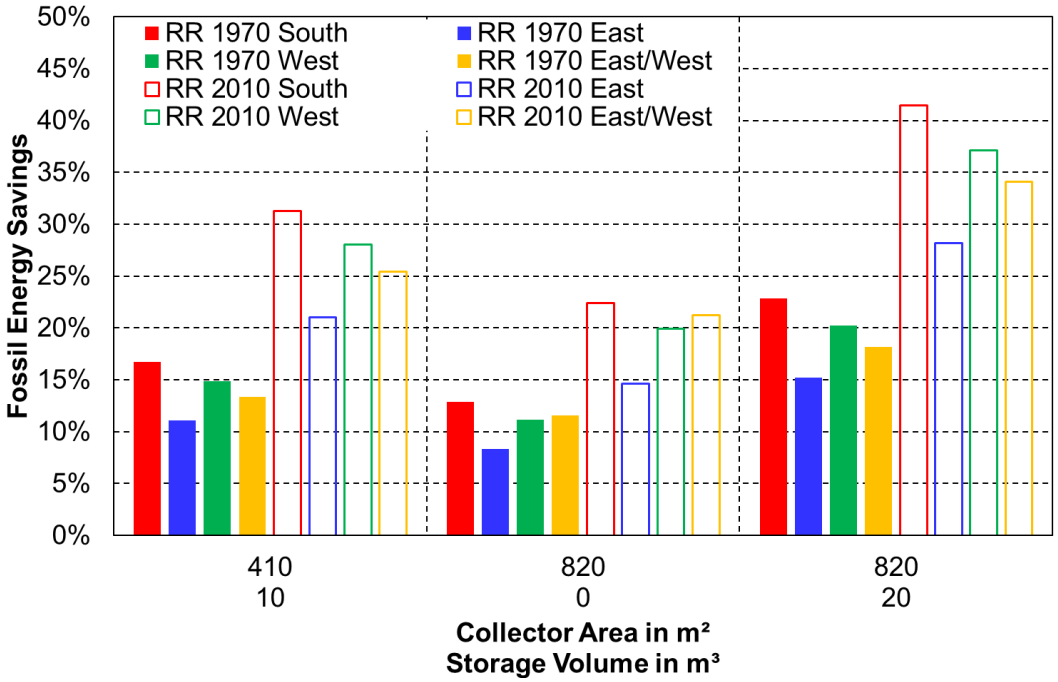

Figure 86: Influence of the collector orientation on the performance of the decentralised plant with RR feed-in

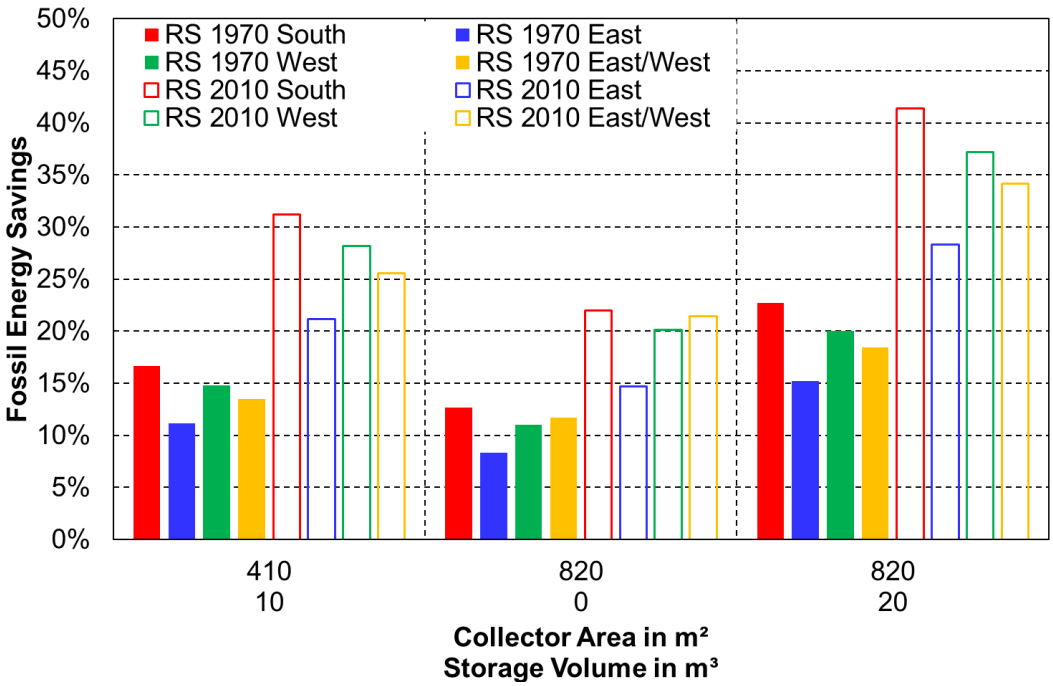

Figure 87: Influence of the collector orientation on the performance of the decentralised plant with RS feed-in

For the systems with unequally distributed plants, the influence on the dimensioning with a total of 410 m² collector area and 10 m³ buffer is described. This system size was selected as it represents a good compromise between the number of installed components and fossil energy savings in the basic variants. The comparison is done with the central or equally distributed variants with the same orientation. The first result column in Table 32 shows the relative fossil energy savings of the east-oriented systems. As already seen for the basic systems, the solar yields and therefore the energy savings are significantly lower. Besides that, several more observations can be made:

- Firstly, the domestic hot water variant is not as far behind the systems with feed-in like for the south variant. This can be explained by the lower irradiation and lower collector temperatures throughout the year. The feed-in temperature is not reached that often and the advantage of the feed-in or central variants therefore not that distinctive.
- Secondly, the decentralised plants outperform the central plants in almost all variants, as they still profit from the lower temperatures of the direct domestic hot water preheating.

For the west orientation (second column), the results are not as significant as for the east orientation. Due to the higher irradiation compared to the east-roofs, the fossil energy savings are closer to the south variants and the ranking is similar.

For the east-west orientation (third column), there is no significant change of the results compared to east or west orientation. The fossil energy savings are in between the two one-sided variants. The savings of the different distribution variants have a similar ranking, too.

Table 32 Fossil energy saving of unequally distributed variants with east, west and east-west orientation compared to basic variants with 410 m² collector area and 10 m³ buffer volume in the renovated district

Hydr. scheme	Central heating station		Building 1		Building 2		Building 3		Building 4		Building 5		Fossil energy savings in %		
	A_{Col}	V_{Buf}	A_{Col}	V_{Buf}	A_{Col}	V_{Buf}	A_{Col}	V_{Buf}	A_{Col}	V_{Buf}	A_{Col}	V_{Buf}	East	West	East/West
RR	410			2		2		2		2		2	15.5	23.1	20.3
RS	410			2		2		2		2		2	16.2	23.6	20.6
RR	410			5								5	14.4	21.5	19.2
RS	410			5								5	14.7	21.6	19.4
RR		10	205								205		14.4	20.3	18.6
RS		10	205								205		14.7	20.7	18.8
RR			205	2		2		2		2	205	2	17.1	23.9	21.6
RS			205	2		2		2		2	205	2	17.8	24.7	22.3
RR			205			3.3		3.3		3.3	205		14.4	20.7	19.2
RS			205			3.3		3.3		3.3	205		15.1	21.4	19.6
RR			205	5							205	5	16.3	22.0	20.6
RS			205	5							205	5	16.5	22.3	20.9
DHW			205	5							205	5	11.9	15.2	14.2
RR		10	82		82		82		82		82		16.4	22.6	20.9
RS		10	82		82		82		82		82		16.9	23.1	21.3
RR			82	5	82		82		82		82	5	18.0	24.6	22.6
RS			82	5	82		82		82		82	5	18.3	24.6	22.7
C	410	10											14.7	21.9	20.0
DHW			82	2	82	2	82	2	82	2	82	2	21.4	27.9	25.5
RR			82	2	82	2	82	2	82	2	82	2	21.0	28.0	25.4
RS			82	2	82	2	82	2	82	2	82	2	21.1	28.2	25.6

As the feed-in option of the smart solar district heating approach has benefits for uneven distributions and load profiles, an additional simulation was done regarding the network with equally distributed plants (82 m², 2 m³) but mixed collector orientations. The pure domestic hot water system, which is the best or at least very close to the best option in terms of energy savings is compared with the RS and RR system for a network with one south, two east and two west collector arrays. Table 33 shows the energy savings for these variants. The disadvantage of the mixed orientation is less for the feed-in systems with 27.0 % compared to the purely local system, which is going down to 25.5 %.

Table 33: Comparison of fossil energy saving of south and mixed orientation

Hydraulic variant	Energy savings with south orientation in %	Energy savings with mixed orientation in %	Change of energy savings with mixed orientation in %
DHW	31.0	25.5	-5.5
RR	31.3	27.0	-4.3
RS	31.2	27.0	-4.2

6.3.2 Variation of Climate

To take into account different climatic conditions in Europe, two additional locations for the district were investigated. These were taken from the reference locations of the *solar keymark*[5], which includes Würzburg (Germany), Stockholm (Sweden), Davos (Switzerland) and Athens (Greece). As the climate in Würzburg is very similar to that in Ingolstadt, this location was dismissed. The same holds true for Athens, as the building structure in Southern Europe is very different from that in Central or Northern Europe. With temperatures between 0 and 20 °C during winter, there can even be cases without any space heating. This makes a test case in such a warm region not suitable for a comparison with the selected system layout at the other locations.

Regarding the weather data, the two other climates have higher respectively lower solar irradiation as well as in one case a lower and in the other case an almost similar average temperature. Table 34 shows the global irradiation, average ambient temperature and resulting annual heat demand for the three locations.

Table 34: Irradiations, temperatures and total heat demand at the investigated locations

Location	Annual global irradiation in MWh/m²	Average ambient temperature in °C	Total annual heat demand of the district in MWh
Ingolstadt	1.120	8.8	408
Stockholm	0.975	7.8	441
Davos	1.339	3.2	518

Having a look at the results for Davos (Table 35, first result column), it becomes clear, that this location enables higher relative fossil energy savings due to the higher heat demand and, at the same time, higher global irradiation. Additionally, the change of the climatic conditions results in a benefit of the equally distributed feed-in systems over the central plant and domestic hot water plants of approximately 3 %.

[5] A quality label for solar thermal collectors, based on European standards, including efficiency tests and solar yield calculations for different locations.

Nevertheless, the central collector array with distributed storages even has similar savings like the equally distributed feed-in systems. While in Ingolstadt, the variants with 82 m² and 5 m³ were equivalent with the 410 m², 2 m³ system, they perform not as good as the 410 m², 2 m³ variant in this location. The disadvantage of a pure domestic hot water system is higher and even the equally distributed system is not more efficient than the central system. This can be explained by the higher fraction of space heating demand, resulting in a better utilisation of the systems that enable a space heating support.

The results for Stockholm are closer to the results of Ingolstadt (Table 35, second column). Due to the lower irradiation, the energy savings are in general lower, although the heat demand is 8 % higher. Besides that, the ranking does not change and still the central collector array with distributed storages, the distributed collector arrays with two storages and the two collector arrays with distributed storages show the best performance and are visibly more efficient than the central basic system.

Table 35: Fossil energy savings of unequally distributed variants compared to basic variants with 410 m² collector area and 10 m³ buffer volume in Davos and Stockholm

Hydr. scheme	Central heating station		Building 1		Building 2		Building 3		Building 4		Building 5		Fossil energy savings in %	
	A_{Col}	V_{Buf}	A_{Col}	V_{Buf}	A_{Col}	V_{Buf}	A_{Col}	V_{Buf}	A_{Col}	V_{Buf}	A_{Col}	V_{Buf}	Davos	Stockholm
RR	410			2		2		2		2		2	31.9	22.4
RS	410			2		2		2		2		2	32.7	23.0
RR	410			5								5	29.8	21.0
RS	410			5								5	29.9	21.0
RR		10	205								205		27.9	19.9
RS		10	205								205		28.7	20.3
RR			205	2		2		2		2	205	2	29.9	22.7
RS			205	2		2		2		2	205	2	31.3	23.5
RR			205			3.3		3.3		3.3	205		27.3	19.9
RS			205			3.3		3.3		3.3	205		28.3	20.5
RR			205	5							205	5	27.5	21.2
RS			205	5							205	5	28.0	21.5
DHW			205	5							205	5	14.5	13.1
RR		10	82		82		82		82		82		29.4	21.5
RS		10	82		82		82		82		82		29.6	22.0
RR			82	5	82		82		82		82	5	29.9	23.0
RS			82	5	82		82		82		82	5	29.6	23.1
C	410	10											29.7	21.1
DHW			82	2	82	2	82	2	82	2	82	2	29.5	25.9
RR			82	2	82	2	82	2	82	2	82	2	32.9	26.0
RS			82	2	82	2	82	2	82	2	82	2	32.9	26.1

6.3.3 Variation of District Density and Heat Demand

The amount of heat transported via the piping system is an important factor for the efficiency of a district heating network. If the connected consumers are too widely spread, the piping losses account for a high fraction of the heat production and the heat generation costs as well as the carbon dioxide emissions get too high in comparison to a solution with individual heat generators for each building. For the non-renovated and the renovated district, a heat demand density of 4.7 MWh/m respectively 2.4 MWh/m of piping length are reached with the basic variants, which is a sufficiently high level. This results in relative losses of 6.8 % respectively 13.2 % of the heat production for the variants without solar thermal plants.

Nevertheless, there may be cases, where buildings are connected via longer networks. Sometimes, the renovation of a building and the resulting lower heat consumption can lead to an inefficient operation of an existing network by decreasing the heat consumption compared to the piping length. Therefore, further variants were investigated, with an enhanced piping length to double the heat losses. In that case, the additional length was set between a separated pair of buildings, 300 m away from the others (top left buildings in the district scheme in Figure 72). This leads to heat losses in the network of 107 MWh for the basic variant without solar thermal plants, meaning 23 % of the total heat generation of the renovated district.

Having a look on the first result column in Table 36, it can be seen, that for all variants the relative fossil energy savings go down between 1.2 % and 4.5 % compared to the renovated basic district. This is due to the generally higher fossil heat generation. The absolute solar yields increase as the load and the network storage capacity are higher. The domestic hot water variants suffer the least from the higher network length. The solar yields do not change compared to the basic district but this is compensated by the lower network losses, making the equally distributed DHW system the most efficient in this case. Regarding the performance of the feed-in strategies, there is an improvement of the RR scheme for the 82 m², 5 m³ and 205 m², 2 m² variants, while the benefit of the RS scheme is even higher for the 205 m², 10 m³ variant.

All buildings were simulated with the same heat demand in the presented cases. In reality, different building types can lead to different space heating demands. The behaviour of residents is highly fluctuating, regarding the consumption of domestic hot water. This may be a temporal deviation, like for day and night shift workers, as well as a generally more wasteful or economical dealing with energy and was seen in the field test. The impact of such variations was investigated with following assumptions:

- Building 1 and building 4 were set to an increased domestic hot water load during

day (shifting of 20 % of the diurnal consumption to day-time).

- In building 2 and building 5, the consumption during day was decreased by 20 %. During night the setting is vice-versa.
- Building 3 was not modified.

This leads to the same annual demand of hot water for the district but a different load curve of the individual buildings. In the basic model, which is set up on measured data from the district in Ingolstadt, 58 % of the tapping is between 6:00 in the morning and 18:00 in the evening. 42 % are during night-time. The modified buildings have 38 % and 62 %, respectively 78 % and 22 % during day and night.

Table 36: Fossil energy savings of unequally distributed variants compared to basic variants with 410 m² collector area and 10 m³ buffer volume in the renovated district with lower density (first column) and modified consumption profile (second column)

Hydr. scheme	Central heating station		Building 1		Building 2		Building 3		Building 4		Building 5		Fossil energy savings in %	
	A_{Col}	V_{Buf}	A_{Col}	V_{Buf}	A_{Col}	V_{Buf}	A_{Col}	V_{Buf}	A_{Col}	V_{Buf}	A_{Col}	V_{Buf}	Density	Demand
RR	410			2		2		2		2		2	25.6	27.3
RS	410			2		2		2		2		2	26.3	28.0
RR	410			5								5	24.1	25.3
RS	410			5								5	24.2	25.4
RR		10	205								205		21.5	23.8
RS		10	205								205		22.9	24.2
RR			205	2		2		2		2	205	2	24.9	27.2
RS			205	2		2		2		2	205	2	23.7	28.0
RR			205			3.3		3.3		3.3	205		22.4	24.2
RS			205			3.3		3.3		3.3	205		23.0	24.9
RR			205	5							205	5	23.0	24.9
RS			205	5							205	5	23.5	25.2
DHW			205	5							205	5	15.2	16.2
RR		10	82		82		82		82		82		23.9	26.0
RS		10	82		82		82		82		82		24.5	26.5
RR			82	5	82		82		82		82	5	25.7	27.6
RS			82	5	82		82		82		82	5	25.5	27.7
C	410	10											23.5	25.4
DHW			82	2	82	2	82	2	82	2	82	2	29.4	30.9
RR			82	2	82	2	82	2	82	2	82	2	28.3	31.1
RS			82	2	82	2	82	2	82	2	82	2	28.5	31.3

The second column in Table 36 shows the fossil energy savings for the renovated district with modified demand profile. Compared to the district with standard demand profile, the order of the dimensioning variants stays the same. There is only a slight decrease of the fossil energy savings of all variants between 0.1 and 0.2 %, while the fossil heat generation of the basic system without solar thermal plants is also reduced by 0.2 %. The same holds true for the central and the equally distributed decentralised variants. Nevertheless, the equally distributed RS-system shows even 0.1 % more

energy savings with this consumption profile. It can be concluded that the simulated variation of the consumption profile has no relevant influence on the results for this dimensioning.

6.4 Advanced Control Strategies

For a final investigation of the system behaviour, two advanced control mechanisms were applied on the network, which include a forced loading of the network by the central collector array in case of imminent stagnation. As a second approach, the autonomous operation of a group of buildings, is investigated to shut down parts of the district heating network during longer periods.

6.4.1 Network Storage

As the pipes in the basic district heating network provide a water volume of approximately 0.37 m³ plus capacity of pipe walls and insulation, it stands to reason to use this volume for additional short-term buffering. As the volume to surface ratio of the pipes is unbeneficial compared to compact storage tanks, it is not reasonable to load the network with fossil energy to higher temperature levels than necessary. On the other hand, the buffering of solar excess heat is a possibility to increase the solar fraction and to reduce stagnation, even if a significant part of the energy may be lost in the network. A variant of the central solar thermal plant was investigated, in which the control was modified to actively load the network in the case of an upcoming stagnation of the collector array. The investigated cases are the renovated district with 410 m² collectors and 10 m³ buffer, 820 m² collectors and 20 m³ buffer as well as the variant with 820 m² and no buffer volume.

The differences in the network temperature can be seen in Figure 88 for a summer day for the variant with 820 m² collector area and without buffer. When the central heating station reaches a temperature of 95 °C, the collector circuit is shut down in the later morning. In the afternoon, after the network and the collectors are again within the operational temperature range, the system is started one more time and works until the evening. The same occurs for the variant with active network storage function (dotted line) but the start of stagnation can be delayed one hour by circulating the fluid in the network and heating up the return pipes (blue dotted line). Table 37 shows the fossil energy savings of the network storage variants compared to the systems with standard operation, which are in the range of 1 % for the variants with sufficient storage volume. The variant without storage shows an increase in solar yield of 42 %, resulting in 4.7 % higher fossil energy savings for this layout. The other two variants

have between 5 % and 6 % higher solar yields. The network losses on the other hand are increased by 5 % for the 410 m², 10 m³ variant, 6 % for the 820 m², 20 m³ variant and more than 7 % for the 820 m², 0 m³ variant.

Table 37: Relative fossil energy savings of the variants with active network loading compared to basic variant with identical dimensioning

Collector area, storage volume	Fossil energy savings without network storage in %	Fossil energy savings with network storage in %	Change of energy savings in %
410 m², 10 m³	25.6	26.6	+1.0
820 m², 0 m³	13.9	18.6	+4.7
820 m², 20 m³	37.1	37.9	+0.8

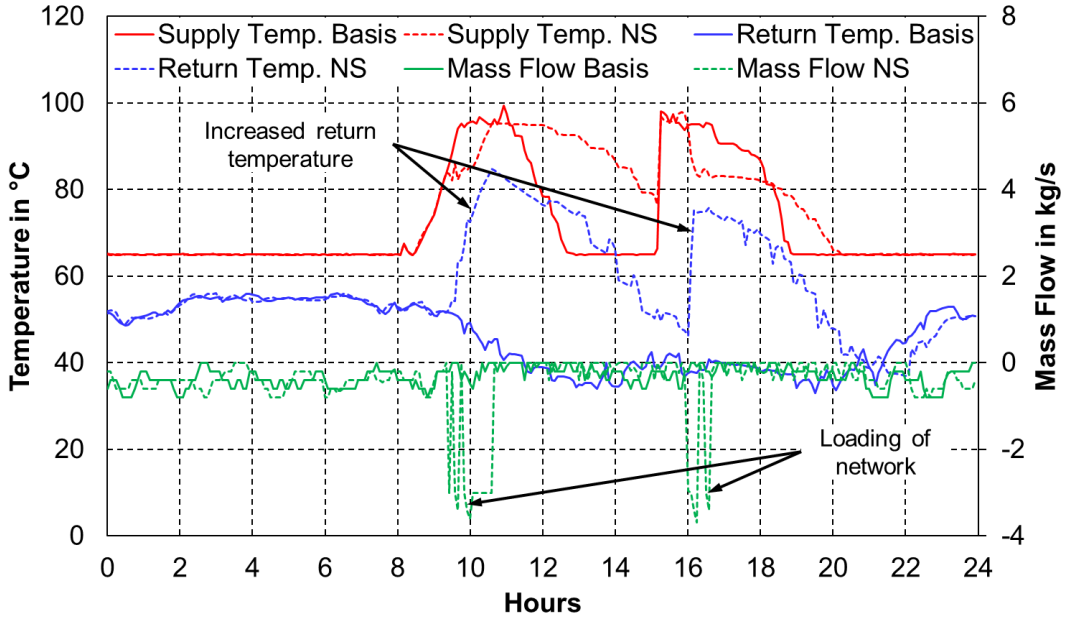

Figure 88: Supply temperatures, return temperatures and mass flows for one summer day of the system with and without network storage for 820 m² collector area and without buffer

All systems with RR and RS scheme perform an automatic heating of the network, as the plants start feeding in, as soon as the buffer temperature exceeds a critical level, respectively draw energy from the network, if high temperatures occur at the central heating station. Therefore, no further investigations are necessary for the other hydraulic variants.

6.4.2 Autonomous Operation

As stated in section 3, one of the advantages of the concept is the independent operation of parts of a district during times of sufficient solar yield at decentralised plants. To assess the effect of such an operation, a modified control strategy was tested on several of the variants with reduced heat consumption density, i.e. two

buildings are further away from the central heating station than in the basic variant. Such an operation is only reasonable in case of a sufficient collector area and buffer volume in these two buildings but with an unequal distribution. Therefore, the investigated cases were limited to the 82 m², 5 m³ variant, the 205 m², 2 m³ variant, the 205 m², 3.3 m³ variant and the 205 m², 5 m³ variant of the renovated district.

The implemented control strategy aims to coordinate the feed-in and consumption of the separated pair of buildings in a way, that the long connection pipe is out of operation as long as possible to reduce the network losses. To enable this operation, the feed-in or consumption signal is not triggered by the central heating station but by the neighbour building. I.e. in the exemplary case of a collector array and a buffer in building 5 but only a buffer in building 4, building 5 starts to feed-in into the network, if the district heating supply temperature is reached and the buffer is on a higher temperature than the buffer in building 4. In this situation, building 4 starts loading the buffer and the flow rate of the feed-in of building 5 is defined by the current consumption flow rate of building 4, including space heating and domestic hot water. This leads to a standstill of the flow in the connection to building 1, 2, 3 and the central heating station. When the temperature differences between producer and consumer are out of defined tolerances, the flow rate control is released and building 5 can also transfer energy to the rest of the network in order to prevent stagnation.

Figure 89 shows this behaviour for a day in summer. The day starts with a period of standstill in all pipes, as the buffers are still loaded from the previous days in both buildings. Around 9:00 in the morning, the temperature in building 5 increases due to solar yields. One hour later, the feed-in starts and building 4 starts the buffer loading at the same time. During a period of two hours with continuing loading, the mass flow in the connection pipe is still zero. This is indicated by the decreasing temperature. At noon, the temperature level gets too high and the coordinated feed-in and loading process of the two buildings is released. From that point on, the connection pipe temperature rises as energy is transferred between this pair of buildings and the rest of the network.

Table 38 shows the relative fossil energy savings of this operation approach compared to the identically dimensioned variants with conventional control algorithm. For the equally distributed storages, an increase of 3.1 % can be observed. The other variants perform between 0.3 % and 1.0 % better.

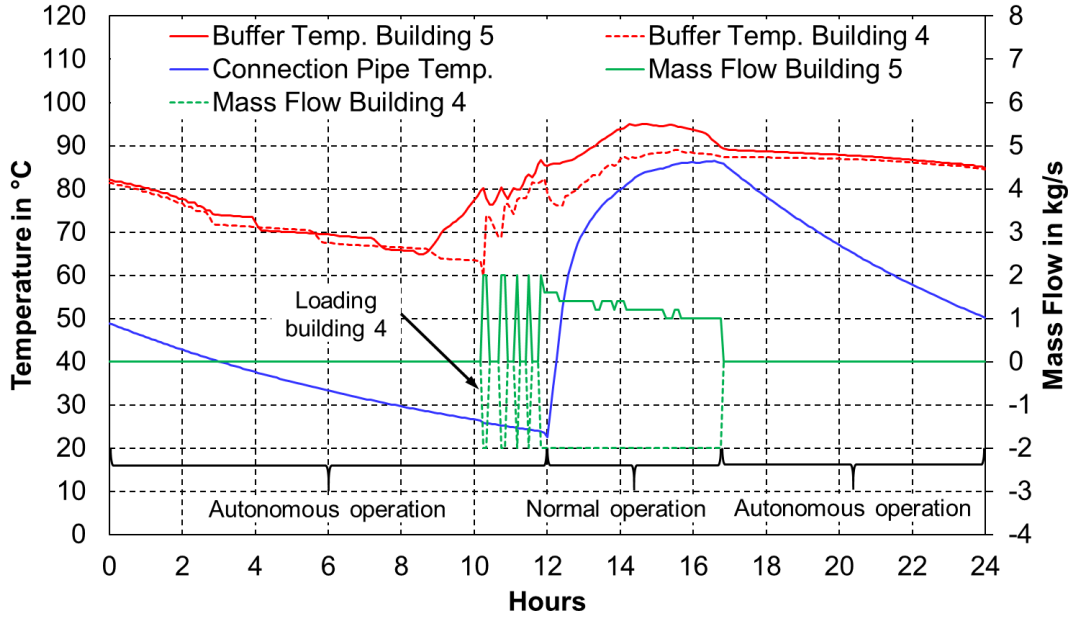

Figure 89: Temperature and mass flow of building 4 and building 5 as well as temperature of the connection pipe to the other buildings during a summer day in the district with lower density and autonomous operation

Table 38: Relative energy savings of the variants with autonomous operation compared to basic variant with identical dimensioning

Collector area, storage volume	Fossil energy savings without autonomous operation in %	Fossil energy savings with autonomous operation in %	Change of energy savings in %
2 x 205 m², 5 x 2 m³	23.7	26.8	+3.1
2 x 205 m², 3 x 3 m³	23.0	23.3	+0.3
2 x 205 m², 2 x 5 m³	23.8	24.5	+0.7
5 x 82 m², 2 x 5 m³	25.5	26.5	+1.0

6.5 Summary

Several Conclusions can be drawn from the results of section 6:

- The integration of feed-in options for equally distributed plants increases the solar yield significantly but has less influence on the fossil energy savings as the additional solar energy primarily leads to increased network losses. This is in particular the case for the renovated buildings (section 6.2.6).
- Decentralised domestic hot water preheating is more efficient than a central solar thermal plant and reduces the district heating piping heat loss.
- A lack of storage volume has a higher influence on domestic hot water preheating

than on the other concepts.

- Even a small buffer volume of 25 l per square meter collector area leads to an increase of the fossil energy savings, while a further increase of the volume has only minor influence.
- If the installation of a central solar thermal plant or equally distributed plants is not possible, the best alternative for the non-renovated district is a central collector array in combination with equally distributed storages.
- For the renovated district, the distribution of at least one component – collectors or storages – leads to reasonable fossil energy savings.
- If south-facing collector arrays are not viable, west orientation is the best alternative for the investigated location. Nevertheless, if no storages are available, a mix of west and east orientation helps improving the fossil energy savings due to a constant solar yield throughout the day.
- For east or west orientation, the decentralised systems with direct local utilisation of the solar yield outperform the central plant even more due to the lower average temperature level.
- Climatic conditions with lower ambient temperatures and higher irradiation help improving the performance of distributed feed-in systems compared to pure domestic hot water plants, while lower irradiation and similar temperatures have no significant influence on the ranking.
- Networks with lower heat demand density lead to lower relative fossil energy savings. Domestic hot water systems are not influenced as much as other concepts due to the generally lower network temperature during summer.
- A temporal variation of the domestic hot water demand has no significant influence on the results.
- A forced overheating of the district heating pipes by a central solar thermal plant can increase the fossil energy savings. The improvement is higher for low available buffer storage volumes.
- The autonomous operation of parts of the district with a shutdown of pipe connections to this part can lead to additional fossil energy savings. The effect is more noticeable for an uneven distribution of collector arrays and buffer storages.

Besides these aspects, close attention has to be paid to the operational costs and, in particular, on the investment costs and of the plants. The following section describes the relation between costs and fossil energy savings of the different approaches in order to derive recommendations for the most promising system solutions.

7 Economic Assessment

One of the main objectives of the field test installation, described in section 4, was to reduce the heat generation costs of decentralised solar thermal systems in urban areas to a level of 8 Ct/kWh to 12 Ct/kWh. This section describes a method for a general calculation of the investment and the heat generation costs, respectively the costs of saved fossil energy of these systems. Several variations of plant layouts and boundary conditions are introduced and the impact on the economic results is documented in comprehensive graphs. This allows the deviation of general design rules for the conception of solar district heating systems.

7.1 Methodology

On the basis of the investment and operating costs of the installed plants combined with the extrapolation of the average annual yields, an economic efficiency evaluation was carried out according to the annuity method, published in VDI 2067 [79]. This method divides the total costs of a plant into capital-related, demand-related, operation-related and other costs.

The calculations were based on the following assumptions:

- 1.5 % interest rate
- 2 % annual price increase of components
- 3 % annual price increase of fossil fuel and electricity
- 2 % annual price increase labour costs

A 2 % increase in prices represents typical long-term inflation rates. 1 % extra increase in energy prices was included, as these are associated with greater volatility and a long-term decline in the supply of fossil fuels. This is also consistent with the average increase in gas prices, as well as electricity prices over the past 15 years [80]. It should be noted that the gas price is not included in the calculation of the solar heat generation costs, respectively the fossil energy saving costs as only the solar thermal system is investigated and not the complete system including the fossil boilers. The imputed interest rate is 1.5 %. This corresponds to the interest rate of the German *KfW (Kreditanstalt für Wiederaufbau)* bank funding programme 271 in the time of the plant set-up, in case of 20 years life and a good solvency. This programme intends to financially support the installation of renewable energy systems. For solar thermal collectors, a lifetime of 20 years is assumed in VDI 2067. This was maintained in the calculations, although experience shows that the actual lifetime of solar thermal systems can be longer. In addition, the calculations with and without funding are

considered. For the variant with funding, the *KfW* program "Renewable Energies Premium" (271) was applied in the version 08/2016. A redemption funding of 30 % is possible for large-scale plants, respectively 40 % if they feed a major part of the heat into a district heating network [81].

In the case of demand-related costs, only the power consumption of the pumps and controllers is required for solar thermal systems. In the field test project, the installed electricity meters were used to determine this electricity consumption. It should be noted that a slightly higher power consumption is given, than it would be the case for solar thermal systems without additional scientific measurement devices. In addition, the start-up phase coincided with lower yields in the considered operation period. Therefore, a long-term electricity consumption of 1 % of the solar yield was defined for all plants. This is confirmed for the RS feed-in systems by the findings of [23], who found that only for high differential pressures in the substation, the feed-in pump power increases significantly. The current electricity costs were set to 28 Ct/kWh for the economic efficiency assessment.

7.2 Results of the Field Test Installation

In addition to the current yield of the plants, the considered optimisations of the system operation introduced in Section 4.8 are included in the analysis. Table 39 shows the investment costs, the solar yield and the calculated solar heat production costs of the realised as well as the optimised plants. The solution with adapted supply temperature and adapted net flow was considered in this case.

Table 39: Economic analysis of the realised and optimised solar thermal plants with and without consideration of funding

	Investment costs in € (€/m²)	**Solar yield in MWh**	**Heat generation costs in Ct/kWh**	
			Without funding	**With funding**
Building 1	82,727 (1,165)	42.5	11.8	8.5
Building 2	52,755 (743)	17.0	18.9	11.9
Building 2 opt.		23.2	13.8	8.7
Building 3	59,443 (837)	32.0	11.7	8.4
Building 3 opt.		32.5	11.5	8.3
Building 4	62,527 (881)	26.0	14.8	10.7
Building 4 opt.		26.6	14.4	10.4

A look at the cost structure of the plants provides information on the relevant starting points for further cost reduction. For each of the four plants, the fractional investments

for each component and labour costs are broken down in Figure 90. In general, savings can be achieved less in the material costs for the collectors, but rather in the installation effort. Simpler assembly methods or a higher level of prefabrication can be useful, since a considerable part of the costs in the "hydraulics" position are spent on personnel. For the economic analysis, investments that are not directly related to the solar thermal systems but were carried out in the course of construction were neglected. These include e.g. the renovation of the roof on building 1 or the relocation of the house electricity connection from the roof to the basement of building 2. In addition, it should be noted that the additional work involved by integrating the metrological devices is included in the costs for hydraulics. The planning costs of the housing association are significant, too. However, some measures are included here, which are not related to the solar thermal systems but to the refurbishment of the building. Unfortunately, this could not be broken down further. The construction of solar thermal plants in the course of any upcoming refurbishment will most probably incur lower costs. On top of that, building 1 contains the installed district heating feed-in, which is not necessary for the current sizing of the system but was desired by the operator (cf. section 4.5.1).

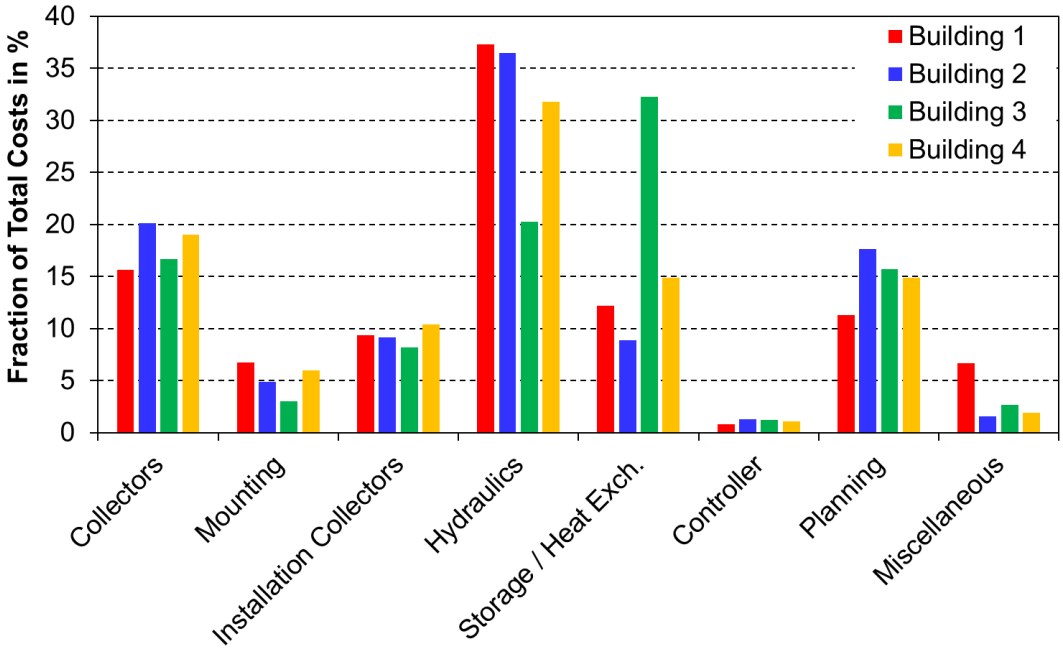

Figure 90: Fraction of single cost aspects for the four realised plants

7.3 Investment Costs for the Simulation Study

Taking the discussion further to the assessment of the variants, investigated in section 6, it is necessary to find out the costs for the differently designed and sized solar thermal systems. Cost data are available of the four realised plants but for different collector array sizes, buffer storage sizes and other components, additional investment

costs have to be defined. There are some data available from literature, that can be compared to the data from the research site.

Opposite to the field test installation, the simulation study is based on exemplary districts, where no actual investment costs are available. To cope with that, a method for calculating the costs for different sizes and numbers of plants was applied, which is based on several cost curves, depending on the component size or number of components. *Task 52* [82] provides figures for the investment costs of large solar thermal plants depending on type and size. In addition to that, the investigated plants from section 2.4 where analysed with focus on the component costs and the total investment, which is available for 21 plants of a comparable size. Other plants in the literature review have several thousand square meters of collector area and are therefore not a suitable data source for the simulated plants with a maximum of 820 m² collector area. Figure 91 shows the curves from *Task 52* in addition to the numbers of the investigated real installations.

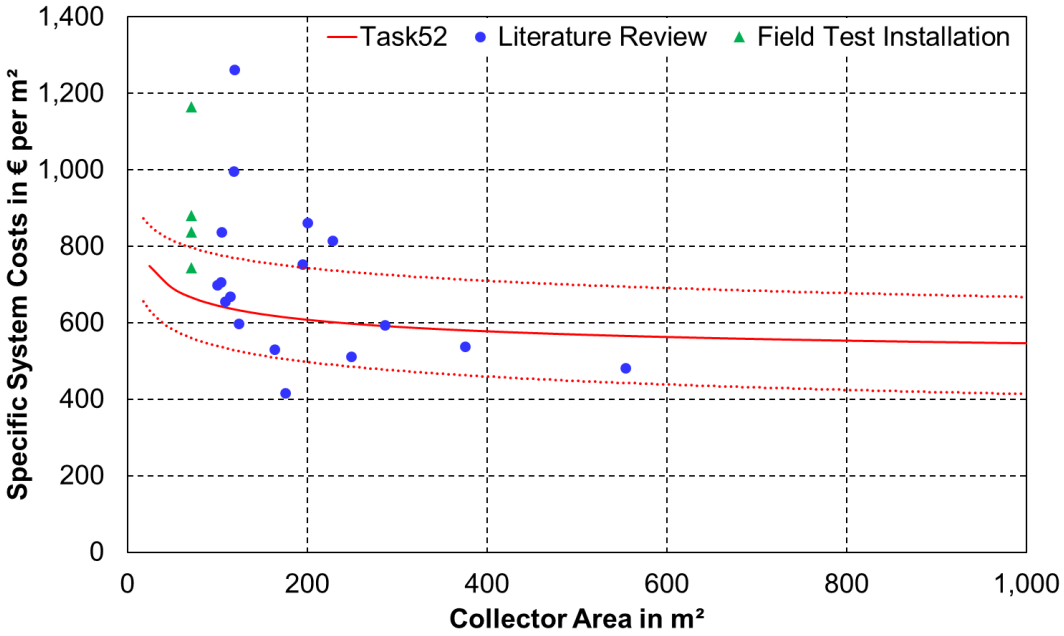

Figure 91: Minimum, maximum (red dotted) and average (red solid) cost curves according to *Task 52*, the plants investigated in the literature review (blue) and the test site plants (green) depending on the collector area

Task 52 states average values as well as minimum and maximum values for the installation costs of different kinds of systems and a cost curve depending on the collector area. The single-family home system with 18 m² collector area is below the smallest investigated variant but in the same region regarding the buffer size (1.5 m³ compared to 2 m³). The system for the multi-family home (100 m²) is close to the 82 m² system but has with 9 m³ a higher storage volume than the investigated decentralised storages. The block heating system with 1,000 m² collector area is close to the largest

investigated system but again has a larger buffer of 100 m³ compared to the maximum of 20 m³ in the simulation study.

As the given numbers are not sufficient to calculate the investment costs of variable combinations of collector area and buffer volume, a more detailed analysis of the component costs of the available plants was necessary. The categories were chosen as already shown in Figure 90. From the values of each category for each plant, average values depending on the system size were derived. All component costs were divided by the collector area to get the specific costs. The only exception is the buffer, which was calculated based on the buffer volume. All costs include the related labour costs to install the components. This is giving several trend-line-functions:

$$Cost_{Coll} = 950 \cdot A_{Coll}{}^{0.685} \quad (22)$$

$$Cost_{Mounting} = 1692 \cdot A_{Coll}{}^{0.2689} \quad (23)$$

$$Cost_{Piping\_Coll} = 4750 + 94 \cdot A_{Coll}{}^{1} \quad (24)$$

$$Cost_{Piping\_System} = 369 \cdot A_{Coll}{}^{0.6302} \quad (25)$$

$$Cost_{Buffer} = (403.5 \cdot V_{Buffer}{}^{-0.4676} + 750) \cdot V_{Buffer} \quad (26)$$

$$Cost_{Control} = 982 \cdot A_{Coll}{}^{0.3378} \quad (27)$$

$$Cost_{Planning} = 161 \cdot A_{Coll}{}^{0.8554} \quad (28)$$

$$Cost_{Misc} = 137 \cdot A_{Coll}{}^{0.7424} \quad (29)$$

with:

A_{Coll}	*collector area*	*m²*
$Cost_{Buffer}$	*costs of buffer storage and heat exchangers*	*€*
$Cost_{Coll}$	*costs of collectors*	*€*
$Cost_{Control}$	*costs of controller and sensors*	*€*
$Cost_{Misc}$	*costs of miscellaneous components*	*€*
$Cost_{Mounting}$	*costs of collector mounting*	*€*
$Cost_{Piping\_Coll}$	*costs of collector piping*	*€*
$Cost_{Piping\_System}$	*costs of system piping*	*€*
$Cost_{Planning}$	*costs of planning*	*€*
V_{Buffer}	*buffer volume*	*m³*

Taking these equations for recalculating the costs for the realised plants from the literature review and field test results in the graph, shown in Figure 92. The real investment is slightly higher in the range from 0 to 250 m² and lower at larger collector areas. This applies for both, the *Task 52* curve and the component-based trend line. Nevertheless, the component-based trend line shows less deviation from the realised installations and has an average deviation across all plants of 2 %.

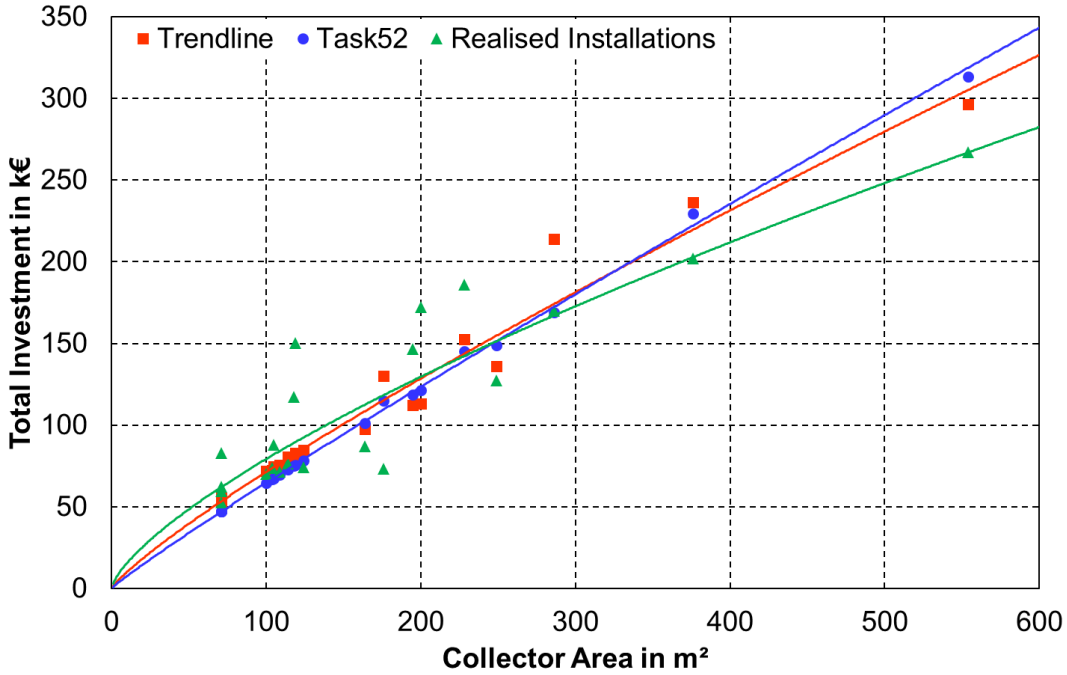

Figure 92: Derived curve of total investment costs compared to the investigated realised installations and the approach of *Task 52*

Due to the decent correlation, the equations can be used to calculate the total investment for the variants of the simulation study. To account for the higher costs of several smaller plants compared to one large plant, each plant is calculated as a separate system with the corresponding costs. I.e. a central system is calculated as one plant with 410 m² collector area and 10 m³ volume, while 5 domestic hot water plants with the same total size are calculated as 5 plants with 82 m² collector area and 2 m³ buffer volume, each.

Besides the investment, *Task 52* also gives values for the annual operation and maintenance costs per square meter installed collector gross area, which are 6.10 €, 5.50 € and 3.50 € for the fixed costs of the single-family, multi-family and block heating systems respectively 1.20 €, 1.40 € and 1.40 € for the variable costs. Nevertheless, as the used method is VDI 2067, the values from this source were taken for maintenance, which result in costs per square meter between 2.59 € for the largest and 11.11 € for the smallest plants.

7.4 Results of the Basic Systems

7.4.1 Equally Distributed Plants

The following results were calculated according to the previously introduced method without funding and value added taxes. Figure 93 shows the annual fossil energy savings of the basic variants, i.e. the plant dimensions according to section 6.2.1, in the non-renovated district. The numbers at each point indicate the total area of the collector arrays and the total buffer volume of the system variants considered. The central systems with 205 m² and 410 m² collector area and sufficient buffer volume reach a cost level of less than 10 Ct/kWh, while the larger collector array systems, particularly without sufficient storage volume, are less economical. All decentralised systems come with higher costs due to the distributed plant installations. The pure domestic hot water system is competitive to the RR and RS systems for smaller collector arrays. When it comes to larger arrays and a lack of buffer volume, the RR and RS systems can utilise their ability of excess feed-in and outperform the DHW system. For many cases, the energy savings are higher with the decentralised systems but the additional solar yield cannot compensate the higher investment.

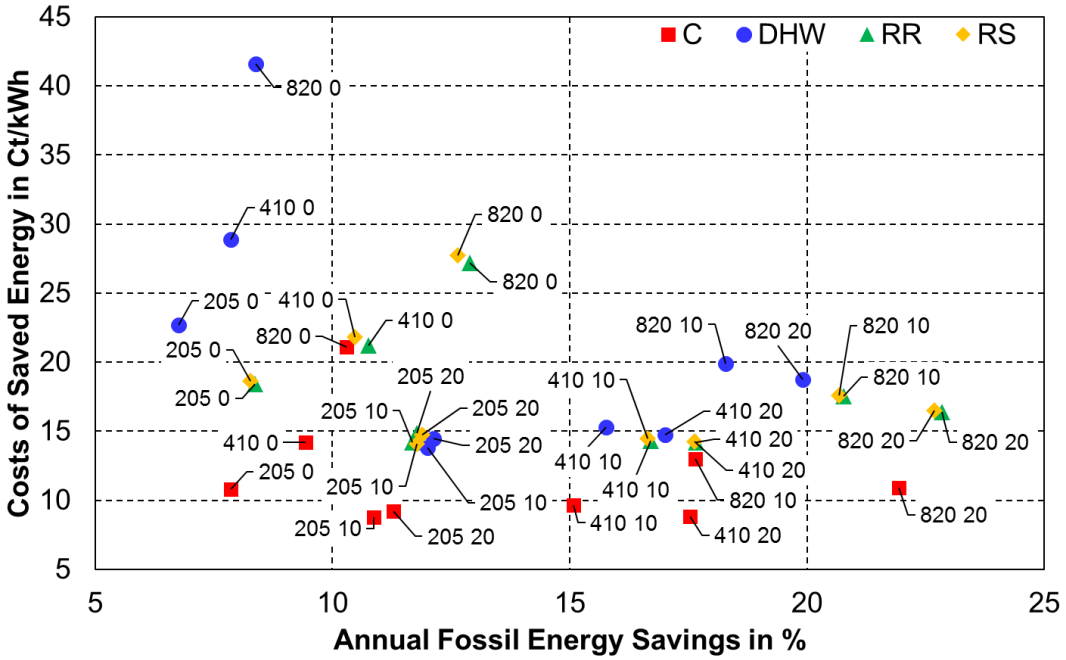

Figure 93: Annual fossil energy savings and costs of saved energy for the non-renovated basic district (numbers indicate the total collector area and buffer volume)

Making the same contemplation with the renovated district shows similar results (Figure 94). The different variants are in the same cost range like their pendants from the non-renovated district. There is a slight offset to higher costs per kWh, as the district with less consumption consequently shows less potential for energy savings.

In general, the difference between RR and RS feed-in is marginal in these cases. Some central variants with sufficient buffer still reach costs below 10 Ct/kWh while a lacking buffer has a much higher negative influence than in the non-renovated district due to the lower potential to directly supply the space heating system.

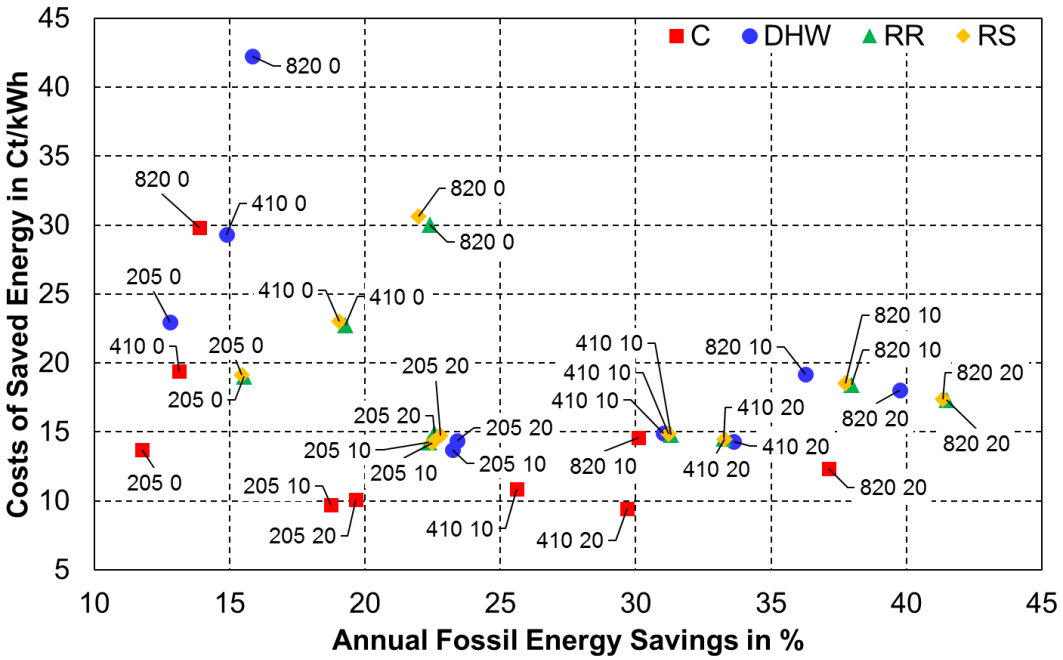

Figure 94: Annual fossil energy savings and costs of saved energy for the renovated basic district (numbers indicate the total collector area and buffer volume)

The conclusions drawn for the equally distributed plants are:

- Maximum fossil energy savings of up to 23 % for RR and RS systems with 820 m² collector area and 20 m³ buffer volume in the non-renovated district
- Fossil energy savings of more than 40 % for renovated district
- Minimum costs of saved energy around 10 Ct/kWh for central variants with 205 m² or 410 m² collector area and 10 m³, respectively 20 m³ buffer volume
- Smaller central plant (205 m²) without buffer in the non-renovated district is still competitive regarding the costs, larger plants and decentralised systems without buffer are less cost efficient
- Costs of saved energy increase for the renovated district due to lower utilisation of available solar heat
- Benefit of decentralised systems over central plants is higher for renovated than for non-renovated district
- Domestic hot water systems are competitive against feed-in systems in case of 205 m² and 410 m² collector area and at least 10 m³ buffer volume
- Lacking storage volume has more negative influence in case of the renovated district

7.4.2 Unequally Distributed Plants

Coming to the unequally distributed plants, i.e. the dimensioning according to section 6.2.7, several conclusions can be drawn. Figure 95 shows the considered systems in comparison to the basic variants of the same size (410 m² collector area and 10 m³ buffer volume at the central plant, respectively 82 m² and 2 m³ per building). The numbers show the size of the single collector arrays and the single buffer storages as described in Table 29. All variants with a central collector array of 410 m² are in a very close range. Only the variant with equally distributed storages (410 2) and RR feed-in shows considerably more energy saving at lower costs than the pure central variant. The variants with two collector arrays of 205 m² have lower costs than the equally distributed systems with five arrays of 82 m². Again, an equal distribution of the storages is the best solution for high energy savings as well as for low costs. The equally distributed collectors with unequally distributed storages (10 m³, 3 x 3.3 m³ or 2 x 5 m³) are the less cost effective, while they have average energy saving potential. For the decentralised collectors, the RR hydraulic is at least competitive and, in some cases, slightly better than the RS system.

There is a wider distribution of the central collector array systems for the renovated district. Still the 410 m², 2 m² RR variant has the lowest costs but the RS variant is very close. On the other hand, the 410 m², 5 m³ RS system does not perform as well as the pure central variant. The distributed collector arrays with 82 m² are again the most expensive systems, while two collector arrays of 205 m² and distributed storages are a good compromise between costs and energy savings (Figure 96).

For the unequally distributed plants, following statements can be derived:

- Maximum fossil energy savings of up to 17 % for equally distributed RR and RS system in the non-renovated district and up to 32 % in the renovated district for equally distributed RR, RS and DHW system
- Minimum costs of below 10 Ct/kWh (non-renovated district), respectively around 10 Ct/kWh (renovated district)
- Best performance with central collector array and equally distributed storages
- Equally distributed collector arrays of 82 m² without equally distributed storages are not recommended
- Two collector arrays of 205 m² enable medium costs at lower (with central storage) or higher (with distributed storages) fossil energy savings

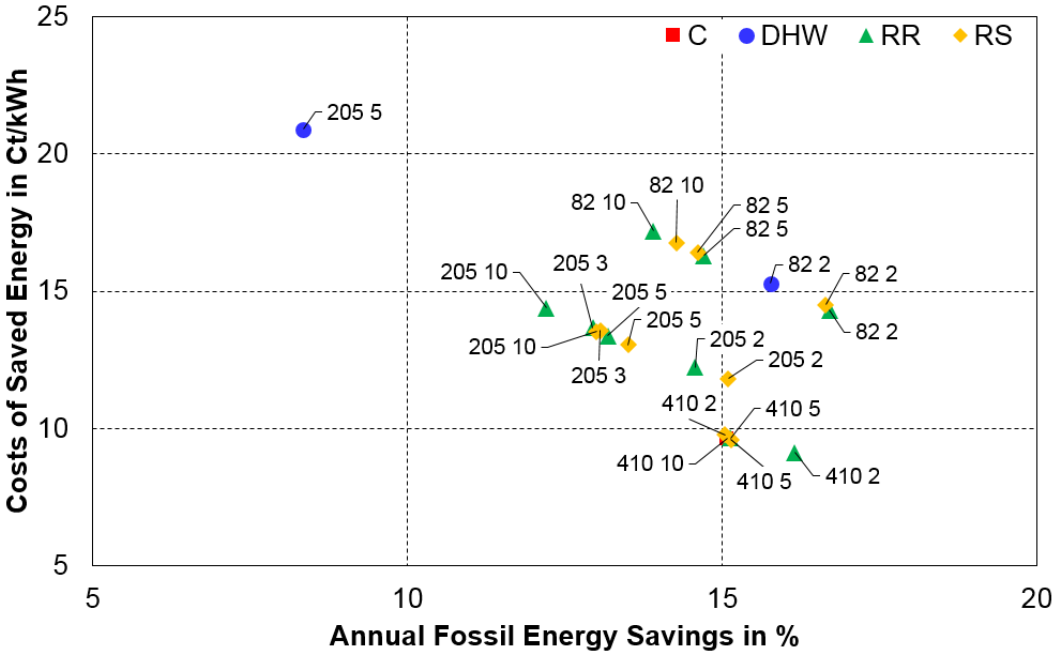

Figure 95: Annual fossil energy savings and costs of saved energy for the unequally distributed plants in the non-renovated district (numbers indicate the area of each collector array and the volume of each buffer)

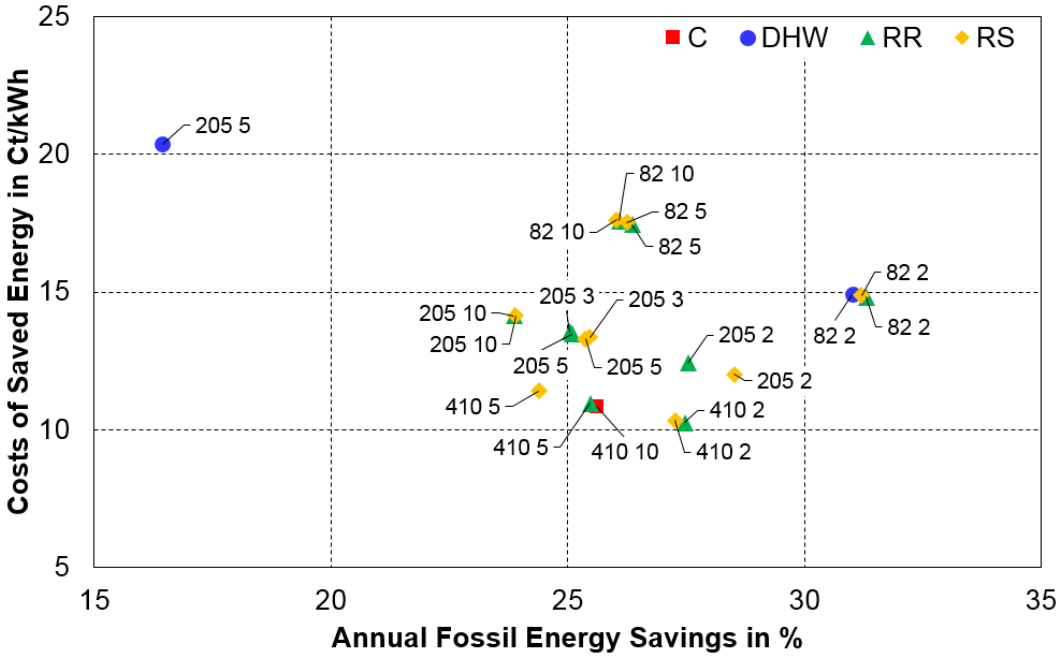

Figure 96: Annual fossil energy savings and costs of saved energy for the unequally distributed plants in the renovated district (numbers indicate the area of each collector array and the volume of each buffer)

7.5 Results of the Systems with Modified Boundary Conditions

7.5.1 Collector Orientation

The three collector orientation variants, which were tested on the equally distributed plants in section 6.3.1, were also applied on the unequally distributed plants. Figure 97, Figure 98 and Figure 99 show the results of the equally distributed and unequally distributed plants for east, west and east-west orientation with a total of 410 m² collector area and 10 m³ buffer volume. For the lower irradiation in case of an east orientation, the domestic hot water plants perform better compared to the feed-in plants. Even the 205 m², 5 m³ variant has no higher costs than the 82 m², 10 m³ variant with RR feed-in but lower energy savings. In general, the benefit of the RS scheme over the RR scheme is higher than for the other orientations. Nevertheless, none of the plants reaches costs below 17 Ct/kWh, making it challenging to compete with fossil heat generation. At the same time, the relative fossil energy savings go down below 18 % for all unequally distributed systems.

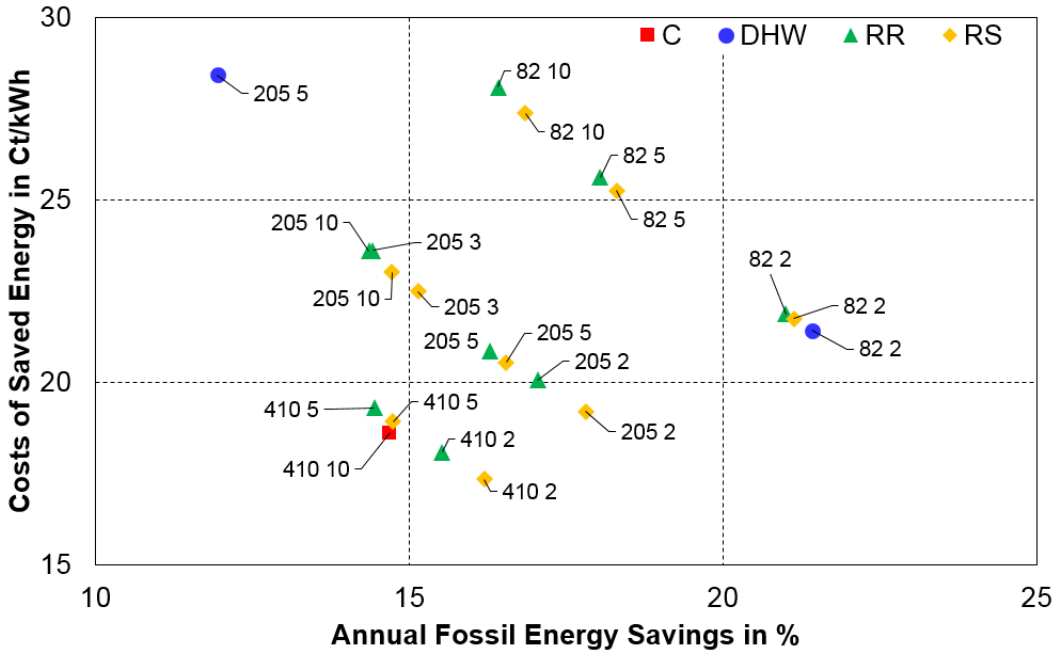

Figure 97: Annual fossil energy savings and costs of saved energy for the unequally distributed plants in the renovated district with east orientation of the collectors (numbers indicate the area of each collector array and the volume of each buffer)

For the west orientation, the results are better and costs of 12 Ct/kWh are reached with some of the variants. The fossil energy savings still are on a level of up to 25 % for the unequally distributed systems. Again, there is a better performance of the RS systems against the RR systems compared to the south orientation.

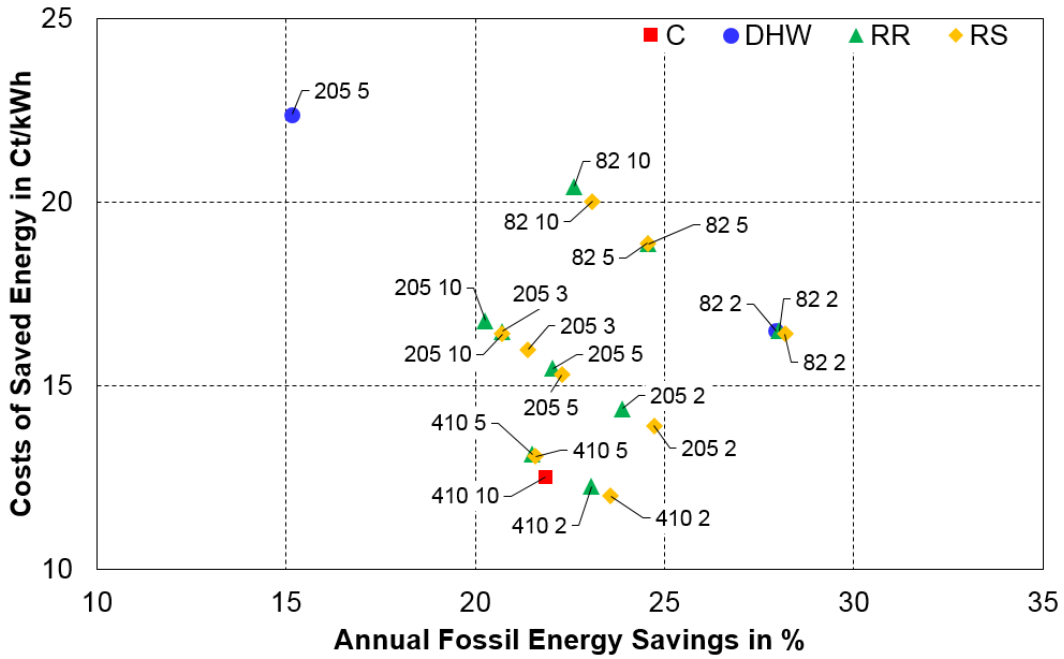

Figure 98: Annual fossil energy savings and costs of saved energy for the unequally distributed plants in the renovated district with west orientation of the collectors (numbers indicate the area of each collector array and the volume of each buffer)

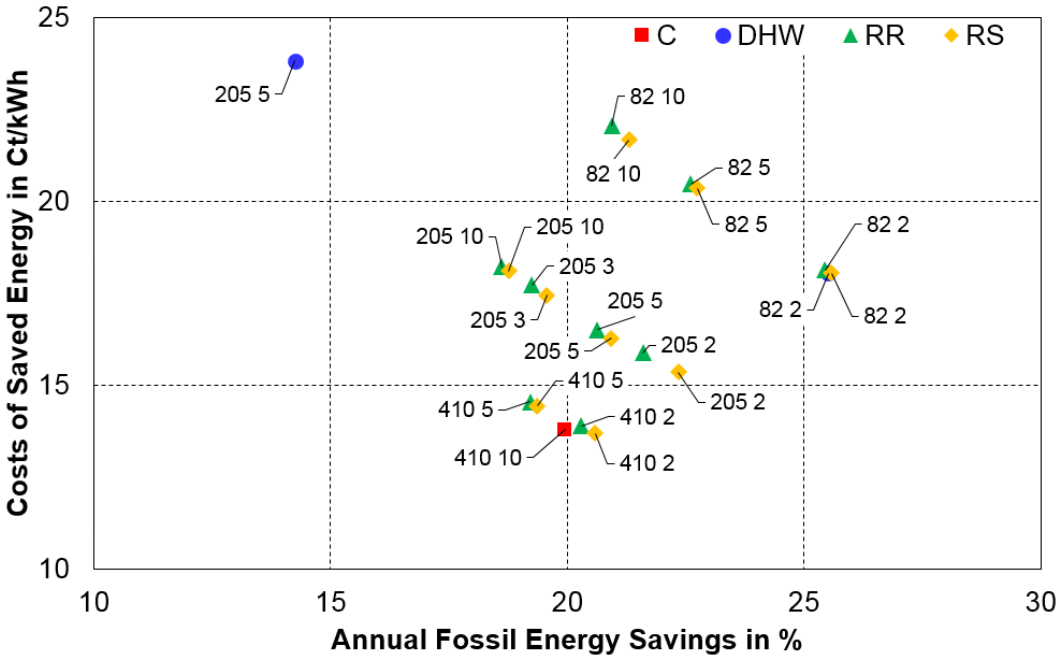

Figure 99: Annual fossil energy savings and costs of saved energy for the unequally distributed plants in the renovated district with east-west orientation of the collectors (numbers indicate the area of each collector array and the volume of each buffer)

The mixed east and west oriented collectors result in fossil energy savings and costs in between the pure east and west systems. The distribution of the different dimensioning variants, on the other hand, is closer to the south oriented systems and the differences between RR and RS scheme small.

Following designs rules can be concluded from these considerations:

- Maximum fossil energy savings for distributed plants with 82 m² and 2 m² per building regardless of collector orientation
- Minimum costs for central collector array of 410 m² and equally distributed storages of 2 m³
- Generally higher costs compared to south orientation
- Lower irradiation (east orientation) results in benefits for domestic hot water systems
- Higher benefit of RS hydraulics compared to south orientation

7.5.2 Climate

A changing climate has remarkable influence on the results, including the relative performance of the variants to each other. Figure 100 shows the unequally distributed plants in Davos. In this sunny but cold location, the difference between the 205 m², 5 m³ domestic hot water system and the other variants is even larger. Nevertheless, the costs of the saved energy are lower for all variants, as the high irradiation and higher space heating consumption increases the solar yield. The systems with one central collector array go down to 7 Ct/kWh. The equally distributed domestic hot water plants do not perform better than the variants with equally distributed collectors and unequally or central storages using RR and RS feed-in.

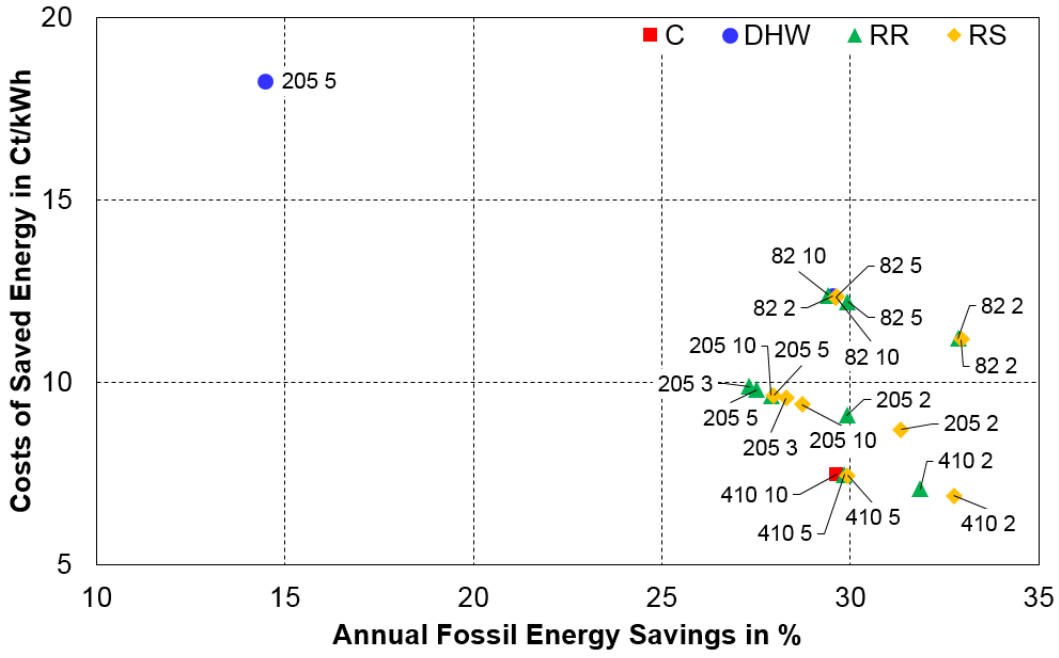

Figure 100: Annual fossil energy savings and costs of saved energy for the unequally distributed plants in the renovated district for Davos climate (numbers indicate the area of each collector array and the volume of each buffer)

Having a look at the results for Stockholm (Figure 101), the correlation between the variants is again different. For the less sunny but warmer climate compared to Davos, the disadvantage of the 205 m², 5 m³ domestic hot water system decreases, as it is more difficult for the other systems to reach the necessary feed-in temperature. None of the variants is below costs of 10 Ct/kWh for the saved energy and, in general, the relative fossil energy savings are lower than for the other locations.

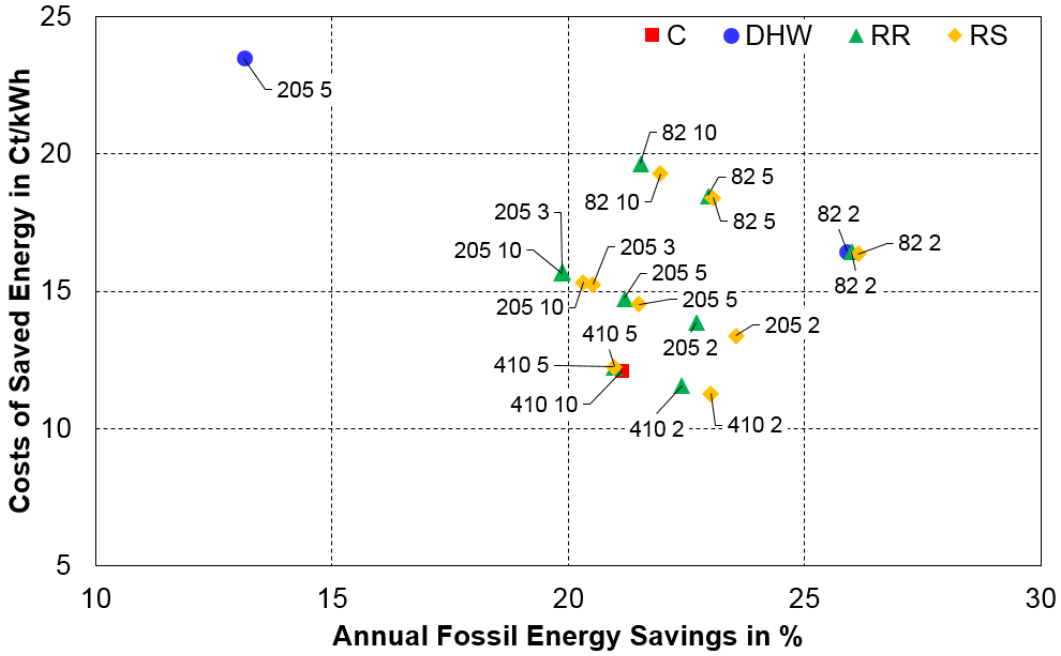

Figure 101: Annual fossil energy savings and costs of saved energy for the unequally distributed plants in the renovated district for Stockholm climate (numbers indicate the area of each collector array and the volume of each buffer)

From the contemplation of the climate conditions it can be concluded that:

- Lower ambient temperature at higher irradiation increases the fossil energy saving of the systems up to 33 % due to higher yields and higher utilisation
- Costs of saved energy of 7 Ct/kwh can be reached for Davos while in Stockholm the costs are higher than 10 Ct/kWh for all variants
- Domestic hot water plants have less disadvantages against feed-in variants in warmer climate with lower irradiation
- A central collector array with equally distributed storages is again the best solution

7.5.3 District Density and Heat Demand

The district with a longer piping distance (cf. section 6.3.3) is more beneficial for pure domestic hot water systems, as for the other variants the feed-in results in even higher network losses than for the basic variants (Figure 102). More than for the other boundary conditions, there is a benefit of the RS hydraulics. This is even true for the

central collector array with distributed storages. On top of that, the 410 m², 5 m³ variants are better than the pure central system. The increased network losses justify the installation of decentralised storages with the resulting lower operation time of the network.

The results for the modified consumption profile, defined in section 6.3.3 show no significant change of the ranking (Figure 103). There is a slight improvement of the decentralised systems compared to the pure central plant but no different general recommendation can be derived for this boundary condition.

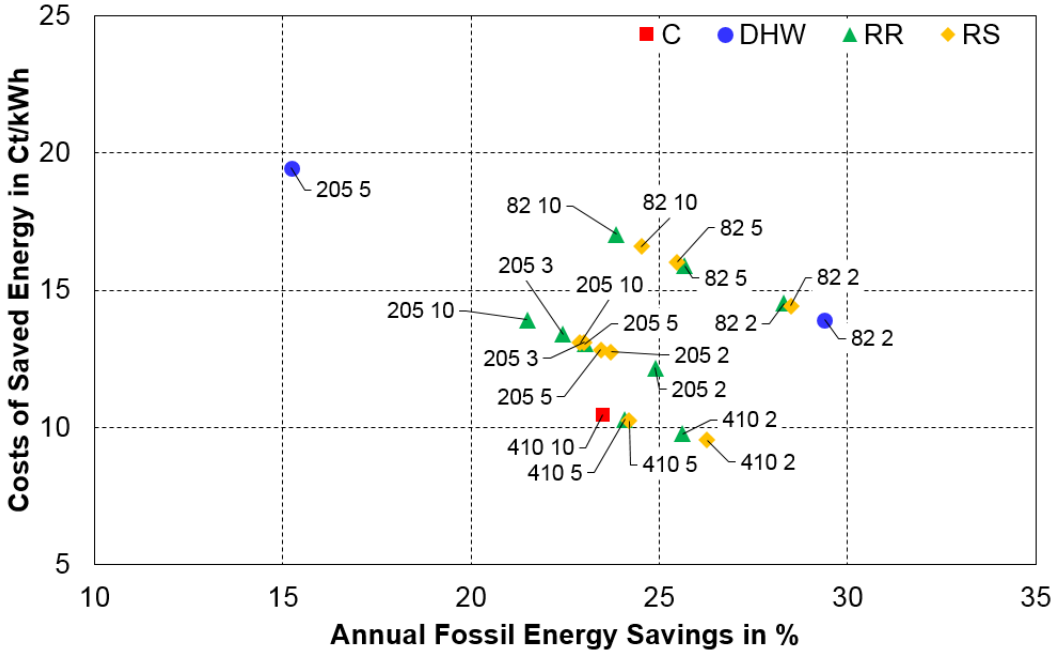

Figure 102: Annual fossil energy savings and costs of saved energy for the unequally distributed plants in the renovated district with lower consumption density (numbers indicate the area of each collector array and the volume of each buffer)

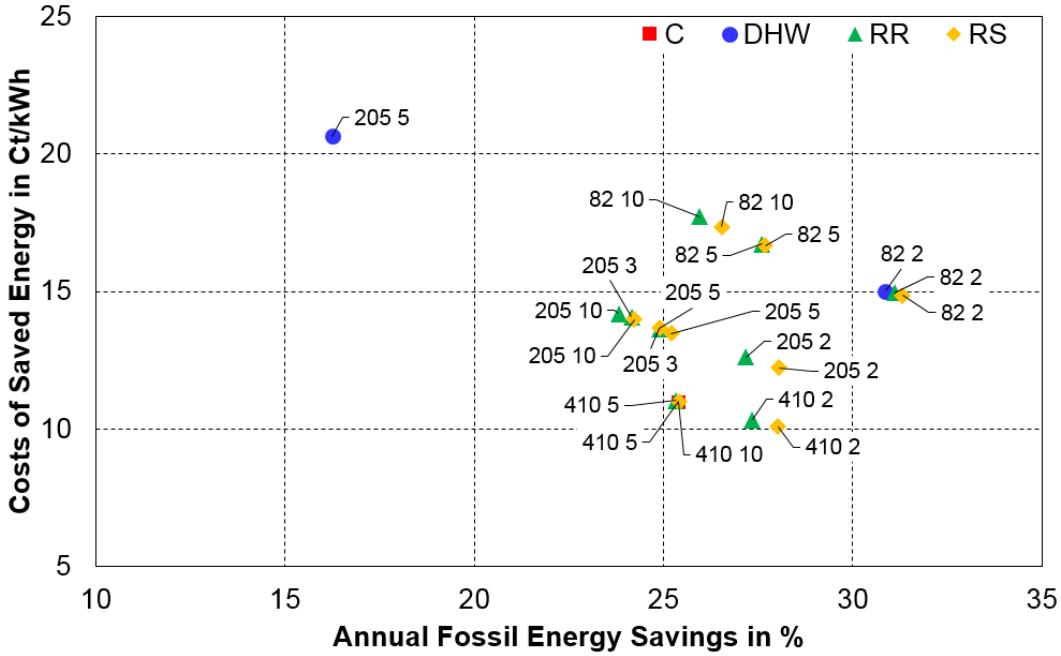

Figure 103: Annual fossil energy savings and costs of saved energy for the unequally distributed plants in the renovated district with modified consumption profile (numbers indicate the area of each collector array and the volume of each buffer)

The variation of the heat density and consumption profiles allows following conclusions:

- Longer piping distances (and heat losses) result in benefits for distributed domestic hot water systems with fossil energy savings of almost 30 %
- The advantage of distributed against central buffer storages is higher than for the basic network length
- The influence of the domestic hot water consumption profile has no relevant influence on the results as all variants come with sufficient buffer volume to compensate this temporal deviation

8 Conclusions and Outlook

Conclusions

The starting point of this thesis was the necessity of increasing the solar fraction in the heat supply of urban areas while at the same time, solar thermal technology suffers from high costs and a lack of suitable areas for the installation of larger plants. To deal with these obstacles, it was the goal to investigate the potential of decentralised integration of several medium-scale solar thermal plants in small district heating networks and use the feed-in of excess heat to reach a decent solar fraction at competitive costs.

An in-depth survey of existing large solar thermal plants was performed to analyse existing hydraulics and control concepts and to assess these systems in terms of solar yield and heat generation costs. This survey showed a wide distribution of efficiency and costs of the plants. While many ambitious projects with seasonal storages suffer from high costs, large ground-mounted systems with only small storage volume perform very well. Subsequently, a field test installation in Ingolstadt, Germany, was planned and four solar thermal plants were integrated into this district heating network. These plants follow three different hydraulic concepts:

- Pure domestic hot water preheating
- Pure feed-in to the network return pipe
- Combination of local use for domestic hot water preheating and feed-in of excess heat into the return pipe

Based on the experience gained during one year of operation, it can be concluded that the decentralised integration of solar thermal systems into an existing network did not reveal any critical technical issues. Challenges were strongly influenced by other conditions, like the availability of personnel for the installation. The integration of solar thermal plants into urban buildings should therefore ideally be carried out in combination with other renovation measures to decrease effort and costs.

The comparison of the different concepts shows, as expected, advantages for a pure feed-in with regard to the low complexity and small space requirement. It stands to reason, that similar systems can be installed in many buildings as an installation wall in the basement is sufficient to accommodate all hydraulic and control components. However, the solar yields strongly depend on the network return temperature and reach an annual value of only 220 kWh/m² at current operation conditions, while the other plants reach values from 325 kWh/m² up to 551 kWh/m². A future optimisation

of the network operation at the study site, also to reduce the distribution losses in the network, is therefore, recommended. This includes, in particular, optimising the network pump control and increasing the temperature spread in the substations, as well as a reduction of the supply temperature in summer.

The pure domestic hot water preheating is the most efficient integration variant, but only allows a limited contribution to the heat supply of the entire district in this case. The simulation-based investigation of a larger sized collector array with the use of the return feed-in directly at the central heat generator showed with 55 % compared to 15 %, a significantly higher solar fraction of the domestic hot water.

The decentralised feed-in systems with additional local use of the solar yield represent the most complex configuration in the investigation. Nevertheless, due to the return feed-in, the hydraulic changes and control effort can still be handled with market-available pumps, valves and controllers. A feed-in to the supply pipe would come along with an even higher complexity as seen from other research projects. An important starting point for further control optimisation is temperature threshold and volume flow during feed-in. In the investigated buildings, monthly solar fractions of more than 100 % during summer were observed.

The solar heat generation costs achieved with the various systems range between 11.7 Ct/kWh and 18.9 Ct/kWh. Taking into account funding and realistic optimisations of the district heating network, the costs can be reduced to a level of 8.3 Ct/kWh to 10.4 Ct/kWh.

In a second step, the field test installation was used to validate the simulation model. This model was subsequently extended by a RS feed-in option for an additional parametric study. Based on a small network of five multi-family buildings, various dimensions of collector arrays and storage volumes were analysed for pure central plants, pure domestic hot water plants and feed-in plants with RR and RS hydraulics. The systems were simulated with and without additional retrofitting measures reducing the space heating demand and temperature levels.

It was shown that a central plant with small- or medium-sized collector area and a storage volume of at least 0.025 m³ per square meter collector area is a better economic solution than an equal distribution of collectors and storages across the buildings. This results in costs below 10 Ct/kWh for the renovated as well as the non-renovated district. On the other hand, the highest fossil energy savings can be reached with distributed plants and large collector arrays.

As a large central plant or a completely equal distribution of the components are not possible in many real cases, a variety of unequally distributed plants was tested. It could be shown that, if possible, a central collector array in combination with distributed storages is a technically and economically promising solution and even performs better than a combination with a large central buffer due to decreased average network temperatures, and hence lower network losses.

If a central collector array cannot be installed, several larger distributed arrays work very well, too. These come with higher investment costs compared to the central variant but still enable competitive heat costs and high fossil energy savings, if they are combined with distributed storages. A distribution of the collectors across all buildings is even more costly and therefore not recommended, if the installation is not combined with sufficient storage volume.

A parametric study on changing boundary conditions, including climate, collector orientation, consumption profiles and piping length of the network confirmed these results. Nevertheless, the differences between the dimensioning and hydraulic integration variants change and solutions, which are not competitive in one district can be a reasonable option in another district. One example are the pure domestic hot water plants, which are outperformed by the feed-in variants in a cold and sunny climate but are competitive, if the climate is less sunny. Another case are collectors with combined east and west orientation. These enable generally less energy savings than south-oriented arrays but are a reasonable solution, if there is no thermal storage available.

The operation of a district heating network with decentralised feed-in offers many degrees of freedom for further optimisation by utilising the distributed plants. This was exemplarily tested by using the network as additional buffer for a central plant as well as operating parts of the network autonomously during periods of solar heat production. These optimisations increased the fossil energy savings by up to 5 %.

It can be summarised that smart decentralised solar district heating is well worth considering regarding the installation of distributed collectors and, in certain, distributed storages. In the analysed cases the benefit of the more complex RS feed-in does not have a significant effect on the fossil energy savings. While the solar yields are generally higher than for the RR systems, this is partly compensated by higher network losses. This, together with the experience gained from the field test installation leads to the recommendation that RR feed-in systems are the preferable solution, if there are no temperature thresholds set by a network operator that might prohibit an increase of the return temperature.

Outlook

To keep the results well structured, regarding the comparison of the different system approaches, only a small part of the wide range of possible locations, building sizes, network sizes and heat demands is shown in this work. As already seen from the results, different boundary conditions can justify different system layouts and each network has to be analysed in detail to get the most efficient and economical solution.

Further studies on this topic are desirable to improve the understanding of the system behaviour. This should be accompanied by further real-life retrofitting projects, allowing a further optimisation of the modelling and cost calculation.

On top of that, optimisations of the control strategies can be done to increase the efficiency of the proposed systems. These optimisations should include an in-depth planning of the network pressure and volume flow conditions.

While this project focussed on the energy management, the results from other presented research should be considered regarding hydraulic details. Another topic should be the testing of different hydraulic schemes inside the buildings, e.g. direct space heating support from buffer or decentralised domestic hot water preparation in the single flats as well as different collector types, which can significantly change the reasonable system design [83].

The influence of changing network temperatures on the efficiency of the heat generator at the central heating station was not further analysed in this work. Depending on the system type, an influence is expected on the performance of the auxiliary heat production. Combined heat and power plants can suffer from an increased return temperature, shifting the overall system efficiency towards the RS feed-in strategy. The same holds true for condensing boilers. The integration of central or even decentralised heat pumps, however, can increase the solar yield due to a lower feed-in threshold. The investigation of the interdependency of different heat sources and the solar thermal plants should be part of future research. In a next step, even the connection to the electricity grid can be analysed in combination with heat pumps, direct electric heating or photovoltaic modules as a supplement or substitution of solar thermal collectors.

Going back to the initial statement, that the solarisation of urban districts with multi-family houses is an essential part of the efforts to reduce carbon dioxide emissions, the results of the work show, that even without accompanying energetic renovation measures, the approach of smart solar district heating can have a significant effect. Solar fractions of up to 17 % are reached with moderate collector areas of 7 m² per

residential unit. If additional energy saving measures, like improving the buildings insulation and reducing temperature levels of the heating system are implemented, the benefit is even higher. Solar fractions of up to 34 % are possible for the same collector areas in the investigated cases. Assuming, that all space heating and domestic hot water demand in Germany would be covered with 17 % solar energy, a total final energy reduction of 143 TWh would be possible. This sums up for 40 % of the necessary renewable heat production in 2050.

References

[1] Bundesministerium für Wirtschaft und Energie, *Energiedaten: Gesamtausgabe*. Berlin, 2018.

[2] Nitsch, J., et al., “Langfristszenarien und Strategien für den Ausbau der erneuerbaren Energien in Deutschland bei Berücksichtigung der Entwicklung in Europa und global”, DLR / IWES / IFNE, 2014.

[3] Wünsch, M., et al., “Beitrag von Wärmespeichern zur Integration erneuerbarer Energien”, Prognos AG, 2011.

[4] Loga, T., et al., *Deutsche Wohngebäudetypologie: Beispielhafte Maßnahmen zur Verbesserung der Energieeffizienz von typischen Wohngebäuden,* 2nd ed. Darmstadt: Institut Wohnen und Umwelt, 2015.

[5] Statistische Ämter des Bundes und der Länder, *Zensus Kompakt … Ergebnisse des Zensus 2011*. Stuttgart, 2011.

[6] Bundesministeriums der Justiz und für Verbraucherschutz, *Verordnung über energiesparenden Wärmeschutz und energiesparende Anlagentechnik bei Gebäuden (Energieeinsparverordnung - EnEV): EnEV 2014*. Berlin, 2015.

[7] Rein, S., et al., “BBSR-Analysen Kompakt 09/2016”, Bundesinstitut für Bau- Stadt- und Raumforschung, Bonn, 2016.

[8] Stryi-Hipp, G., et al., “GroSol Studie zu großen Solarwärmeanlagen”, Bundesverband Solarwirtschaft, 2007.

[9] Eicker, U., *Solare Technologien für Gebäude: Grundlagen und Praxisbeispiele,* 2nd ed. Wiesbaden: Vieweg+Teubner Verlag / Springer Fachmedien Wiesbaden GmbH, 2012.

[10] Duffie, J. A., Beckman, W. A., *Solar engineering of thermal processes,* 4th ed. Hoboken: Wiley, 2013.

[11] Bollin, E., et al., *Automation regenerativer Wärme und Kälteversorgung von Gebäuden: Komponenten, Systeme, Anlagenbeispiele,* 1st ed. Wiesbaden: Vieweg+Teubner Verlag, 2009.

[12] Krimmling, J., *Energieeffiziente Nahwärmesysteme: Grundwissen, Auslegung, Technik für Energieberater und Planer,* 1st ed. Stuttgart: Fraunhofer-IRB-Verlag, 2011.

[13] Szablinski, D., “Energetische Optimierung von solar unterstützten Nahwärmesystemen” Dissertation, Ruhr-Universität Bochum, 2004.

[14] Skagestad, B., Mildenstein, P., “District Heating and Cooling Connection Handbook”, International Energy Agency, 2002.

[15] Gerhardy, K., “Das DVGW-Arbeitsblatt W 551 und die 3-Liter-Regel”, *energie wasser praxis*, vol. 2012, no. 2, pp. 42–45, 2012.

[16] Solites Steinbeis Research Institute for Solar and Sustainable Thermal Energy Systems, *Solar District Heating - The SDH Projects Website.* [Online] Available: www.solar-district-heating.eu. Accessed on: Nov. 12 2018.

[17] Mangold, D., “Solar district heating guidelines - Collection of Fact Sheets”, SDH, 2012.

[18] Peuser, F. A., et al., “Abschlussbericht zum Projekt 032 9601 L gefördert mit Mitteln des BMU Teil I (veröffentlichter Teil): Wissenschaftlich-technische Ergebnisse”, Zfs - Rationelle Energietechnik GmbH, 2006.

[19] Schäfer, K. et al., “Dezentrale Einspeisung von Solarthermie in Wärmenetze - technische Analyse von realisierten Anlagen” in *Ostbayerisches Technologie-Transfer-Institut e.V. - 24. Symposium Thermische Solarenergie*, Bad Staffelstein, 2014.

[20] Dalenbäck, J.-O., “Decentralised SDH Systems - Swedish Experience”, presented at *1st International Solar District Heating Conference*, Malmö, 2013.

[21] Papillon, P., Paulus, C., “Design and Recommendations for Decentralized Solar District Heating Systems in France” in *13th Conference of International Building performance Simulation Association*, Chambéry, 2013.

[22] Lennermo, G., Lauenberg, P. “Variation in Differential Pressure at a District Heating Prosumer Substation” in *3rd International Solar District Heating Conference*, Toulouse, 2015.

[23] Schäfer, K. et al., “DEZENTRAL - Dezentrale Einspeisung in Nah- und Fernwärmesysteme unter besonderer Berücksichtigung der Solarthermie”, Solites Steinbeis Research Institute for Solar and Sustainable Thermal Energy Systems, 2015.

[24] Heymann, M., Rühling, K., “Integration of Solar Thermal Systems into District Heating - Results of a Case Study done in the R&D Project DEZENTRAL” in *3rd International Solar District Heating Conference,* Toulouse, 2015.

[25] Rosemann, R., Löser, J., Rühling, K., “Controller Development for a Combined Supply and Feed-In Substation and Testing Through Emulation” in *3rd International Solar District Heating Conference,* Toulouse, 2015.

[26] Lundh, M., Dalenbäck, J.-O., “Swedish solar heated residential area with seasonal storage in rock: Initial evaluation”, *Renewable Energy*, vol. 33, no. 4, pp. 703–711, 2007.

[27] Spliethoff, H. et al., “Begleitforschung Solare Nahwärme Am Ackermannbogen in München - SNAB”, Bayerisches Zentrum für Angewandte Energieforschung e.V., 2010.

[28] Gustafsson, J., Delsing, J., van Deventer, J., “Improved district heating substation efficiency with a new control strategy”, *Applied Energy*, vol. 87, no. 6, pp. 1996–2004, 2010.

[29] Felsmann, C., “TRNSYS-TUD Simulation von Wärmenetzen”, presented at *Symposium Integrale planung und Simulation in Bauphysik und Gebäudetechnik*, Dresden, 2012.

[30] Guigas, M., “Abschlussbericht Solare Nahwärme Fellbach”, Stadtwerke Fellbach, 2000.

[31] Rehrmann, U., Mies, M., “Kurzbericht zum Langzeitverhalten Solaranlage Cohnsches Viertel Hennigsdorf”, ZfS, 2010.

[32] Mies, M., Rehrmann, U., “Abschlussbericht für das Projekt Cohnsches Viertel Hennigsdorf”, ZfS, 2007.

[33] Mies, M., Rehrmann, U., “Abschlussbericht für das Anlagenmonitoring Nahwärme Wiershäuser Weg Hann. Münden Berichtszeitraum: bis Oktober 2010”, ZfS, 2010.

[34] Rehrmann, U., Mies, M., “Kurzbericht zum Langzeitverhalten Neubaugebiet „Badener Hof“ Heilbronn”, ZfS, 2010.

[35] Mies, M., et al., “Abschlussbericht für das Projekt Neubaugebiet "Badener Hof" Heilbronn”, ZfS, 2006.

[36] Mies, M., Rehrmann, U., “Abschlussbericht für das Projekt Wohngebäude Magdeburger Str. Hannover Berichtszeitraum: bis Dezember 2009”, ZfS, 2010.

[37] Rehrmann, U., “Solaranlage zur Nahwärmeunterstützung Wohnsiedlung Stuttgart Burgholzhof”, ZfS, 2000.

[38] Peuser, F. A., et al., “Abschlussbericht für das Projekt Wohnsiedlung Burgholzhof Stuttgart”, ZfS, 2007.

[39] Miedaner, O., Pauschinger, T., “Nutzung der Solarthermie bei der Bestandssanierung im städtischen Umfeld - Beispielhafte Umsetzung einer lokalen Initiative in Stuttgart” in *Ostbayerisches Technologie-Transfer-Institut e.V. - 23. Symposium Thermische Solarenergie*, Bad Staffelstein, 2013.

[40] Croy, R., Wirth, H. P., “1. Zwischenbericht für das Projekt Solaranlage im Wohngebiet ehemaliger Schlachthof in Speyer”, ZfS, 2006.

[41] Croy, R., Wirth, H. P., “4. Zwischenbericht für das Projekt Solaranlage im Wohngebiet ehemaliger Schlachthof in Speyer”, ZfS, 2009.

[42] Croy, R., “Abschlussbericht für das Projekt Solaranlage im Wohngebiet ehemalige Kaserne Normand in Speyer”, ZfS, 2009.

[43] Mies, M., Rehrmann, U., “Abschlussbericht für das Projekt Nahwärme Gorch-Fock-Weg Norderney Berichtszeitraum: bis Dezember 2009”, ZfS, 2010.

[44] Bollin, E., “Solar unterstützte Nahwärmeversorgung Holzgerlingen”, Hochschule Offenburg, 2012.

[45] Bühl, J., et al., “Förderprogramm ”Solarthermie 2000” Teilprogramm 2 Zwischenbericht zur 3. Messperiode (Nov. 2004 - Nov. 2005) (Kugelberg Weißenfels)”, Technische Universität Ilmenau, 2006.

[46] TU Chemnitz, *Solarthermie2000.* [Online] Available: https://www.tu-chemnitz.de/mb/SolTherm/ST2000/auswahl.htm. Accessed on: Sep. 15 2018.

[47] Benner, M. et al., “Solar unterstützte Nahwärmeversorgung mit und ohne Langzeit-Wärmespeicher 1998-2003”, Institut für Thermodynamik und Wärmetechnik, 2004.

[48] Bollin, E., et al., “Schlussbericht Solaranlage Wohngebäude Wilmersdorfer Straße Freiburg”, Fachhochschule Offenburg, 2003.

[49] Schlosser, M., et al., “Langzeitmonitoring Solar unterstützte Nahwärmeversorgung Hamburg-Bramfeld” in *Ostbayerisches Technologie-Transfer-Institut e.V - 17. Symposium Thermische Solarenergie*, Bad Staffelstein, 2007.

[50] Schlosser, M., Fisch, M. N., “Wissenschaftliche Begleitung der solar unterstützten Nahwärmeversorgung Hamburg-Bramfeld” in *Ostbayerisches Technologie-Transfer-Institut e.V. - 23. Symposium Thermische Solarenergie*, Bad Staffelstein, 2013.

[51] Bodmann, M., “Solar unterstützte Nahwärmeversorgung Hamburg-Bramfeld” in *Ostbayerisches Technologie-Transfer-Institut e.V - 15. Symposium Thermische Solarenergie*, Bad Staffelstein, 2005.

[52] Gries, A., “Solarsiedlung Gelsenkirchen-Lindenhof”, EnergieAgentur.NRW, Düsseldorf, 2008.

[53] Croy, R., Wirth, H. P., “Analyse und Evaluierung großer Kombianlagen zur Trinkwassererwärmung und Raumheizung”, Zfs - Rationelle Energietechnik GmbH, 2006.

[54] Croy, R., “Projekthistorie zum Abschlussworkshop Integration von Heizkesseln in Wärmeverbundsysteme mit großen Solaranlagen”, presented at *Abschlussworkshop Integration von Heizkesseln in Wärmeverbundsysteme mit großen Solaranlagen*, Wolfenbüttel, 2012.

[55] Bodmann, M., Fisch, M. N., “Betriebserfahrungen der solar unterstützten Nahwärmeversorgung in Hannover, Steinfurt und Hamburg” in *Ostbayerisches Technologie-Transfer-Institut e.V - 13. Symposium Thermische Solarenergie*, Bad Staffelstein, 2003.

[56] Gries, A., “Solarsiedlung Steinfurt-Borghorst”, EnergieAgentur.NRW, Düsseldorf, 2008.

[57] Milles, U., “Solar unterstützte Nahwärme”, BINE Informationsdienst, Bonn, 2000.

[58] Schmidt, T., et al., “Langzeit-Wärmespeicher für solare Nahwärme”, in *ForschungsVerbund Sonnenenergie Workshop Wärmespeicherung*, Köln, 2001.

[59] Mangold, D., “Einführung in die solare Nahwärme mit saisonalem Wärmespeicher Hirtenwiesen 2 in Crailsheim”, presented at T*reffen der Arbeitsgruppe Solare Nah- und Fernwärme*, Crailsheim, 2010.

[60] Marx, R., et al., “Erste Messergebnisse der solar unterstützten Nahwärmeversorgung in Crailsheim” in *Ostbayerisches Technologie-Transfer-Institut e.V - 19. Symposium Thermische Solarenergie*, Bad Staffelstein, 2009.

[61] Schneider, B., “Sonnenenergie in der Erde speichern”, BINE Informationsdienst, Bonn, 2013.

[62] Croy, R., Wirth, H. P., “Abschlussbericht für das Projekt Solaranlage in den Wohnhochhäusern Frankfurt Peter-Fischer-Allee (ehemals Windthorststraße)”, ZfS, 2010.

[63] Croy, R., Wirth, H. P., “Kurzbericht zum Langzeitverhalten Solaranlage im Mehrfamilienhaus Baumgartner-/Ganghoferstraße in München”, ZfS, 2009.

[64] Croy, R., Wirth, H. P., “Abschlussbericht für das Projekt Solaranlage im Mehrfamilienhaus Baumgartner-/Ganghoferstraße in München”, ZfS, 2003.

[65] Grimmig, B. et al., “Zusammenfassung WG 'Karl-Marx': Humboldtring Potsdam Deutschland”, SOLARGE, Hannover, 2008.

[66] Reuß, M. et al., “Solare Nahwärme Attenkirchen - Erfahrungen beim Bau und im Betrieb” in *Ostbayerisches Technologie-Transfer-Institut e.V - 17. Symposium Thermische Solarenergie*, Bad Staffelstein, 2007.

[67] Schmidt, T., Müller-Steinhagen, H., “Die solar unterstützte Nahwärmeversorgung mit saisonalem Aquifer-Wärmespeicher in Rostock - Ergebnisse nach vier Betriebsjahren” in *5. Symposium Erdgekoppelte Wärmepumpen, 8. Geothermische Fachtagung*, Landau in der Pfalz, 2004.

[68] Solarge, *Solarge Website*. [Online] Available: www.solarge.org. Accessed on: Apr. 18 2015.

[69] Arcon, *Arcon Website.* [Online] Available: www.arcon.dk. Accessed on: Jun. 26 2013.

[70] Danish District Heating Association, *Solvarmedata.* [Online] Available: www.solvarmedata.dk. Accessed on: Jul. 12 2013.

[71] Zech, D. et al., “Technologien, Emissionen, Kosten – ein Überblick über Möglichkeiten der Wärmeversorgung von Wohngebäuden mit Erneuerbaren Energien”, Institut für Energiewirtschaft und Rationelle Energieanwendung, 2009.

[72] Fink, C., Riva, R., “Solar-supported heating networks in multi-storey residential buildings”, AEE INTEC, 2004.

[73] Rühling, K. et al., “Dezentrale Einspeisung in Nah- und Fernwärmesysteme unter besonderer Berücksichtigung der Solarthermie”, Technische Universität Dresden, 2015.

[74] Verein Deutscher Ingenieure, *VDI 6002 Blatt 1 - Solare Trinkwassererwärmung - Allgemeine Grundlagen - Systemtechnik und Anwendung im Wohnungsbau*, 2014.

[75] Hafner, B., Plettner, J., Wemhöner, C., Wenzel, T. “Conventional And Renewable eNergy systems Optimization Toolbox”, Solar-Institut Jülich, 1999.

[76] Recknagel, H. et al., *Taschenbuch für Heizung + Klimatechnik, 77th* ed. München: Deutscher Industrieverlag GmbH, München, 2015

[77] DIN EN 12975, *Sonnenkollektoren - Allgemeine Anforderungen*, 2018.

[78] Bundeskartellamt, *Sektoruntersuchung Fernwärme*. Bonn, 2012.

[79] Verein Deutscher Ingenieure, *VDI 2067 - Wirtschaftlichkeit gebäudetechnischer Anlagen*, 2012.

[80] Statistisches Bundesamt (Destatis), *Daten zur Energiepreisentwicklung*. Wiesbaden, 2020.

[81] KfW Bankengruppe, “Merkblatt Erneuerbare Energien 'Premium'”, Frankfurt, 2018.

[82] Mauthner, F., Herkel, S., “Technology and Demonstrators: Technical Report Subtask C - Part C1: Classification and benchmarking of solar thermal systems in urban environments”, International Energy Agency Solar Heating and Cooling Programme, 2016.

[83] Beckenbauer, D. et al., “Solar Retrofitting In Urban District Heating Networks - Influence of the Collector Type on the Solar Yield” in *3rd International Solar District Heating Conference,* Toulouse, 2015.

Appendix

Photographs of the field test system

Following photographs show the plants at the field test site to provide a better impression of the system layouts and sizes.

Building 2

Figure 104: Building 2 – four parallel collector arrays (top left), solar station between primary solar circuit and district heating return pipe (top right) and full view (bottom)

Building 1

Figure 105: Building 1 – 40°-inclined collectors on flat roof (top left), solar station (top right), parallel connected buffers in the basement (mid right) and full view (bottom)

Building 3

Figure 106: Building 3 – newly installed flat plate collectors (top left), existing evacuated tube collectors (top right) on west roof and full view (bottom)

Building 4

Figure 107: Building 4 – 40°-inclined collectors on the south roof (top left), controller, metrological equipment and feed-in components (top right) and full view (bottom)